

Evolutionary Analysis of MYBs-bHLH- WD40 Protein Complexes Formation and Their Functional Relationship *in Planta*

Inaugural-Dissertation

zur

Erlangung des Doktorgrades

der Mathematisch-Naturwissenschaftlichen Fakultät

der Universität zu Köln

vorgelegt von

Bipei Zhang

aus Zhejiang, China

Köln

2018

Berichtersteller/in: Prof. Dr. Martin Hülskamp

Prof. Dr. Ute Höcker

Prüfungsvorsitzender: Prof. Dr. Wolfgang Werr

Tag der mündlichen Prüfung: 16 Mai, 2018

KURZZUSAMMENFASSUNG

Der flavonoid-basierte Pigmentbiosyntheseweg in fast allen höheren Pflanzen wird von einem ternären Komplex bestehend aus R2R3MYB, bHLH und WD40 Proteinen (MBW-Komplex) aktiviert. Einige zusätzliche Funktionen des MBW-Komplexes entwickelten sich in der Gruppe der Rosiden: Trichommusterbildung, Wurzelhaarmusterbildung und Samenmantelschleimhautproduktion in Arabidopsis (*A. thaliana*) und Arabis (*A. alpina*), sowie Samenhaarbildung in Baumwolle (*G. hirsutum*). Diese neuen regulativen Aufgaben des MBW-Komplexes in epidermaler Zelldifferenzierung divergierten eventuell bei der evolutionären Trennung der Rosiden von den Asteriden, jedoch sind die Details dieser Entwicklung noch nicht bekannt.

Dieser Studie vorausgehende Ergebnisse aus unserer Gruppe zeigten neue stereochemische Konformationen der MBW Komponenten, die das klassische ternäre TTG1-GL3-GL1 Model ergänzten (z.B. alternative Dimere wie TTG1-GL3 und GL1-GL3). Dies führte zu folgender Frage: Welche evolutive Bedeutung hat diese alternative Dimerformation der MBW Komponenten in Pflanzen? Hierzu haben wir in dieser Studie die stereochemischen Eigenschaften von MBW Proteinen aus verschiedenen Pflanzenspezies mithilfe von Dreifach-LUMIER-Tests charakterisiert. Unter Verwendung der Ergebnisse der untersuchten Wechselbeziehungen der MBW Komponenten, konnten wir einen sehr genauen phylogenetischen Baum rekonstruieren. Dieses Ergebnis hebt die evolutionäre Relevanz dieser neuen stereochemischen Eigenschaften der MBW Komponenten hervor. Des Weiteren wurden besonders relevante Bereiche für variable stereochemische Eigenschaften innerhalb der bHLH Proteine vorhergesagt.

Es wird angenommen, dass Trichom- und Wurzelhaarmusterbildung neue evolutive Merkmale sind und dass diese aus der Duplizierung und Diversifizierung der Gene hervorgegangen sind, welche die Flavoniodbiosynthese regulieren. Die genaue Reihenfolge, in der diese Merkmale entstanden sind, ist jedoch bisher unklar.

Wir führten artübergreifende Komplementärstudien mit homologen MBW Proteinen in *A. thaliana* Mutanten durch, um die funktionalen Unterschiede der MBW Proteine in den fünf TTG1 regulierten morphologischen Merkmalen besser zu definieren.

AtTTG1-AtGL3-AtGL1 gilt als der wichtigste regulatorische MBW-Komplex für die Trichommusterbildung auf Blättern. Diese regulatorische Einheit liegt nicht nur in trimerer Konformation vor (synergistische Wechselwirkung), sondern auch in zwei

alternativen Dimeren (antagonistische Wechselwirkung), die wiederum verschiedene nachgeschaltete Gene regulieren. Ein wahrscheinlich noch wichtigerer Aspekt ist, dass abhängig von den relativen Konzentrationen dieser drei Proteine zu einander, verschiedene Promotoren differentiell aktiviert werden, was sich wiederum auf das Verhältnis der Konformationen auswirkt (alternative Dimere vs trimerer Komplex). Im Rahmen dieser Studie wurde versucht durch Simulationen ein regulatorisches Modell aufzustellen, welches die verschiedene Proportionalität der alternativen Dimere beschreibt. Dazu wurde quantitativ bestimmt, wie AtTTG1 und AtGL1 um die Bindung mit AtGL3 konkurrieren. Diese experimentellen Studien wurden durch mathematische Modelle von Anna Deneer, Waageningen, ergänzt.

ABSTRACT

It is well established that a network of three classes of proteins consisting of R2R3MYB, bHLH factors and WD40 repeat protein acted in concert as a ternary complex (i.g. MBW protein complex) to activate the flavonoid-based pigment biosynthetic pathway in most high plants. Several additional functions evolved in rosids: e.g. trichome patterning, root hair patterning and seed coat mucilage production in *Arabidopsis* (*A. thaliana*) or *Arabis* (*A. alpina*) and seed hair formation in cotton (*G. hirsutum*). New roles of MBW complexes controlling epidermal cell fate in rosids may have diverged since the evolutionary separation of rosid and asterid, although the details of this are still not clear.

Previous studies in our lab revealed novel stereochemistry of MBW components, i.g. alternative dimers TTG1-GL3 and GL1-GL3, which revised the conventional TTG1-GL3-GL1 ternary model. However, it raises one major question: what are the evolutionary implications of such alternative dimers formation among MBW components in plants? In this study, we characterized the stereochemistry of MBW proteins in different plant species by triple LUMIER assay. Using the inter-relation of MBW components as the criterion, we achieved a highly accordant phylogenetic tree suggesting the evolutionary relevance of this novel stereochemistry of MBW components. Potential critical sites in bHLH proteins accounting for diversified MBW stereochemistry were predicted.

In *Arabidopsis*, MBW genes which control trichome and root hair patterning traits are assumed to evolve from the duplication and diversification of flavonoid controlling genes, therefore trichome and root hair traits are considered as evolutionary current inventions. However, the exact evolving order of these traits still remains to be confirmed. To better define functional divergence of the MBW proteins in the five TTG1 related traits, we performed cross-species complementary assays with MBW homologs in *Arabidopsis* mutants.

Among MBW protein complexes in *Arabidopsis*, AtTTG1-AtGL3-AtGL1 is considered to be the predominant regulatory complex in leaf trichome formation. This regulatory unit is not only represented by a single trimeric complex (synergetic inter-relation) but also by two alternative dimers (antagonistic inter-relation) that in turn regulate different downstream genes. Probably even more important is the finding that different promoters become activated depending on the relative concentration of these three

proteins, as this should translate into different ratios of alternative dimers and trimers. In this study, we attempted to simulate regulatory models in the context of differential proportion of alternative dimers through quantitatively determining AtTTG1 and AtGL1 competing for the binding to AtGL3. These experimental studies were complemented by mathematical modeling by Anna Deneer, Wageningen.

ACKNOWLEDGEMENTS

I would like to express my gratitude to various individuals. This thesis could never have been completed without the support of a lot of people.

First and foremost, I would like to thank my supervisors, Prof. Dr. Martin Hüskamp, who give me the precious opportunity to pursue science and also have faith in my progress with great patience, support and advice. I have learned a lot from you and realize how kind and generous you've been teachers and supervisors.

I want to thank all my present and past members in my laboratory especially Sabine Lohmer, Irene Klinkhammer, Heike Wolff and Lisa Stephan, who provides warm and comfortable surroundings for study and research. They are always helping me whenever I bother them for the questions of translation or anything else, besides, they encourages me when I was down in spirits. Additionally, I would like to appreciate Anna Deneer as an excellent collaborator gave her full aide and support in this thesis accomplishment.

Special thanks to Dr. Stefanie Herberth, who helped me a lot in the project introduction. I am aslo very grateful to Dr. Andrea Schrader for her instruction in the flavonoid related content.

I would like to thank Prof. Dr. Ute Höcker, and Prof. Dr. Wolfgang Werr who gave me an exceptional doctoral committee.

Finally, this thesis is dedicated to my family. Many full-heart thanks to my parents, without their boundless love, affection and selfless sacrifice, I would not have been what I am today. From the bottom of my heart I thank my best girl friend Dr. Fanglei Liu for her suggestions and accompany to overcome any obstacle I have met throughout my study and life.

剧辛乐毅感恩分，输肝剖胆效英才。

--唐 李白《行路难》



TABLE OF CONTENTS

KURZZUSAMMENFASSUNG.....	I
ABSTRACT.....	III
ACKNOWLEDGEMENTS.....	V
TABLE OF CONTENTS	VI
LIST OF FIGURES	VIII
LIST OF TABLES	XI
ABBREVIATIONS.....	XII
1. General Introduction	2
1.1 Structures of MBW proteins.....	2
1.1.1 R2R3MYBs.....	2
1.1.2 bHLHs.....	2
1.1.3 WD40 Repeats	2
1.2 MBW complexes are conserved regulatory modules of flavoid biosynthesis pathway during the course of plant evolution.....	4
1.3 The molecular role of each component in the MBW protein complex.....	9
1.4 The stereochemistry of MBW protein complexes <i>in planta</i>	10
1.5 Objectives of the thesis	12
2. Evolutionary diversification of the inter-relation of MBW components in plants.....	14
2.1 Summary	14
2.2 Introduction.....	14
2.3 Results.....	16
2.3.1 Both synergetic and antagonistic models are recruited by MBW proteins in <i>Arabidopsis thaliana</i>	16
2.3.2 Antagonistic inter-relation of MBW components is a common protein behavior involved in regulating trichome development in rosids.....	20
2.3.3 Stereochemistry of MBW proteins in asterids and monocots.....	25
2.3.4 Proximity in bHLHs phylogenetic tree is perfectly accordant with their protein behavior similarity.....	28
2.4 Discussion	32
3. Evolutionary analysis of MBW function by phenotypic rescue in <i>Arabidopsis thaliana</i>	36
3.1 Summary	36
3.2 Introduction.....	36
3.3 Results.....	39
3.3.1 <i>AtTTG1</i> orthologs functionally substitute <i>AtTTG1</i> in term of all 5 traits	39
3.3.2 <i>bHLHs</i> have overlapping but differential regulatory capabilities in limitative traits.....	39
3.3.3 <i>R2R3MYBs</i> specifically rescue <i>gl1</i> or <i>pap1pap2</i> for one trait	41
3.3.4 Inter-species MBW pairwise interaction	46
3.4 Discussion	49

3.4.1 bHLH proteins redundantly and distinctly rescue AtTTG1- dependent traits, which provide an essential basic point for learning functional divergence of the MBW proteins	49
3.4.2 Hetero-MBW complex formation is in concert with rescue of AtTTG1-dependent traits in <i>Arabidopsis</i> mutant by MBW orthologs	50
4. Quantitative Analysis of TTG1, GL3 and GL1 Protein Complex Formation	52
4.1 Summary	52
4.2 Results	52
4.2.1 The comparison of GL3 binding affinity with GL1, TTG1 and itself	52
4.2.2 Effect of GL1 on the TTG1 binding to GL3 in dependence of the relative protein concentration	54
4.2.3 Quantitative analysis of GL1 and TTG1 effect on GL3 homo- dimerisation	55
4.2.4 Quantitative analysis of the interaction of GL3 with inhibitors TRY and CPC	56
4.2.5 The inhibitory effect comparison between distinct binding site competition and same binding site competition by mathematic modeling	58
4.3 Discussion	60
PERSPECTIVE	62
5. Materials and Methods	64
5.1 General Materials	64
5.1.1 Buffers and Solutions	64
5.1.2 Organisms	68
5.1.3 Oligonucleotides	68
5.1.4 Constructs	72
5.2 Methods	77
5.2.1 LUMIER (LUminescence-based Mammalian IntERactome)	77
5.2.2 Yeast two hybrid	78
5.2.3 Manipulation of plants and seeds	79
5.2.4 DNA extraction, amplification and cloning	82
5.2.5 Biochemical Methods	86
APPENDIX A Pairwise interaction analyses	87
APPENDIX B Protein motif analysis	126
APPENDIX C Western blot analysis of protein expressed in HEK cell	127
APPENDIX D Quantitative analyses of TTG1, GL3 and GL1 Protein Complex Formation	130
REFERENCES	144
Erklärung	i
Lebenslauf	ii

LIST OF FIGURES

Figure 1.1 Schematic depiction of the general R2R3MYB, bHLH and WD40 proteins structures.....	4
Figure 1.2 MBW proteins are common and conserved modules involved in regulating flavonoid biosynthesis throughout the plant kingdom.....	6
Figure 1.3 MBW Regulatory network model in Arabidopsis.....	7
Figure 1.4 GL1 and TTG1 compete for binding to GL3 in Arabidopsis.....	11
Figure 1.5 Putative stereochemistry of MYB-bHLH-WD40 protein complexes in Arabidopsis.....	11
Figure 2.1 Schematic representation of ternary MBW complexes regulating anthocyanin biosynthesis and trichome formation in plants.....	15
Figure 2.2 Inter-relation of MBW proteins in Arabidopsis thaliana.....	18
Figure 2.3 Inter-relation of MBW proteins in other rosids.....	22
Figure 2.4 Inter-relation of MBW proteins in asterid and monocot.....	27
Figure 2.5 Molecular phylogenetic analysis of bHLH proteins.....	29
Figure 2.6 Amino acids in bHLHs might feature bHLHs behavior.....	30
Figure 2.7 Potential evolutionary model for stereochemistry of MBW proteins in the context of traits regulation.....	34
Figure 3.1 The flavonoid pigment biosynthetic pathway in Arabidopsis.....	37
Figure 3.2 Rescue of 5 TTG1-dependent traits in Arabidopsis mutant by MBW genes from different plant species.....	42
Figure 3.3 Phenotypes of mutants rescued by different MBW genes.....	44
Figure 3.4 Analysis of inter-species MBW pairwise interaction by LUMIER pulldown assays.....	47
Figure 4.1 GL3 binding affinity analyses.....	53
Figure 4.2 Quantitative analysis of TTG1 and GL1 competing for the binding to GL3.....	55
Figure 4.3 Quantitative analysis of TTG1 and GL1 effect on GL3 homodimerisation.....	56
Figure 4.4 Analysis of GL3 binding affinity with inhibitors TRY and CPC.....	57
Figure 4.5 The inhibitory effect comparison between GL1 on GL3-TTG1 (distinct binding site competition) and TRY on GL1-GL3 (same binding site competition).....	59
Figure 4.6 Dynamic balance of multiple orders of complexes formed by TTG1, GL3 and GL1.....	61
Figure 5.1 Gateway BP and LR reactions.....	84
Figure S1 Protein–protein interactions among members of the MBW regulatory complex in cotton (A), petunia (B) and maize (C) determined by Yeast two hybrids assays.....	87
Figure S2 Sequence information of each motif in bHLH proteins.....	126
Figure S3 Western blot analysis of proteins fused with 3HA.....	127
Figure S4 Likelihood profile.....	129

LIST OF TABLES

Table 1.1 MBW (R2R3-MYB-bHLH-WDR) proteins (putatively) regulating flavonoid biosynthesis from different plant species.....	8
Table 2.1 The profile of MBW genes in 5 plant species.....	20
Table 5.1 Oligonucleotides.....	69
Table 5.2 Constructs used in this study.....	72
Table 5.3 Transgenic plant lines.....	79
Table S1 Pairwise interaction of MBW components in Arabidopsis (<i>A. thaliana</i>).....	89
Table S2 Pairwise interaction of MBW components in Arabis (<i>A. alpine</i>).....	94
Table S3 Pairwise interaction of MBW components in Cotton (<i>G.hirsutum</i>).....	97
Table S4 Pairwise interaction of MBW components in Petunia (<i>P. hybrida</i>).....	101
Table S5 Pairwise interaction of MBW components in Maize (<i>Z.mays</i>).....	103
Table S6 Interaction between WD40 homologs and bHLHs/R2R3MYBs in Arabidopsis.....	106
Table S7 Interaction between bHLH homologs and AtTTG1/R2R3MYBs in Arabidopsis.....	113
Table S8 Interaction between R2R3MYB homologs and AtTTG1/bHLHs in Arabidopsis.....	120
Table S 9-1 Binding affinity analysis of TTG1 (or GL1) and GL3 by titration.....	130
Table S10 Binding affinity analysis of TRY (or CPC) and GL3 by titration LUMIER.....	133
Table S11 Binding affinity analysis of TRY (or CPC) and GL3 by titration LUMIER.....	135
Table S12 Quantitative analysis of GL1 or TTG1 effect on GL3-GL3 dimerization by dosage-dependent LUMIER.....	136
Table S13 Quantitative analysis of GL1 effect on TTG1-GL3 interaction by dosage-dependent LUMIER.....	138
Table S14 Quantitative analysis of TRY or CPC effect on GL3-GL1 interaction by dosage-dependent LUMIER.....	140
Table S15 ANOVA test of effect of GL1 on the TTG1 binding to GL3.....	142

ABBREVIATIONS

- Aa** *Arabidopsis alpina*
- aa** amino acids
- A, C, G, T** adenine, cytosine, guanine, thymine
- AD** GAL4 activation domain
- Amp** ampicillin
- AN** anthocyanin
- ATP** adenosine triphosphate
- At** *Arabidopsis thaliana*
- AGI** code Arabidopsis gene locus identifiers assigned by TAIR
- B** BOOSTER
- BAN** BANYULS
- BD** GAL4 binding domain
- bHLH** basic HELIX-LOOP-HELIX
- Bo** *Brassica oleracea*
- BP** BP cloning strategy (Invitrogen)
- bp** base pair
- Br** *Brassica rapa*
- BSA** bovine serum albumin
- C1** COLORLESS1
- CaMV** Cauliflower Mosaic Virus
- ChIP** Chromatin Immunoprecipitation
- Col** Columbia
- COP1** CONSTITUTIVELY PHOTOMORPHOGENIC 1
- CPC** CAPRICE
- cDNA** complementary DNA
- CDS** coding sequence
- Ct** cycle threshold
- DEL** DELILA
- DFR** DIHYDROFLAVONOL 4-REDUCTASE
- dH₂O** distilled water
- DNA** deoxyribonucleic acid
- dNTP** deoxy-ribonucleotide triphosphate
- DMSO** dimethyl sulfoxide
- DTT** dithiothreitol
- E. coli** *Escherichia coli*
- EB** ethidium bromide
- EBG** early biosynthetic gene
- EGL3** ENHANCER OF GLABRA3
- EDTA** ethylenediaminetetraacetate

EMS ethyl methanesulfonate
ER Endoplasmic reticulum
Eudicot Eudicotyledons
et al. 'And others'
F3'5'H flavonoid 3', 5'-hydroxylase
F3'H flavonoid 3'-hydroxylase
F3H flavanone 3-hydroxylase
Fh *Freesia hybrida*
FLS flavonol synthase
g, mg, ug, ng gram, milligram, microgram, nanogram
g glabra
Gh *Gossypium hirsutum*
GL3 GLABRA3
GUS β -glucuronidase
h, min, s hour, minute, second
HCl hydrochloric acid
HI *Humulus lupulus*
In *Ipomoea nil*
IN1 INTENSIFIER1
JAF JOHNaNDFRANCESCA
Kan kanamycin
kb kilo base pair
LAR leucoanthocyanidin reductase
LAP1 LEGUME ANTHOCYANIN PRODUCTION 1
LBG late biosynthetic gene
l, ml, ul litre, millilitre, microlitre
LB lysogeny broth medium
LDOX LEUCOANTHOCYANIDIN DIOXYGENASE
Ler *Landsberg erecta* Arabidopsis accession
Lj *Lotus japonicus*
M, mM, uM molar, millimolar, micromolar
MBW MYB-bHLH-WD40 protein complex
Md *Malus domestica*
Mt *Medicago truncatula*
mm, nm, um millimetre, nanometer, micrometer
mRNA messenger ribonucleic acid
Monocot monocotyledon
MS Murashige and Skoog medium
MUT MUTABILIS
MYB MYELOBLASTOSIS (homolog)
MYBL MYB-like

MYBPA MYB transcription factors regulating PA synthesis
MYC MYELOCYTOMATOSIS (homolog)
MYB myeloblastosis
Nt *Nicotiana tabacum*
Os *Oryza sativa*
P1 PERICARP COLOR1
Pa *Picea abies*
PAP production of anthocyanin pigment
PAs proanthocyanidins
PAC1 PALE ALEURONE COLOR1
PAR PROANTHOCYANIDIN REGULATOR
PCR polymerase chain reaction
Pf *Perilla frutescens*
Ph *Petunia hybrida*
PH pH
PL PURPLE LEAF
Pm *Picea mariana*
Pp *Physcomitrella patens*
Pp *Prunus persica*
Pt *Pinus taeda*
Ptr *Populus trichocarpa*
35S 35S RNA promoter of cauliflower mosaic virus
qPCR quantitative polymerase chain reaction
qRT-PCR quantitative reverse transcriptase polymerase chain reaction
R RED
RHL1 ROOT HAIRLESS1
RLC RED LEAF COTTON
ROS ROSEA
RSL ROOT HAIR DEFECTIVE SIX-LIKE
RNA ribonucleic acid
RNase ribonuclease
rpm revolutions per minute
RT-PCR reverse transcriptase polymerase chain reaction
SDS sodium dodecyl sulfate
sec second(s)
Si *Setaria italica*
SPA SUPPRESSOR OF PHYA-105
SPL SQUAMOSA PROMOTER BINDING PROTEIN-LIKE
TAE tris, acetic acid, EDTA
Taq *Thermus aquaticus*
t-DNA transfer DNA

TE tris and EDTA

TFs transcription factors

T_m melting temperature

TRY TRIPTYCHON

TT1, 2, 8 TRANSPARENT TESTA2, 8

TTG1, 2, 3, 4 TRANSPARENT TESTA GLABRA1, 2,3,4

U units

UTR untranslated region

UV ultraviolet

V voltage

VE VENOSA

Vv *Vitis vinifera*

v/v volume per volume

w/v weight per volume

WER WEREWOLF

WDR WD40 repeats

WT wild type

X-gluc C₁₄H₁₃BrCINO₇, as a reagent to detect β -glucuronidase

Zm *Zea mays*

3-AT 3-amino-1,2,4-triazole

CHAPTER I

GENERAL INTRODUCTION

1. General Introduction

1.1 Structures of MBW proteins

1.1.1 R2R3MYBs

Myeloblastosis proteins (MYB) are found in all eukaryotic organisms [1, 2]. First identified in the *v-myb* oncogene of the avian myeloblastoma virus, later in the human proto-oncogene *c-myb* and other related factors. MYB proteins in general contain up to three imperfect repeats: R1, R2 and R3 with R2 and R3 representing the minimum DNA-binding domain and containing cooperative recognition helices [2-6]. Few plant 4R-MYB proteins are reported (e.g. in soy bean) [7, 8]. R2R3-MYB proteins are the most abundant plant specific MYB proteins in plants [1, 4, 5, 9]. R2R3-MYBs form also the largest class of MYB with 126 genes in Arabidopsis. Based on the conservation of the DNA binding domain and variability of the C terminal domains, R2R3-MYB proteins have been divided into at least 25 subgroups with various biological functions [10, 11]. The first cloned plant MYB gene was *Colorless1 (C1)* from maize (*Zea mays*), which regulates anthocyanidin accumulation [12]. *C1* was the gene disrupted in McClintock's experiments underlying her discovery of transposable elements [13].

1.1.2 bHLHs

Plant bHLH proteins of subgroup IIIf and MYB proteins containing the bHLH interaction motif [DE]L_{x2}[RK]L_{x3}L_{x6}L_{x3}R directly interact [14]. Subgroup IIIf bHLH proteins are already present in mosses [15]. Similar to R2R3-MYB proteins, the first cloned plant bHLH proteins originated from maize. In 1989 the *R (Red 1)* and *B (Booster 1)* gene were cloned [16, 17]. The basic helix-loop-helix (bHLH) motif was first discovered and described in murine muscle development transcription factors and found to mediate dimerization and DNA binding [18]. It consists of a basic region at the N-terminus that binds specific DNA motifs and an HLH region that mainly forms homo- and heterodimers with bHLH proteins [19]. More than 130 bHLH genes are found in Arabidopsis and have been divided into 12 subgroups [20].

1.1.3 WD40 Repeats

WD40 repeat (WDR) proteins are strongly conserved in eukaryotes within their WD40 repeats [21]. They have evolved in plants in various protein families with diverse function: e.g. signal transduction, cytoskeletal dynamics, chromatin modification or transcriptional regulation [21]. This is in part due to diversification of regulators and targets up- and downstream the WDR proteins that act as interaction platform,

constituents for protein complexes and sites of transient protein contacts [21]. WDR proteins are characterized by different numbers of WD40 repeats (usually 4-10 in plants) [21]. WDR proteins share a stretch of about 40 amino acids in one WD40 repeat that usually ends with Trp-Asp (WD) [22]. Four and more WD40 repeats in one protein can form so called β -propellers, a cylindrical formed series of four-stranded antiparallel beta sheets [21, 23]. In the mammalian G-protein subunit $G\beta$, it is shown that the first and last WD40 repeat contribute to the same beta-blade [23]. There are 237 WDR proteins with more than four repeats in Arabidopsis [21]. Six of these are TRANSPARENT TESTA GLABRA1 (TTG1), CONSTITUTIVELY PHOTOMORPHOGENIC 1 (COP1) and the four SUPPRESSOR OF PHYA-105 (SPA) proteins [24-27]. As shown in Figure 1.1, each such repeat folds into a 4-strand β -sheet. Among the Arabidopsis WDR proteins, TTG1 has been identified for the pleiotropic phenotypes of the corresponding mutants affected in flavonoid biosynthesis and various epidermal cell fates [28]. The interactions between the R2R3-MYB and the R/B-like bHLH (subgroup III_f) are probably among the best-described cooperation of transcription factors in plants [29-35]. These involved the R3 repeat of the MYB (with a conserved motif [D/E]LX2[R/K]X3LX6LX3R) and the N-terminus MYB-interacting region (MIR) of the bHLHs, which contains an arginine residue conserved among the bHLHs of the III_f subgroup.

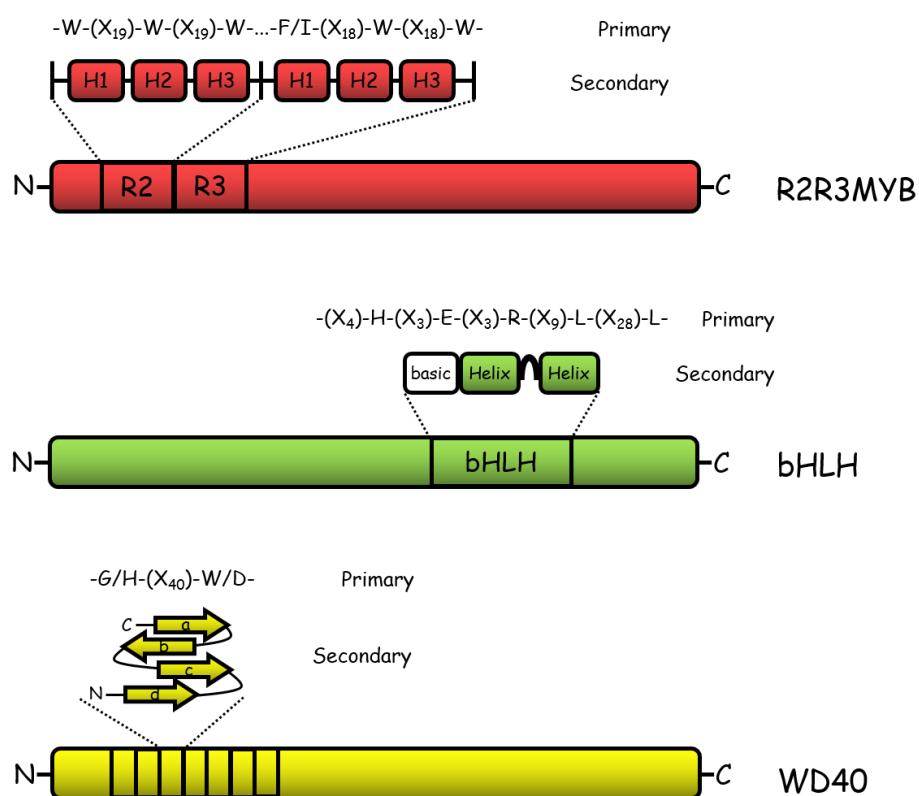


Figure 1.1 Schematic depiction of the general R2R3MYB, bHLH and WD40 proteins structures.
(Modified from [34, 36])

1.2 MBW complexes are conserved regulatory modules of flavoid biosynthesis pathway during the course of plant evolution

The flavonoid biosynthetic pathway is found in a wide range of land plants, even in the bryophytes (mosses) and it has been suggested that synthesis of flavones, flavanones, and flavonols may have evolved first to provide chemical messengers and then UV sunscreens [37, 38]. Maize (*Zea mays*), petunia (*Petunia hybrida*) and snapdragon (*Antirrhinum majus*) emerged as the major models for the study of flavonoid biosynthesis and genes encoding R2R3-MYB and bHLH proteins were identified as regulators of anthocyanin structural genes, demonstrating broad conservation of this regulatory mechanism in these plants [39-50]. By then, the relationship between WD40 proteins and the R2R3MYB/bHLH transcriptional regulators had not been revealed. The first anthocyanin regulatory locus that was cloned from petunia, *AN11*, encoded a protein containing five WD40-repeats [51]. Further support for the formation of an MBW complex in plants came from interaction studies conducted in *A. thaliana* [29]. Similarly,

the maize PAC1 (WD40) is specifically involved in the anthocyanin pathway but can complement all *ttg1* phenotypes in Arabidopsis, and it became the first identified TTG1-like protein in the monocot [42, 52]. Later WD40 proteins were found to regulate the anthocyanin pathway in other plants such as *Arabis alpina*, *Perilla frutescens*, *Ipomoea nil*, *Medicago truncatula* and *Malus domestica* [42, 53-57]

Regularly, new orthologs are identified which might be of relevance for breeding purposes. Not only allelism tests and rescue experiments within the respective species are employed – if applicable - to explore the ortholog's function when mutants or *TTG1* variants are identified. More often, the function of the orthologs is estimated using the model species *A. thaliana*. In cross-species rescue experiments, TTG1 orthologs from other species are expected to take over AtTTG1 function at least in part within respective TTG1-MBW complexes containing the ortholog of AtTTG1. This year, for example, ectopic expression of SiTTG1 (a newly identified TTG1 ortholog in *Setaria italica*) in the *A. thaliana ttg1-13* background was shown to fully rescued the glabrous trichome and the anthocyanidin phenotype. This suggests that SiTTG1 is a member of flavonoid regulators in monocots [58]. Another example is *BrTTG1*, that was isolated from a brown-seeded hairy *Brassica rapa* and found to functionally complement an *A. thaliana ttg1* mutant, while another orthologue isolated from *Brassica rapa* yellow-seeded glabrous germplasm was not functional [59].

It needs to be mentioned that promoter sequences and MBW components might have differentially evolved in the respective other species and thereby lead to shifts in TTG1-MBW function, nevertheless, newly identified orthologs also provide novel insights into evolutionary aspects of TTG1-MBWs: MBW complexes have been identified as common and conserved flavonoid biosynthesis regulators, similarly reported for various land plants - although in several cases not all components have been identified or characterized (Figure 1.2 and Table 1.1). Recently, MBW complexes (PaWD40-1-PabHLH1/2-PaMYB29/32/33/35) were characterized in Norway spruce (*Picea abies*) and shown to be involved in the regulation of the flavonoid biosynthesis pathway [60]. This reveals a full MBW regulator in gymnosperms which were previously thought to be devoid of TTG1 orthologs [61].

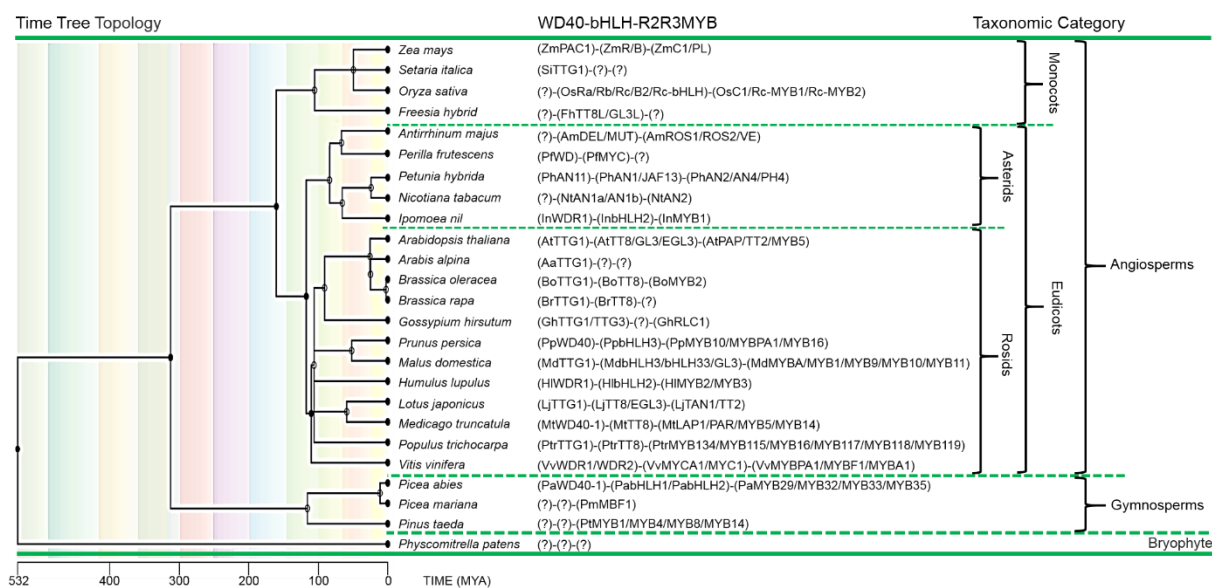


Figure 1.2 MBW proteins are common and conserved modules involved in regulating flavonoid biosynthesis throughout the plant kingdom.

Phylogeny of selected land plants is reflected by time tree topology on the left (conducted in TimeTree database [62]). Functionally characterized MBW proteins from different plant species are listed in the middle (flavonoid pathway exclusive). Question marks indicate unidentified components. For a full list of proteins and references, please refer to Table 1.1.

Interestingly, in the rosid clade, besides regulation of the flavonoid biosynthesis pathway, combinatorial MBW complexes evolved several extra functions: for instance trichome patterning, root hair patterning and seed coat mucilage production in *A. thaliana* [35, 63-72] (Figure 1.3) or *Arabis alpina* [57] and seed hair formation in cotton (*Gossypium hirsutum*) [73-76]. These observations imply that a common regulatory MBW module has been adapted for controlling specific epidermal cell fates in rosids. However, such pleiotropic functions of MBW complexes have neither been observed in the Asterid clade nor in monocots. Based on this, a speculation is raised: new roles of MBW complexes in controlling epidermal cell fate may have diverged since the evolutionary separation of these major plant groups, although the details of this are still not clear [77, 78]. This is supported by the findings that multicellular trichome and conical cell formation in asterids, like *Antirrhinum* and *Solanaceae* species, are regulated by MIXTA-like R2R3-MYB-related proteins in which the bHLH interaction motif ([DE]L_{x2}[RK]_{x3}L_{x6}L_{x3}R) is devoid. MIXTA genes overexpression in rosids do not affect trichome formation [78-80]. AtGL1, a trichome patterning specific-R2R3-MYB protein, was grouped phylogenetically together with AtPAP and AtTT2, which act in the regulation of the flavonoid biosynthesis pathway. This clade is distinct from the MIXTA-

like regulators branch [81-83]. It is assumed that duplication and subsequent divergence, as known for other protein families [84], has been the driving force to evolve new roles of MBW complexes and other epidermal cell fates in rosids as compared to asterids [85].

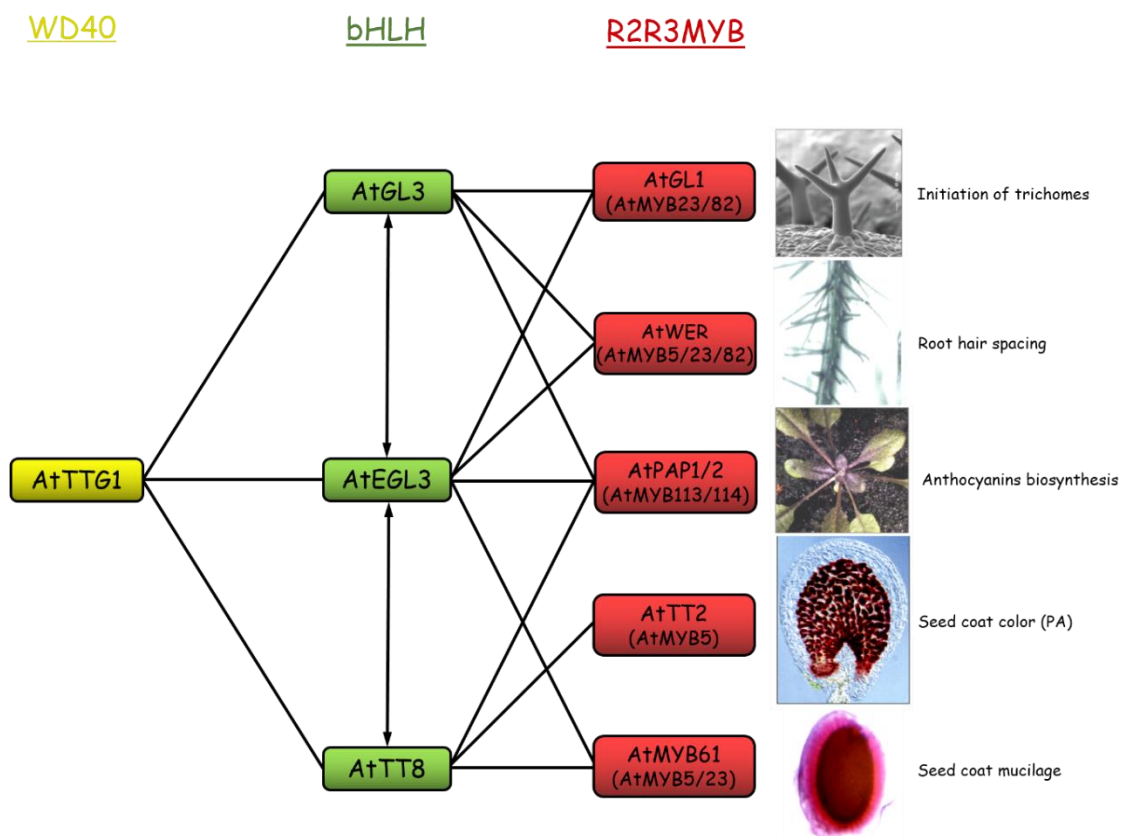


Figure 1.3 MBW Regulatory network model in Arabidopsis.

This reticulated model shows all of the known bHLH and myb transcriptional regulators that function the TTG1-dependent pathways. (Modified from [66, 86, 87])

Table 1.1 MBW (R2R3-MYB-bHLH-WDR) proteins (putatively) regulating flavonoid biosynthesis from different plant species.

Species	MBW Proteins			References
	WD40	bHLH	R2R3MYB	
<i>Zea mays</i>	ZmPAC1	ZmR/B ZmIN1(repressor)	ZmC1; ZmPL ZmP1(independence of WDR and bHLH)	[33, 41-43, 88-92]
<i>Setaria italica</i>	SiTTG1			[58]
<i>Oryza sativa</i>		OsRa/Rb/Rc OsB2 OsRc-bHLH	OsC1; OsRc-MYB1/2	[93-96]
<i>Freesia hybrida</i>		FhTT8L FhGL3L		[97]
<i>Antirrhinum majus</i>		AmDEL AmMUT	AmROS1/2; AmVE AmMYB308/330 (repressors)	[50, 98-100]
<i>Perilla frutescens</i>	PfWD (cytosol)	PfMYC		[53]
<i>Petunia hybrida</i>	PhAN11 (cytosol)	PhAN1 PhJAF13	PhAN2/4; PhPH4 PhMYB27(repressor)	[44-49, 51, 83]
<i>Nicotiana tabacum</i>		NtAN1a/b	NtAN2	[101]
<i>Ipomoea nil</i>	InWDR1 InWDR2*	InbHLH2 InbHLH1/3*	InMYB1 InMYB2/3*	[54]
<i>Arabidopsis thaliana</i>	AtTTG1	AtTT8 AtGL3 AtEGL3 AtMYC1*	AtPAP1/2; AtMYB113/114; AtTT2; AtMYB5 AtMYB4 (repressor)	[28, 31, 32, 66, 102-111]
<i>Arabis alpina</i>	AaTTG1			[57]
<i>Brassica oleracea</i>	BoTTG1	BoTT8 BoEGL3*	BoMYB2 BoMYB12*BoTT2*	[112]
<i>Brassica rapa</i>	BrTTG1	BrTT8		[113, 114]
<i>Gossypium hirsutum</i>	GhTTG1/3	GhDEL61/65* GhMYC1*	GhRLC1	[73-76]
<i>Prunus persica</i>	PpWD40	PpbHLH3	PpMYB10.1/10.3; PpMYBPA1; PpMYB16 PpMYB111(a repressor)	[111, 115-117]
<i>Malus domestica</i>	MdTTG1	MdbHLH3 MdbHLH33 MdGL3	MdMYB1/9/10/11; MdMYBA	[55, 118, 119]
<i>Humulus lupulus</i>	HiWDR1	HibHLH2	HIMYB2/3 HIMYB7(a repressor)	[120]
<i>Lotus japonicus</i>	LjTTG1	LjTT8, LjEGL3 LjRHL1*	LjTAN1; LjTT2a/b/c	[121]
<i>Medicago truncatula</i>	MtWD40-1	MtTT8 MtEGL3*	MtLAP1; MtPAR; MtMYB5/14 MtMYB2 (a repressor)	[56, 122-126]

Table 1.1 Cont.

Species	WD40	bHLH	R2R3MYB	References
<i>Populus trichocarpa</i>	PtrTTG1	PtrTT8	PtrMYB134/115/116/117 /118/119; PtrMYB182 (a repressor)	[127-129]
<i>Vitis vinifera</i>	VvWDR1/2	VvMYCA1 VvMYC1	VvMYBPA1; VvMYBF1; VvMYBA1	[130-134]
<i>Picea abies</i>	PaWD40-1	PabHLH1/2 PabHLH3*	PaMYB29/32/33/35 PaMYB30/31/34*	[60]
<i>Picea mariana</i>			PmMBF1	[135]
<i>Pinus taeda</i>			PtMYB1/4/8/14	[136, 137]
<i>Physcomitrella patens</i>		PpRSL1/2* (rhizoid development)		[138]

* functions in flavonoid biosynthesis regulation remain to be confirmed. Note, not for all proteins full MBW complexes have been described (so far). Some might turn out not to be present in these species as MBW complexes.

1.3 The molecular role of each component in the MBW protein complex

The exact molecular role of each of the three components of MBW protein complexes is also not yet fully understood. For instance, some evidences suggest that the bHLHs can bind DNA, and its direct binding may be dispensable [139, 140]. On the contrary, mutations of the MYB-interacting region can induce bHLH transcriptional activity, suggesting that MYB plays the regulatory role [141]. Last, WD40 is dispensable for the activity MBW complexes *in vitro*, however we cannot exclude that some heterologous proteins can replace the WD40 *in planta* [31, 142].

One attractive hypothesis is that the WD40 is necessary to prevent the effect of a negative regulator, allowing stabilization and/or nuclear localization of the MBW complexes, or controlling the interaction with chromatin factors [29, 31, 34, 51, 140, 143, 144]. Nevertheless, the later hypotheses are difficult to reconcile with the positive effect of WD40 in transient expression in protoplasts from Arabidopsis, maize or moss or in yeast experiments [31, 140, 142]. In addition, the ectopic expression of different bHLHs can (partially) complement *ttg1* mutants in Arabidopsis [66] and TTG1 has a quantitative effect on TT8 activity [31], suggesting that the TTG1 protein plays a

role at the post-translational level by regulating its activity in a quantitative manner, which in turn demonstrates a stabilization role for TTG1.

1.4 The stereochemistry of MBW protein complexes *in planta*

Based on plenty of former investigations, the MBW proteins are considered to act together in a transcriptional activating complex in which both the R2R3MYB and the WD40 proteins bind to the bHLH protein. Higher ordered complexes are possible due to homodimerization or heterodimerization of bHLH proteins [29, 33, 43, 66, 145, 146]. Three components of MBW complex forming a trimeric complex, work in coordination to activate their downstream effector genes. In Arabidopsis, the concept of trimeric MBW activation complex was derived from yeast two-hybrid data showing that GL1 interacts with GL3 and that GL3 interacts with TTG1 [29]. This view was also adapted for MBW proteins from other plant species [34, 81, 147, 148].

Contrasting the current view of MBW complexes, our former study have shown that in the context of trichome patterning in Arabidopsis alternative dimers are formed, rather than a single ternary complex [149]. We have provided the evidence that these three MBW proteins form either GL1-GL3 or GL3-TTG1 dimers. The formation of each dimer is counteracted by the respective third protein in yeast three-hybrid assays, pulldown experiments (luminescence-based mammalian interactome), and fluorescence lifetime imaging microscopy-fluorescence resonance energy transfer studies. We further showed that two target promoters, TRIPTYCHON (TRY) and CAPRICE (CPC), were differentially regulated: GL1 represses the activation of the TRY promoter by GL3 and TTG1, and TTG1 suppressed the activation of the CPC promoter by GL1 and GL3. The data suggested that the transcriptional activation by the MBW complex involved alternative complex formation and that the two dimers could differentially regulate downstream genes (Figure 1.4). This finding adds another level of complexity to the stereochemistry of MBW protein complexes, however the precise stereochemistry of the MBW protein complexes still remains to be further confirmed *in planta* (Figure 1.5).

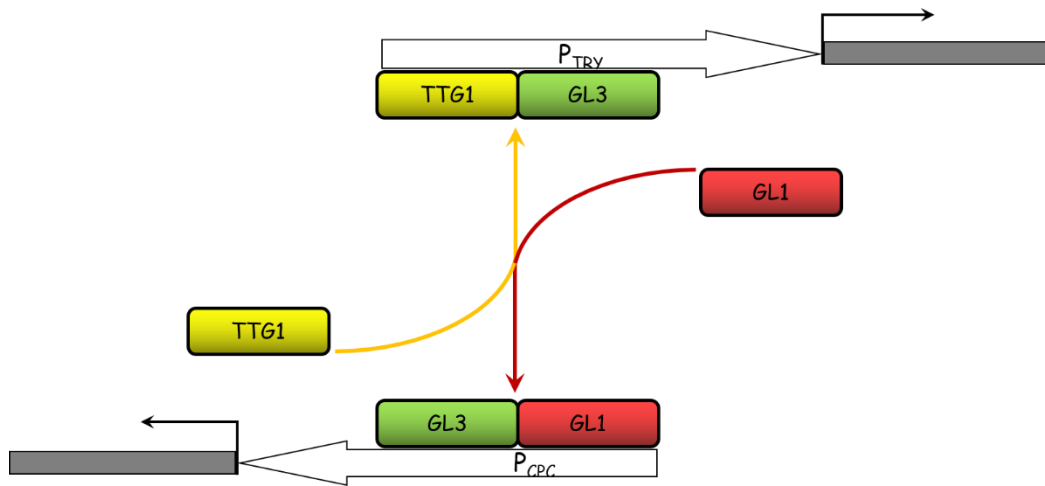


Figure 1.4 GL1 and TTG1 compete for binding to GL3 in Arabidopsis.

The interaction between TTG1 and GL3 could be counteracted by GL1, and vice versa. Alternative dimer alone is sufficient to activate *CPC* and *TRY* respectively (adapted from [149]).

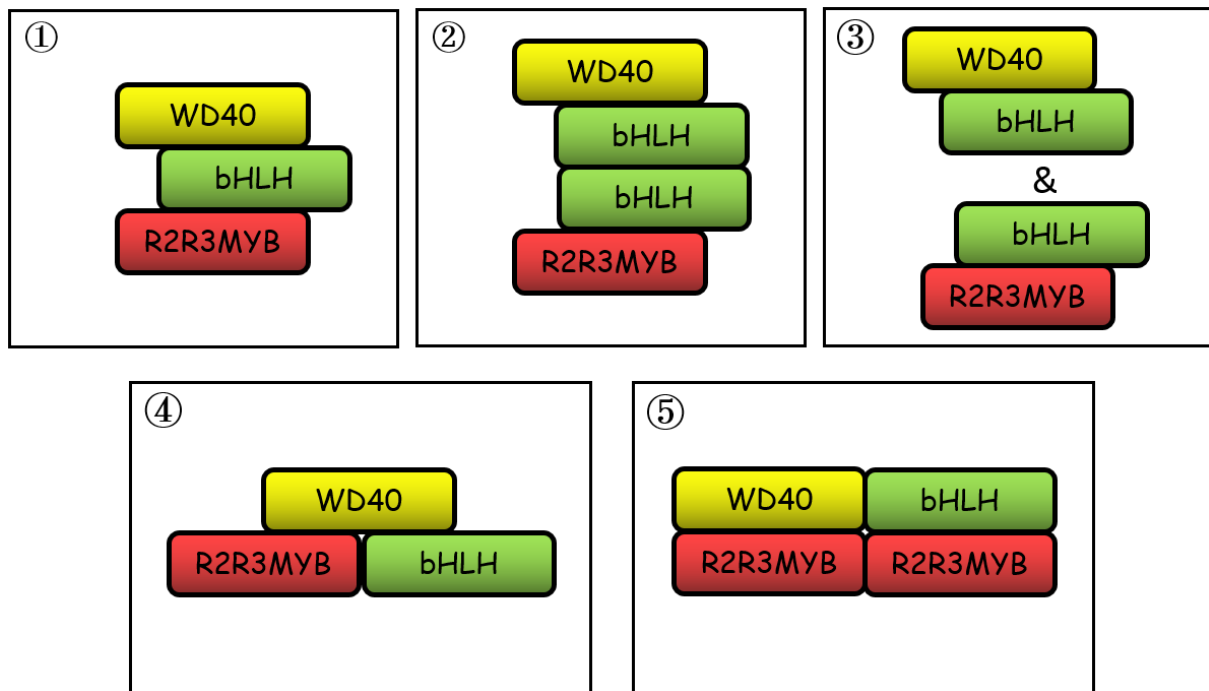


Figure 1.5 Putative stereochemistry of MYB-bHLH-WD40 protein complexes in Arabidopsis.

1.5 Objectives of the thesis

At the start of my PhD, our understanding of the regulatory model of the MYB-bHLH-WD40 (MBW) complexes in Arabidopsis was becoming clearer, however some questions still needed to be answered.

Within the framework of this PhD thesis we wished to develop evolutionary diversification of stereochemistry of MBW protein complexes and integrate it into their function in determining the epidermal cell fates in plants. For this purpose we have tried to answer a set of linked but different basic questions:

I. What are the evolutionary implications of alternative dimer formations among MBW components?

- Is it an evolutionarily conserved mechanism recruited by all plants or an occasional case in Arabidopsis?

II. Are there any functional correlations of diverse stereochemistry of MBW complexes in terms of TTG1-dependent traits?

- Are there any correlations between MBW proteins' behavior and functions involved in the control of epidermal cell fates?

III. How will alternative dimer formation change the current patterning models?

- How does dynamic balance of TTG1, GL3 and GL1 determine multiple orders of protein complexes formation

CHAPTER II

EVOLUTIONARY DIVERSIFICATION OF

INTER-RELATION OF MBW

COMPONENTS IN PLANTS

2. Evolutionary diversification of the inter-relation of MBW components in plants

2.1 Summary

R2R3MYB, basic helix-loop-helix (bHLH), and WD40 factors comprise evolutionarily conserved MBW complexes. It is a common regulatory module controlling flavonoid biosynthesis throughout the plant kingdom. Interestingly, the role of the MBW complex evolved an extra trait in rosids: trichome formation (in the context of leaf, root or seed) but not in asterids, suggesting that the MBW regulatory systems may have diverged since the evolutionary separation of asterids and rosids. Our previous data have shown that in *Arabidopsis* MBW proteins can form two alternative dimers: MB and BW, which adds another level of complexity to the stereochemistry of MBW protein complexes. However, this raises one major question: what are the evolutionary implications of such alternative dimers formation among MBW components in plants? In this study, we characterized the inter-relation of MBW components in different plant species by triple LUMIER assays. Using the interaction behavior as the criterion, we arrived at the well-established phylogenetic tree suggesting the evolutionary relevance of alternative dimers. Finally, potential vital sites in bHLH proteins accounting for differential inter-relation of MBW components were predicted by amino acids alignment.

2.2 Introduction

Investigation of the MBW complex in plants obtains a rich and interesting research history beginning with genetic studies on one of the most intensely researched metabolic systems in plants, i.e. the flavonoid biosynthetic regulation. Identified as common and conserved flavonoid biosynthesis regulating complexes, MBW proteins have been characterized in angiosperms as well as in gymnosperms [60].

In all plants studied so far MBW complexes determine the spatio-temporal expression of target genes those account for tissue-specific accumulation of flavonoid. Apart from regulation of the flavonoid biosynthesis pathway in plants, combinatorial MBW complexes evolved several extra functions in rosids: for instance trichome patterning, root hair patterning and seed coat mucilage production in *Arabidopsis* [35, 63-72] or *Arabis* (*A. alpine*) [57] and seed hair formation in cotton (*G. hirsutum*) [73-76] (Figure 2.1). These observations imply that a common regulatory MBW module has been adapted for controlling specific epidermal cell fates in rosids.

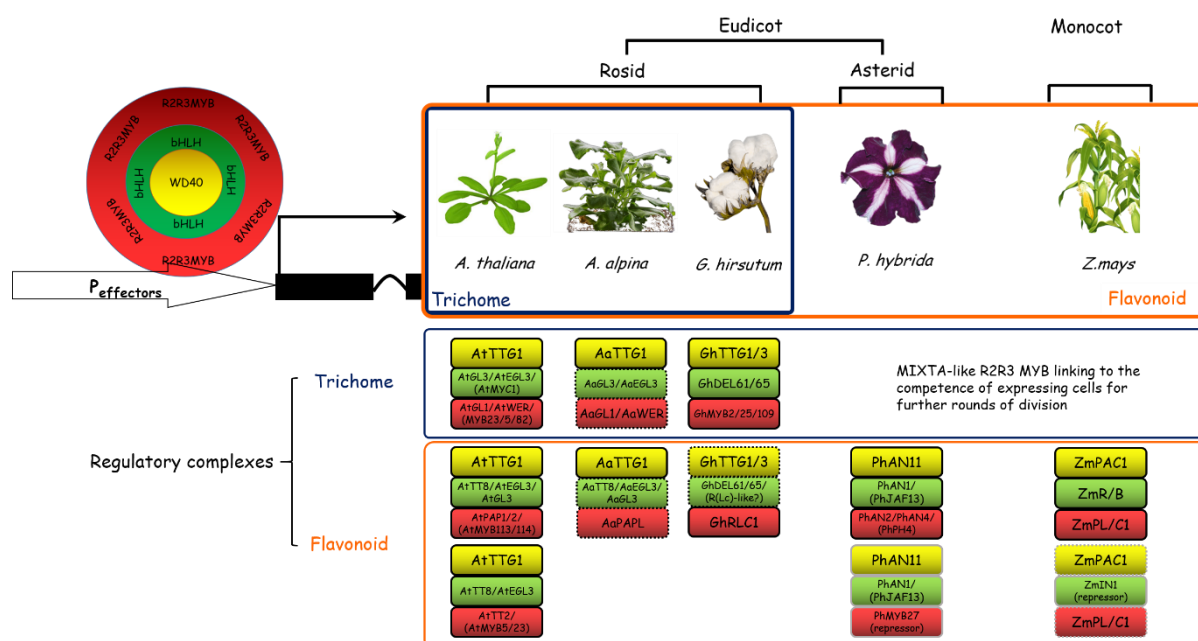


Figure 2.1 Schematic representation of ternary MBW complexes regulating anthocyanin biosynthesis and trichome formation in plants.

Different plant species include: Arabidopsis (*A. thaliana*), Arabis (*A. alpina*), petunia (*P. hybrida*), and maize (*Z. mays*). Blocks in full line indicate demonstrated regulatory mechanisms, while blocks in dotted lines indicated potential regulatory mechanisms. Blocks in grey line indicate negative regulation. (Adapted from [34, 148, 150-152]).

Petunia and Arabidopsis represent model species from the two major groupings of dicotyledonous plants, the asterids and rosids, respectively. Studies of the role of the MBW complex in controlling trichome/hair production suggest that the MBW regulatory systems may have diverged since the evolutionary separation of these major plant groups, although the details of this are still not clear [77, 78].

The study of stereochemistry of MBW protein complexes was essentially based on yeast two-hybrid data in different plant species [29, 34, 81, 147, 148]. It was generally considered that three components of MBW complex, forming a trimeric complex, work in coordination to activate their downstream effector genes.

Contrasting the current view of MBW complexes, our former study has shown that in the context of trichome patterning alternative dimers are formed, rather than a single ternary complex in Arabidopsis [149]. We've provided the evidence that these three MBW proteins form either GL1-GL3 or GL3-TTG1 dimers. The formation of each dimer is counteracted by the respective third protein in yeast three-hybrid assays, pulldown experiments (luminescence-based mammalian interactome), and fluorescence lifetime

imaging microscopy-Förster resonance energy transfer studies. It was further shown that two target promoters, TRIPTYCHON (TRY) and CAPRICE (CPC), are differentially regulated by alternative dimers. This new observation gives rise to one major question: what are the evolutionary implications of such alternative dimers formation among MBW components in plants? In this study, we characterized the stereochemistry of MBW proteins in different plant species by triple LUMIER assay. After dissecting the interplay of the regulatory components of MBW complexes, differentially involved in the control of epidermal cell fates, we made a bid to elucidate the evolutionary relevance of alternative dimers.

2.3 Results

2.3.1 Both synergetic and antagonistic models are recruited by MBW proteins in *Arabidopsis thaliana*.

Our previous finding that AtGL1 and AtWER can interfere with the interactions between AtTTG1 and GL3 triggered us to explore whether it is a general phenomenon in multiple combinations of MBW proteins or if it is specific to certain combinations. To this end, we initially refined a comprehensive network model of MBW proteins in *Arabidopsis thaliana* by integrating pairwise LUMIER data in our hands and other previous data (Table S1). This was necessary as the pairwise interaction data are not fully conclusive in the literature [29, 31, 32, 66, 153].

Protein interactions were found between the 4 bHLH proteins and all R2R3MYBs tested, despite AtMYB61 showed weak interaction with 4 bHLH proteins. Homo- and hetero-dimerization were found in all bHLH proteins here. Self-interactions in AtMYC1 and AtTT8 were novel observations (Figure 2.2A Table S1).

Based on the network, we then proceeded to quantitatively analyze the effect of different R2R3MYBs on the interaction between AtTTG1 (WD40) and 4 bHLH proteins, respectively, by triple LUMIER (luminescence-based mammalian interactome mapping) pulldown assays [154].

The ProtA-fused bHLH proteins (AtGL3, AtEGL3, AtTT8 and AtMYC1) were immunoprecipitated with IgG beads and the amounts of co-immunoprecipitated Renilla luciferase-fused AtTTG1 were quantified when adding a certain amount of YFP-tagged R2R3MYB proteins. As shown in Figure 2.2B, AtTTG1/AtGL3 interaction substantially dropped by adding AtGL1, AtWER, AtTT2 or AtMYB61; whereas two anthocyanin specific R2R3MYBs, i. e. AtPAP1 and AtPAP2 enhanced their interaction. A similar

inter-relation was found in AtTTG1-AtEGL3 combination. Interestingly, all of the R2R3MYB proteins here did enhance the interaction between AtTTG1 and AtTT8, by contrast, AtTTG1-AtMYC1 interaction was significantly counteracted by each R2R3MYB protein.

Taken together, both synergetic (trimer and/or multimer) and antagonistic (alternative dimers) inter-relation of MBW proteins exist in Arabidopsis. And 4 combinations of AtTTG1/bHLH presented 3 different inter-relation patterns.

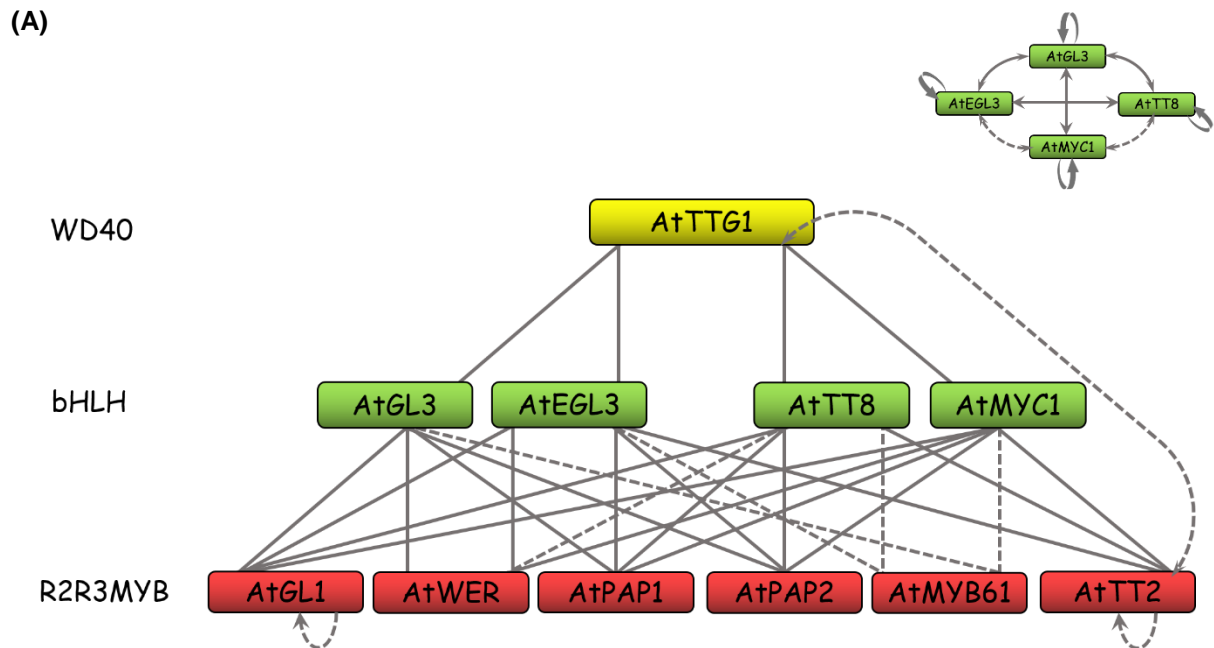


Figure 2.2 Inter-relation of MBW proteins in *Arabidopsis thaliana*.

(A). Comprehensive network model of MBW in *Arabidopsis thaliana* demonstrated by yeast two hybrids and pairwise LUMIER pulldown assays. It shows all known bHLHs and R2R3MYBs transcriptional regulators that function in five TTG1-dependent traits. Homo- and hetero-dimerization of bHLHs are depicted separately on upper-right. Dash lines indicate weak interaction among the proteins.

(B)

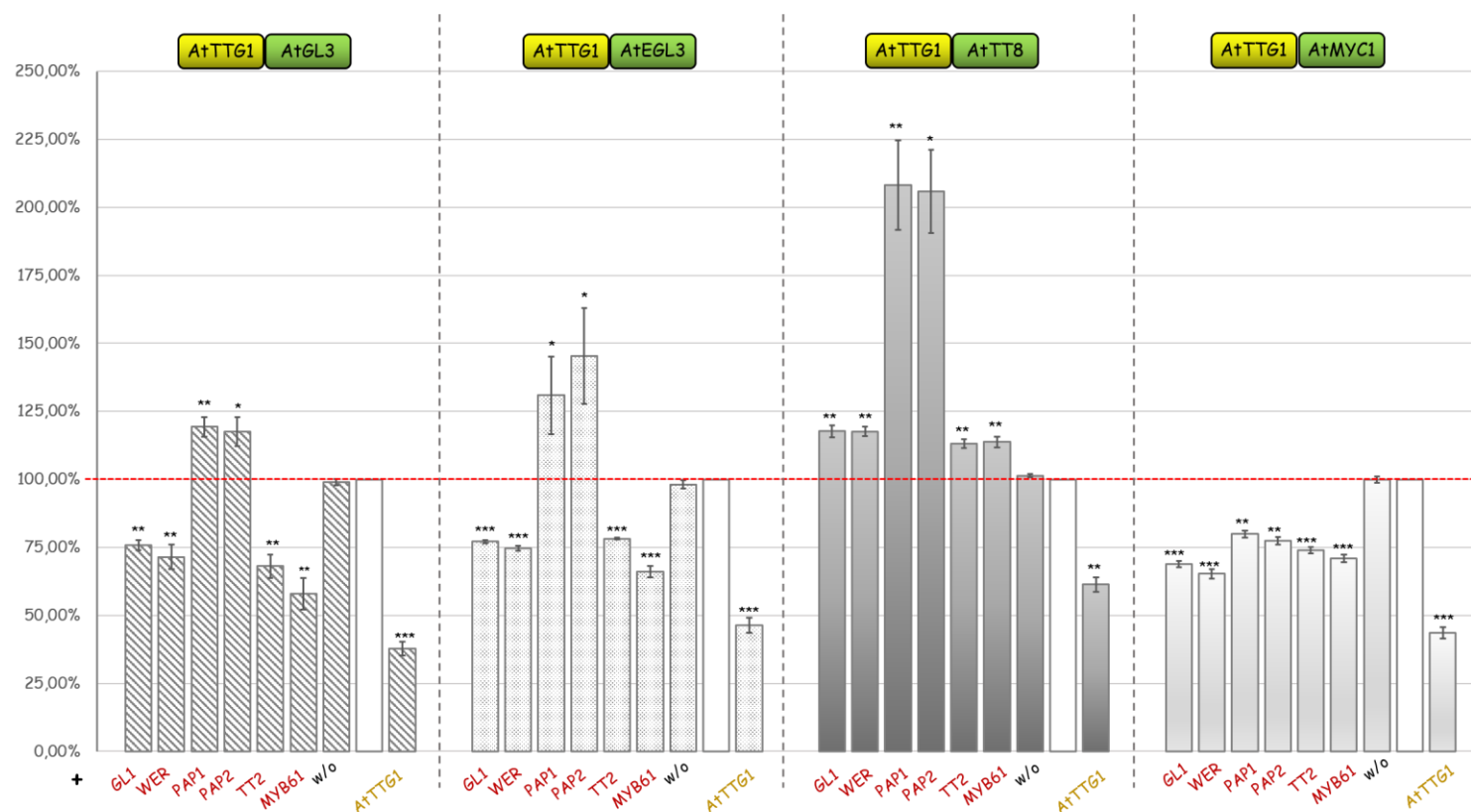


Figure 2.2 Cont. Inter-relation of MBW proteins in *Arabidopsis thaliana*.

(B) The effect of different R2R3MYBs on the interaction between AtTTG1 (WD40) and 4 bHLHs, respectively. Triple LUMIER pulldown assays are used to quantify relative pulldown efficiency (pulldown ratio) of Renilla Luciferase fused TTG1 and ProtA fused bHLHs in the presence of YFP tagged R2R3MYB factors. The pulldown ratio is normalized to the combination AtTTG1 and bHLHs without additional R2R3MYB proteins (defined as 100% in hollow columns). As a negative control, YFP only protein without any other CDS is also included (w/o), meanwhile YFP-tagged AtTTG1 is antagonistic-positive control. Each value represents mean \pm standard errors ($n = 3$ biological replicates). *** indicates that pulldown ratio is extremely significant different from that of the reference (hollow column) by Student's t test ($0.0001 \leq P < 0.001$); ** indicates very significant difference ($0.001 \leq P < 0.01$); * indicates significant difference ($0.01 \leq P < 0.05$).

2.3.2 Antagonistic inter-relation of MBW components is a common protein behavior involved in regulating trichome development in rosids.

It is assumed that the duplication of components of the MBW gene cassette and subsequent divergence of rosid and asterid was the driving force to evolve a new role of the MBW complex in trichome development of rosids [81]. As a typical representative in rosids, *Arabidopsis* gave a perfect starting point for the stereochemistry investigation of MBW proteins. In order to further determine whether alternative complex formation is a common behavior of the MBW proteins in rosids, we implemented the same scheme in other two rosids: *Arabis* (*Arabis alpina*) and cotton (*Gossypium hirsutum*) as the MBW genes were well-identified in these species (Table 2.1).

Table 2.1 The profile of MBW genes in 5 plant species.

Gene	Locus	GenBank Accession	cDNA Length (bp)	Donor	References
Arabidopsis (<i>A.thaliana</i> n=5)					
GL1	AT3G27920	NM_113708	687	our lab	[67, 155-157]
WER	AT5G14750	NM_121479	612	our lab	[63]
PAP1	AT1G56650	NM_104541	747	our lab	[106, 108, 158]
PAP2	AT1G66390	NM_105310	750	our lab	
TT2	AT5G35550	NM_122946	777	our lab	[31, 104]
MYB61	AT1G09540	NM_100825	1101	our lab	[72]
GL3	AT5G41315	NM_148067	1914	our lab	[29, 65, 66, 108, 109, 159]
EGL3	AT1G63650	NM_202351	1791	our lab	[65, 66, 108]
MYC1	AT4G00480	NM_001160722	1473	our lab	[70, 71]
TT8	AT4G09820	NM_117050	1557	our lab	[66, 102, 103]
TTG1	AT5G24520	NM_122360	1026	our lab	[105]
Arabis (<i>A.alpina</i> n=8)					
GL1	AALP_AA5G050100	LT669792	675	our lab	this work
WER	AALP_AA8G149800	LT669795	618	our lab	this work
PAPL	AALP_AAs71396U000200	KL980989	741	our lab	this work
GL3	AALP_AA6G320200	LT669793	1884	our lab	[150]
EGL3	Chr2	LT669789	1806	our lab	[150]
MYC1	AALP_AA6G006500	LT669793	1683	our lab	this work
TT8	AALP_AA6G192900	LT669793	1590	our lab	this work
TTG1	AALP_AA8G421800	KFK27728	1032	our lab	[57]
Cotton (<i>G.hirsutum</i> 2n=52)					
MYB2		AF034130	597	our lab	[160-163]
MYB25		AY464054	1104	our lab	[164]

Table 2.1 Cont.

Gene	Locus	GenBank Accession	cDNA Length (bp)	Donor	References
<i>RLC1</i>		NM_001327615	744	our lab	[75]
<i>DEL65</i>		AF336280	1863	our lab	[76, 151]
<i>DEL61</i>		AF336279	1875	our lab	
<i>TTG1</i>		AF530907	1032	our lab	[74]
<i>TTG2</i>		AF530909	1041	our lab	
<i>TTG3</i>		AF530911	1038	our lab	
<i>TTG4</i>		AF530912	1041	our lab	
Petunia (<i>P.hybrida</i> n=7)					
<i>AN2</i>		AAF66727	765	Ronald Koes	[44, 48, 49]
<i>AN4</i>		EB175066	768	Ronald Koes	
<i>PH4</i>		AY973324	843	Ronald Koes	
<i>AN1</i>		AF020543	2007	Ronald Koes	[46, 47]
<i>JAF13</i>		AF260918	1884	Ronald Koes	[45]
<i>AN11</i>		U94748	1014	Ronald Koes	[51]
Maize (<i>Z.mays</i> n=10)					
<i>C1</i>		AY237128	822	GRASSIUS	[41, 43, 88, 89]
<i>PL</i>		AAA19821	819	GRASSIUS	
<i>P1</i>		AY702552	1005	GRASSIUS	
<i>R(Lc)</i>		M26227	1830	GRASSIUS	[40, 165]
<i>R(S)</i>		X57276	1671	our lab	[166]
<i>B</i>		M26227	1848	GRASSIUS	[39, 167]
<i>PAC1</i>		AY115485	1059	GRASSIUS	[42]
<i>MP1</i>		AY339884	1251	our lab	

In a first step, we confirmed the network model of MBW proteins in Arabis and cotton, respectively (Figure 2.3A and C, Figure S1, Table S2 and S3). Like in Arabidopsis, a single copy of AaTTG1 in Arabis was able to interact with 4 bHLH proteins which was potentially involved in five TTG1-dependent traits, although the regulatory mechanism was not fully understood (Figure 2.3A and Table S2) [57].

There were four copies of WD40 proteins in cotton (i.e. GhTTG1, GhTTG2, GhTTG3 and GhTTG4), but only GhTTG1 and GhTTG3 could interact with bHLH proteins, which was consistent with the fact that only GhTTG1 and GhTTG3 function in seed fiber development (Figure 2.3C) [74].

As a second step, quantitative analyses of inter-relation were carried out. In Arabis, the results revealed a suppression of AaTTG1-AaGL3 and AaTTG1-AaEGL3 interaction by AaGL1, AaWER or AaMYB23 suggested alternative complex formation,

however, a putative anthocyanin-specific R2R3MYB3 (i.e. AaPAPL) promoted their interaction suggesting a synergetic trimer or multimer formation. Similar with those in *Arabidopsis*, the combination of AaTTG1-AaMYC1 showed antagonistic exclusive inter-relation with any R2R3MYB here, whereas the combination of AaTTG1-AaTT8 showed synergetic exclusive inter-relation (Figure 2.3B). As shown in Figure 2.3D, two fiber (seed trichome)-specific R2R3MYBs (i.e. GhMYB2 and GhMYB25) dramatically counteracted the interaction of GhTTG1-GhDEL65 as well as GhTTG1-GhDEL61, while the anthocyanin-specific GhRLC1 did not.

These results demonstrated that alternative complex formation was a common behavior of MBW components those were involved in regulating trichome development in rosids.

(A)

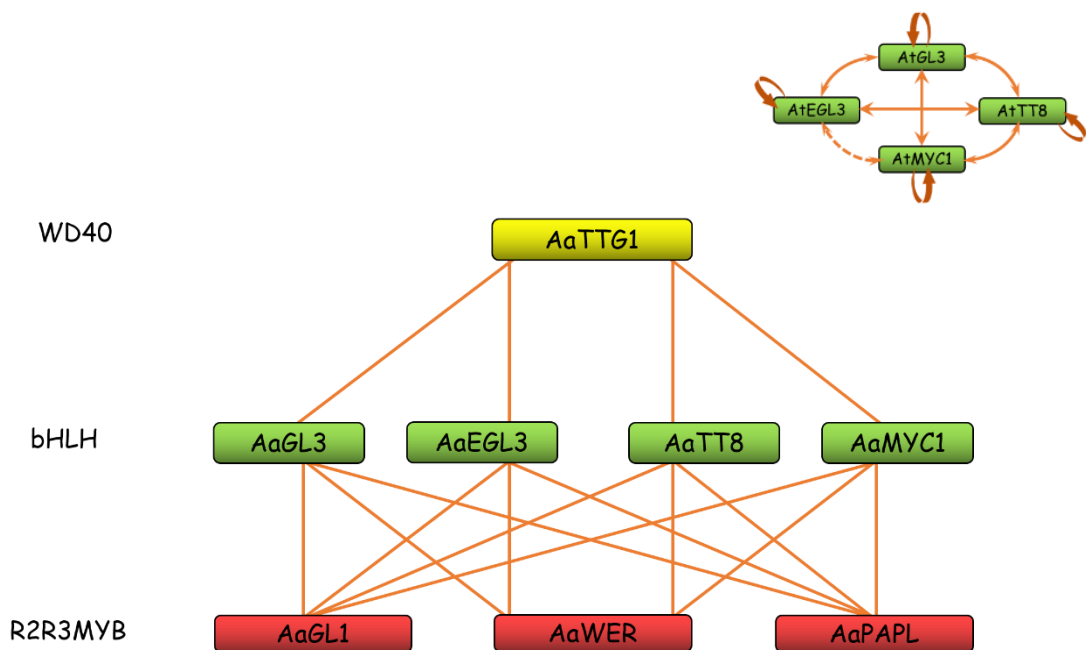
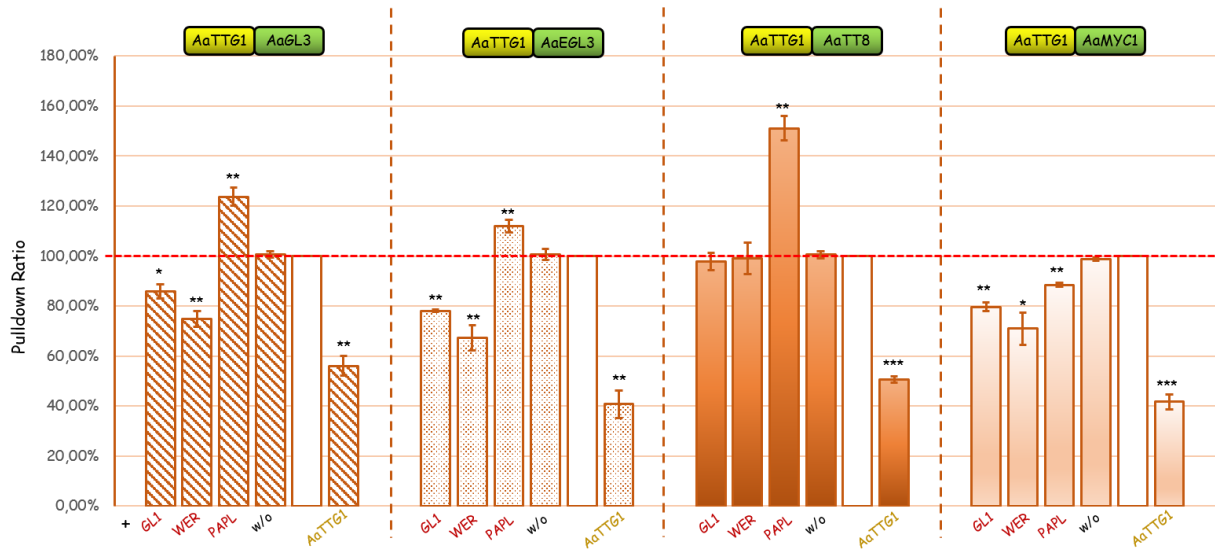
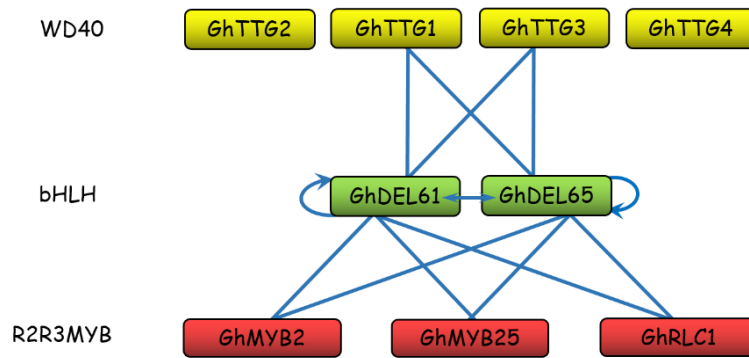


Figure 2.3 Inter-relation of MBW proteins in other rosids: *Arabis alpina* (Aa) and *Gossypium hirsutum* (Gh).

(B)



(C)



(D)

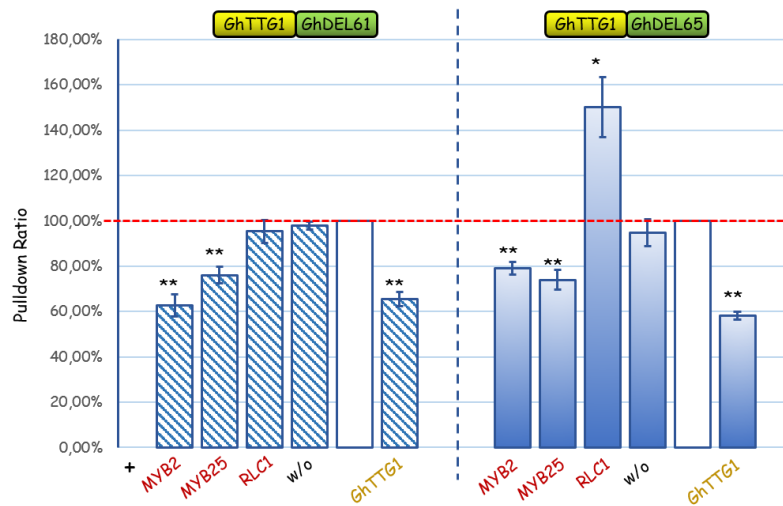


Figure 2.3 Cont. Inter-relation of MBW proteins in other rosids: *Arabis alpina* (Aa) and *Gossypium hirsutum* (Gh).

(A) A comprehensive network model of MBW proteins in *Arabis alpina* demonstrated by yeast two hybrids and pairwise LUMIER pulldown assays. It shows all MBW components identified up-to-date that potentially function in five TTG1-dependent traits.

(B) The effect of four putative R2R3MYBs in *Arabis alpina* on the interaction between AaTTG1 (WD40) and 4 bHLH homologs, respectively. Triple LUMIER pulldown assays are used to quantify relative pulldown efficiency (pulldown ratio) of Renilla Luciferase fused AaTTG1 and ProtA fused bHLHs in the presence of YFP tagged R2R3MYB factors.

(C) A comprehensive reticulated network model of MBW proteins in *Gossypium hirsutum* demonstrated by yeast two hybrids and pairwise LUMIER pulldown assays. MBW components presented here are able to regulate seed hair formation (specified by MYB2 and MYB25) or anthocyanin biosynthesis (specified by RLC1) potentially.

(D) The effect of three R2R3MYBs in *Gossypium hirsutum* on the interaction between GhTTG1 (WD40) and 2 bHLH homologs, respectively. Triple LUMIER pulldown assays are used to quantify relative pulldown efficiency (pulldown ratio) of Renilla Luciferase fused GhTTG1 and ProtA fused bHLHs in the presence of YFP tagged R2R3MYB factors.

(A) and (C) Any positive interaction is indicated by a full line (*Arabis alpina* in tangerine; *Gossypium hirsutum* in turquoise). Homo- and hetero-dimerization of bHLHs are depicted by arrow lines. Dash lines indicate weak interaction.

(B) and (D) Each value represents mean \pm standard errors (n = 3 biological replicates). *** indicates that pulldown ratio is extremely significant different from that of the reference (hollow column) by Student's t test ($0.0001 \leq P < 0.001$); ** indicates very significant difference ($0.001 \leq P < 0.01$); * indicates significant difference ($0.01 \leq P < 0.05$).

2.3.3 Stereochemistry of MBW proteins in asterids and monocots.

It is widely known that MBW complexes in asterids and monocots are only able to regulate flavonoid pigmentation rather than trichome development. If indeed two alternative dimers are a common stereochemistry of MBW proteins in rosids, the question arises how they behave in asterids and monocots. Towards this end we studied inter-relation of MBW proteins in petunia (*Petunia hybrida*, representative for asterid) and maize (*Zea mays*, a representative for monocot), respectively.

When we determined the pairwise interactions in our hands as a basis for the three protein interaction assays, some contradictions were found: homodimerisation of AN1 was *de novo* verified by yeast two-hybrid and pairwise LUMIER assay [47, 146] (Figure 2.4A, Table S4, and Figure S1B); however we could not confirm the interaction between B and R2R3MYBs in maize, for which reason we excluded B from three protein interaction assays [39, 43] (Figure 2.4C).

As expected, no counteraction was observed in all combinations of AN11/AN1/MYBs (Figure 2.4B). Likewise, the interaction between PAC1 and R remained unchanged by adding C1 or even increased by adding PL (Figure 2.4D). These results suggested a synergetic inter-relation.

Interestingly, AN11-JAF13 interaction was strongly reduced in the presence of any R2R3MYB proteins (AN2, AN4 or PH4), indicating antagonistic inter-relation of AN11-JAF13/MYBs. JAF13 is functionally and evolutionary distinct from AN1 and R. Ectopic JAF13 expression induces anthocyanin accumulation in tissues that are already slightly pigmented, but does not alter the pattern of pigmentation; however, no loss-of-function mutants are known for *jaf13* in petunia [45-47, 146]. In our work (Chapter III), overexpression of JAF13 in *gl3egl3tt8* could reduce N-file root hair which implied JAF13 is functionally similar with AtMYC1 other than AN1 (Figure 3.2B).

Taking into account all of these results, we made the assumption that the functional and evolutionary divergence of bHLH proteins might determine different inter-relation of MBW components.

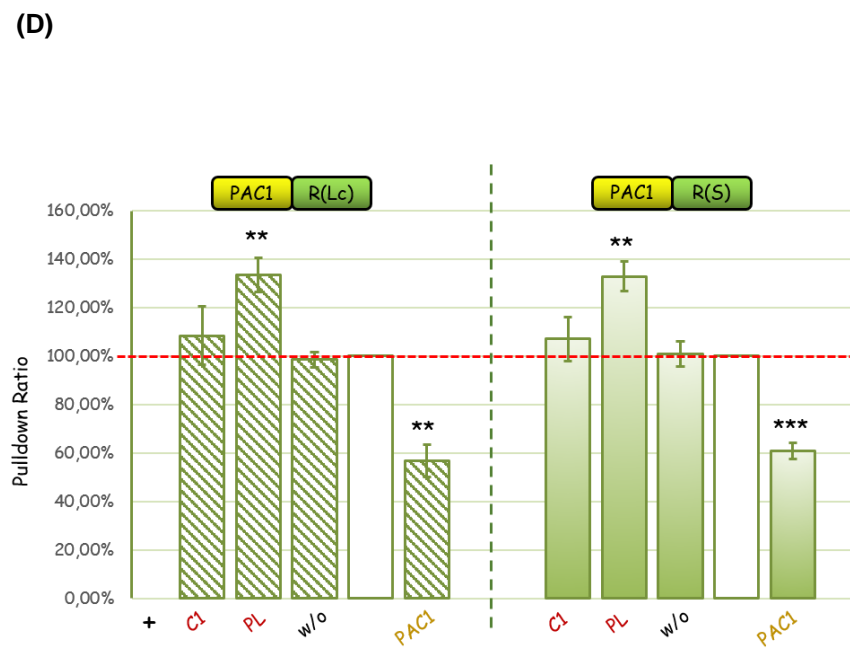
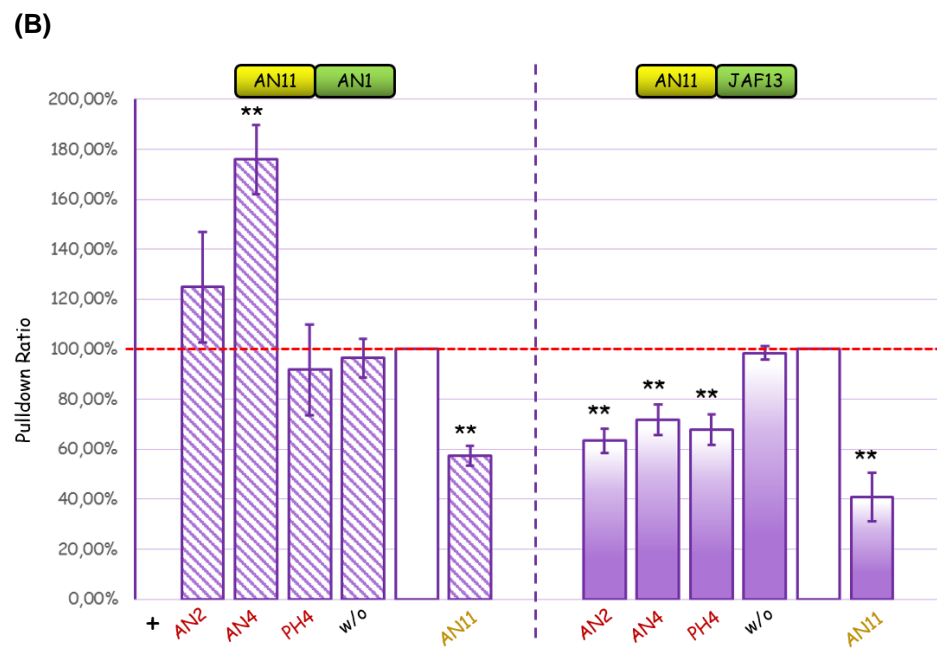
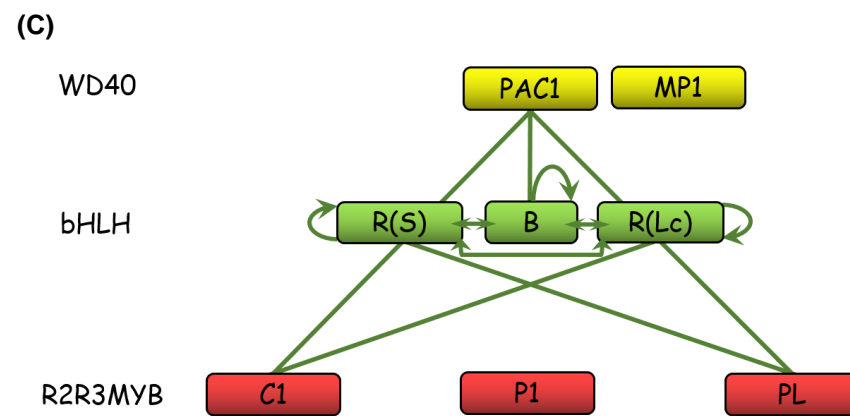
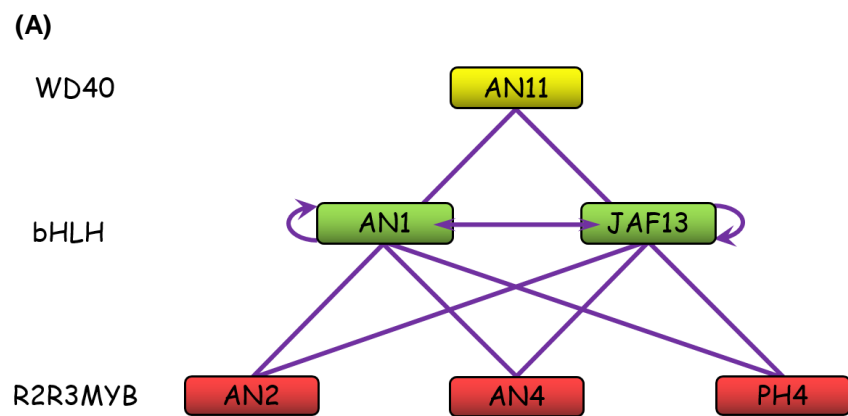


Figure 2.4 Inter-relation of MBW proteins in asterid and monocot: *Petunia hybrida* (Ph) and *Zea mays* (Zm).

(A) A comprehensive network model of MBW proteins in *Petunia hybrida* demonstrated by yeast two hybrids and pairwise LUMIER pulldown assays.

(B) The effect of 3 different R2R3MYBs on the interaction between AN11 (WD40) and 2 bHLHs, respectively. Triple LUMIER pulldown assays are used to quantify relative pulldown efficiency (pulldown ratio) of Renilla Luciferase fused AN11 and ProtA fused bHLHs in the presence of YFP tagged R2R3MYB factors. The pulldown ratio is normalized to the combination AN11 and bHLHs without additional R2R3MYB proteins (hollow column). As a negative control, YFP only protein without any other CDS is also included (w/o), meanwhile YFP tagged AN11 is antagonistic-positive control. Each value represents mean \pm standard errors ($n = 3$ biological replicates). *** indicates that pulldown ratio is extremely significant different from that of the reference (hollow column) by Student's t test ($0.0001 \leq P < 0.001$); ** indicates very significant difference ($0.001 \leq P < 0.01$); * indicates significant difference ($0.01 \leq P < 0.05$).

(C) A comprehensive network model of MBW proteins in *Zea mays* demonstrated by yeast two hybrids and pairwise LUMIER pulldown assays.

(D) The effect of C1 and PL on the interaction between PAC1 (WD40) and R (bHLH), respectively. Triple LUMIER pulldown assays are used to quantify relative pulldown efficiency (pulldown ratio) of Renilla Luciferase fused PAC1 and ProtA fused bHLHs in the presence of YFP tagged R2R3MYB factors. The pulldown ratio is normalized to the combination PAC1 and bHLHs without additional R2R3MYB proteins (hollow column). As a negative control, YFP only protein without any other CDS is also included (w/o), meanwhile YFP tagged PAC1 is antagonistic-positive control. Each value represents mean \pm standard errors ($n = 3$ biological replicates). *** indicates that pulldown ratio is extremely significant different from that of the reference (hollow column) by Student's t test ($0.0001 \leq P < 0.001$); ** indicates very significant difference ($0.001 \leq P < 0.01$); * indicates significant difference ($0.01 \leq P < 0.05$).

2.3.4 Proximity in bHLHs phylogenetic tree is perfectly accordant with their protein behavior similarity.

Given that bHLH proteins play a bridging role in MBW complex formation, it is conceivable that bHLHs proteins are the overriding factor to determine the stereochemistry of MBW complexes. In order to confirm whether the diversification of MBW components inter-relations could be categorized by evolutionary divergence of bHLH proteins, we generated a phylogenetic tree based on full protein sequences of bHLH proteins included in this work. As shown in Figure 2.5, two main clades (i.e. blue and orange) were classified by phylogenetic proximity of bHLH proteins.

Intriguingly, these two clades coincided with inter-relations of the corresponding MBW components: MBW combinations with bHLH proteins in orange clade behaved synergetically in their own species, while those with bHLH proteins in blue clade behave antagonistic inter-relation. It was worth to mention that a subclade containing GhDEL65, GhDEL61, AtGL3, AaGL3, AtEGL3 and AaEGL3 was also a partially synergetic clade in the context of combinations with anthocyanin-specific R2R3MYBs, suggesting that synergetic inter-relation might be indispensable for MBW complexes regulating in anthocyanin biosynthesis pathway.

We also predicted some important amino acids in bHLHs, which might feature their protein behavior by sequence alignment (Figure 2.6).

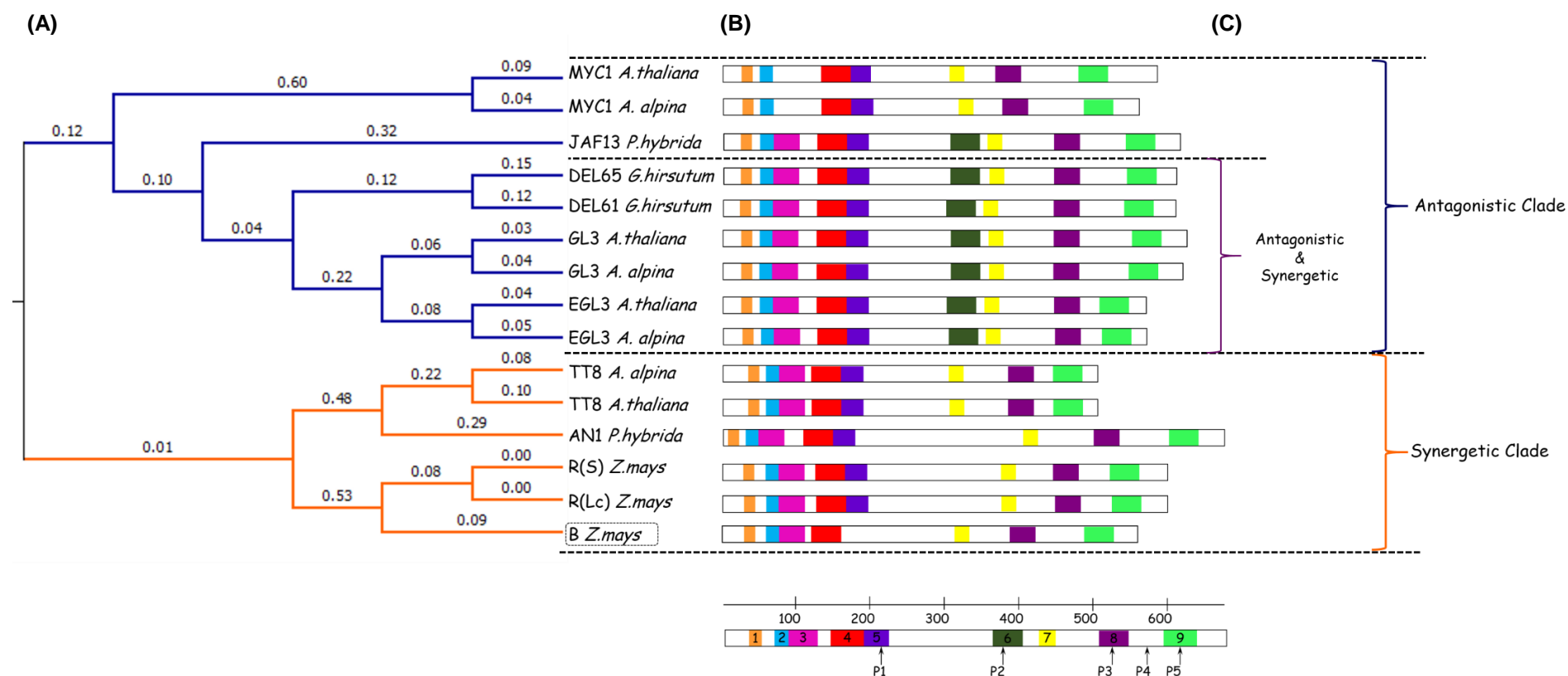


Figure 2.5 Molecular phylogenetic analysis of bHLH proteins.

(A) The phylogenetic trees were constructed using aligned full length of the bHLH proteins. The evolutionary history was inferred by using the Maximum Likelihood method based on the JTT matrix-based model [168]. Evolutionary analyses were conducted in MEGA6 [169].

(B) MEME analysis of bHLH proteins motifs [<http://alternate.meme-suite.org>] [170]. The motifs, numbered 1–9, are depicted as different colored boxes. The sequence information for each motif is provided in Figure S2. Motifs 8 correspond to the bHLH domain. P1 to P5 underlying arrows indicated predicted vital positions in bHLH proteins motifs.

(C) Protein behaviors classification. Block in dotted line indicated protein behavior to be confirmed.

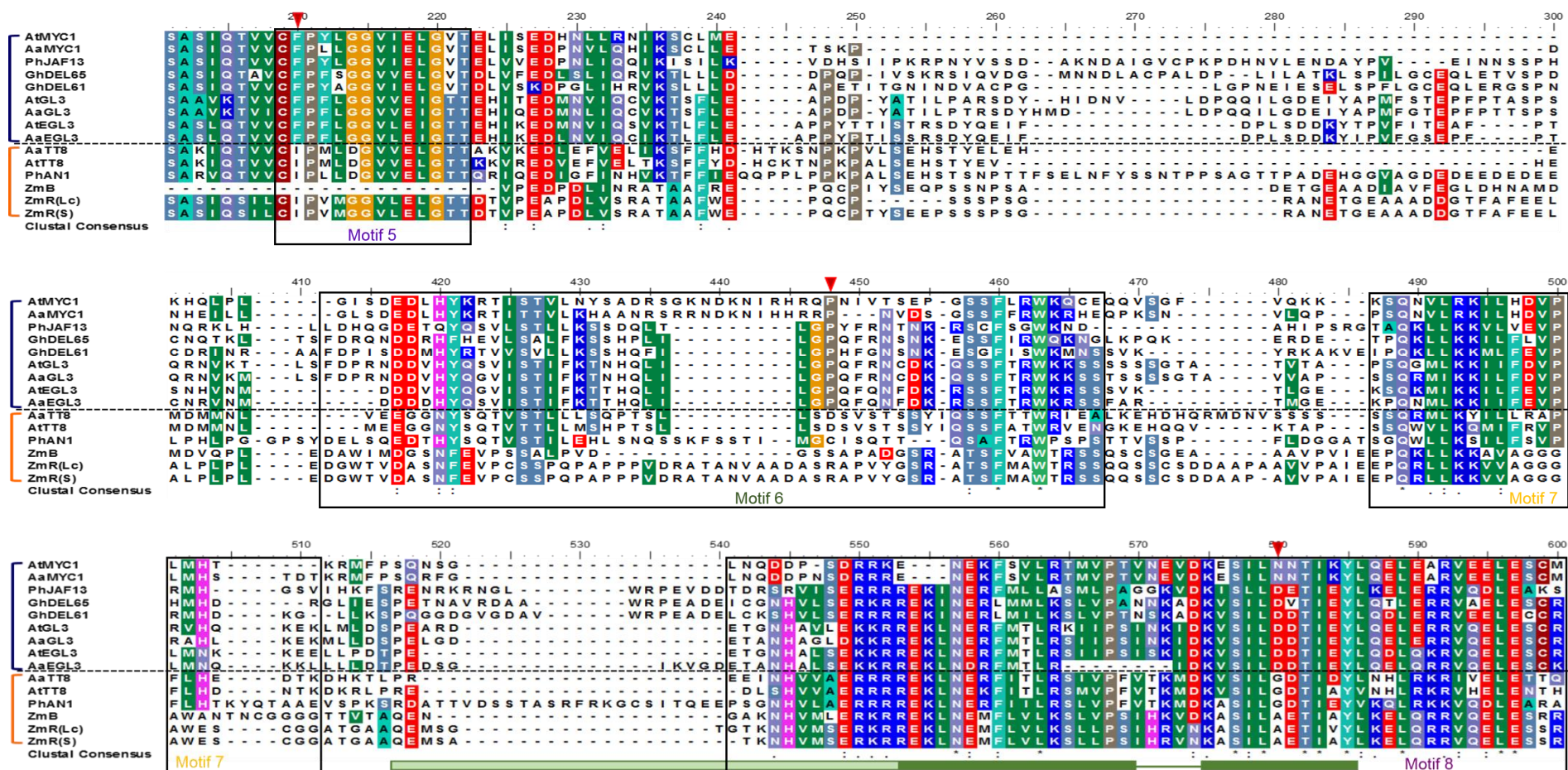


Figure 2.6 Amino acids in bHLHs might feature bHLHs behavior.

Sequence alignment of bHLH proteins from five different plant species. Red triangles indicate vital positions in amino acids that might determine protein behavior difference between antagonistic clade (in dark blue bracket) and synergetic clade (in orange bracket).

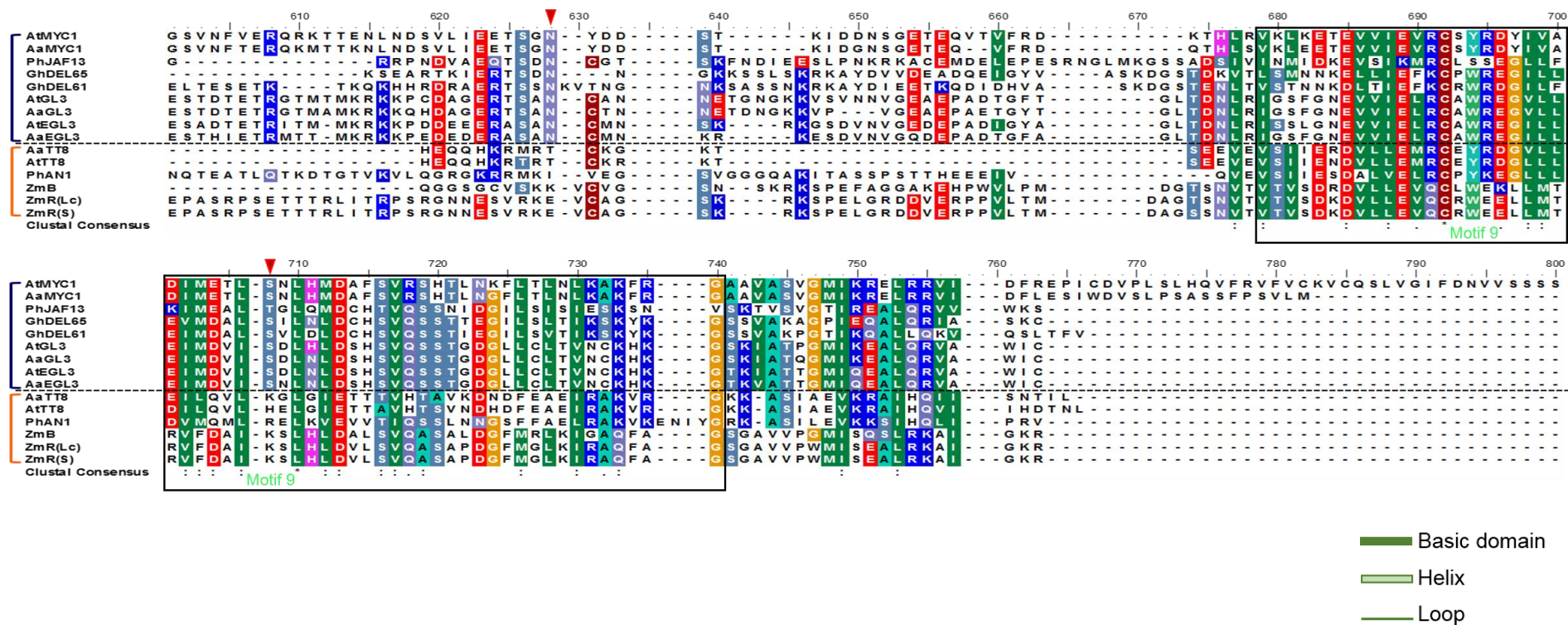


Figure 2.6 Cont. Amino acids in bHLHs might feature bHLHs behavior.

Sequence alignment of bHLH proteins from five different plant species. Red triangles indicate vital positions in amino acids that might determine protein behavior difference between antagonistic clade (in dark blue bracket) and synergetic clade (in orange bracket).

2.4 Discussion

To date, studies show that throughout the plant kingdom flavonoid biosynthesis pathway is regulated by certain MBW (R2R3MYB-bHLH-WD40) complexes [87]. In this study, we examined in more detail the regulatory network that surrounds core MBW protein complexes, in particular with regard to stereochemistry of MBW components in different plant species. This has enabled an integrated MBW regulatory model to be developed and comparison of the data for rosids to asterid, as well as eudicot to monocot.

2.4.1 Alternative dimer formation among MBW components is not an occasional phenomenon but bearing certain evolutionary implications in plants

Previous studies in our lab revealed a new stereochemistry of MBW proteins in *Arabidopsis*, which refreshed the classic view of trimeric MBW complexes, i.e. in the context of trichome patterning alternative dimers were formed: GL1-GL3 and GL3-TTG1 [149]. The formation of each dimer could be counteracted by the third protein (e.g. TTG1 counteracts the formation of GL1-GL3 dimer, and *vice versa*). Here, we define such competitive behavior among MBW components as the antagonistic inter-relation. Correspondingly, non-competitive behavior is the synergetic inter-relation. As a typical representative in rosids, *Arabidopsis* recruits both synergetic and antagonistic models in the inter-relation of MBW components which correlates with their functional diversification in terms of 5 AtTTG1-dependent traits (Figure 2.2). As expected, similar phenomena were also observed in other rosids: *Arabis* (*A. alpina*) and cotton (*G. hirsutum*) (Figure 2.3).

Duplication of MBW gene cassettes and subsequent divergence of rosids and asterids were deemed the driving force to evolve a new role of MBW complexes in rosids trichome development [81]. Therefore, we explored inter-relations of MBW components in asterid and monocot as comparison. For a strong knowledge base for the flavonoid-related MBW protein complexes in *petunia* (*P. hybrida*) and *maize* (*Z. mays*), we selected them as representative model species in asterid and monocot, respectively. Based on the results for combinations of PhAN1 and ZmR, synergetic inter-relation only is present in their own species. However, PhJAF13 combinations showed strongly antagonistic inter-relation of AN11/JAF13/MYBs (Figure 2.4B) which acts in a AtMYC1 or AaMYC1-like manner (Figure 2.2B and Figure 2.3B).

These observations indicate the inter-relation of MBW components differing from one combination to another is not in accordance with species divergence of asterid and rosid, nor eudicot and monocot.

By establishing a phylogenetic tree of bHLH proteins, we revealed a general rule behind distinct inter-relations of MBW components. Two main clades classified by phylogenetic proximity of bHLH proteins are coincided with inter-relations of the corresponding MBW components, which suggests the evolutionary relevance of alternative dimers.

2.4.2 MBW protein complexes regulating flavonoid biosynthesis tend to behave with synergetic inter-relation, while those regulating trichome development are antagonistic-bias.

MBW complexes determine the spatiotemporal expression of flavonoid biosynthesis target genes that account for tissue-specific accumulation of flavonoids. Some MBW complexes from monocots can control the expression of enzymes of the entire pathway, while others specifically control late flavonoid biosynthesis genes in eudicots [171]. Nevertheless, the bHLH interaction motif ([DE]Lx₂[RK]x₃Lx₆Lx₃R) found in R2R3-MYB members of MBW complexes is highly conserved among higher plant species [172], suggesting that at least MYB and bHLH interactions arose early during the event of land plant evolution.

AtTT8/AtPAP (anthocyanin-specific) and AtTT8/AtTT2 (proanthocyanidin-specific) are well-known predominant flavonoid biosynthesis regulators in *Arabidopsis* [31, 66, 103, 104, 108, 143, 173], moreover, AtGL3/AtPAP and AtEGL3/AtPAP have minor effects on the anthocyanin biosynthetic pathway [66, 109]. All these MBW complexes above behave synergetically within their respective components (Figure 2.2B). Likewise, in *Arabis* and cotton, the inter-relation of MBW components potentially involved in the flavonoid biosynthetic pathway are synergetic as well, although their function *in vivo* are still not well characterized (Figure 2.3). Such correlation is also supported by data in maize and petunia (Figure 2.4). Interestingly, antagonistic-exclusive inter-relation among PhJAF13 combinations may explain why no loss-of-function mutants are known for *jaf13* in petunia (i.g. JAF13 does not compensate for the loss of AN1, as *an1* mutants completely lack anthocyanins despite expressing JAF13) [45-47, 146].

In rosids, besides regulation of the flavonoid biosynthesis pathway, combinatorial MBW complexes evolved several extra functions: for instance, leaf trichome and root

hair (broad term of trichome) patterning specified by AtGL1 and AtWER, respectively, with its bHLH partners: AtGL3, AtEGL3 or AtMYC1 in *Arabidopsis* [29, 65-71]; And their orthologs (AaGL3, AaEGL3 and AaMYC1 with combinations of AaGL1 or AaWER) in *Arabis* are thought to regulate trichome development in *Arabis* despite being devoid of loss-of-function mutants [57]; Seed hair (broad term of trichome) formation in cotton is also under the control of GhDEL61/65 and their R2R3MYBs partners (e.g. well-investigated GhMYB2 and GhMYB25) [73, 74, 76, 151, 160, 161, 164]. Interestingly, our data shows that all of these MBW complexes behave with antagonistic inter-relation. These observations imply that a new regulatory MBW module has been adapted for controlling specific epidermal cell fates in rosids.

Alltogether, MBW protein complexes regulating flavonoid biosynthesis tend to behave with synergetic inter-relation as an ancient stereochemistry, while those regulating trichome development are antagonistic-bias as a modern stereochemistry. Additionally, higher ordered complexes are possible to work as compatible structures between them due to homodimerization or heterodimerization of bHLH proteins (Figure 2.7)

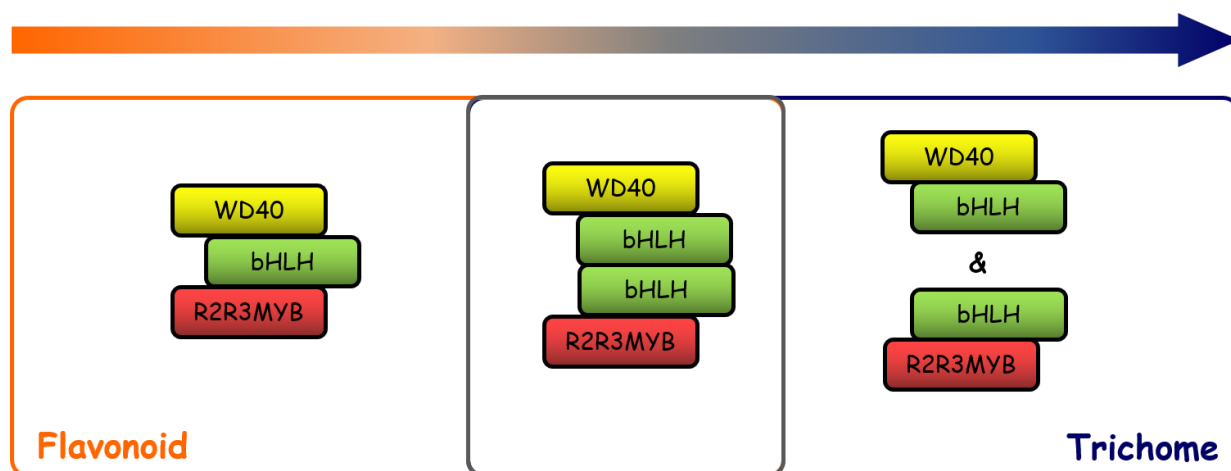


Figure 2.7 Potential evolutionary model for stereochemistry of MBW proteins in the context of traits regulation.

CHAPTER III

**EVOLUTIONARY ANALYSIS OF MBW
FUNCTION BY PHENOTYPIC RESCUE IN**
Arabidopsis thaliana

3. Evolutionary analysis of MBW function by phenotypic rescue in *Arabidopsis thaliana*

3.1 Summary

In *Arabidopsis*, the WD40 repeat protein is represented by the single copy gene *TTG1* comprising MBW complexes, which have been implicated in five epidermal cell traits: anthocyanin and proanthocyanidin biosynthesis, seed coat mucilage production, trichome and root hair patterning. These are so called *TTG1*-dependent traits. MBW genes which control trichome and root hair patterning traits are assumed to evolve from the duplication and diversification of flavonoid controlling genes, therefore trichome and root hair traits are considered as evolutionary current inventions. However, the exact evolving order of these traits still remains to be confirmed. To better define functional divergence of the MBW proteins in the five *TTG1*-dependent traits, and then come to address functional relevance of diverse stereochemistry of MBW complexes in term of *TTG1*-dependent traits, we performed inter-species complementary assays with MBW homologs in *Arabidopsis* mutants.

3.2 Introduction

Arabidopsis flowers are naturally colorless but flavonoid-based pigments are produced in the seed coat (testa), giving *Arabidopsis* seeds particular brown color. Hence the identification of pigment mutants in *Arabidopsis* has primarily focused on convenient screens for yellow (no pigment) or light colored (reduced pigment) seed, otherwise known as *transparent testa (tt)* mutants [105, 174]. However, the seed coat pigments are not anthocyanins but a related pigment known as proanthocyanidins (PAs) produced in a branch of the flavonoid pathway (Figure 3.1). Although PA and anthocyanin biosynthesis share many steps of the flavonoid pathway, there are specific genes (both structural and regulatory) dedicated to the production of PAs. Conversely, the nature of *tt* screens did not allow for the isolation of anthocyanin-specific mutants. However, the developmental profiles of anthocyanin pigment production and structural gene expression in young *Arabidopsis* seedlings have been well characterized [175].

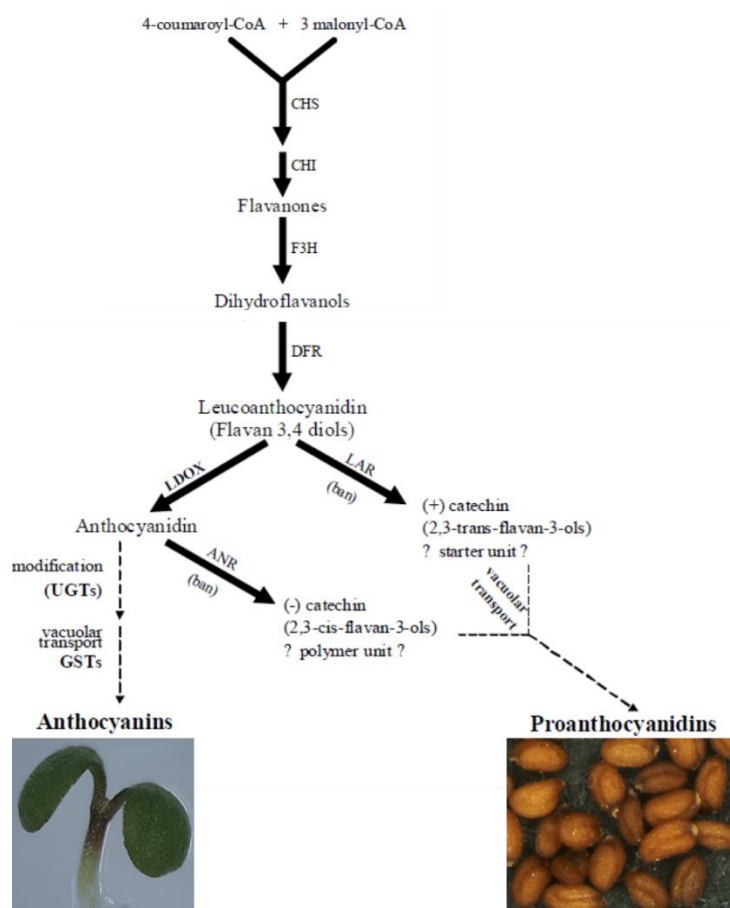


Figure 3.1 The flavonoid pigment biosynthetic pathway in Arabidopsis.

(Adapted from [87, 147])

The first of the transparent testa mutants identified was *transparent testa glabra1 (ttg1)* [105]. This mutant had pleiotropic phenotypes. Not only are *ttg1* seeds and plants devoid of all flavonoid-based pigments (PAs and anthocyanins), they also show a range of developmental defects: a lack of the trichome; a loss of cell patterning in the root epidermis resulting in the over-production of root hair cells in N-files; and undifferentiated cells of the epidermal layer of the seed coat resulting in a lack of seed coat mucilage normally produced by the testa epidermis during seed development. This immediately suggested a regulatory role for the *TTG1* locus in the development of several widespread and seemingly unrelated characteristics linked only by their epidermal origin (Fig 1.3). Eventually, a chromosome walk to *TTG1* locus was shown to encode a WD40 protein [28].

The *tt* mutant screen approach described above yielded in a pair of *TTG1*-dependent regulators, *TT8* and *TT2* [102, 173]. *TT8* and *TT2* encode a bHLH and R2R3MYB protein, respectively, that together regulate specifically the biosynthesis of PA pigments in Arabidopsis seed coat. *tt8* and *tt2* mutants show no other *ttg1*-like mutant

phenotypes, even showing normal expression of anthocyanins in young seedlings where anthocyanins are developmentally produced and TT8 is also expressed. This suggested the existence of more TTG1-dependent Myb and bHLH *Arabidopsis* proteins controlling the various co-regulated epidermal pathways originally defined by the *ttg1* mutant. Meanwhile, another pair of R2R3MYB-bHLH regulator GL1-GL3 was found during isolation of the reduced trichome mutant *glabra3 (gl3)* and was *glabra1 (gl1)* [29]. However neither *gl1* nor *gl3* mutants were pleiotropic like *ttg1* mutants. This again strongly hinted other TTG1-dependent R2R3MYB and bHLH proteins in *Arabidopsis*.

The genetic identification of *enhancer of glabra3 (EGL3)* gave rise to another pleiotropic mutant *gl3 egl3* that exhibited glabrous leave and differentiated root hairs in all cell files, as does *ttg1*. In addition, a clear-cut qualitative anthocyanin deficit and less mucilage were also found in *gl3 egl3* double mutant through quantitatively weaker than *ttg1*. Later, the *gl3 egl3 tt8* triple mutant, which is essentially phenotypically indistinguishable from the most severe *ttg1* mutations, were produced as well [66].

Recently, Squamosa Promoter Binding Protein-Like (SPLs) are reported to potentially rearrange the MBW complex, attenuating its transcriptional activity to control trichome distribution. Elevated SPL4/5 levels recruit TTG1, and therefore interfere with the stability of the MBW complex, mimicking the *ttg1*-like trichome disorder [176].

In this work, we performed cross-species rescue assays in order to reveal correlations between MBW proteins' behavior and functions involved in the control of epidermal cell fates.

3.3 Results

3.3.1 *AtTTG1* orthologs functionally substitute *AtTTG1* in term of all 5 traits

The discovery of the Arabidopsis *ttg1* mutant provided an unique platform for the study of how TTG1 homologs functionally diverge in terms of five TTG1-dependent traits. It was of particular interest, whether the TTG1 like WD40 proteins from other plant species could complement not only *ttg1* defects in anthocyanin production, but other *ttg1* defects as well. An overexpression vector, referred to as 35S-*WD40*, which included full length of CDS, was transformed into one severe *ttg1* allele, named *ttg1-1* [28, 105]. As a positive control, endogenous *AtTTG1* was also cloned and transformed in parallel. (Figure 3.2B).

To determine if the 35S-*WD40* transgene complements the *ttg1* defect in 5 traits individually, we focused on various observations as follows (Figure 3.2A):

- a) Trichome: All primary transformant (T1 progeny) seedlings were screened for trichomes on true leaves regardless of number and patterning.
- b) Root hair: N-file hairs were counted with 1-week-old basta-resistant T2 seedlings (root phenotypes associated with *ttg1* mutants are difficult to score, therefore were not examined rigorously).
- c) Anthocyanin: 4 DAG T2 progeny germinated on MS with 3% sugar were examined in the hypocotyl.
- d) In view of the seed phenotypes were maternally derived, we examined T2 seeds for both proanthocyanidin and mucilage observations regardless segregation.

As shown in figure 3.2B, except for *GhTTG2*, *GhTTG4* and *ZmMP1*, these WD40 genes were functional homologues to the Arabidopsis thaliana *TTG1* gene. The results presented here were congruent with previous research on maize and cotton *TTG1* homologs [52, 74]. Lastly, in rescued lines, when anthocyanin phenotype was complemented, all phenotypes were complemented.

3.3.2 *bHLHs* have overlapping but differential regulatory capabilities in limitative traits

As the *gl3 egf3 tt8* triple mutant essentially phenocopied *ttg1*, we produced the *gl3 egf3 tt8* triple mutant in *Col* background by crossing. All 35S-*bHLH* (CDS) overexpression

constructs were transformed into triple mutants. Complementary analyses were carried out as described above.

All of bHLHs genes here were able to suppress the mucilage defect of *gl3 egl3 tt8*, except for *AtGL3* and *ZmB*. Our evidence reconfirmed *AtGL3* played no role in mucilage production (Figure 3.2B) [66].

Out of our expectation, none of these bHLHs overexpression lines rescued transparent testa (i.e. yellow seed coat) of the *gl3 egl3 tt8* triple mutant (Figure 3.2B) although 1 out of 20 *ZmR(Lc)* overexpression lines produced light brown seeds (Data not shown). In view of promoter effect, 35S was swapped for the *AtTT8* promoter (*proTT8*). Nevertheless, no bHLH gene could confer any brown seeds (Data not shown). Interestingly, after constructs were transformed into *tt8* single mutant rather than *gl3 egl3 tt8* triple mutant, we observed *AtTT8*, *AaTT8*, *PhAN1* and *ZmR* fairly rescued seed coat color while *proTT8-AtEGL3* lines had light brown seeds (Figure 3.2C). It suggested seed coat color rescue was *AtGL3* and/or *AtEGL3* dependent to some extent through unclear ways.

Among the bHLHs tested, *PhJAF13* and *ZmB* did not rescued anthocyanin biosynthesis in the Arabidopsis triple mutant (Figure 3.2B). These results were incompatible with the function of these genes in their own species [45, 167]. Furthermore, we first discovered *GhDEL61/65* were able to suppress the anthocyanin defect in the Arabidopsis mutant. B-Peru can substitute for R function in the seed, and only one functional allele at either locus is required for pigment synthesis [39, 167]. bHLHs (CDS) overexpression trichome phenotype was easy to be characterized: substantial trichomes were found in *AtGL3*, *AtEGL3*, *AaGL3*, *AaEGL3* and *ZmR* overexpressed T1 seedlings from the first true leaf although their trichome patterning were irregular from wild type (Figure 3.2B and 3.3A).

AtMYC1 is a quantitative trait gene for trichome density, when trichome is already initiated [70]. The genomic sequence of *DEL61* or *DEL65* driven by promoter *AtGL3* could complement trichome production in Arabidopsis *gl3 egl3* double mutant [76, 151]. It implied these bHLHs might be under spatio- and temporal control by their virtual promoters and introns.

Although we did not carry out intensive quantification of root hair production, all bHLHs which rescued the trichome phenotype were also able to significantly suppress root hair differentiation with varying levels in N files, but not fully suppress as wild type. In addition, *AtMYC1*, *AaMYC1*, *GhDEL61* and *GhDEL65* overexpression lines showed

partial loss of N file hairs as well. To our surprise, PhJAF13 which is involved in anthocyanin biosynthesis in petunia did rescue the root hair phenotype moderately in Arabidopsis (Figure 3.2B and 3.3B)

3.3.3 *R2R3MYBs* specifically rescue *gl1* or *pap1pap2* for one trait

In view of the fact that *ttg1* phenocopied multiple *R2R3MYBs* mutant has not been available now, we just picked trichome and anthocyanin traits for phenotypic analysis of *R2R3MYB* homologs (trichome trait is considered as a recent evolutionary invention while anthocyanin is an ancient trait in plants [81]).

The specificity for these TTG1-dependent traits is ultimately bound to *R2R3MYBs*. *gl1* and *pap* mutations only affect trichome and anthocyanin, respectively, although phenotypes are not completely defective due to some partially redundant paralogous *R2R3MYBs*. For instance, minor trichomes are still visible on leaf margins in *gl1* mutants and faint anthocyanin can be detected in *pap1 pap2* mutants.

AaGL1, which has high sequence similarity to AtGL1, also exhibited function in trichome production in Arabidopsis. GhMYB2 and GhMYB25 were two *R2R3MYB* genes encoding cotton seed hair regulators, however, GhMYB25 could not rescue trichome phenotype of *gl1* mutant. GhMYB3 was homologous to GhMYB2 and rescued trichomes as GhMYB2 (Figure 3.2B). It was worthwhile to note that trichomes with irregular patternings were initiated from 3rd and 4th leaves other than 1st and 2nd in AtGL1, AaGL1, GhMYB2 or GhMYB3 overexpression lines (Figure 3.3D). Interestingly, denser trichomes were observed on leaf margins from 5th leaf in either AtTT2 or ZmPL overexpression lines suggesting these two *R2R3MYBs* might effect trichome phenotypes through some unknown bypasses (Figure 3.3D).

Anthocyanin was not visible in *pap1 pap2* double mutants, while AaPAPL, PhAN2, PhAN4 and PhPH4 restored anthocyanin biosynthesis defect of *pap1pap2* at a comparable level with AtPAP (Figure 3.2B). Moreover, GhRLC1, ZmC1, ZmPL and ZmP1 overexpression lines showed substantial anthocyanin at relatively lower levels (Data not shown).

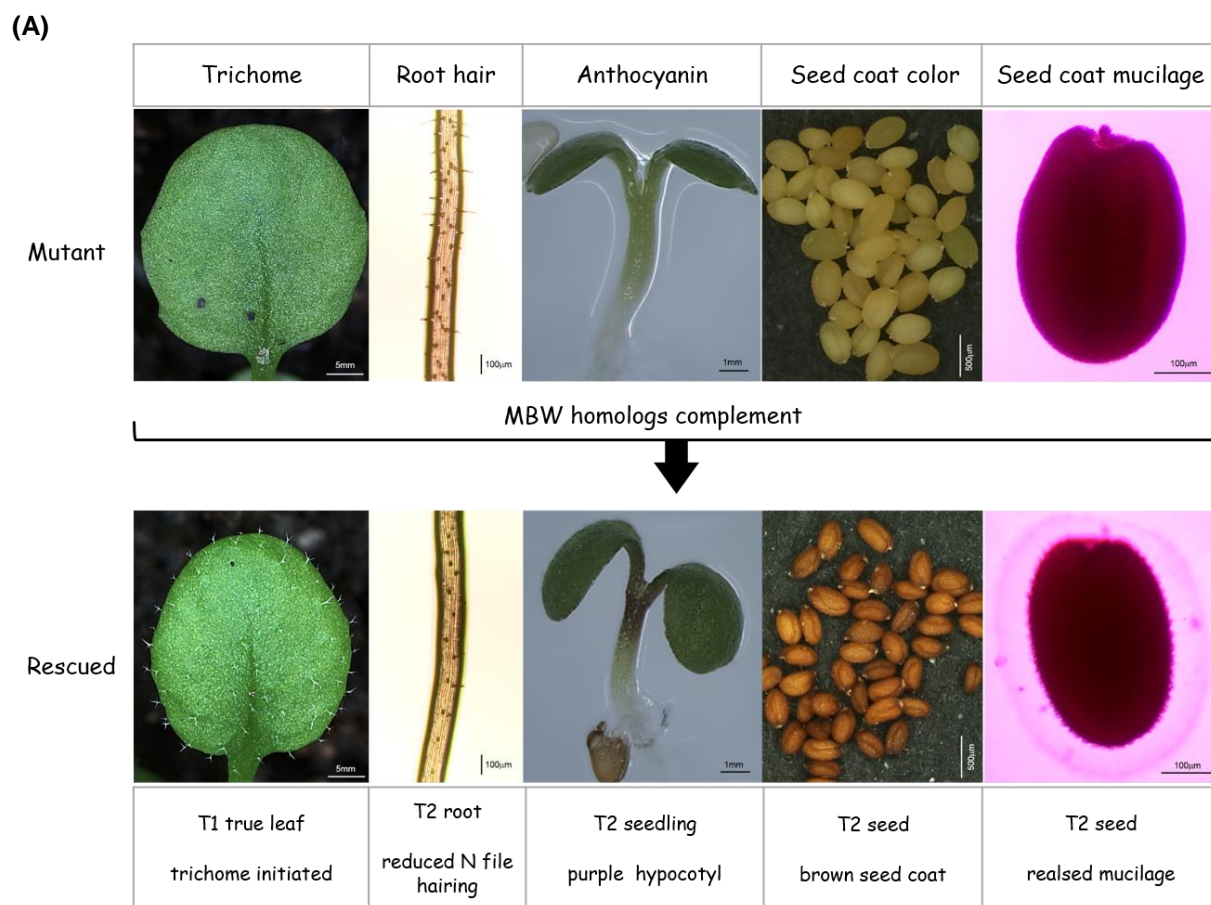


Figure 3.2 Rescue of 5 *TTG1*-dependent traits in *Arabidopsis* mutant by MBW genes from different plant species.

(A) Schematic depiction of rescue strategy.

(B)

	<i>ttg1/35S-</i>	Trichome	Root hair	Anthocyanin	Seed coat color	Seed coat mucilage
WD40	<i>TT61 A.thaliana</i>	25/27	23/27	22/27	25/27	25/27
	<i>TT61 A. alpina</i>	15/16	13/16	12/16	13/16	14/16
	<i>TT61 G.hirsutum</i>	35/50	33/50	33/50	35/50	35/50
	<i>TT62 G.hirsutum</i>	0/15	0/15	0/15	0/15	0/15
	<i>TT63 G.hirsutum</i>	14/19	12/19	12/19	13/19	13/19
	<i>TT64 G.hirsutum</i>	0/16	0/16	0/16	0/16	0/16
	<i>AN11 P.hybrida</i>	12/15	12/15	12/15	12/15	12/15
	<i>PAC1 Z.mays</i>	34/35	30/35	30/35	32/35	34/35
	<i>MPI Z.mays</i>	0/12	0/12	0/12	0/12	0/12
	<i>gl3egl3tt8/35S-</i>					
bHLH	<i>GL3 A.thaliana</i>	18/20	14/20	18/20	0/20	0/20
	<i>EGL3 A.thaliana</i>	15/20	10/20	10/20	0/20	9/20
	<i>MYC1 A.thaliana</i>	0/20	9/20	0/20	0/20	14/20
	<i>TT8 A.thaliana</i>	0/20	0/20	13/20	0/20	18/20
	<i>GL3 A. alpina</i>	25/28	16/28	24/28	0/28	13/28
	<i>EGL3 A. alpina</i>	10/13	7/13	10/13	0/13	(6/13) ^a
	<i>MYC1 A. alpina</i>	0/10	5/10	0/10	0/10	6/10
	<i>TT8 A. alpina</i>	0/20	0/20	12/20	0/20	18/20
	<i>DEL61 G.hirsutum</i>	0/20	12/20	9/20	0/20	17/20
	<i>DEL65 G.hirsutum</i>	0/20	13/20	10/20	0/20	18/20
	<i>AN1 P.hybrida</i>	0/20	0/20	11/20	0/20	10/20
	<i>JAF13 P.hybrida</i>	0/19	10/19	0/19	0/19	18/19
	<i>R(Lc) Z.mays</i>	20/24	13/24	20/24	0/24	(10/24) ^a
	<i>R(S) Z.mays</i>	20/22	15/22	20/22	0/22	(4/22) ^a
	<i>B Z.mays</i>	0/10	0/10	0/10	0/10	0/10
	<i>gl1/35S-</i> <i>pap1pap2/35S-</i>					
R2R3 MYB	<i>GL1 A.thaliana</i>	17/18	n.d.	0/16	n.d.	n.d.
	<i>WER A.thaliana</i>	0/16	n.d.	0/16	n.d.	n.d.
	<i>PAP1 A.thaliana</i>	0/16	n.d.	18/18	n.d.	n.d.
	<i>PAP2 A.thaliana</i>	0/16	n.d.	13/18	n.d.	n.d.
	<i>TT2 A.thaliana</i>	(9/16) ^b	n.d.	0/16	n.d.	n.d.
	<i>MYB61 A.thaliana</i>	0/16	n.d.	0/16	n.d.	n.d.
	<i>GL1 A. alpina</i>	14/16	n.d.	0/16	n.d.	n.d.
	<i>WER A. alpina</i>	0/16	n.d.	0/16	n.d.	n.d.
	<i>PAPL A. alpina</i>	0/16	n.d.	17/18	n.d.	n.d.
	<i>MYB23 A. alpina</i>	0/16	n.d.	0/16	n.d.	n.d.
	<i>MYB2 G.hirsutum</i>	14/16	n.d.	0/15	n.d.	n.d.
	<i>MYB3 G.hirsutum</i>	15/16	n.d.	0/15	n.d.	n.d.
	<i>MYB25 G.hirsutum</i>	0/16	n.d.	0/15	n.d.	n.d.
	<i>RLC1 G.hirsutum</i>	0/16	n.d.	6/12	n.d.	n.d.
	<i>AN2 P.hybrida</i>	0/16	n.d.	10/16	n.d.	n.d.
	<i>AN4 P.hybrida</i>	0/16	n.d.	13/16	n.d.	n.d.
	<i>PH4 P.hybrida</i>	0/16	n.d.	7/14	n.d.	n.d.
	<i>C1 Z.mays</i>	0/16	n.d.	8/12	n.d.	n.d.
	<i>PL Z.mays</i>	(6/16) ^b	n.d.	7/12	n.d.	n.d.
	<i>P1 Z.mays</i>	0/16	n.d.	9/15	n.d.	n.d.

Figure 3.2 Cont. Rescue of 5 TTG1-dependent traits in Arabidopsis mutant by MBW genes from different plant species

(B) T1 or T2 lines transformed by pAMPAT-35S-GW showing phenotypic rescue (rescued lines / total number of lines) in *ttg1*, *gl3/egl3/tt8*, *gl1* and *pap1/pap2* mutant, respectively. Any trait rescued is indicated by grey filling block.

a. Partially rescued; b. Trichome on leaf margin is restored; c. Seed coat is light brown.

(C)

<i>tt8/pro TT8-</i>	Trichome	Root hair	Anthocyanin	Seed coat color	Seed coat mucilage
<i>GL3 A.thaliana</i>	0/20	n.d.	n.d.	0/20	n.d.
<i>EGL3 A.thaliana</i>	0/20	n.d.	n.d.	(5/20) ^c	n.d.
<i>MYC1 A.thaliana</i>	0/20	n.d.	n.d.	0/20	n.d.
<i>TT8 A.thaliana</i>	0/20	n.d.	n.d.	18/20	n.d.
<i>GL3 A.alpina</i>	0/20	n.d.	n.d.	0/20	n.d.
<i>EGL3 A.alpina</i>	0/20	n.d.	n.d.	0/20	n.d.
<i>MYC1 A.alpina</i>	0/20	n.d.	n.d.	0/20	n.d.
<i>TT8 A.alpina</i>	0/20	n.d.	n.d.	15/20	n.d.
<i>DEL61 G.hirsutum</i>	0/20	n.d.	n.d.	0/20	n.d.
<i>DEL65 G.hirsutum</i>	0/20	n.d.	n.d.	0/20	n.d.
<i>ANI P.hybrida</i>	0/20	n.d.	n.d.	12/20	n.d.
<i>JAF13 P.hybrida</i>	0/20	n.d.	n.d.	0/20	n.d.
<i>R(Lc) Z.mays</i>	0/20	n.d.	n.d.	20/20	n.d.
<i>R(S) Z.mays</i>	0/20	n.d.	n.d.	19/20	n.d.
<i>B Z.mays</i>	0/20	n.d.	n.d.	0/20	n.d.

Figure 3.2 Cont. Rescue of 5 TTG1-dependent traits in Arabidopsis mutant by MBW genes from different plant species.

(C) T1 or T2 lines transformed by pAMPAT-pro*TT8*-bHLHs showing phenotypic rescue (rescued lines/total number of lines) in *tt8* single mutant.

n.d. Not done

(A)

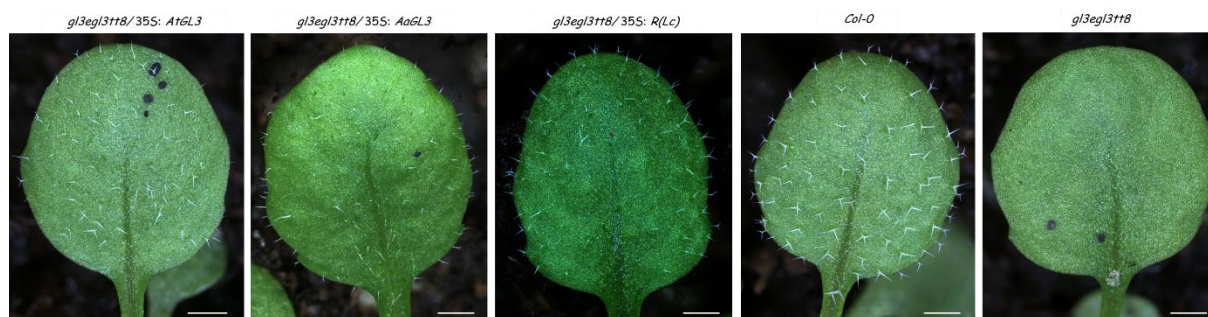
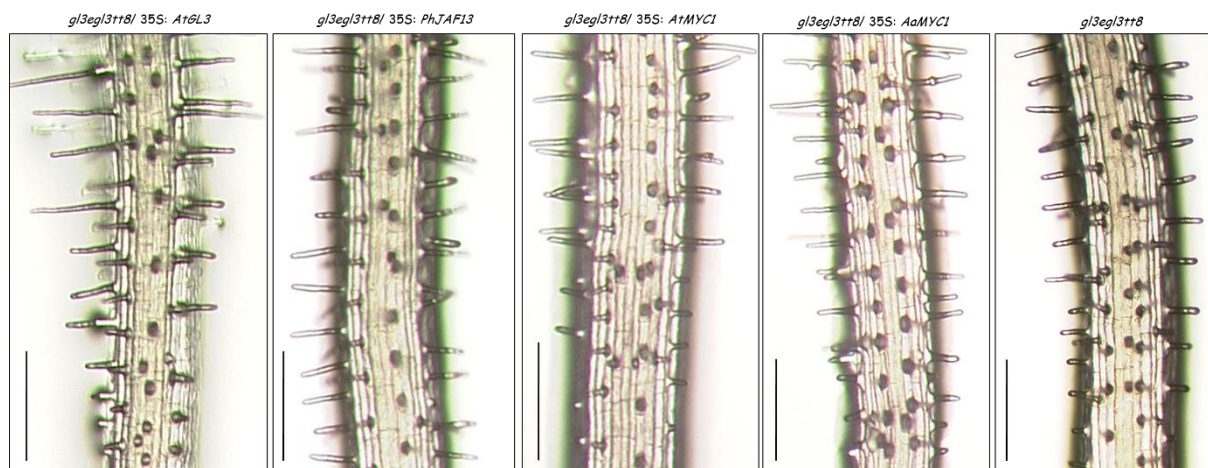


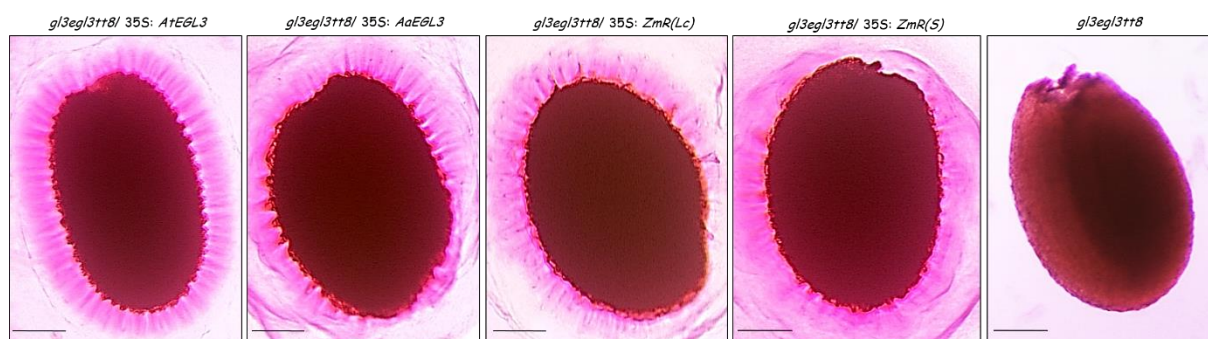
Figure 3.3 Phenotypes of mutants rescued by different MBW genes.

(A) The 3rd true leaf trichome phenotype of *gl3egl3tt8* triple mutant rescued by 35S: *bHLHs* in 10-day-old T1 seedling. (Scale bar = 5 mm)

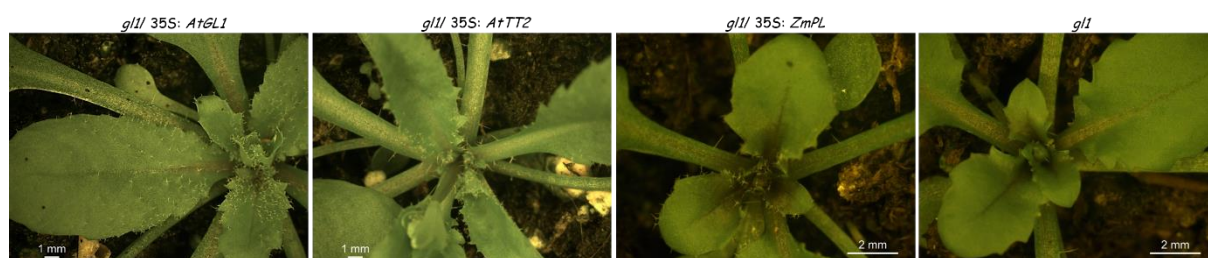
(B)



(C)



(D)



(E)

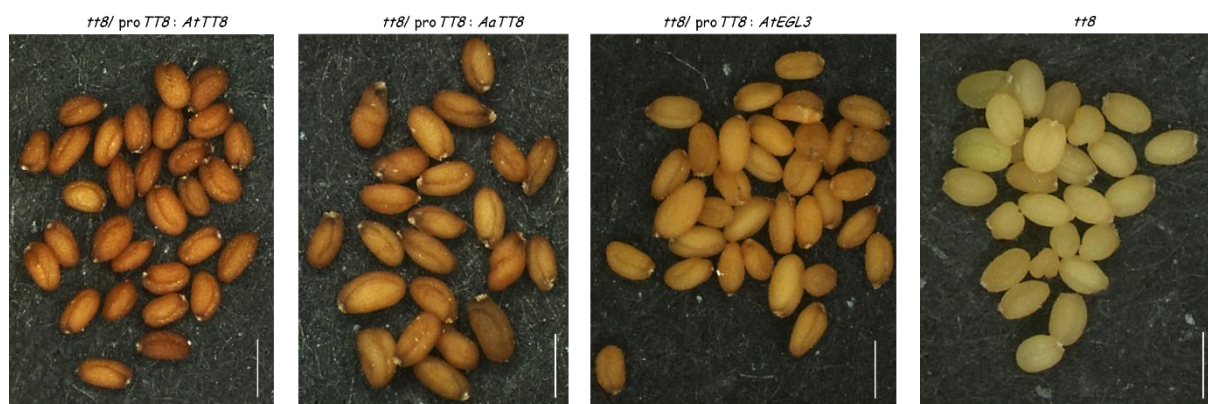


Figure 3.3 Cont. Phenotypes of mutants rescued by different MBW genes

(B) Root hair phenotype of *gl3egl3tt8* triple mutant rescued by 35S::*bHLHs* in T2 seedlings. (Scale bar =200 μ m)

(C) Seed coat mucilage phenotype of *gl3egl3tt8* triple mutant rescued by 35S: *bHLHs* in T2 progeny. (Scale bar =100 μm)

(D) Trichome phenotype of *gl1* single mutant rescued by 35S:*R2R3MYBs* in 3-week-old T1 seedlings.

(E) Seed coat color of *tt8* single mutant rescued by pro *TT8*: *bHLHs* in T2 generations. (Scale bar =500 μm)

3.3.4 Inter-species MBW pairwise interaction

Since some orthologs of Arabidopsis MBW genes were able to restore TTG1-dependent traits, we proposed that hetero-MBW complexes formation backed phenotypic rescue. To this end, we performed inter-species MBW proteins interaction assay with LUMIER.

In the combination of bHLH proteins from Arabidopsis and AaTTG1, strong renilla luciferase activity signal were detected demonstrating AaTTG1 indeed interacted with 4 bHLH proteins from Arabidopsis. Similar results were found in GhTTG1/bHLH, PhAN11-bHLH and ZmPAC1-bHLH combinations. GhTTG3, another ortholog of AtTTG1, was able to interact with AtGL3, AtEGL3 and AtMYC1 but not AtTT8. These results were well correlated with data in phenotypic rescue, i.e. AtTTG1 orthologs that could interact with 4 bHLH proteins had capacities in rescuing 5 TTG1-dependent traits, and *vice versa* (GhTTG2, GhTTG4 and ZmMP1 were devoid of rescuing ability). Additionally, GhTTG3 also weakly interacted with AtTT2, which might explain the fact that GhTTG3 fairly rescued seed coat color despite loss of interaction with AtTT8 (Figure 3.4 and Table S6).

All of bHLH proteins tested could firmly bind to AtTTG1. On the contrary, renilla luciferase activity of all bHLHs-AtMYB61 (a seed coat mucilage specific R2R3MYB) combinations were barely detectable. Except for ZmB, other bHLHs were found to interact with trait-specific AtR2R3MYBs, respectively, in spite of negative signals in AaEGL3-AtPAP2 combinations (Figure 3.4B and Table S7).

Similar to intra-specific data, most of R2R3MYBs from other species were not able to directly interact with AtTTG1, however, the combination of ZmPL-AtTTG1 showed a weak signal which used to be found in AtTT2-AtTTG1 combination (Figure 3.4 and Table S). As expected, all of 4 Arabidopsis bHLH proteins was also confirmed to bind to hetero-R2R3MYBs but not to GhMYB25 or ZmP1 (Figure 3.4B and Table S8).

To sum up, hetero-MBW complex formation was in concert with the rescue of TTG1-dependent traits in Arabidopsis mutant by MBW orthologs.

(A)

		ProtA_fused											
		A+TTG1	A+GL3	A+EGL3	A+TT8	A+MYC1	A+GL1	A+WER	A+PAP1	A+PAP2	A+TT2	A+MYB61	w/o
Renilla_fused	A+TTG1	-	+	+	+	+	-	-	-	-	-	-	-
	A+GL3	+	+	+	+	+	+	+	+	+	+	-	-
	A+EGL3	+	+	+	+	w	+	+	+	+	+	-	-
	A+TT8	+	+	+	+	w	+	w	+	+	+	-	-
	A+MYC1	+	+	w	w	+	+	+	+	+	+	-	-
	A+GL1	-	+	+	+	+	w	-	-	-	-	-	-
	A+WER	-	+	+	w	+	-	-	-	-	-	-	-
	A+PAP1	-	+	+	+	+	-	-	-	-	-	-	-
	A+PAP2	-	+	+	+	+	-	-	-	-	-	-	-
	A+TT2	w	+	+	+	+	-	-	-	-	w	-	-
	A+MYB61	-	w	w	w	w	-	-	-	-	-	-	-
	w/o	-	-	-	-	-	-	-	-	-	-	-	-

Figure 3.4 Analysis of inter-species MBW pairwise interaction by LUMIER pulldown assays.

(A) MBW pairwise interaction in *Arabidopsis thaliana* as a positive control.

w/o: Empty vector without CDS fusion.

+ : Positive interaction (Luciferase activity $\geq 2.5\%$)

w : Weak interaction (Luciferase activity = 1.5%~2.5%)

- : No interaction (Luciferase activity $< 1.5\%$)

(B)

		ProtA_ or Renilla_											
		A+TTG1	A+GL3	A+EGL3	A+TT8	A+MYC1	A+GL1	A+WER	A+PAP1	A+PAP2	A+TT2	A+MYB61	w/o
ProtA_ or Renilla_	AaTTG1		+/+	+/+	+/+	+/+	-/-	-/-	-/-	-/-	-/-	-/-	-/-
	GhTTG1		+/+	+/+	+/+	+/+	-/-	-/-	-/-	-/-	-/-	-/-	-/-
	GhTTG2		-/-	-/-	-/-	-/-	-/-	-/-	-/-	-/-	-/-	-/-	-/-
	GhTTG3		+/w	+/+	-/-	+/+	-/-	-/-	-/-	-/-	w/w	-/-	-/-
	GhTTG4		-/-	-/-	-/-	-/-	-/-	-/-	-/-	-/-	-/-	-/-	-/-
	PhAN11		+/+	+/+	+/+	+/+	-/-	-/-	-/-	-/-	-/-	-/-	-/-
	ZmPAC1		+/+	+/+	+/+	+/+	-/-	-/-	-/-	-/-	-/-	-/-	-/-
	ZmMP1		-/-	-/-	-/-	w/-	-/-	-/-	-/-	-/-	-/-	-/-	-/-
	AaGL3	+/+					+/+	+/+	+/+	w/+	+/+	-/-	-/-
	AaEGL3	+/+					+/+	+/+	w/w	-/-	+/+	-/-	-/-
	AaTT8	+/+					+/+	+/+	+/+	+/+	+/+	-/w	-/-
	AaMYC1	+/+					+/+	+/+	+/+	+/+	+/+	-/-	-/-
	GhDEL61	+/+					+/+	+/+	+/+	+/w	+/+	-/-	-/-
	GhDEL65	+/+					+/+	+/+	+/+	+/+	+/+	-/-	-/-
	PhAN1	+/+					+/+	+/+	+/+	+/+	+/+	-/-	-/-
	PhJAF13	+/+					+/+	+/+	+/+	w/w	+/+	-/-	-/-
	ZmR(Lc)	+/+					+/+	+/+	+/+	+/+	+/+	-/-	-/-
	ZmR(S)	+/+					+/+	+/+	+/+	+/+	+/+	-/-	-/-
	ZmB	+/+					-/-	-/-	-/-	-/-	-/-	-/-	-/-
	AaGL1	-/-	+/+	+/+	+/+	+/+							-/-
	AaWER	-/-	+/+	+/+	+/+	+/+							-/-
	AaPAP1	-/-	+/+	+/+	+/+	+/+							-/-
	AaMYB23	-/-	+/+	+/+	+/+	+/+							-/-
	GhMYB2	-/-	+/+	+/+	+/+	+/+							-/-
	GhMYB3	-/-	+/+	+/+	+/+	+/+							-/-
	GhMYB25	-/-	-/-	-/-	-/-	-/-							-/-
	GhRCL1	-/-	+/+	+/+	+/+	+/+							-/-
	PhAN2	-/-	+/+	+/+	+/+	+/+							-/-
	PhAN4	-/-	+/+	+/+	+/+	+/+							-/-
	PhPH4	-/-	+/+	+/+	+/+	+/+							-/-
	ZmC1	-/-	+/+	+/+	+/+	+/+							-/-
	ZmPL	w/w	+/+	+/+	+/+	+/+							-/-
ZmP1	-/-	-/-	-/-	-/-	-/-							-/-	
w/o	-/-	-/-	-/-	-/-	-/-	-/-	-/-	-/-	-/-	-/-	-/-	-	

Figure 3.4 Cont. Analysis of inter-species MBW pairwise interaction by LUMIER pulldown assays.

(B) Interaction is assessed by recombination Renilla luciferase fused MBW homologs from different plant species (*Arabis alpine* [Aa], *Gossypium hirsutum* [Gh], *Petunia hybrid* [Ph] and *Zea mays* [Zm]) with protein A (protA) fused MBW in *Arabidopsis thaliana* [At] and vice versa. All proteins are single-expressed in human cells (HEK293TN) and immunoprecipitated with IgG Dynabeads.

3.4 Discussion

Regularly, new orthologs are identified, which might be of relevance for breeding purposes. Not only are allelism tests and rescue experiments within the respective species conducted (if applicable) to explore the ortholog's function, when mutants are identified. More often, the function of the orthologs is estimated by using the model species *A. thaliana*. In cross-species rescue experiments, *MBW* orthologs from other species are expected to take over *AtMBW* function at least in part within respective *MBW* complexes.

3.4.1 bHLH proteins redundantly and distinctly rescue AtTTG1-dependent traits, which provide an essential basic point for learning functional divergence of the MBW proteins

AtTTG1 is the head of an evolutionarily-conserved gene regulatory network, regulating five *AtTTG1*-dependent traits with adaptive value for the plant. Similarly, *AtTTG1*-like WD40 proteins in other species are indispensable for respective *MBW* regulatory traits in their own species as well. These *AtTTG1* orthologs which are functionally active in their own species are able to substitute *AtTTG1* in term of 5 traits, regardless of their intraspecific functions, and vice versa (Figure 3.2B).

The bHLH factors act redundantly towards the different traits. All of *bHLHs* genes here (at least partially) suppress the mucilage defect of *gl3 egl3 tt8* except for *AtGL3* and *ZmB*, suggesting seed coat mucilage probably the most ancient and conserved trait during the plant evolution (Fig 3.2B). Based on the data, it seems that root hair and anthocyanin traits are equally positioned at the second conserved place, nevertheless it needs to be mentioned that the function of PhJAF13 and ZmR in *Arabidopsis* have shifted and duplicated due to some unclear mechanisms (e.g. the hierarchical and feedback regulation of *MBW* genes in *Arabidopsis* [146]). Therefore, anthocyanin is a more conserved trait than root hair. Trichome and seed coat color (proanthocyanidin) are evolutionarily recent traits, because two distinct groups of bHLHs rescue the respective trait (apart from pleiotropic ZmR) (Figure 3.2B and 3.2C).

The highest specificity of the trait regulation by *MBW* protein complexes exists on the level of the R2R3MYB factors. All R2R3MYBs tested here still retain their intraspecific function in *Arabidopsis* without shifts or duplications, while GhMYB25 lost its function.

3.4.2 Hetero-MBW complex formation is in concert with rescue of AtTTG1-dependent traits in *Arabidopsis* mutant by MBW orthologs

Most orthologs of *Arabidopsis* MBW genes are able to restore TTG1-dependent traits to varying degrees, suggesting hetero-MBW complex formation might back phenotypic rescue. The result of inter-species MBW proteins interaction LUMIER assay supports our speculation. Three AtTTG1 orthologs (i.g. GhTTG2, GhTTG4 and ZmMP1) devoid of rescuing any traits fail to form hetero-MBW complexes in *Arabidopsis*, which is consistent with their intra-specific data (Figure 3.4B ,Table S3 and Table S5) [74]. Besides, none of *Arabidopsis* bHLH proteins bind to GhMYB25, which is again in concert with the loss of its function in *Arabidopsis* (Figure 3.2B and Figure 3.4B). Similarly, in bHLH proteins, ZmB which lost its function in *Arabidopsis* is found not able to interact with trait-specific AtR2R3MYBs. Although the other bHLH proteins that are able to form hetero-MBW complexes in terms of all 5 traits, not every bHLH protein could rescue all 5 traits (Figure 3.2B and Figure 3.4B). One question might be raised referring to AtMYB61 combinations: why are almost bHLHs able to restore seed coat mucilage regardless of their negative binding with AtMYB61? One explanation might be that other functionally redundant R2R3MYBs probably take over AtMYB61 for the mucilage trait, e.g. MYB5, MYB23 and so on [104, 177]). From these results, we could conclude that hetero-MBW complexes formation is necessary, but not a sufficient condition for rescue of TTG1-dependent traits in *Arabidopsis* mutants.

In addition, the direct interaction of ZmPL-AtTTG1 and AtTT2-AtTTG1 might lead to minor trichome formation on the leaf border in *gl1* mutants by ZmPL or AtTT2 overexpression (Figure 3.3D and Figure 3.4B).

CHAPTER IV

**QUANTITATIVE ANALYSIS OF TTG1,
GL3 AND GL1 PROTEIN COMPLEX
FORMATION**

4. Quantitative Analysis of TTG1, GL3 and GL1 Protein Complex Formation

4.1 Summary

TTG1, GL3 and GL1 are three key MBW factors that regulate leaf trichome formation in *Arabidopsis*. The introduction of two alternative dimers (i.g. TTG1-GL3 and GL3-GL1) complicates previous trichome patterning models based on one ternary protein complex (i.g. TTG1-GL3-GL1). In particular, it is unknown, which relative concentrations of dimers and ternary complexes are to be expected. Towards this end, I performed quantitative LUMIER assays to determine the relative binding affinities and quantified the dosage dependent competition in titration experiments. These experimental studies were complemented by mathematical modeling by Anna Deneer, Wageningen.

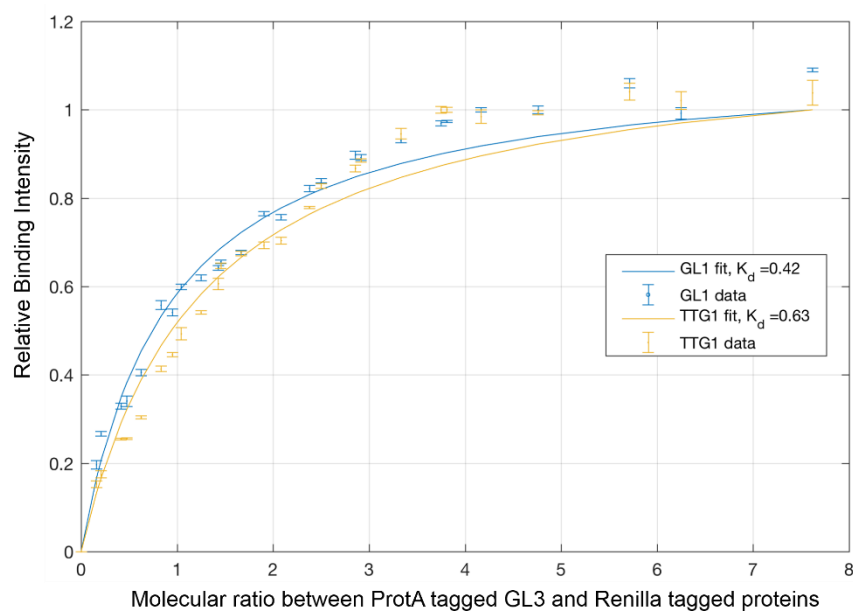
4.2 Results

4.2.1 The comparison of GL3 binding affinity with GL1, TTG1 and itself

As TTG1 and GL1 bind to different regions of the GL3 protein [29, 66, 67], it is conceivable that the observed competitive binding to GL3 is due to intramolecular changes of protein folding, also known as an allosteric regulation. To describe the formation of dimers and trimers quantitatively, it is necessary to determine the binding constant/dissociation constant of GL3 TTG1 and GL3 GL1. Towards this end, we performed pulldown experiments by LUMIER assays [149, 178]. The amount of ProtA tagged GL3 was kept constant and a dilution series of Luciferase-tagged GL1 and TTG1 was added for the titration experiments. To enable a comparison of the relative amounts of GL3 and GL1 or TTG1 protein all proteins carried an additional HA-tag. The relative amounts of the three proteins were determined by a quantitative analysis of western blots using the HA-antibody (Figure S3). Data analysis was done by Anna Deneer, Wageningen University. She determined the best fit curve for my data (Figure 4.1) and calculated the dissociation constants (K_ds). As we do not know the absolute protein concentrations, these K_ds are relative K_ds that enable a comparison of the binding affinity of all proteins to GL3. As showed in Figure 4.1A, she estimated the K_ds for GL1-GL3 at 0.42 and that for TTG1-GL3 at 0.63, respectively. The difference between the two K_ds is statistically significant suggesting that the binding affinity of GL3 has higher affinity with GL1 than TTG1 (Figure S4A). Additionally, the binding

affinity of GL3-GL3 (i.g. GL3 homodimerization) was estimated in a similar range of GL1-GL3 (Note that dimerization of the same tagged GL3 was not counted here) (Figure 4.1B and Figure S4B). Therefore, we take into account GL3 homo-dimerization in our analysis.

(A)



(B)

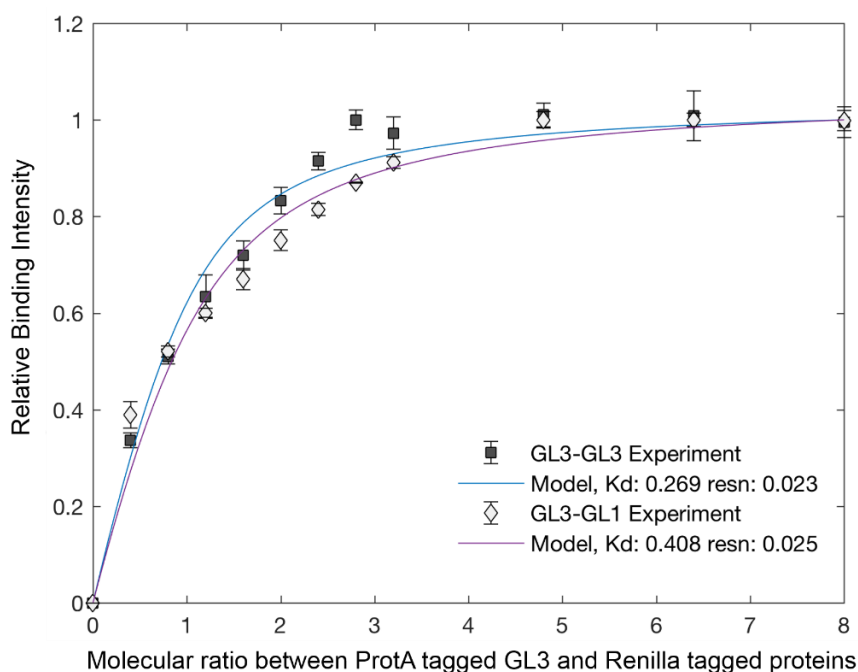


Figure 4.1 GL3 binding affinity analyses

(A) Binding affinity comparison of TTG1-GL3 (yellow) and GL1-GL3 (blue). Each value represents mean \pm standard errors (n = 3 technical replicates). Kd values are estimated by Anna Deneer, Wageningen University based data of this work (Table S9).

(B) Binding affinity comparison of GL3-GL3 (blue) and GL1-GL3 (violet). Each value represents mean \pm standard errors (n = 3 technical replicates). Kd values are estimated by Anna Deneer, Wageningen University based data of this work (Table S11).

4.2.2 Effect of GL1 on the TTG1 binding to GL3 in dependence of the relative protein concentration

To further investigate the details of TTG1 and GL1 competing for the binding to GL3, I quantified the effect of GL1 (or TTG1) on the interaction between GL3 and TTG1 (or GL1) by dosage-dependent LUMIER assay. When adding increasing amounts of GL1, the relative binding intensity of TTG1-GL3 dropped to ~ 63.72%. The maximal inhibition was found at a molecular ratio of TTG1 to GL1 of about 1:1. Interestingly, a rebound from lowest value was found before it plateaued at around 81.63% (after GL1 out-amounted TTG1 by approximate twice) suggesting effect of GL1 might shift to synergetic-dominant on TTG1-GL3 interaction by a certain out-amounted GL1 (Figure 4.3 and Table S13). Whereas decreasing-only effect of YFP tagged TTG1 on the interaction between ProtA tagged GL3 and Renilla_LUC tagged TTG1 was found in the control (Table S13), indicating the formation of multiple orders of complexes shifted dynamically in dependence of the relative protein concentration.

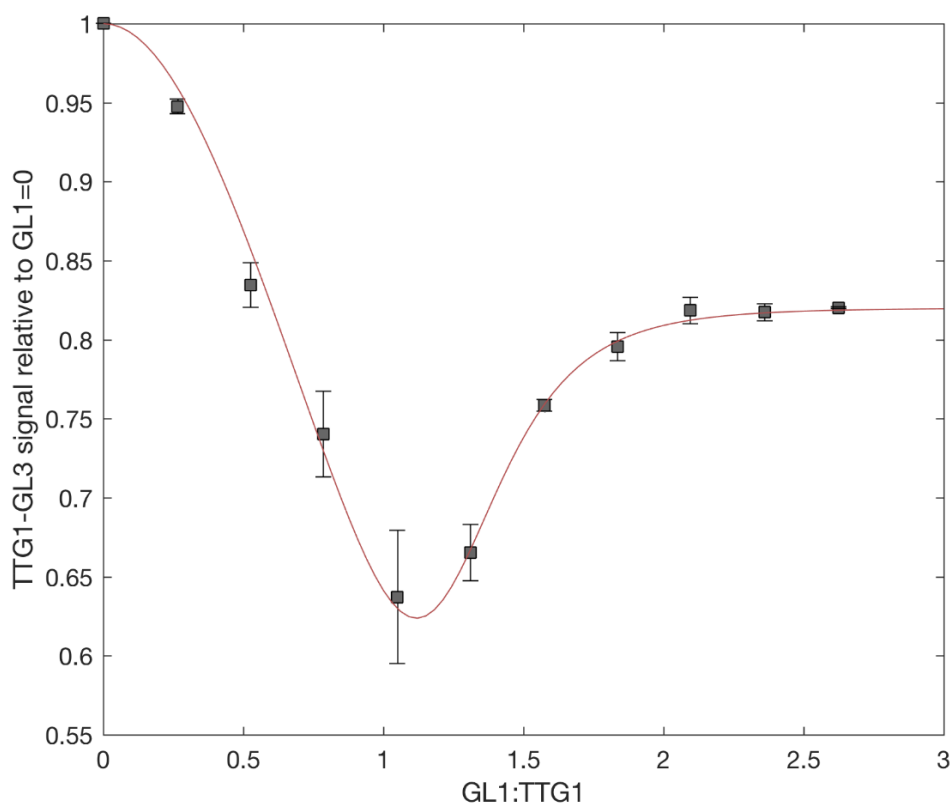


Figure 4.2 Quantitative analysis of TTG1 and GL1 competing for the binding to GL3.

The effect of incremental amount of GL1 on binding intensity of TTG1 and GL3 indicated by grey spares. Each value represents mean \pm standard errors ($n = 2$ biological replicates). ANOVA test showed that there is significant difference between the different levels of GL1 ($p < 0.001$, referring to Table S15)

Model (red line) fits to $f(x) = \frac{\sum_{i=0} a_i x^{n_i}}{\sum_{i=0} b_i x^{m_i}}$. $n = \{0, 10\}$ $m = \{0, 2, 10\}$.

Modeling by Anna Deneer, Wageningen University based data of this work (Table S13).

4.2.3 Quantitative analysis of GL1 and TTG1 effect on GL3 homo-dimerisation

As GL3 can dimerize [29, 65, 66], it is possible that higher order complexes are formed. To test, whether GL3 dimerization is influenced by binding of GL3 to TTG1 or GL1, we used ProtA tagged GL3 to precipitate Renilla_Luciferase tagged GL3 in the presence of different amounts of TTG1 and GL1 (Figure 4.2 and Table S12). In these experiment we found no differences of the GL3 dimerization upon addition of TTG1 and GL1 indicating that GL3 dimerization is not modulated by GL1 or TTG1 binding, which in turn suggested homodimerization of GL3 is independent of other protein binding reactions.

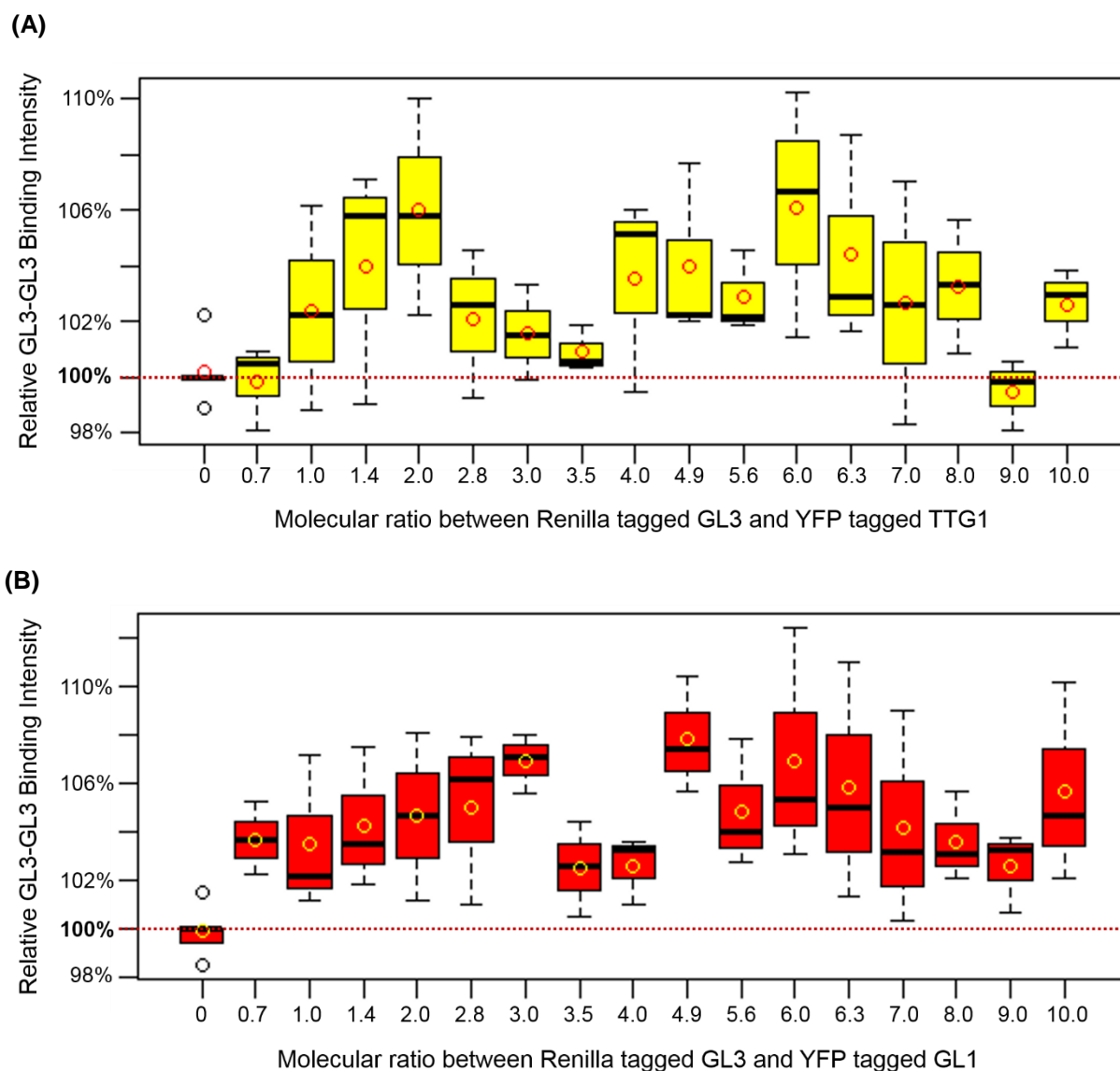


Figure 4.3 Quantitative analysis of TTG1 and GL1 effect on GL3 homodimerisation.

(A) Binding intensity of ProtA tagged GL3 and Renilla_LUC tagged GL3 was determined in the presence of incremental amount of YFP tagged TTG1. Binding intensity was normalized to the reference that was determined without additional TTG1 (defined as 100%).

(B) Binding intensity of ProtA tagged GL3 and Renilla_LUC tagged GL3 was determined in the presence of incremental amount of YFP tagged GL1. Binding intensity was normalized to the reference that was determined without additional GL1 (defined as 100%).

Each value represents mean \pm standard errors ($n = 3$ technical replicates). By Student's t test, no significant difference from the reference was achieved ($P \geq 0.05$).

4.2.4 Quantitative analysis of the interaction of GL3 with inhibitors

TRY and CPC

A second important type of protein-protein interactions of GL3 is that with the trichome inhibitors TRY and CPC. TRY and CPC binding to GL3 occurs in the same region of

GL3 as GL1 binding. Therefore TRY/CPC compete for binding with GL1 to GL3. The binding of TRY/CPC to GL3 leads to a transcriptionally inactive complex whereas GL1 bound to GL3 results in a transcriptionally active complex [179]. To quantitatively assess this competition I aimed to determine the dissociations constants of TRY/CPC with GL3. Using ProtA tagged GL3 and Renilla_LUC tagged TRY/CPC, I performed titration experiments and Anna Deneer determined the best fitting curves (Figure 4.4). As compared to GL1 we observed slopes with a reduced steepness and the K_d values were clearly much higher for TRY ($K_d = 1,6$) and CPC ($K_d = 7,28$). This suggests that TRY and CPC levels need to be higher than GL1 for competition. To test this assumption, we did a titration series by studying the GL3-GL1 interaction in the presence of different amounts of TRY. We found a concentration dependent reduction of GL1 binding to GL3 (Figure 4.5B and Table S14). Surprisingly, GL3-GL1 binding intensity dropped to the lowest level and was stable at ~20% in the presence of equimolar amount of GL1 and TRY (Table S14).

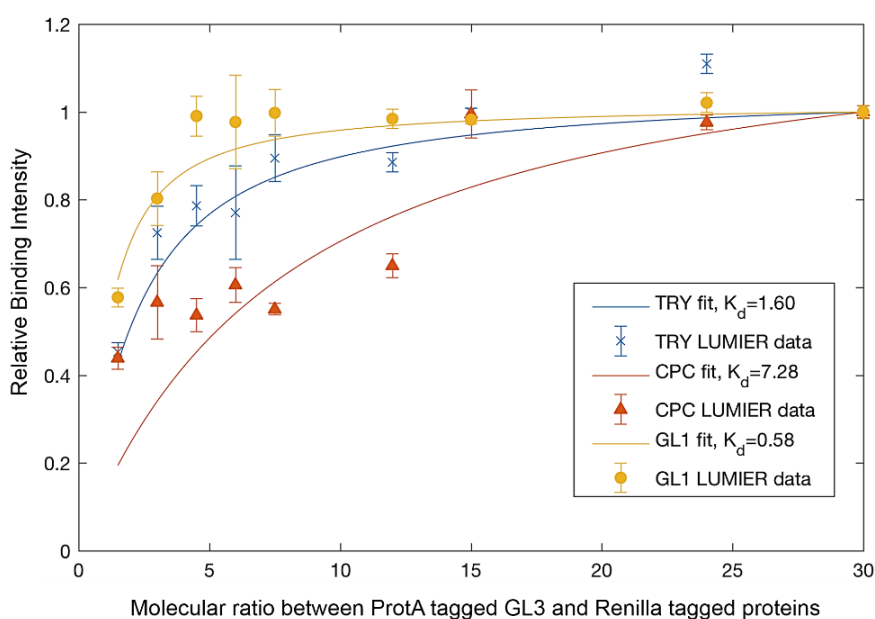


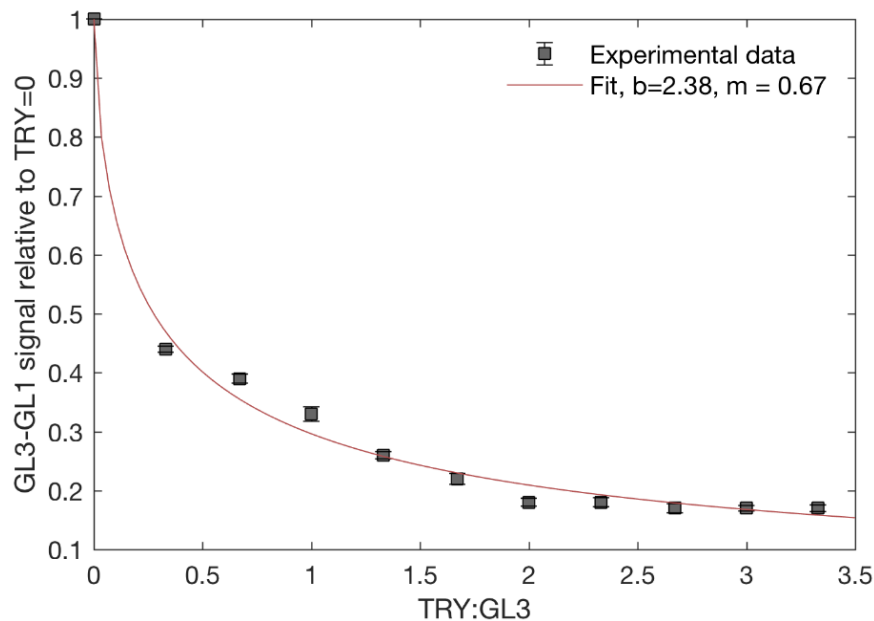
Figure 4.4 Analysis of GL3 binding affinity with inhibitors TRY and CPC.

Binding affinity comparison of GL1-GL3 (yellow), TRY-GL3 (blue) and CPC-GL3 (red). Each value represents mean \pm standard errors ($n = 3$ technical replicates). K_d values are estimated by Anna Deneer, Wageningen University based data of this work (Table S10).

4.2.5 The inhibitory effect comparison between distinct binding site competition and same binding site competition by mathematic modeling

Based on above data, we estimated coefficient of inhibition of GL1 on GL3-TTG1 interaction (decreasing phase at the first 5 points) via mathematic modeling (Figure 4.5A which was carried out by Anna Deener, Wageningen University). Likewise, same approaches were applied in the estimation of TRY inhibitory effect on GL3-GL1 interaction as a same bind site competition control (Figure 4.5B). As expected, modeling showed the inhibitory coefficient caused by distinct binding site competition ($b = 0.53$, i.g. GL1 on GL3-TTG1) was much lower than that caused by same binding site competition ($b = 2.38$, i.g. TRY on GL3-GL1), suggesting GL1 might also work as a weak synergist on GL3-TTG1 interaction in the beginning. It was worth be mentioned, decreasing points in Figure 4.5A better fitted to the model with $m = 2$, rather than $m = 1$, indicating that initially a dimer of GL1 inhibiting the GL3-TTG1 binding, which was consistent with the fact that GL1 was able to form homodimer [180].

(A)



(B)

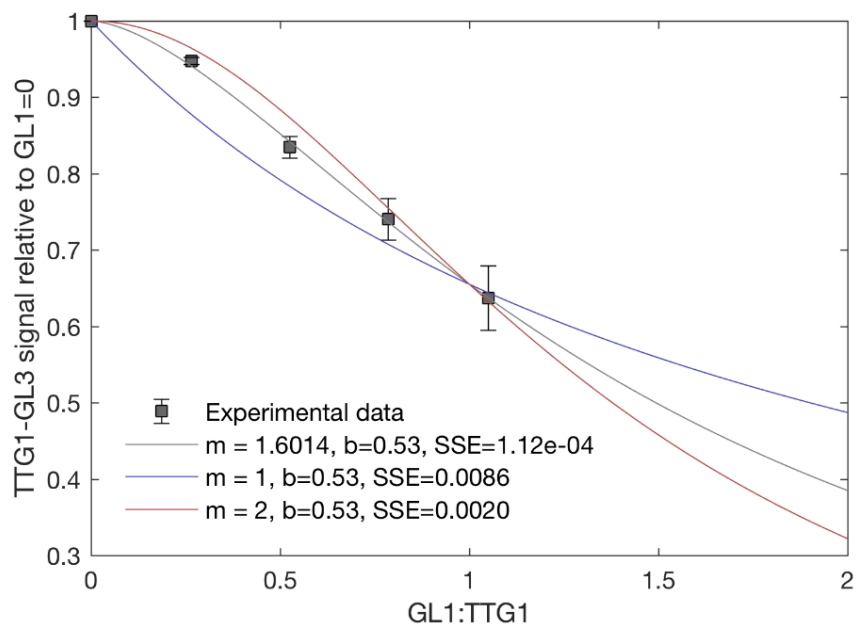


Figure 4.5 The inhibitory effect comparison between GL1 on GL3-TTG1 (distinct binding site competition) and TRY on GL1-GL3 (same binding site competition).

(A) Model fits to initial decrease $f(x) = \frac{1}{(1+bx^m)}$. It represents an inhibitory effect of GL1, where m indicates the complex order. Grey line best fits with estimates for b (coefficient of inhibition) and m (GL1 unit) given in legend. SSE: sum of squared error for nearest integers of m . Blue line is a first order complex ($m = 1$, with GL1 monomer) while red line fits to a second order complex ($m = 2$, with GL1 dimer). [Modeling by Anna Deneer, Wageningen University based data of this work (Table S13).]

(B) The effect of incremental amount of TRY on binding intensity of GL1-GL3 indicated by grey spares. Each value represents mean \pm standard errors ($n = 2$ biological replicates). Model fits to R3MYB inhibitor (TRY) decreasing GL1-GL3 binding. Model (red line) best fits with estimates for b (coefficient of inhibition) and m (TRY unit). [Modeling by Anna Deneer, Wageningen University based data of this work (Table S14).]

4.3 Discussion

Mechanisms beneath the regulation of trichome formation in *Arabidopsis* are sophisticated networks involving multiple stereochemistry of MBW protein complexes. Here, we used GL1-GL3-TTG1 as a representative MBW complex modulating trichome formation to quantitatively decipher how alternative dimers (GL1-GL3 and GL3-TTG1) refresh the current trichome patterning model.

Since the observation of antagonistic inter-relation among GL1, GL3 and TTG1 was first presented by Martina Pesch [149], we had been seeking for its functional relevance on trichome morphogenesis for long time. However, quantitative analyses of morphogenesis *in vivo* was messy operations. To this end, mathematic simulation was recruited based on our doable experimental data. First of all, aiming to provide critical parameters for following mathematic modelings we estimated GL3 binding affinity with TTG1, GL1 and itself, respectively. Moreover, from binding affinity estimation, it is assumed that GL3 tends to form homo-dimer firmly regardless of the presence of TTG1 and GL1 (Figure 4.1). On the basis of quantitative analyses of TTG1 and GL1 competing for the binding to GL3, The effect of incremental amount of GL1 on binding intensity between TTG1 and GL3 was in three different phases (Figure 4.2): 1) dissociation between TTG1 and GL3 as the inhibitory effect of GL1 in the beginning; 2) rebinding of TTG1 and GL3 as reduced inhibitory and/or increased synergetic effect of GL1 when the amount of GL1 exceeded that of TTG1; 3) balancing after GL1 out-amounted TTG1 by approximate twice. Mathematic modeling showed the inhibitory coefficient of GL1 effect on GL3-TTG1 was much lower than that caused by the same binding site competition (Figure 4.5), suggesting even in the very beginning of decreasing phase, GL1 probably also synergized the GL3-TTG1 interaction although in subordinate effect.

Due to the complicated inter-relation of these three components in the dosage-dependent assay, it is conceivable that the formation of multiple orders of complexes shifts dynamically in dependence of the relative protein concentration *in vivo* as well (Figure 4.6).

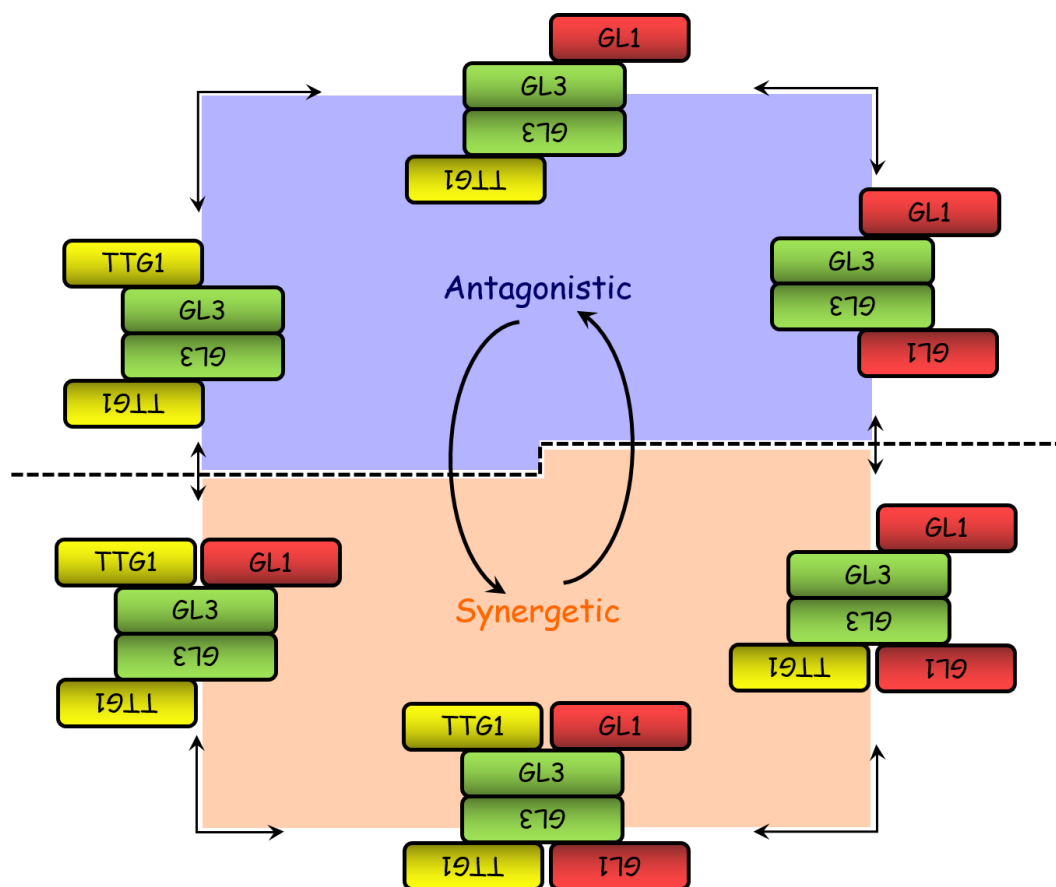


Figure 4. 6 Dynamic balance of multiple orders of complexes formed by TTG1, GL3 and GL1.

We propose homodimerized GL3 interact with TTG1 and/or GL1. Provided GL3-TTG1 complex is a starting point, antagonistic inter-relation firstly occurs in the incremental presence of GL1 (blue region, the inhibitory-dominant GL1 competes TTG1 for binding to GL3); As GL1 out-amounts TTG1 (orange region), synergist role of GL1 significantly effects on complexes formation although inhibitory effect is still dominant resulting in the decreasing output; Finally, multiple orders of complexes balances dynamically after GL1 exceeds doublemolar level of TTG1. [Note: an initial homodimer of GL1 (not indicated in the figure) is assumed to inhibit the interaction of GL3-TTG1.]

PERSPECTIVE

In depth quantitative analyses of inter-relation of MBW components from different plant species revealed that the existence of diverse inter-relation among MBW components in the perspective of the event of plant evolution. These results emphasized that the critical role of three MBW components. Nevertheless, factors that cause distinct protein behavior are still remained as a unexplored field (for instance, positions in bHLH proteins and PAP-like MYBs). In addition, why plants recruit different stereochemistry of MBW proteins (i.g. the functional relevance of different MBW protein behavior *in vivo*) could be a central question driving future research.

As dominant regulators in Arabidopsis leaf trichome initiation and patterning, TTG1, GL3 and GL1 work in a dynamic balance with various phases in term of dimers, trimers and multimers. The competition between TTG1 and GL1 for binding to GL3 differs from the same binding site competition (e.g. GL1 and R3MYB inhibitors competing for the same site on GL3). In this regard, a lot of work remains to be carried out to decipher the competition mechanism behind interactions among TTG1, GL3 and GL1 (e.g. an allosteric-like regulation induced competition for binding to GL3). Furthermore, building a connection between differential proportion of multiple orders of protein complexes and trichome morphogenesis is our final aim.

CHAPTER V

MATERIALS AND METHODS

5. Materials and Methods

5.1 General Materials

All chemicals and antibiotics used comply analytical quality and were obtained from Sigma-Aldrich (Munic, Steinheim), Roth (Karlsruhe), Merck (Darmstadt), and Duchefa (Haarlem, Netherlands).

DNA modifying enzymes (restriction enzymes, Taq polymerase, Pfu polymerase, Phusion polymerase, T4 ligase) as well as the pJET Cloning Kit were used from MBI-fermentas (Thermo Fisher Scientific, USA). DNA preparation kits (Mini, Midi, Maxi, gel extraction, purification) were supplied from QIAGEN (Hilden), Fermentas (Thermo Fisher Scientific, USA), peqlab (Erlangen), Roche (Mannheim), and Invitrogen (Karlsruhe).

5.1.1 Buffers and Solutions

If not stated otherwise, all buffers and solutions were prepared with distilled 0.2µm filtered H₂O. All buffers used for gel filtration columns were additionally 0.2µm filtered after preparation and vacuumed for 45 min before usage.

Bacterium Culture

	Concentration	Content
LB pH 7.0	10 g/l	Peptone
	5 g/l	Yeast extract
	5 g/l	Sodium Chloride
	15 g/l	Agar
YEB pH 7.0	5 g/l	Beef extract
	1 g/l	Yeast extract
	5 g/l	Peptone
	5 g/l	Sucrose
	0.5 g/l	MgCl ₂
	15 g/l	Agar

Yeast Culture

	Concentration	Content
YPAD	20 g/l	Bacto-peptone
	10 g/l	Bacto-yeast extract
	40 mg/l	Adenine sulfate
	20 g/l	Agar
	2%	Glucose

	Concentration	Content
SD medium pH 5.8	1.7 g/l	Yeast nitrogen base
	5 g/l	Ammonium sulfate
	0,6 g/l	Drop-out supplement
	100 mg/l	Leucine
	20 mg/l	Histidine
	50 mg/l	Tryptophan
	100 mg/l	Adenine
	18 g/l	Agar
	2%	Glucose
	0 - 15 mM	3-AT

Plant Culture

	Concentration	Content
MS pH 5.7	4.33 g/l	Murashige and Skoog with vitamins
	1% (3%)	Sucrose
	10 g/l	Plant agar

	Concentration	Content
Plant DNA Extraction Buffer pH 7.5	200 mM	Tris-HCl
	150 mM	NaCl
	25 mM	EDTA
	0.5%	SDS

Western Blot

	Component	Stacking gel		Separating gel		
		5%	7.5%	10%	12.5%	15%
SDS-PAGE	Gel buffer (ml)	0.345	2.815	2.815	2.815	2.815
	H ₂ O (ml)	1.835	2.670	2.045	1.420	0.800
	10% SDS (μl)	27.5	75	75	75	75
	30% acrylamide (ml)	0.460	1.875	2.500	3.125	3.750
	TEMED (μl)	3	6	6	6	6
	10% APS (μl)	15	60	60	60	60

Stacking gel buffer: 1 M TRIS/HCl pH 6.8 **Separating gel buffer:** 1 M TRIS/HCl pH 8.8

	Concentration	Content
10 x SDS running buffer	144 g/l	Glycine
	30 g/l	Tris
	10 g/l	SDS

	Concentration	Content		Concentration	Content
10 x Carbonate blotting buffer	8.4 g/l	NaHCO ₃	Towbin buffer	7,36 g/l	Glycine
	3.1 g/l	Na ₂ CO ₃		1,21 g/l	TRIS
	8.3 ml	10% SDS		100 ml	MeOH (add fresh)

	Concentration	Content
10 x PBS	25.6 g/l	Na ₂ HPO ₄ ·7H ₂ O
	80 g/l	NaCl
	2 g/l	KCl
	2 g/l	KH ₂ PO ₄

PBS-T: 1 x PBS containing 0.1% TWEEN 20

Antibodies

Primary antibody (usually in 2% milk in TBS)		Secondary antibody (usually in 5% milk in TBS)	
α-HA (Roche, unconjugated)	1:4000	α-rat IgG-HRP	1:5000
α-CSN4 (Biomol)	1:1000	α -rabbit IgG-HRP	1:80000
α-RBX1 (Biomol)	1:2000	α -rabbit IgG-HRP	1:80000
α-CUL4 (Genschik)	1:2000	α -rabbit IgG-HRP	1:80000
α-GFP (Roche monoclonal)	1:5000	α -mouse IgG-HRP	1:50000
α-HSC70 (Stressgen)	1:20000	α -mouse IgG-HRP	1:50000
α-HSP90 (SantaCruz)	1:10000	α -rabbit IgG-HRP	1:80000
α-PEPC (Rockland/Biomol)	1:5000	α -rabbit IgG-HRP	1:80000
α-Tubulin (Sigma)	1:10000	α -mouse IgG-HRP	1:50000
α-Histone H3 (Abcam)	1:5000	α -rabbit IgG-HRP	1:80000
α-HA-HRP (Roche)	1:1000		

	Concentration	Content
TAE pH 7.5	200 mM	Tris-HCl
	150 mM	NaCl
	25 mM	EDTA
	0.5%	SDS

Antibiotics	Stock solution	Final concentration
Kanamycin	100 mg/ml	50 mg/l
Ampicillin	100 mg/ml	50 mg/l
Gentamicin	50 mg/ml	50 mg/l
Chloramphenicol	30 mg/ml	30 mg/l
Rifampicin	25 mg/ml	25 mg/l
Cefotaxime	200 mg/ml	200 mg/l

LUMIER

	Concentration	Content
HEK cell lysis buffer	22 mM	Tris/HCl pH 7.5
	275 mM	NaCl
	11 mM	Na ₂ EDTA pH 8.0
	1.1%	Triton X-100
	10 mM	DTT
	1 tablet/10 ml	Complete (Roche) protease inhibitor cocktail
	Concentration	Content
Renilla detection buffer	1.1 M	NaCl
	2.2 mM	Na ₂ EDTA pH 8.0
	220 mM	K _x PO ₄ pH 5.1
	10 mM	DTT
	0.44 mg/ml	BSA
	0.1%(v/v)	Renilla luciferase substrate (coelenterazine)

5.1.2 Organisms

Bacterial Strains

Name	Organism	Application
<i>DH5α</i>	<i>E. coli</i>	general cloning
<i>DB3.1</i>	<i>E. coli</i>	Gateway cloning with <i>ccdB</i>
BL21(DE3)	<i>E. coli</i>	protein expression in bacteria
LBA4404	<i>Rhizobium radiobacter</i>	cell culture transformation (<i>Arabidopsis</i>)
pBBR1MCS.virGN54D	<i>Rhizobium radiobacter</i>	plant transformation (<i>Arabidopsis</i> and <i>Nicotiana</i>)
GV3101 pMP90RK	<i>Rhizobium radiobacter</i>	plant transformation (<i>Arabidopsis</i> and <i>Nicotiana</i>)

Yeast Strains

Name	Genotype	Application
Y187	<i>MATα</i> , <i>ura3-52</i> , <i>his3-200</i> , <i>ade2-101,112</i> <i>gcn2::LEU2</i> , <i>trp1-901</i> , <i>leu2-3</i> , <i>gal4-Δ</i> , <i>gal80-Δ</i> , <i>met-</i> , <i>URA3::GAL1_{UAS}-GAL1_{TATA}-LacZ</i> , <i>MEL1</i>	Screening
AH109	<i>MATα</i> , <i>trp1-901</i> , <i>leu2-3</i> , <i>112</i> <i>gcn2::LEU2</i> , <i>ura3-52</i> , <i>his3-200</i> , <i>gal4-Δ</i> , <i>gal80-Δ</i> , <i>LYS2:: GAL1_{UAS}- GAL1_{TATA}-HIS3-GAL1_{TATA}-LacZ</i>	Yeast two-hybrid
YM4271	<i>MATα</i> , <i>ura3-52</i> , <i>his3-200</i> , <i>ade2-101</i> , <i>lys2-801</i> , <i>leu2-3,112</i> <i>gcn2::LEU2</i> , <i>trp1-901</i> , <i>tyr1-501</i> , <i>gal4-Δ512</i> , <i>gal80-Δ538</i> , <i>ade5::hisG</i>	Yeast one-hybrid

5.1.3 Oligonucleotides

All primers were obtained from either Invitrogen (Karlsruhe) or Sigma (Munic, Steinheim). For detailed information about all primers that I used, see table 5.1 below.

Table 5.1 Oligonucleotides

Primer ID	Primer Name	Primer Sequence
pBP0001	attB-AN11-F	GGGGACAAGTTTGTACAAAAAAGCAGGCTTAATGGAAAATTCAAGTCAAGA
pBP0002	attB-AN11-R	GGGGACCACTTTGTACAAGAAAGCTGGGTTTACTTTAAGCAATTGCAACT
pBP0003	attB-JAF13-F	GGGGACAAGTTTGTACAAAAAAGCAGGCTTAATGGCTATGGGATGCAAAGA
pBP0004	attB-JAF13-R	GGGGACCACTTTGTACAAGAAAGCTGGGTTAGATTTCCAGACTACTCGCT
pBP0005	attB-AN1-F	GGGGACAAGTTTGTACAAAAAAGCAGGCTTAATGCAGCTGCAAACCATGTT
pBP0006	attB-AN1-R	GGGGACCACTTTGTACAAGAAAGCTGGGTTTTAACTCTAGGGATTAAGT
pBP0007	attB-AN2-F	GGGGACAAGTTTGTACAAAAAAGCAGGCTTAATGAGTACTTCTAATGCATC
pBP0008	attB-AN2-R	GGGGACCACTTTGTACAAGAAAGCTGGGTTCTAACTAACTAAATCCATA
pBP0009	attB-AN4-F	GGGGACAAGTTTGTACAAAAAAGCAGGCTTAATGAAAACCTTCTGTTTTTAC
pBP0010	attB-AN4-R	GGGGACCACTTTGTACAAGAAAGCTGGGTTCTATAGTAATTCCCAGAGGT
pBP0011	attB-PH4-F	GGGGACAAGTTTGTACAAAAAAGCAGGCTTAATGAGAACCCCATCATCATC
pBP0012	attB-PH4-R	GGGGACCACTTTGTACAAGAAAGCTGGGTTCTAACTGGGATTATATTGAT
pBP0013	attB-PAC1-F	GGGGACAAGTTTGTACAAAAAAGCAGGCTTAATGGACCCACCCAAGCCGCC
pBP0014	attB-PAC1-R	GGGGACCACTTTGTACAAGAAAGCTGGGTTGACCCTAAGAAGCTGGACCT
pBP0015	attB-MP1-F	GGGGACAAGTTTGTACAAAAAAGCAGGCTTAATGGGCGGAGTCGGCGAAGG
pBP0016	attB-MP1-R	GGGGACCACTTTGTACAAGAAAGCTGGGTTTCAGACCCTGAGAATCTGAA
pBP0017	attB-R-F	GGGGACAAGTTTGTACAAAAAAGCAGGCTTAATGGCGCTTTCAGCTTCCCG
pBP0018	attB-R-R	GGGGACCACTTTGTACAAGAAAGCTGGGTTTCACCGCTTCCCTATAGCTT
pBP0019	attB-B-F	GGGGACAAGTTTGTACAAAAAAGCAGGCTTAATGGCCCTGTCTGCTTGTCC
pBP0020	attB-B-R	GGGGACCACTTTGTACAAGAAAGCTGGGTTCTCTTCCGATAGCCTTCC
pBP0021	attB-PL-F	GGGGACAAGTTTGUACAAAAAAGCAGGCTTAATGGGCCGCAGGGCTTGCTG
pBP0022	attB-PL-R	GGGGACCACTTTGTACAAGAAAGCTGGGTTAACCAGCUTGCTCAGCAGTAT
pBP0023	attB-C1-F	GGGGACAAGTTTGTACAAAAAAGCAGGCTTAATGGGGAGGAGGGCGTGTTG
pBP0024	attB-C1-R	GGGGACCACTTTGTACAAGAAAGCTGGGTTTCACGCAAGCTGCCCGGCCG
pBP0025	attB-P1-F	GGGGACAAGTTTGTACAAAAAAGCAGGCTTAATGGGGAGGGCGCCGTGCTG
pBP0026	attB-P1-R	GGGGACCACTTTGTACAAGAAAGCTGGGTTGAACGAGTCGGACAGGAGCC
pBP0027	GhACT1-F	CTGTGATAATGGAAGTGAATGGT
pBP0028	GhACT1-R	TATCATCCAGTTGCTCACAATACCAT
pBP0029	attB-GhTTG1-F	GGGGACAAGTTTGTACAAAAAAGCAGGCTTAATGGAGAATTCAACTCAGGA
pBP0030	attB-GhTTG1-R	GGGGACCACTTTGTACAAGAAAGCTGGGTTTCAAACCTTTGAGAAGCTGCA
pBP0031	attB-GhTTG2-F	GGGGACAAGTTTGTACAAAAAAGCAGGCTTAATGGCCGCTAGCAGCGATCC
pBP0032	attB-GhTTG2-R	GGGGACCACTTTGTACAAGAAAGCTGGGTTTCATACCCTGAGAATCTGAA
pBP0033	attB-GhTTG3-F	GGGGACAAGTTTGTACAAAAAAGCAGGCTTAATGGAGAATTCAACTCAAGA
pBP0034	attB-GhTTG3-R	GGGGACCACTTTGTACAAGAAAGCTGGGTTTCAAACCTTTGAGAAGCTGCA

Table 5.1 Cont.

Primer ID	Primer Name	Primer Sequence
pBP0035	attB-GhTTG4-F	GGGGACAAGTTTGTACAAAAAAGCAGGCTTAATGACGGCCACCAGCGATCC
pBP0036	attB-GhTTG4-R	GGGGACCACTTTGTACAAGAAAGCTGGGTTTCATACCTTAGAATCTGAA
pBP0037	attB-GhDEL61-F	GGGGACAAGTTTGTACAAAAAAGCAGGCTTAATGGCTACTACTGGGGTTCA
pBP0038	attB-GhDEL61-R	GGGGACCACTTTGTACAAGAAAGCTGGGTTTTACACAAAGGTTAAAGATT
pBP0039	attB-GhDEL65-F	GGGGACAAGTTTGTACAAAAAAGCAGGCTTAATGTCTACTGGAGTTCAACA
pBP0040	attB-GhDEL65-R	GGGGACCACTTTGTACAAGAAAGCTGGGTTTCAACACTTGCTAGCAATTC
pBP0041	attB-GhMYB2-F	GGGGACAAGTTTGTACAAAAAAGCAGGCTTAATGGCTCCAAAGAAGGCTGG
pBP0042	attB-GhMYB2-R	GGGGACCACTTTGTACAAGAAAGCTGGGTTTTATACCATTGCTAATGGAT
pBP0043	attB-GhMYB3-F	GGGGACAAGTTTGTACAAAAAAGCAGGCTTAATGGAGCAAATTTGTCCT
pBP0044	attB-GhMYB3-R	GGGGACCACTTTGTACAAGAAAGCTGGGTTTTAAACTTAAACCGTCGT
pBP0045	attB-GhMYB25-F	GGGGACAAGTTTGTACAAAAAAGCAGGCTTAATGCAGCAGTCTCCATGTAG
pBP0046	attB-GhMYB25-R	GGGGACCACTTTGTACAAGAAAGCTGGGTTTCAAAGACAGAAGAACCAG
pBP0047	attB-GhMYB109-F	GGGGACAAGTTTGTACAAAAAAGCAGGCTTAATGCTCCCGCCGCCATGGC
pBP0048	attB-GhMYB109-R	GGGGACCACTTTGTACAAGAAAGCTGGGTTCTAGCTAAGATGAAAAGAAG
pBP0049	attB-GhRLC1-F	GGGGACAAGTTTGTACAAAAAAGCAGGCTTAATGGAGGGCTCATCTTTAAG
pBP0050	attB-GhRLC1-R	GGGGACCACTTTGTACAAGAAAGCTGGGTTCTATGGGTTGAACACATTCC
pBP0051	LBb1.3	ATTTTGCCGATTTCCGGAAC
pBP0052	SALK_048673 LP	CGAGGAAGACAACCAACCAG
pBP0053	SALK_048673 RP	AGTTCCACAACCCATCAAGC
pBP0054	SALK_030966 LP	GGCCATAAAACGACAAGAAG
pBP0055	SALK_030966 RP	TACCACGTTTTCTGATCTCCG
pBP0056	AtGL3-3HA_attB-F	GGGGACAAGTTTGTACAAAAAAGCAGGCTTAATGGCTACCGGACAAAACAG
pBP0057	AtGL3-3HA-R	GAACATCGTATGGGTAACAGATCCATGCAAC
pBP0058	AtTTG1-3HA_attB-F	GGGGACAAGTTTGTACAAAAAAGCAGGCTTAATGGATAATTCAGCTCCAGA
pBP0059	AtTTG1-3HA-R	GAACATCGTATGGGTAACACTCTAAGGAGCTGC
pBP0060	3HA(GL3)-F	GTTGCATGGATCTGTTACCCATACGATGTTTCTGACTATGCGGGCTATCCGTATGACGTC
pBP0061	3HA(TTG1)-F	GCAGCTCCTTAGAGTTTACCCATACGATGTTTCTGACTATGCGGGCTATCCGTATGACGTC
pBP0062	3HA-R	AGCGTAATCTGGAACGTCATATGGATAGGATCCTGCATAGTCCGGGACGTCATACGGATAGC
pBP0063	3HA-attB-R	GGGGACCACTTTGTACAAGAAAGCTGGGTTTCAAGCGTAATCTGGAACGT
pBP0064	ProTT8-SgsI-F	GGCGCGCCTTACCCATTATTTTTCTACAATTATGTGGT
pBP0065	ProTT8-XhoI-R	TCTCGAGGCTCTCTCTCTAAAAATCTTATAACTTTG
pBP0066	TRY-attb-F	GGGGACAAGTTTGTACAAAAAAGCAGGCTTAATGGATAAACTGACCGTCCG
pBP0067	TRY(3HA)-R	CATCGTATGGGTAGGAAGGATAGATAGAAAAGCGAG
pBP0068	(TRY)3HA-F	CTATCCTTCTACCCATACGATGTTTCTGACTATGCGGGCTATCCGTATGACGTC

Table 5.1 Cont.

Primer ID	Primer Name	Primer Sequence
pBP0069	CPC-attb-F	GGGGACAAGTTTGTACAAAAAAGCAGGCTTAATGTTTCGTTTCAGACAAGGC
pBP0070	CPC(3HA)-R	GAACATCGTATGGGTATTTCTAAAAAAGTCTCTTCGTCT
pBP0071	(CPC)3HA-F	TTAGGAAATACCCATACGATGTTTCCTGACTATGCGGGCTATCCGTATGACGTC
pBP0072	GL3-F	CGTCTTCAACATTGGTGAAGGAATG
pBP0073	GL3-R _S	TGGTACCAATCTCAACGACTCCTCCAA
pBP0074	GL3-R _L	GCGCTTCTTCTCTAAAACCGCATGGT
pBP0075	ACT2-F	AGTGGTCGTACAACCGGTATTGT
pBP0076	ACT2-R _S	GATGGCATGAGGAAGAGAGAAAC
pBP0077	ACT2-R _L	GAAGCAAGAATGGAACCACCGAT
pBP0078	5'sgsI-pGL3	GGCGCGCCCGATCACTCAAATAGTAAT
pBP0079	3'XhoI-GL3-ex3	CTCGAGGTGGTACCAATCTCAACGACT

5.1.4 Constructs

All CDS entry clones were generated by amplifying the CDSs from start to stop codon from *Arabidopsis thaliana* (*At*), *Arabis alpina* (*Aa*), *Gossypium hirsutum* (*Gh*), *Petunia hybrid* (*Ph*) and *Zea mays* (*Zm*) and then cloning into pENTR1A/ pENTR4 or BP recombination in pDONR201/207. All constructs used and created in this work are listed in Table 5.2.

Table 5.2 Constructs used in this study

Application	Plasmid name	Created by
Yeast vector	pC-ACT2-attR_w/o	Martina Pesch
	pC-ACT2-attR_GhTTG1	me
	pC-ACT2-attR_GhTTG2	me
	pC-ACT2-attR_GhTTG3	me
	pC-ACT2-attR_GhTTG4	me
	pC-ACT2-attR_AN11	me
	pC-ACT2-attR_PAC1	me
	pC-ACT2-attR_MP1	me
	pC-ACT2-attR_GhDEL61	me
	pC-ACT2-attR_GhDEL65	me
	pC-ACT2-attR_PhAN1	me
	pC-ACT2-attR_PhJAF13	me
	pC-ACT2-attR_ZmR(Lc)	me
	pC-ACT2-attR_ZmR(S)	me
	pC-ACT2-attR_ZmB	me
	pC-ACT2-attR_GhMYB2	me
	pC-ACT2-attR_GhMYB3	me
	pC-ACT2-attR_GhMYB25	me
	pC-ACT2-attR_GhRLC1(geno)	me
	pC-ACT2-attR_GhRLC1(CDS)	me
	pC-ACT2-attR_PhAN2	me
	pC-ACT2-attR_PhAN4	me
	pC-ACT2-attR_PhPH4	me
	pC-ACT2-attR_ZmC1	me
	pC-ACT2-attR_ZmPL	me
	pC-ACT2-attR_ZmP1	me
	pAS-attR_w/o	Martina Pesch
	pAS-attR_GhTTG1	me
	pAS-attR_GhTTG2	me
	pAS-attR_GhTTG3	me
	pAS-attR_GhTTG4	me
	pAS-attR_AN11	me
	pAS-attR_PAC1	me
	pAS-attR_GhDEL61	me
pAS-attR_GhDEL65	me	
pAS-attR_PhAN1	me	
pAS-attR_PhJAF13	me	
pAS-attR_ZmR(Lc)	me	
pAS-attR_ZmR(S)	me	
pAS-attR_ZmB	me	
pAS-attR_GhMYB2	me	
pAS-attR_GhMYB3	me	
pAS-attR_GhMYB25	me	
pAS-attR_GhRLC1(geno)	me	

	pAS-attR_GhRLC1(CDS)	me
	pAS-attR_PhAN2	me
	pAS-attR_PhAN4	me
	pAS-attR_PhPH4	me
	pAS-attR_ZmC1	me
	pAS-attR_ZmPL	me
	pAS-attR_ZmP1	me
LUMIER vectors	pcDNA3-Rluc-GW_AtTTG1	me
	pcDNA3-Rluc-GW_AtTTG1-3HA	me
	pcDNA3-Rluc-GW_AtGL3	me
	pcDNA3-Rluc-GW_AtGL3-3HA	me
	pcDNA3-Rluc-GW_AtEGL3	me
	pcDNA3-Rluc-GW_AtTT8	me
	pcDNA3-Rluc-GW_AtMYC1	me
	pcDNA3-Rluc-GW_AtGL1	me
	pcDNA3-Rluc-GW_AtWER	me
	pcDNA3-Rluc-GW_AtPAP1	me
	pcDNA3-Rluc-GW_AtPAP2	me
	pcDNA3-Rluc-GW_AtTT2	me
	pcDNA3-Rluc-GW_AtMYB61	me
	pcDNA3-Rluc-GW_AaTTG1	me
	pcDNA3-Rluc-GW_AaGL3	me
	pcDNA3-Rluc-GW_AaEGL3	me
	pcDNA3-Rluc-GW_AaTT8	me
	pcDNA3-Rluc-GW_AaMYC1	me
	pcDNA3-Rluc-GW_AaGL1	me
	pcDNA3-Rluc-GW_AaWER	me
	pcDNA3-Rluc-GW_AaPAPL	me
	pcDNA3-Rluc-GW_AaMYB23	me
	pcDNA3-Rluc-GW_GhTTG1	me
	pcDNA3-Rluc-GW_AtMYB61	me
	pcDNA3-Rluc-GW_GhTTG1	me
	pcDNA3-Rluc-GW_GhTTG2	me
	pcDNA3-Rluc-GW_GhTTG3	me
	pcDNA3-Rluc-GW_GhTTG4	me
	pcDNA3-Rluc-GW_AN11	me
	pcDNA3-Rluc-GW_PAC1	me
	pcDNA3-Rluc-GW_MP1	me
	pcDNA3-Rluc-GW_GhDEL61	me
	pcDNA3-Rluc-GW_GhDEL65	me
	pcDNA3-Rluc-GW_PhAN1	me
	pcDNA3-Rluc-GW_PhJAF13	me
	pcDNA3-Rluc-GW_ZmR(Lc)	me
	pcDNA3-Rluc-GW_ZmR(S)	me
	pcDNA3-Rluc-GW_ZmB	me
	pcDNA3-Rluc-GW_GhMYB2	me
	pcDNA3-Rluc-GW_GhMYB3	me
	pcDNA3-Rluc-GW_GhMYB25	me
	pcDNA3-Rluc-GW_GhRLC1(geno)	me
	pcDNA3-Rluc-GW_GhRLC1(CDS)	me
	pcDNA3-Rluc-GW_PhAN2	me
	pcDNA3-Rluc-GW_PhAN4	me
	pcDNA3-Rluc-GW_PhPH4	me
	pcDNA3-Rluc-GW_ZmC1	me
	pcDNA3-Rluc-GW_ZmPL	me
	pcDNA3-Rluc-GW_ZmP1	me

pcDNA3-Rluc-GW_w/o	Martina Pesch
pTREX-dest30-ntProtA_AtTTG1	me
pTREX-dest30-ntProtA_AtTTG1-3HA	me
pTREX-dest30-ntProtA_AtGL3	me
pTREX-dest30-ntProtA_AtGL3-3HA	me
pTREX-dest30-ntProtA_AtEGL3	me
pTREX-dest30-ntProtA_AtTT8	me
pTREX-dest30-ntProtA_AtMYC1	me
pTREX-dest30-ntProtA_AtGL1	me
pTREX-dest30-ntProtA_AtWER	me
pTREX-dest30-ntProtA_AtPAP1	me
pTREX-dest30-ntProtA_AtPAP2	me
pTREX-dest30-ntProtA_AtTT2	me
pTREX-dest30-ntProtA_AtMYB61	me
pTREX-dest30-ntProtA_AaTTG1	me
pTREX-dest30-ntProtA_AaGL3	me
pTREX-dest30-ntProtA_AaEGL3	me
pTREX-dest30-ntProtA_AaTT8	me
pTREX-dest30-ntProtA_AaMYC1	me
pTREX-dest30-ntProtA_AaGL1	me
pTREX-dest30-ntProtA_AaWER	me
pTREX-dest30-ntProtA_AaPAPL	me
pTREX-dest30-ntProtA_AaMYB23	me
pTREX-dest30-ntProtA_GhTTG1	me
pTREX-dest30-ntProtA_AtMYB61	me
pTREX-dest30-ntProtA_GhTTG1	me
pTREX-dest30-ntProtA_GhTTG2	me
pTREX-dest30-ntProtA_GhTTG3	me
pTREX-dest30-ntProtA_GhTTG4	me
pTREX-dest30-ntProtA_AN11	me
pTREX-dest30-ntProtA_PAC1	me
pTREX-dest30-ntProtA_MP1	me
pTREX-dest30-ntProtA_GhDEL61	me
pTREX-dest30-ntProtA_GhDEL65	me
pTREX-dest30-ntProtA_PhAN1	me
pTREX-dest30-ntProtA_PhJAF13	me
pTREX-dest30-ntProtA_ZmR(Lc)	me
pTREX-dest30-ntProtA_ZmR(S)	me
pTREX-dest30-ntProtA_ZmB	me
pTREX-dest30-ntProtA_GhMYB2	me
pTREX-dest30-ntProtA_GhMYB3	me
pTREX-dest30-ntProtA_GhMYB25	me
pTREX-dest30-ntProtA_GhRLC1(geno)	me
pTREX-dest30-ntProtA_GhRLC1(CDS)	me
pTREX-dest30-ntProtA_PhAN2	me
pTREX-dest30-ntProtA_PhAN4	me
pTREX-dest30-ntProtA_PhPH4	me
pTREX-dest30-ntProtA_ZmC1	me
pTREX-dest30-ntProtA_ZmPL	me
pTREX-dest30-ntProtA_ZmP1	me
pTREX-dest30-ntProtA_w/o	Martina Pesch
pTREX-dest30-ntYFP_AtTTG1	me
pTREX-dest30-ntYFP_AtGL3	me
pTREX-dest30-ntYFP_AtEGL3	me
pTREX-dest30-ntYFP_AtTT8	me
pTREX-dest30-ntYFP_AtMYC1	me
pTREX-dest30-ntYFP_AtGL1	me
pTREX-dest30-ntYFP_AtWER	me
pTREX-dest30-ntYFP_AtPAP1	me

	pTREX-dest30-ntYFP_ <i>AtPAP2</i>	me
	pTREX-dest30-ntYFP_ <i>AtTT2</i>	me
	pTREX-dest30-ntYFP_ <i>AtMYB61</i>	me
	pTREX-dest30-ntYFP_ <i>AaTTG1</i>	me
	pTREX-dest30-ntYFP_ <i>AaGL3</i>	me
	pTREX-dest30-ntYFP_ <i>AaEGL3</i>	me
	pTREX-dest30-ntYFP_ <i>AaTT8</i>	me
	pTREX-dest30-ntYFP_ <i>AaMYC1</i>	me
	pTREX-dest30-ntYFP_ <i>AaGL1</i>	me
	pTREX-dest30-ntYFP_ <i>AaWER</i>	me
	pTREX-dest30-ntYFP_ <i>AaPAPL</i>	me
	pTREX-dest30-ntYFP_ <i>AaMYB23</i>	me
	pTREX-dest30-ntYFP_ <i>GhTTG1</i>	me
	pTREX-dest30-ntYFP_ <i>AtMYB61</i>	me
	pTREX-dest30-ntYFP_ <i>GhTTG1</i>	me
	pTREX-dest30-ntYFP_ <i>GhTTG2</i>	me
	pTREX-dest30-ntYFP_ <i>GhTTG3</i>	me
	pTREX-dest30-ntYFP_ <i>GhTTG4</i>	me
	pTREX-dest30-ntYFP_ <i>AN11</i>	me
	pTREX-dest30-ntYFP_ <i>PAC1</i>	me
	pTREX-dest30-ntYFP_ <i>MP1</i>	me
	pTREX-dest30-ntYFP_ <i>GhDEL61</i>	me
	pTREX-dest30-ntYFP_ <i>GhDEL65</i>	me
	pTREX-dest30-ntYFP_ <i>PhAN1</i>	me
	pTREX-dest30-ntYFP_ <i>PhJAF13</i>	me
	pTREX-dest30-ntYFP_ <i>ZmR(Lc)</i>	me
	pTREX-dest30-ntYFP_ <i>ZmR(S)</i>	me
	pTREX-dest30-ntYFP_ <i>ZmB</i>	me
	pTREX-dest30-ntYFP_ <i>GhMYB2</i>	me
	pTREX-dest30-ntYFP_ <i>GhMYB3</i>	me
	pTREX-dest30-ntYFP_ <i>GhMYB25</i>	me
	pTREX-dest30-ntYFP_ <i>GhRLC1(geno)</i>	me
	pTREX-dest30-ntYFP_ <i>GhRLC1(CDS)</i>	me
	pTREX-dest30-ntYFP_ <i>PhAN2</i>	me
	pTREX-dest30-ntYFP_ <i>PhAN4</i>	me
	pTREX-dest30-ntYFP_ <i>PhPH4</i>	me
	pTREX-dest30-ntYFP_ <i>ZmC1</i>	me
	pTREX-dest30-ntYFP_ <i>ZmPL</i>	me
	pTREX-dest30-ntYFP_ <i>ZmP1</i>	me
	pTREX-dest30-ntYFP_w/o	Alexandra Steffens
Plant vectors	pAMPAT-35S-GW_ <i>AtTTG1</i>	me
	pAMPAT-35S-GW_ <i>AtGL3</i>	me
	pAMPAT-35S-GW_ <i>AtEGL3</i>	me
	pAMPAT-35S-GW_ <i>AtTT8</i>	me
	pAMPAT-35S-GW_ <i>AtMYC1</i>	me
	pAMPAT-35S-GW_ <i>AtGL1</i>	me
	pAMPAT-35S-GW_ <i>AtWER</i>	me
	pAMPAT-35S-GW_ <i>AtPAP1</i>	me
	pAMPAT-35S-GW_ <i>AtPAP2</i>	me
	pAMPAT-35S-GW_ <i>AtTT2</i>	me
	pAMPAT-35S-GW_ <i>AtMYB61</i>	me
	pAMPAT-35S-GW_ <i>AaTTG1</i>	me
	pAMPAT-35S-GW_ <i>AaGL3</i>	me
	pAMPAT-35S-GW_ <i>AaEGL3</i>	me
	pAMPAT-35S-GW_ <i>AaTT8</i>	me
	pAMPAT-35S-GW_ <i>AaMYC1</i>	me
	pAMPAT-35S-GW_ <i>AaGL1</i>	me

pAMPAT-35S-GW_AaWER	me
pAMPAT-35S-GW_AaPAPL	me
pAMPAT-35S-GW_AaMYB23	me
pAMPAT-35S-GW_GhTTG1	me
pAMPAT-35S-GW_GhTTG2	me
pAMPAT-35S-GW_GhTTG3	me
pAMPAT-35S-GW_GhTTG4	me
pAMPAT-35S-GW_AN11	me
pAMPAT-35S-GW_PAC1	me
pAMPAT-35S-GW_MP1	me
pAMPAT-35S-GW_GhDEL61	me
pAMPAT-35S-GW_GhDEL65	me
pAMPAT-35S-GW_PhAN1	me
pAMPAT-35S-GW_PhJAF13	me
pAMPAT-35S-GW_ZmR(Lc)	me
pAMPAT-35S-GW_ZmR(S)	me
pAMPAT-35S-GW_ZmB	me
pAMPAT-35S-GW_GhMYB2	me
pAMPAT-35S-GW_GhMYB3	me
pAMPAT-35S-GW_GhMYB25	me
pAMPAT-35S-GW_GhRLC1(geno)	me
pAMPAT-35S-GW_GhRLC1(CDS)	me
pAMPAT-35S-GW_PhAN2	me
pAMPAT-35S-GW_PhAN4	me
pAMPAT-35S-GW_PhPH4	me
pAMPAT-35S-GW_ZmC1	me
pAMPAT-35S-GW_ZmPL	me
pAMPAT-35S-GW_ZmP1	me
pAMPAT-proTT8-GW_AtGL3	me
pAMPAT-proTT8-GW_AtEGL3	me
pAMPAT-proTT8-GW_AtTT8	me
pAMPAT-proTT8-GW_AtMYC1	me
pAMPAT-proTT8-GW_AaGL3	me
pAMPAT-proTT8-GW_AaEGL3	me
pAMPAT-proTT8-GW_AaTT8	me
pAMPAT-proTT8-GW_AaMYC1	me
pAMPAT-proTT8-GW_GhDEL61	me
pAMPAT-proTT8-GW_GhDEL65	me
pAMPAT-proTT8-GW_PhAN1	me
pAMPAT-proTT8-GW_PhJAF13	me
pAMPAT-proTT8-GW_ZmR(Lc)	me
pAMPAT-proTT8-GW_ZmR(S)	me
pAMPAT-proTT8-GW_ZmB	me
pAMPAT-35S:GUS	me
pAMPAT-proGL3:GUS	me
pAMPAT-proGL3:GL3(intron2)-GUS	me

5.1.4.1 Yeast vectors

Fusions of the CDSs to the GAL4 binding domain were produced in pAS-attR through LR reaction. As a negative control, the vector pAS-attR was recombined with pENTR1A-w/o-ccdB.

Meanwhile, the CDSs of each gene were fused to the coding sequence for the GAL4 activation domain via LR in pC-ACT2-attR. As a negative control, the vector pC-ACT2-attR was recombined with pENTR1A-w/o-*ccdB*.

5.1.4.2 LUMIER vectors

Three different destination vectors were used for subsequent LR reactions. pcDNA3-Rluc-GW and pTREX-dest30 (Invitrogen) enable the N-terminal fusion of *Renilla reniformis* and *Staphylococcus aureus* protein, respectively, were described before [178].

Defined genes were N-terminal fused to the *Staphylococcus aureus* protein A sequence in pTREX-dest30-ntProtA by LR reaction. As negative control, the vector pTREX-dest30-ntProtA was recombined with pENTR1A-w/o-*ccdB*.

Renilla reniformis Luciferase-gene generated by LR reaction, fusing the full-length *Renilla* luciferase sequence N-terminal to the coding sequences in pcDNA3-Rluc-GW. Also pENTR1A-w/o-*ccdB* was recombined to this vector as a negative control.

YFP-tagged proteins and the control without any CDS were created by LR recombination of pTREX-dest30-YFP with the respective entry clones.

5.1.4.3 Plant vectors

All CDS or genomic fragments of MBW homologs were cloned into Donor vectors by BP reactions (Invitrogen). Then recombination of the corresponding entry clones with the 35S promoter driven vector pAMPAT-35S-GW (GenBank accession no. AY436765 [149]).

5.2 Methods

5.2.1 LUMIER (LUminescence-based Mammalian IntERactome)

5.2.1.1 6-well plate for pairwise assay

For LUMIER assays, each protein was transiently expressed in HEK293TM cells (BioCat/SBI: LV900A-1) as hybrid proteins either with the *Staphylococcus aureus* protein A or with the *Renilla reniformis* luciferase fused to their amino N termini. Transfection and cell harvesting was done as described before [149, 178]. After 48 hours, the medium was removed; cells were washed three times with PBS.

Lysis of cells with 150 µl-250 µl lysis buffer for each well. Combination of two hybrid proteins was approached after 1hr lysis. Each combination was prepared in duplicate. Protein immunoprecipitation with sheep-anti-rabbit IgG-coated magnetic beads in a

magnetic holder and luminescence measurement after pulldown in a microtitre plate reader was done as described previously [178]. The pulldown was also performed with untransfected cells or with cells solely expressing Luciferase-protein to exclude any nonspecific signal from the cell lysate and non-specific binding of Luciferase-protein to the beads, respectively.

The percentage of Rluc on the beads compared with the lysate was calculated by dividing the Rluc activity on the beads by the Rluc activity in the same amount of lysate used in the pull-down assay (Input).

5.2.1.2 9-cm petri dish for triple-components assay

The third protein was N termini fused with YFP in the backbone of pTREXdest30. Lysis of cells with 750µl-1000µl lysis buffer for each plate. Combination of three proteins was approached after 1hr lysis and normalization of YFP signal (TECAN). Each combination was prepared in duplicate and the total volume for incubation were equilibrated by untransfected cell lysate. The combination without additional YFP-fused protein was used as the reference. Cells solely expressing YFP-protein was also performed to exclude any nonspecific interference signal.

5.2.2 Yeast two hybrid

The yeast two-hybrid assays, using the yeast strain *AH109*, were done as described previously [181]. The transformed yeast cells were selected by plating them onto synthetic dropout selection medium lacking Leu and Trp (SD-LW). Interactions were analyzed by plating co-transformed yeast cells on synthetic dropout interaction medium lacking Leu, Trp, and His supplemented with 5, 10, and 15mM 3-amino-1, 2, 3-triazole (SD-LWH).

5.2.2.1 Yeast transformation

Yeast strain *AH109* was transformed by the LiAc-method. Cells were grown overnight in 10 ml YPAD medium. On the next day, 0.5-1 ml of the overnight culture was used to inoculate 50 ml YPAD and subsequently incubated at 30° C for 3-4 h at 250 rpm. At $OD_{600} = 0.7-1.0$ (sufficient for 10-15 transformations), cells were centrifuged at 3000 g for 5 min. The pellet was washed with 10 ml 0.1 M LiAc-solution (pH 7.5) and again centrifuged at 3000 g for 5 min. $n \times 240 \mu\text{l}$ PEG 3350, $n \times 36 \mu\text{l}$ 1 M LiAc, $n \times 50 \mu\text{l}$ ssDNA (2 mg/ ml, cooked for 10 min at 100°C) and $n \times 25 \mu\text{l}$ H₂O were added to the pellet whereby n stand for the number of transformations. The yeast cell suspension was mixed for 30 s and 350 µl was added to 2 µl of each DNA construct. DNA and

cells were mixed for 30 s and incubated for 40 min at 42°C. The cells were pelleted by centrifugation (3300 g, 30 s), re-suspended in 100 µl H₂O and plated on SD-LW plates.

5.2.3 Manipulation of plants and seeds

5.2.3.1 Arabidopsis strains and plant growth

The mutant alleles used in this study: *ttg1-1* is in the *Ler* background [28, 105]; *gl3-3* is in the *Col* background [182]; *egl3-77439* is in the *Col* background (TAIR accession 1008704039); *tt8-048673* is in the *Col* background (TAIR accession 1005848854); *gl3/egl3* in the *Col* background [183]; *gl3/egl3/tt8* (homozygous progeny by crossing *gl3/egl3* with *tt8-048673*); *gl1* in the *Col* background [157]. *pap1* insertion mutant seedlings (pst16228) is in the *No-0* background [184]; *pap2* in the *Col* background (salk_093731, TAIR accession 1005457343); *pap1/pap2* is generated by crossing *pap1* and *pap2*. Plants were grown on soil at 24°C with 16 h of light per day. All transgenic plant lines used and created in this work are listed in Table 5.3.

Table 5.3 Transgenic plant lines

Insertion (plasmid name)	Background	Created by
pAMPAT-35S-GW-AtTTG1	<i>ttg1-1</i>	me
pAMPAT-35S-GW-AaTTG1	<i>ttg1-1</i>	me
pAMPAT-35S-GW-GhTTG1	<i>ttg1-1</i>	me
pAMPAT-35S-GW-GhTTG2	<i>ttg1-1</i>	me
pAMPAT-35S-GW-GhTTG3	<i>ttg1-1</i>	me
pAMPAT-35S-GW-GhTTG4	<i>ttg1-1</i>	me
pAMPAT-35S-GW-PhAN11	<i>ttg1-1</i>	me
pAMPAT-35S-GW-ZmPAC1	<i>ttg1-1</i>	me
pAMPAT-35S-GW-ZmMP1	<i>ttg1-1</i>	me
pAMPAT-35S-GW-AtGL3	<i>gl3/egl3/tt8</i>	me
pAMPAT-35S-GW-AtEGL3	<i>gl3/egl3/tt8</i>	me
pAMPAT-35S-GW-AtTT8	<i>gl3/egl3/tt8</i>	me
pAMPAT-35S-GW-AtMYC1	<i>gl3/egl3/tt8</i>	me
pAMPAT-35S-GW-AaGL3	<i>gl3/egl3/tt8</i>	me
pAMPAT-35S-GW-AaEGL3	<i>gl3/egl3/tt8</i>	me
pAMPAT-35S-GW-AaTT8	<i>gl3/egl3/tt8</i>	me
pAMPAT-35S-GW-AaMYC1	<i>gl3/egl3/tt8</i>	me
pAMPAT-35S-GW-GhDEL61	<i>gl3/egl3/tt8</i>	me
pAMPAT-35S-GW-GhDEL65	<i>gl3/egl3/tt8</i>	me
pAMPAT-35S-GW-PhAN1	<i>gl3/egl3/tt8</i>	me
pAMPAT-35S-GW-PhJAF13	<i>gl3/egl3/tt8</i>	me
pAMPAT-35S-GW-ZmR(Lc)	<i>gl3/egl3/tt8</i>	me
pAMPAT-35S-GW-ZmR(S)	<i>gl3/egl3/tt8</i>	me
pAMPAT-35S-GW-ZmB	<i>gl3/egl3/tt8</i>	me
pAMPAT-ProTT8-GW-AtGL3	<i>gl3/egl3/tt8</i>	me
pAMPAT-ProTT8-GW-AtEGL3	<i>gl3/egl3/tt8</i>	me
pAMPAT-ProTT8-GW-AtTT8	<i>gl3/egl3/tt8</i>	me
pAMPAT-ProTT8-GW-AtMYC1	<i>gl3/egl3/tt8</i>	me
pAMPAT-ProTT8-GW-AaGL3	<i>gl3/egl3/tt8</i>	me
pAMPAT-ProTT8-GW-AaEGL3	<i>gl3/egl3/tt8</i>	me
pAMPAT-ProTT8-GW-AaTT8	<i>gl3/egl3/tt8</i>	me
pAMPAT-ProTT8-GW-AaMYC1	<i>gl3/egl3/tt8</i>	me

Table 5.3. Cont.

Insertion (plasmid name)	Background	Created by
pAMPAT-ProTT8-GW-GhDEL61	<i>gl3/egl3/tt8</i>	me
pAMPAT-ProTT8-GW-GhDEL65	<i>gl3/egl3/tt8</i>	me
pAMPAT-ProTT8-GW-PhAN1	<i>gl3/egl3/tt8</i>	me
pAMPAT-ProTT8-GW-PhJAF13	<i>gl3/egl3/tt8</i>	me
pAMPAT-ProTT8-GW-ZmR(Lc)	<i>gl3/egl3/tt8</i>	me
pAMPAT-ProTT8-GW-ZmR(S)	<i>gl3/egl3/tt8</i>	me
pAMPAT-ProTT8-GW-ZmB	<i>gl3/egl3/tt8</i>	me
pAMPAT-ProTT8-GW-AtGL3	<i>tt8</i>	me
pAMPAT-ProTT8-GW-AtEGL3	<i>tt8</i>	me
pAMPAT-ProTT8-GW-AtTT8	<i>tt8</i>	me
pAMPAT-ProTT8-GW-AtMYC1	<i>tt8</i>	me
pAMPAT-ProTT8-GW-AaGL3	<i>tt8</i>	me
pAMPAT-ProTT8-GW-AaEGL3	<i>tt8</i>	me
pAMPAT-ProTT8-GW-AaTT8	<i>tt8</i>	me
pAMPAT-ProTT8-GW-AaMYC1	<i>tt8</i>	me
pAMPAT-ProTT8-GW-GhDEL61	<i>tt8</i>	me
pAMPAT-ProTT8-GW-GhDEL65	<i>tt8</i>	me
pAMPAT-ProTT8-GW-PhAN1	<i>tt8</i>	me
pAMPAT-ProTT8-GW-PhJAF13	<i>tt8</i>	me
pAMPAT-ProTT8-GW-ZmR(Lc)	<i>tt8</i>	me
pAMPAT-ProTT8-GW-ZmR(S)	<i>tt8</i>	me
pAMPAT-ProTT8-GW-ZmB	<i>tt8</i>	me
pAMPAT-35S-GW-AtGL1	<i>gl1</i>	me
pAMPAT-35S-GW-AtWER	<i>gl1</i>	me
pAMPAT-35S-GW-AtPAP1	<i>gl1</i>	me
pAMPAT-35S-GW-AtPAP2	<i>gl1</i>	me
pAMPAT-35S-GW-AtTT2	<i>gl1</i>	me
pAMPAT-35S-GW-AtMYB61	<i>gl1</i>	me
pAMPAT-35S-GW-AaGL1	<i>gl1</i>	me
pAMPAT-35S-GW-AaWER	<i>gl1</i>	me
pAMPAT-35S-GW-AaPAPL	<i>gl1</i>	me
pAMPAT-35S-GW-AaMYB23	<i>gl1</i>	me
pAMPAT-35S-GW-GhMYB2	<i>gl1</i>	me
pAMPAT-35S-GW-GhMYB3	<i>gl1</i>	me
pAMPAT-35S-GW-GhMYB25	<i>gl1</i>	me
pAMPAT-35S-GW-GhRCL1	<i>gl1</i>	me
pAMPAT-35S-GW-PhAN2	<i>gl1</i>	me
pAMPAT-35S-GW-PhAN4	<i>gl1</i>	me
pAMPAT-35S-GW-PhPH4	<i>gl1</i>	me
pAMPAT-35S-GW-ZmC1	<i>gl1</i>	me
pAMPAT-35S-GW-ZmPL	<i>gl1</i>	me
pAMPAT-35S-GW-ZmP1	<i>gl1</i>	me
pAMPAT-35S-GW-AtGL1	<i>pap1/pap2</i>	me
pAMPAT-35S-GW-AtWER	<i>pap1/pap2</i>	me
pAMPAT-35S-GW-AtPAP1	<i>pap1/pap2</i>	me
pAMPAT-35S-GW-AtPAP2	<i>pap1/pap2</i>	me
pAMPAT-35S-GW-AtTT2	<i>pap1/pap2</i>	me
pAMPAT-35S-GW-AtMYB61	<i>pap1/pap2</i>	me
pAMPAT-35S-GW-AaGL1	<i>pap1/pap2</i>	me
pAMPAT-35S-GW-AaWER	<i>pap1/pap2</i>	me
pAMPAT-35S-GW-AaPAPL	<i>pap1/pap2</i>	me
pAMPAT-35S-GW-AaMYB23	<i>pap1/pap2</i>	me
pAMPAT-35S-GW-GhMYB2	<i>pap1/pap2</i>	me
pAMPAT-35S-GW-GhMYB3	<i>pap1/pap2</i>	me
pAMPAT-35S-GW-GhMYB25	<i>pap1/pap2</i>	me
pAMPAT-35S-GW-GhRCL1	<i>pap1/pap2</i>	me

Table 5.3. Cont.

Insertion (plasmid name)	Background	Created by
pAMPAT-35S-GW- <i>PhAN2</i>	<i>pap1/pap2</i>	me
pAMPAT-35S-GW- <i>PhAN4</i>	<i>pap1/pap2</i>	me
pAMPAT-35S-GW- <i>PhPH4</i>	<i>pap1/pap2</i>	me
pAMPAT-35S-GW- <i>ZmC1</i>	<i>pap1/pap2</i>	me
pAMPAT-35S-GW- <i>ZmPL</i>	<i>pap1/pap2</i>	me
pAMPAT-35S-GW- <i>ZmP1</i>	<i>pap1/pap2</i>	me

5.2.3.2 Seed sterilization

The sterilization solution is prepared by dissolution of 10 ml hypochloride sodium in 40 ml of distilled water supplement with 0.1% tween-20. 1 ml of sterilization solution is used to incubate 20 mg of seeds for 15 min, after seeds are washed with 75% ethanol for seconds. Thoroughly rinse the seeds by distill water several time in clean bench.

5.2.3.3 *Arabidopsis* crossing

For the most efficient crossings, we use a mother plant that have developed 5-6 inflorescences, and a father plants have formed siliques that indicate the pollen is fine. The emasculation of buds is performed with tweezer and manually pollinated with the mature anthers taken from the male plant. The seeds issues from the cross have to be harvest at maturity before silique dehiscence.

5.2.3.4 Genetic transformation of *Arabidopsis*

5 ml of YEB liquid medium with the appropriate antibiotics are inoculated with an isolated agrobacterium colony and cultured for 36 h at 28°C in a shaker (200 rpm). 1 ml of this pre-culture is used to inoculate 250 ml of YEB liquid medium. Incubation in a shaker (200 rpm) is performed to obtain stationary phase (OD=1.5-2.0, around 16-24h). Collect Agrobacterium cells by centrifugation at 4,000g for 10 min at room temperature, and gently resuspend cells in 1 volume of freshly made 5% (wt/vol) sucrose solution with a stirring bar. Add Silwet L-77 to a concentration of 0.02% (vol/vol) (100 ml per 500 ml of solution) and mix well immediately before dipping. Invert plants and dip aerial parts of plants in the Agrobacterium cell suspension for 10 s with gentle agitation. Drain the treated plants for 3–5 s. Cover dipped plants with a plastic cover or wrap them with plastic film. Lay down the treated plants on their sides for 16–24 h to maintain high humidity. The seeds harvested are sown in a selective solid medium or soil to obtain the primary transformed plants (T1 progeny) [185].

5.2.3.5 Trichome analysis

The first true leaf of soil-grown T1 progeny was labelled as leaf 1 and the following ones accordingly. Leaves 1–6 of two-week-old seedlings were observed for trichome analysis.

5.2.3.6 Root hair file analysis

H-files of 7-day-old 1/2MS plate-grown T2 progeny seedlings were microscopically identified by the position over cortical cell boundaries. Following 10 to 15 H-file cells per root and zone, the number of cells and root hairs in the flanking N-files was determined. Further, the length of continuous stretches of N-file cells carrying a root hair was determined.

5.2.3.7 Anthocyanin analysis

T2 progeny seedlings were grown on ½ MS germination medium containing 3% sucrose, and observed under Canon EOS 5D Mark (Canon, Krefeld, Germany) by Siegfried Werth or a Leica stereomicroscope (MZ FLIII) with the Multi-Focus and Montage option of the Leica Application Suite V3 (Leica Microsystems, Wetzlar, Germany).

5.2.3.8 Seed coat color analysis

T1 progeny seeds were captured using a Canon EOS 5D Mark (Canon, Krefeld, Germany) by Siegfried Werth or a Leica stereomicroscope (MZ FLIII) with the Multi-Focus and Montage option of the Leica Application Suite V3 (Leica Microsystems, Wetzlar, Germany).

5.2.3.8 Ruthenium red staining of seed mucilage

Whole seeds (T2 progeny) were allowed to imbibe in 0.2% w/v aqueous ruthenium red (Sigma) solution with 0.5% agar before solidification. Observe seeds after 3-4 h under light microscopy and pictures taken using the DISKUS software (Carl H. Hilgers-Technisches Büro, Germany) (Modified from [64]) .

5.2.4 DNA extraction, amplification and cloning

5.2.4.1 Plasmid extraction

Mini-preparations of plasmidic DNA are made from 5 ml of bacterial cultures brought at saturation, using the GeneJET Plasmid Miniprep Kit recommendations of the manufacturer. In order to obtain bigger DNA quantities, the culture volume is adapted to the type of plasmid (from 25 to 500 ml depending of the number of plasmid copies by cell).

5.2.4.2 DNA extraction from vegetal tissues

This method consists in a fast DNA extraction to be carried out genotyping (DNA is preferentially used during a month after extraction because of possible DNA degradation due to some impurities presence). Harvest a younger leaf and transfer it into an eppendorf tube. Process with a pestle and add 400 µl of extraction buffer and vortex for 5 s. Then centrifuge for 1 min at 13000 rpm to precipitate the proteins. Transfer 300 µl of supernatant to a new tube and add 300 µl of isopropanol and mix well. Incubate for 2 min. Centrifuge 5 min at 13000 rpm to precipitate the DNA. Then discard the supernatant and let pellet dry. Re-suspend in 50 µl of distilled water.

5.2.4.3 RNA extraction and cDNA synthesis

The extraction is made through RNeasy Mini Kit (Qiagen, Cat No./ID: 74106) which is added of a DNA degradation step by “RNase-free” DNase (Thermo). First-strand cDNA was then synthesized from the total RNA (1 µg) using the RevertAid H Minus 1st strand cDNA synthesis (Thermo) as described by manufacturer’s instruction.

5.2.4.4 DNA amplification by Polymerase Chain Reaction (PCR)

Use 0.5 U of Phusion polymerase for 20 µl of reaction medium: 5 µl of 10X HF buffer, 1.5 µl of dNTP mix (final concentration at 0.2 mM), 1.5 µl of 10 uM each oligonucleotide (final concentration at 0.5 µM), 10 pg - 1 µg DNA template. Usually, the PCR reaction consist in a denaturation phase, 3 min to 98°C; followed by 28~36 cycles comprising: denaturation, 30s at 94°C; oligonucleotide hybridization, 30s at 55-60°C; elongation, 1min/1000bp at 72°C; then a final 10 min elongation step at 72°C. These conditions are adapted according to the GC/AT ratio.

5.2.4.5 DNA analysis

DNA electrophoresis in an agarose gel allows qualitative and semi-quantitative analyzis. The electrophoresis is performed in 1X TAE buffer with a power of 120-150V. The gel is made by hot agarose dissolution in 1X TAE, usually 1% (w/v), varying between 0.5 to 3% depending on the size of the DNA fragments to be separated (small fragments should use high concentration). Ethidium bromide is added at a 10 ng/µl final concentration just before polymerization. The samples containing the charge loading buffer in a 1/10 proportion are runed into the gel. After migration, the DNA is visualized under “UV radiation” (Gel Doc™ XR+ Gel Documentation System, BioRad, USA).

5.2.4.6 Gateway® cloning by recombination

This type of recombination uses the specific sites, discovered in the λ phage by Landy (1989) [186]. The two steps of recombination are: i) introduction of the insert in the entry vector by a recombination type BP and ii) transfer of the insert to a destination vector by a recombination type LR (Figure 5.1, adapted from [187]).

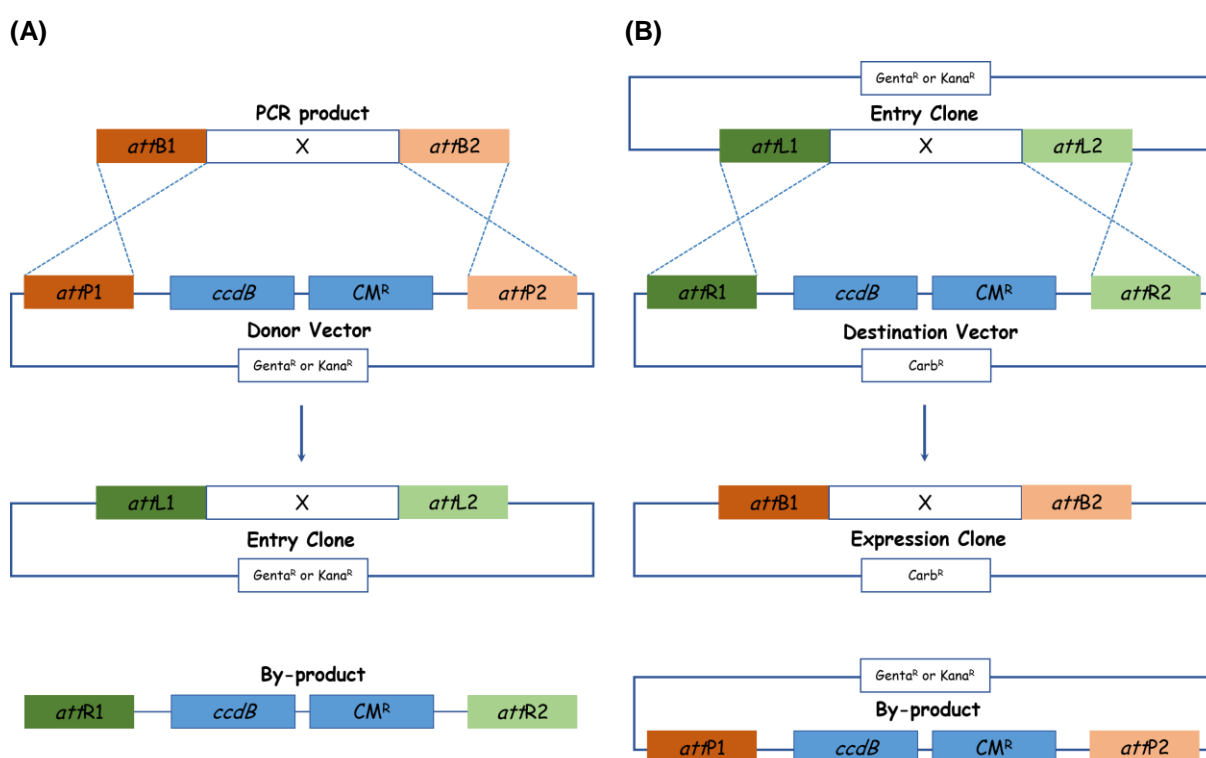


Figure 5.1 Gateway BP and LR reactions.

(Adapted from [187])

(A) BP recombination of a PCR product "X" flanked by attB sites with a Gateway donor vector *pDNOR207* (Genta^R) or *pDNOR201* (Kana^R).

(B) LR recombination of an entry clone bearing a DNA fragment "X" with a Gateway destination vector.

5.2.4.7 DNA Sequencing

The Roche PCR purification kit (Roche Diagnostics Deutschland GmbH, Mannheim, Germany) was used to purify the PCR product before sequencing. LightRUN™ sequencing service based on Sanger sequencing from GATC Biotech AG (European Genome and Diagnostics Centre, Constance, Germany) was used to sequence PCR products and plasmids.

5.2.4.8 Transformation

Escherichia coli transformation

E. coli strain DH5- α (F⁻, ϕ 80lacZ Δ M15, Δ (lacZYA-argF), U169, deoR, recA1, endA1, hsdR17, (rk⁻, mk⁺), phoA, supE44, thi-1, gyrA96, relA1, λ -) (Hanahan 1983) was used for classical cloning with the pUC18, CloneJET™ PCR Cloning Kit as well as Gateway® Cloning vectors. *E. coli* strain DB3.1 (F⁻ gyrA462endA1 glnV44 Δ (sr1-recA) mcrBmrrhsdS20 (rB⁻, mB⁻) ara14 galK2 lacY1 proA2 rpsL20 (Smr) xyl5 Δ leumtl1) [188, 189] was used for amplification of empty vectors containing the Gateway®-Cassette which encodes for the ccdB gene (toxic for DH5 α). Competent *E. coli* cells were transformed by heat shock method. For retransformations (plasmid amplification), Gateway®-cloning, classical cloning as well as for CloneJET™ PCR Cloning, the total volume of a LR, BP, ligation reaction or 1 μ l DNA (re-transformation) was added to 50 μ l of CaCl₂-competent *E. coli* cells. The cell-plasmid mixture was incubated for 20 min on ice. To induce plasmid uptake by bacteria, a heat shock at 42°C of 1 min was applied, followed by incubation on ice for five minutes. 800 μ l of LB medium (w/o antibiotics) was added and the cell suspension was grown for 1 h at 37°C at 850 rpm. The cells were pelleted at 6000 rpm for 4 min and re-suspended in a total volume of 50 μ l LB medium. The cells were streaked on LB agar plates containing appropriate antibiotics for selection of positive colonies. For re-transformation, the centrifugation step was omitted and 100 μ l of the 800 μ l culture was used. The plates were incubated overnight at 37°C and positive colonies were inoculated in liquid culture on the next day.

Agrobacterium tumefaciens transformation

The *A. tumefaciens* strain GV3101PMP90RK [190], harbouring resistance genes against rifampicin and gentamycin was used for transformation of *A. thaliana* with the plant expression vector pAMPAT-GW. CaCl₂-competent *A. tumefaciens* cells were transformed by heat shock. Plasmid DNA (2 μ l) was added to 50 μ l of the CaCl₂-competent *A. tumefaciens* cells and incubated on ice for 20 min. The cells were then subjected to a 2 min heat shock at 42°C. 950 μ l of YEB medium without antibiotics was added and the cell suspension was grown for 2 h at 28°C at 850 rpm. 100 μ l of the culture was plated on YEB-agar plates containing the appropriate antibiotic combination. The plates were incubated at 28°C for 2 days and positive colonies were inoculated in liquid culture. The liquid cultures were incubated at 28°C for 2 days.

Confirmed *Agrobacteria* cultures were used for plant transformation or stored at -80°C in glycerol stocks (800 µl culture + 800 µl 50% glycerol, quick freezing in liquid nitrogen).

5.2.5 Biochemical Methods

5.2.5.1 Protein Extraction from HEK Cells

Three milliliters of HEK-cell culture was transfected with 1.5 µg plasmid DNA using the transfection reagent Lipofectamin (Invitrogen) and cultivated at 37 °C and 5% CO₂. Transfected cells were harvested after 48 hours by centrifugation at 600 g for 10 min and washed twice with 10 ml of standard PBS buffer. Then, 200 µl of lysis buffer were added to the sample pellet at 4 °C. After centrifugation at 4 °C and 15 000 g for 20 min, samples can be used for either Protein A/RLuc co-precipitation or western blot.

5.2.5.2 Western Blot

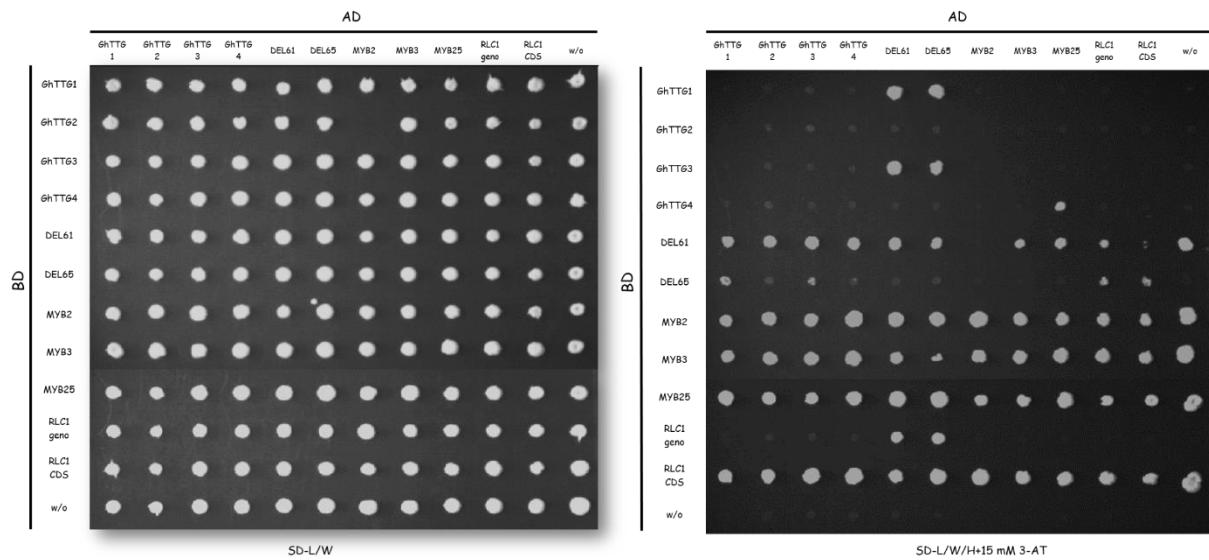
Western blot experiments were performed as described in Molecular Cloning [191]. Materials were used as follows: PVDF membrane (Roth), Super Signal West Femto Maximum Sensitivity Substrate (Thermo Scientific), Mini Trans-Blot Cells (BioRad) for wet western blotting, Mini Protean Cells (BioRad) for SDS gel electrophoresis, and Prestained Protein Ladder (Fermentas).

5.2.5.3 Histochemical detection of GUS activity

GUS stainings were essentially done as previously [192]. After staining for 16 h at 37°C, tissues were cleared and leaves were inspected by light microscopy and pictures taken using the DISKUS software (Carl H. Hilgers -Technisches Büro, Germany). Trichome numbers were determined on the third and fourth fully expanded leaf of soil-grown seedlings.

APPENDIX A Pairwise interaction analyses

(A)



(B)

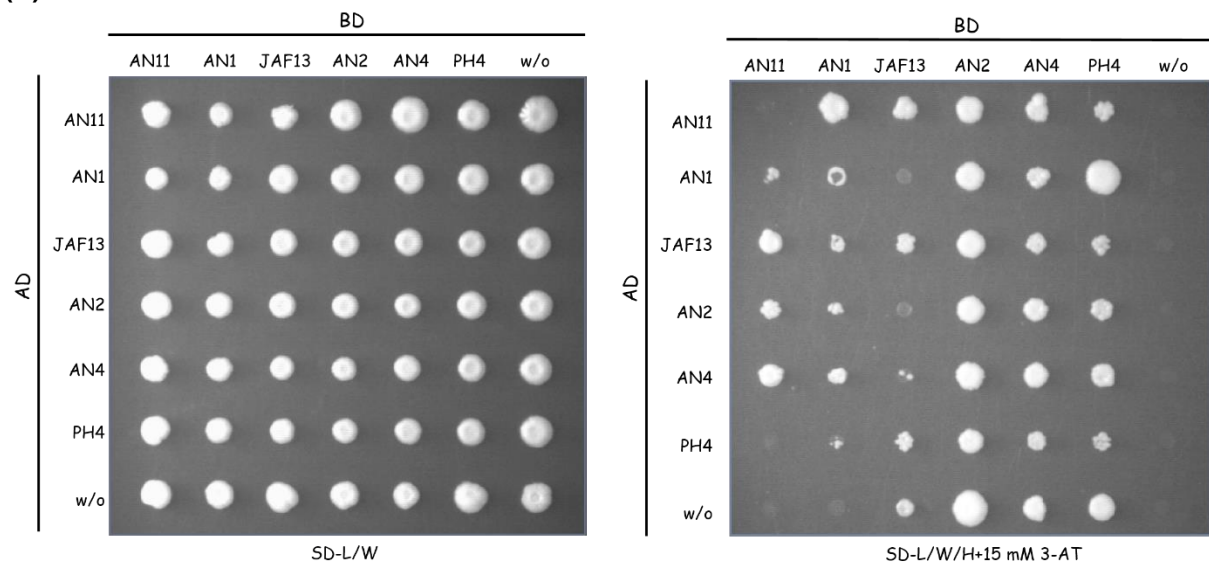


Figure S1 Protein–protein interactions among members of the MBW regulatory complex in cotton (A), petunia (B) and maize (C) determined by Yeast two hybrids assays.

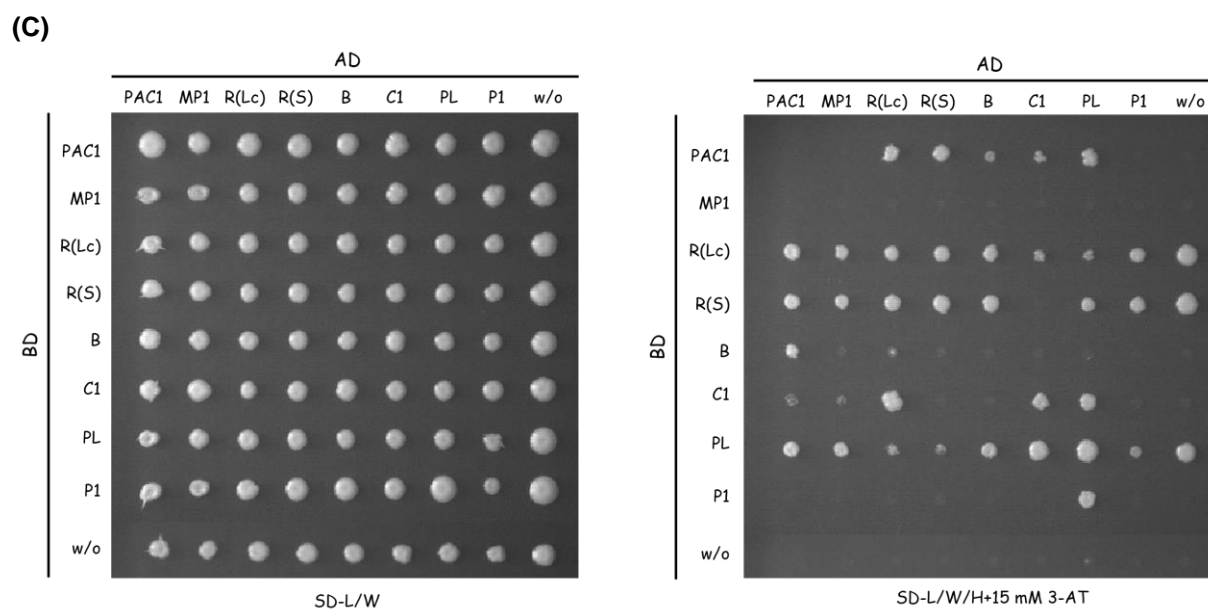


Figure S1 Cont. Protein–protein interactions among members of the MBW regulatory complex in cotton (A), petunia (B) and maize (C) determined by Yeast two hybrids assays.

Left: Growth on synthetic dropout selective medium lacking Leu, Trp (SD-L/W) for 5 days at 30°C as control; Right: Growth on synthetic dropout interaction medium lacking Leu, Trp, and His, supplemented with 15 mM 3-AT for 5 days at 30°C.

AD, GAL4 activation domain; BD, GAL4 DNA binding domain.

Table S1 Pairwise interaction of MBW components in Arabidopsis (*A. thaliana*).

ProtA fusion	Luciferase fusion	Luciferase activity: pulldown/input ratio (%)		References
AtTTG1	AtTTG1	0.35±0.00	-	[31]
AtTTG1	AtGL3	27.43±0.02	+	[29, 66, 153]
AtTTG1	AtEGL3	10.58±0.12	+	[66]
AtTTG1	AtTT8	4.79±0.03	+	[31, 103]
AtTTG1	AtMYC1	59.70±1.09	+	[70, 178]
AtTTG1	AtGL1	0.67±0.00	-	[70]
AtTTG1	AtWER	0.60±0.00	-	This work
AtTTG1	AtPAP1	0.31±0.00	-	This work
AtTTG1	AtPAP2	0.63±0.00	-	This work
AtTTG1	AtTT2	1.95±0.05	w	[31, 103]
AtTTG1	AtMYB61	0.61±0.00	-	This work
AtTTG1	w/o	0.55±0.01	-	This work
AtGL3	AtTTG1	8.45±0.05	+	[29, 66, 153]
AtGL3	AtGL3	5.44±0.04	+	[29, 65, 66]
AtGL3	AtEGL3	2.70±0.01	+	[66]
AtGL3	AtTT8	2.71±0.00	+	This work
AtGL3	AtMYC1	2.59±0.03	+	[35] conflict
AtGL3	AtGL1	47.21±2.18	+	[29, 66, 69, 153, 178, 193]
AtGL3	AtWER	78.89±3.23	+	[32, 65, 194]
AtGL3	AtPAP1	29.99±1.17	+	[66, 103]
AtGL3	AtPAP2	22.59±2.14	+	[66]
AtGL3	AtTT2	33.40±3.09	+	[103]
AtGL3	AtMYB61	2.17±0.35	w	This work
AtGL3	w/o	0.48±0.04	-	This work
AtEGL3	AtTTG1	8.40±0.15	+	[66]
AtEGL3	AtGL3	3.21±0.06	+	[66]
AtEGL3	AtEGL3	2.89±0.02	+	[65, 66]
AtEGL3	AtTT8	4.09±0.01	+	This work
AtEGL3	AtMYC1	2.25±0.02	w	This work
AtEGL3	AtGL1	10.44±0.10	+	[32, 66, 193]
AtEGL3	AtWER	7.19±0.13	+	[32, 194]

Table S1 Cont.

ProtA fusion	Luciferase fusion	Luciferase activity: pull-down/input ratio (%)		References
AtEGL3	AtPAP1	7.85±0.06	+	[32, 103]
AtEGL3	AtPAP2	6.25±0.04	+	[32, 66]
AtEGL3	AtTT2	7.38±0.02	+	[32, 103]
AtEGL3	AtMYB61	2.33±0.05	w	This work
AtEGL3	w/o	0.45±0.00	-	This work
AtTT8	AtTTG1	4.32±0.13	+	[31]
AtTT8	AtGL3	3.13±0.16	+	This work
AtTT8	AtEGL3	2.66±0.08	+	This work
AtTT8	AtTT8	2.94±0.04	+	[31] conflict
AtTT8	AtMYC1	2.23±0.01	w	This work
AtTT8	AtGL1	3.72±0.05	+	[32]
AtTT8	AtWER	2.28±0.01	w	[32]
AtTT8	AtPAP1	15.91±0.12	+	[32]
AtTT8	AtPAP2	15.69±0.11	+	[32]
AtTT8	AtTT2	18.99±0.12	+	[31, 32, 103]
AtTT8	AtMYB61	2.13±0.03	w	This work
AtTT8	w/o	0.55±0.00	-	This work
AtMYC1	AtTTG1	31.75±1.89	+	[70, 178]
AtMYC1	AtGL3	2.39±0.30	+	[35] conflict
AtMYC1	AtEGL3	2.30±0.04	w	This work
AtMYC1	AtTT8	2.39±0.03	w	This work
AtMYC1	AtMYC1	3.06±0.04	+	[35] conflict
AtMYC1	AtGL1	21.17±0.12	+	[32, 35, 178]
AtMYC1	AtWER	11.54±0.19	+	[32, 35]
AtMYC1	AtPAP1	17.20±0.60	+	[32]
AtMYC1	AtPAP2	15.34±0.31	+	[32]
AtMYC1	AtTT2	18.26±1.37	+	[32]
AtMYC1	AtMYB61	2.36±0.23	w	This work
AtMYC1	w/o	0.57±0.00	-	This work
AtGL1	AtTTG1	0.58±0.00	-	[70]

Table S1 Cont.

ProtA fusion	Luciferase fusion	Luciferase activity: pull-down/input ratio (%)		References
AtGL1	AtGL3	19.61±0.59	+	[29, 66, 69, 153, 178, 193]
AtGL1	AtEGL3	17.76±0.75	+	[32, 66]
AtGL1	AtTT8	26.51±1.66	+	[32]
AtGL1	AtMYC1	22.61±0.30	+	[32, 35, 178]
AtGL1	AtGL1	1.81±0.05	w	[180]
AtGL1	AtWER	0.61±0.01	-	This work
AtGL1	AtPAP1	0.63±0.00	-	This work
AtGL1	AtPAP2	0.59±0.03	-	This work
AtGL1	AtTT2	0.58±0.01	-	This work
AtGL1	AtMYB61	0.54±0.02	-	This work
AtGL1	w/o	0.57±0.02	-	This work
AtWER	AtTTG1	0.60±0.00	-	This work
AtWER	AtGL3	16.56±0.32	+	[32, 65, 194]
AtWER	AtEGL3	19.88±0.74	+	[32, 194]
AtWER	AtTT8	2.44±0.98	w	[32]
AtWER	AtMYC1	14.42±0.29	+	[32, 35]
AtWER	AtGL1	0.62±0.03	-	This work
AtWER	AtWER	0.61±0.04	-	This work
AtWER	AtPAP1	0.63±0.03	-	This work
AtWER	AtPAP2	0.60±0.02	-	This work
AtWER	AtTT2	0.58±0.00	-	This work
AtWER	AtMYB61	0.57±0.01	-	This work
AtWER	w/o	0.58±0.00	-	This work
AtPAP1	AtTTG1	0.61±0.01	-	This work
AtPAP1	AtGL3	19.93±0.23	+	[66, 103]
AtPAP1	AtEGL3	22.60±0.79	+	[32, 103]
AtPAP1	AtTT8	25.83±0.85	+	[32]
AtPAP1	AtMYC1	17.15±0.59	+	[32]
AtPAP1	AtGL1	0.65±0.01	-	This work
AtPAP1	AtWER	0.61±0.01	-	This work
AtPAP1	AtPAP1	0.63±0.02	-	This work

Table S1 Cont.

ProtA fusion	Luciferase fusion	Luciferase activity: pull-down/input ratio (%)		References
AtPAP1	AtPAP2	0.60±0.04	-	This work
AtPAP1	AtTT2	0.58±0.02	-	[103]
AtPAP1	AtMYB61	0.62±0.03	-	This work
AtPAP1	w/o	0.57±0.02	-	This work
AtPAP2	AtTTG1	0.94±0.08	-	This work
AtPAP2	AtGL3	19.56±0.41	+	[66]
AtPAP2	AtEGL3	12.44±0.17	+	[32, 66]
AtPAP2	AtTT8	35.22±0.39	+	[32]
AtPAP2	AtMYC1	17.15±0.99	+	[32]
AtPAP2	AtGL1	0.65±0.01	-	This work
AtPAP2	AtWER	0.60±0.01	-	This work
AtPAP2	AtPAP1	0.65±0.02	-	This work
AtPAP2	AtPAP2	0.60±0.04	-	This work
AtPAP2	AtTT2	0.66±0.02	-	This work
AtPAP2	AtMYB61	0.62±0.03	-	This work
AtPAP2	w/o	0.55±0.02	-	This work
AtTT2	AtTTG1	0.82±0.02	-	[31]
AtTT2	AtGL3	20.33±0.59	+	[103]
AtTT2	AtEGL3	22.59±0.35	+	[32, 103]
AtTT2	AtTT8	28.63±0.74	+	[31, 32, 103]
AtTT2	AtMYC1	19.59±0.99	+	[32]
AtTT2	AtGL1	0.65±0.00	-	This work
AtTT2	AtWER	0.61±0.03	-	This work
AtTT2	AtPAP1	0.63±0.00	-	[103]
AtTT2	AtPAP2	0.60±0.00	-	This work
AtTT2	AtTT2	1.87±0.02	w	[31]
AtTT2	AtMYB61	0.62±0.01	-	This work
AtTT2	w/o	0.57±0.00	-	This work
AtMYB61	AtTTG1	0.60±0.01	-	This work
AtMYB61	AtGL3	0.85±0.04	-	This work

Table S1 Cont.

ProtA fusion	Luciferase fusion	Luciferase activity: pull-down/input ratio (%)		References
AtMYB61	AtEGL3	0.89±0.02	-	This work
AtMYB61	AtTT8	1.19±0.06	-	This work
AtMYB61	AtMYC1	0.88±0.01	-	This work
AtMYB61	AtGL1	0.64±0.04	-	This work
AtMYB61	AtWER	0.60±0.02	-	This work
AtMYB61	AtPAP1	0.63±0.02	-	This work
AtMYB61	AtPAP2	0.60±0.00	-	This work
AtMYB61	AtTT2	0.58±0.02	-	This work
AtMYB61	AtMYB61	0.62±0.02	-	This work
AtMYB61	w/o	0.57±0.00	-	This work
w/o	AtTTG1	0.54±0.01	-	This work
w/o	AtGL3	0.69±0.07	-	This work
w/o	AtEGL3	0.71±0.05	-	This work
w/o	AtTT8	0.70±0.09	-	This work
w/o	AtMYC1	0.68±0.01	-	This work
w/o	AtGL1	0.69±0.01	-	This work
w/o	AtWER	0.58±0.08	-	This work
w/o	AtPAP1	0.60±0.02	-	This work
w/o	AtPAP2	0.62±0.04	-	This work
w/o	AtTT2	0.57±0.03	-	This work
w/o	AtMYB61	0.65±0.01	-	This work
w/o	w/o	0.54±0.00	-	This work

The proteins were single-expressed in human cells (HEK293TN) and immunoprecipitated with IgG Dynabeads. Data are mean ± s.d. (n = 3).

w/o: Empty vector without CDS fusion.

+ : Positive interaction (Luciferase activity ≥ 2.5%)

W : Weak interaction (Luciferase activity = 1.5% ~ 2.5%)

- : No interaction (Luciferase activity < 1.5%)

Table S2 Pairwise interaction of MBW components in *Arabidopsis* (*A. alpine*).

ProtA fusion	Luciferase fusion	Luciferase activity: pull-down/input ratio (%)		References
AaTTG1	AaTTG1	0.63±0.01	-	This work
AaTTG1	AaGL3	4.06±0.39	+	This work
AaTTG1	AaEGL3	4.54±0.27	+	This work
AaTTG1	AaTT8	5.53±0.11	+	This work
AaTTG1	AaMYC1	4.33±0.19	+	This work
AaTTG1	AaGL1	0.61±0.02	-	This work
AaTTG1	AaWER	0.62±0.02	-	[150]
AaTTG1	AaPAPL	0.65±0.01	-	This work
AaTTG1	w/o	0.55±0.01	-	This work
AaGL3	AaTTG1	7.74±0.29	+	This work
AaGL3	AaGL3	3.87±0.04	+	This work
AaGL3	AaEGL3	2.69±0.03	+	This work
AaGL3	AaTT8	4.77±0.07	+	This work
AaGL3	AaMYC1	3.76±0.09	+	This work
AaGL3	AaGL1	15.74±1.63	+	This work
AaGL3	AaWER	14.84±1.00	+	This work
AaGL3	AaPAPL	10.38±0.35	+	This work
AaGL3	w/o	0.58±0.01	-	This work
AaEGL3	AaTTG1	8.12±0.54	+	This work
AaEGL3	AaGL3	3.83±0.20	+	This work
AaEGL3	AaEGL3	3.09±0.05	+	This work
AaEGL3	AaTT8	5.01±0.17	+	This work
AaEGL3	AaMYC1	2.23±0.04	w	This work
AaEGL3	AaGL1	5.74±1.19	+	This work
AaEGL3	AaWER	6.84±1.06	+	This work
AaEGL3	AaPAPL	5.38±0.61	+	This work
AaEGL3	w/o	0.57±0.01	-	This work
AaTT8	AaTTG1	8.51±1.31	+	This work
AaTT8	AaGL3	2.96±0.12	+	This work
AaTT8	AaEGL3	1.91±0.02	w	This work

Table S2 Cont.

ProtA fusion	Luciferase fusion	Luciferase activity: pull-down/input ratio (%)		References
AaTT8	AaTT8	3.62±0.17	+	This work
AaTT8	AaMYC1	2.83±0.04	+	This work
AaTT8	AaGL1	4.74±0.36	+	This work
AaTT8	AaWER	3.97±0.19	+	This work
AaTT8	AaPAPL	4.25±0.08	+	This work
AaTT8	w/o	0.58±0.01	-	This work
AaMYC1	AaTTG1	6.93±0.16	+	This work
AaMYC1	AaGL3	3.31±0.07	+	This work
AaMYC1	AaEGL3	1.97±0.04	w	This work
AaMYC1	AaTT8	3.62±0.17	+	This work
AaMYC1	AaMYC1	2.83±0.04	+	This work
AaMYC1	AaGL1	4.74±0.36	+	This work
AaMYC1	AaWER	3.97±0.19	+	This work
AaMYC1	AaPAPL	4.25±0.08	+	This work
AaMYC1	w/o	0.58±0.01	-	This work
AaGL1	AaTTG1	0.60±0.02	-	This work
AaGL1	AaGL3	9.56±0.14	+	This work
AaGL1	AaEGL3	8.22±0.47	+	This work
AaGL1	AaTT8	8.80±0.17	+	This work
AaGL1	AaMYC1	11.28±0.38	+	This work
AaGL1	AaGL1	0.64±0.01	-	This work
AaGL1	AaWER	0.62±0.02	-	This work
AaGL1	AaPAPL	0.62±0.00	-	This work
AaGL1	w/o	0.57±0.00	-	This work
AaWER	AaTTG1	0.62±0.02	-	This work
AaWER	AaGL3	14.37±0.69	+	This work
AaWER	AaEGL3	14.44±0.64	+	This work
AaWER	AaTT8	15.52±1.38	+	This work
AaWER	AaMYC1	13.59±1.00	+	This work
AaWER	AaGL1	0.66±0.02	-	This work
AaWER	AaWER	0.60±0.01	-	This work

Table S2 Cont.

ProtA fusion	Luciferase fusion	Luciferase activity: pull-down/input ratio (%)		References
AaWER	AaPAPL	0.61±0.00	-	This work
AaWER	w/o	0.57±0.00	-	This work
AaPAPL	AaTTG1	0.61±0.02	-	This work
AaPAPL	AaGL3	13.90±0.52	+	This work
AaPAPL	AaEGL3	8.59±0.29	+	This work
AaPAPL	AaTT8	35.31±3.17	+	This work
AaPAPL	AaMYC1	20.96±2.38	+	This work
AaPAPL	AaGL1	0.61±0.01	-	This work
AaPAPL	AaWER	0.63±0.02	-	This work
AaPAPL	AaPAPL	0.63±0.01	-	This work
AaPAPL	w/o	0.59±0.01	-	This work

Table S3 Pairwise interaction of MBW components in Cotton (*G.hirsutum*).

BD or ProtA fusion	AD or Luciferase fusion	Yeast two hybrid	LUMIER	References
GhTTG1	GhTTG1	-	0.45±0.06 -	This work
GhTTG1	GhTTG2	-	0.47±0.05 -	This work
GhTTG1	GhTTG3	-	0.59±0.05 -	This work
GhTTG1	GhTTG4	-	0.57±0.05 -	This work
GhTTG1	GhDEL61	+	6.18±0.89 +	This work
GhTTG1	GhDEL65	+	13.86±2.80 +	
GhTTG1	GhMYB2	-	0.55±0.07 -	This work
GhTTG1	GhMYB25	-	0.61±0.04 -	This work
GhTTG1	GhRLC1	-	0.61±0.06 -	This work
GhTTG1	w/o	-	0.50±0.03 -	This work
GhTTG2	GhTTG1	-	0.52±0.08 -	This work
GhTTG2	GhTTG2	-	0.57±0.02 -	This work
GhTTG2	GhTTG3	-	0.59±0.04 -	This work
GhTTG2	GhTTG4	-	0.56±0.05 -	This work
GhTTG2	GhDEL61	-	0.58±0.05 -	This work
GhTTG2	GhDEL65	-	0.61±0.04 -	This work
GhTTG2	GhMYB2	-	0.59±0.04 -	This work
GhTTG2	GhMYB25	-	0.61±0.04 -	This work
GhTTG2	GhRLC1	-	0.59±0.07 -	This work
GhTTG2	w/o	-	0.49±0.03 -	This work
GhTTG3	GhTTG1	-	0.48±0.08 -	This work
GhTTG3	GhTTG2	-	0.57±0.04 -	This work
GhTTG3	GhTTG3	-	0.59±0.05 -	This work
GhTTG3	GhTTG4	-	0.56±0.05 -	This work
GhTTG3	GhDEL61	+	6.90±0.11 +	[76]
GhTTG3	GhDEL65	+	14.83±3.27 +	[76]
GhTTG3	GhMYB2	-	0.57±0.03 -	This work
GhTTG3	GhMYB25	-	0.63±0.06 -	This work
GhTTG3	GhRLC1	-	0.61±0.07 -	This work
GhTTG3	w/o	-	0.49±0.04 -	This work

Table S3 Cont.

BD or ProtA fusion	AD or Luciferase fusion	Yeast two hybrid	LUMIER	References
GhTTG4	GhTTG1	-	0.53±0.09 -	This work
GhTTG4	GhTTG2	-	0.51±0.05 -	This work
GhTTG4	GhTTG3	-	0.58±0.05 -	This work
GhTTG4	GhTTG4	-	0.56±0.05 -	This work
GhTTG4	GhDEL61	-	0.58±0.03 -	This work
GhTTG4	GhDEL65	-	0.65±0.05 -	This work
GhTTG4	GhMYB2	-	0.57±0.06 -	This work
GhTTG4	GhMYB25	-	0.64±0.05 -	This work
GhTTG4	GhRLC1	-	0.60±0.07 -	This work
GhTTG4	w/o	-	0.49±0.03 -	This work
GhDEL61	GhTTG1	A	8.86±0.40 +	This work
GhDEL61	GhTTG2	A	0.56±0.05 -	This work
GhDEL61	GhTTG3	A	7.59±0.27 +	[76]
GhDEL61	GhTTG4	A	0.57±0.06 -	This work
GhDEL61	GhDEL61	A	3.60±0.11 +	[76]
GhDEL61	GhDEL65	A	4.86±3.27 +	[76]
GhDEL61	GhMYB2	A	39.53±8.13 +	[76, 161]
GhDEL61	GhMYB25	A	5.84±0.12 +	[161]
GhDEL61	GhRLC1	A	42.22±5.83 +	This work
GhDEL61	w/o	A	0.49±0.04 -	This work
GhDEL65	GhTTG1	+	20.93±5.04 +	[151]
GhDEL65	GhTTG2	-	0.56±0.03 -	This work
GhDEL65	GhTTG3	+	15.54±2.20 +	[76]
GhDEL65	GhTTG4	-	0.56±0.03 -	This work
GhDEL65	GhDEL61	w	3.74±0.11 +	[76]
GhDEL65	GhDEL65	w	3.86±3.27 +	[76]
GhDEL65	GhMYB2	+	43.67±6.25 +	[76, 161]
GhDEL65	GhMYB25	+	4.83±0.38 +	[161]
GhDEL65	GhRLC1	+	40.60±3.77 +	This work
GhDEL65	w/o	-	0.50±0.03 -	This work

Table S3 Cont.

BD or ProtA fusion	AD or Luciferase fusion	Yeast two hybrid	LUMIER	References
GhMYB2	GhTTG1	A	0.63±0.04 -	This work
GhMYB2	GhTTG2	A	0.58±0.04 -	This work
GhMYB2	GhTTG3	A	0.61±0.03 -	This work
GhMYB2	GhTTG4	A	0.57±0.05 -	This work
GhMYB2	GhDEL61	A	13.72±0.41 +	[76, 161]
GhMYB2	GhDEL65	A	17.80±1.71 +	[76, 161]
GhMYB2	GhMYB2	A	0.66±0.06 -	This work
GhMYB2	GhMYB25	A	0.59±0.06 -	This work
GhMYB2	GhRLC1	A	0.63±0.07 -	This work
GhMYB2	w/o	A	0.51±0.02 -	This work
GhMYB25	GhTTG1	A	0.64±0.07 -	This work
GhMYB25	GhTTG2	A	0.53±0.04 -	This work
GhMYB25	GhTTG3	A	0.57±0.06 -	This work
GhMYB25	GhTTG4	A	0.51±0.04 -	This work
GhMYB25	GhDEL61	A	7.99±0.30 +	[161]
GhMYB25	GhDEL65	A	9.48±0.85 +	[161]
GhMYB25	GhMYB2	A	0.60±0.07 -	This work
GhMYB25	GhMYB25	A	0.62±0.04 -	This work
GhMYB25	GhRLC1	A	0.67±0.07 -	This work
GhMYB25	w/o	A	0.52±0.04 -	This work
GhRLC1	GhTTG1	A	0.65±0.06 -	This work
GhRLC1	GhTTG2	A	0.55±0.04 -	This work
GhRLC1	GhTTG3	A	0.60±0.06 -	This work
GhRLC1	GhTTG4	A	0.53±0.04 -	This work
GhRLC1	GhDEL61	A	9.64±0.26 +	This work
GhRLC1	GhDEL65	A	9.38±1.17 +	This work
GhRLC1	GhMYB2	A	0.60±0.05 -	This work
GhRLC1	GhMYB25	A	0.66±0.03 -	This work
GhRLC1	GhRLC1	A	0.68±0.06 -	This work
GhRLC1	w/o	A	0.49±0.03 -	This work

Table S3 Cont.

BD or ProtA fusion	AD or Luciferase fusion	Yeast two hybrid	LUMIER	References
w/o	GhTTG1	-	0.67±0.06 -	This work
w/o	GhTTG2	-	0.55±0.03 -	This work
w/o	GhTTG3	-	0.62±0.05 -	This work
w/o	GhTTG4	-	0.56±0.03 -	This work
w/o	GhDEL61	-	0.53±0.02 -	This work
w/o	GhDEL65	-	0.61±0.03 -	This work
w/o	GhMYB2	-	0.64±0.05 -	This work
w/o	GhMYB25	-	0.64±0.03 -	This work
w/o	GhRLC1	-	0.67±0.07 -	This work
w/o	w/o	-	0.49±0.04 -	This work

A : Autoactivation

Table S4 Pairwise interaction of MBW components in *Petunia* (*P. hybrida*).

BD or ProtA fusion	AD or Luciferase fusion	Yeast two hybrid	LUMIER		References
AN11	AN11	-	0.58±0.08	-	[146]
AN11	AN1	+	18.45±0.65	+	[146]
AN11	JAF13	+	26.77±4.24	+	[146]
AN11	AN2	+	0.59±0.02	-	[146]
AN11	AN4	+	0.55±0.02	-	This work
AN11	PH4	-	0.56±0.07	-	This work
AN11	w/o	-	0.48±0.03	-	[146]
AN1	AN11	+	29.75±3.68	+	[146]
AN1	AN1	+	9.19±2.91	+	[47, 146] conflict
AN1	JAF13	-	17.06±3.46	+	[47, 48, 146]
AN1	AN2	+	47.21±5.22	+	[146]
AN1	AN4	+	50.39±7.63	+	This work
AN1	PH4	w	51.89±8.89	+	[48]
AN1	w/o	-	0.49±0.05	-	[48]
JAF13	AN11	A	31.80±4.51	+	[146]
JAF13	AN1	A	5.77±0.54	+	[47, 146]
JAF13	JAF13	A	8.99±1.26	+	[47, 48, 146]
JAF13	AN2	A	48.26±8.02	+	[146]
JAF13	AN4	A	51.39±8.81	+	This work
JAF13	PH4	A	50.73±6.53	+	[48]
JAF13	w/o	A	0.50±0.04	-	[48]
AN2	AN11	A	0.59±0.00	-	This work
AN2	AN1	A	18.17±0.66	+	This work
AN2	JAF13	A	26.08±6.27	+	This work
AN2	AN2	A	0.55±0.03	-	This work
AN2	AN4	A	0.56±0.04	-	This work
AN2	PH4	A	0.59±0.03	-	This work
AN2	w/o	A	0.47±0.06	-	This work
AN4	AN11	A	0.55±0.02	-	This work

Table S4 Cont.

BD or ProtA fusion	AD or Luciferase fusion	Yeast two hybrid	LUMIER	References
AN4	AN1	A	19.65±2.43 +	This work
AN4	JAF13	A	32.21±4.02 +	This work
AN4	AN2	A	0.58±0.02 -	This work
AN4	AN4	A	0.57±0.02 -	This work
AN4	PH4	A	0.58±0.01 -	This work
AN4	w/o	A	0.48±0.05 -	This work
PH4	AN11	A	0.57±0.04 -	This work
PH4	AN1	A	31.94±6.10 +	This work
PH4	JAF13	A	42.77±4.48 +	This work
PH4	AN2	A	0.58±0.03 -	This work
PH4	AN4	A	0.56±0.01 -	This work
PH4	PH4	A	0.59±0.03 -	This work
PH4	w/o	A	0.50±0.01 -	This work
w/o	AN11	-	0.55±0.03 -	This work
w/o	AN1	-	0.60±0.02 -	This work
w/o	JAF13	-	0.62±0.05 -	This work
w/o	AN2	-	0.59±0.03 -	This work
w/o	AN4	-	0.52±0.02 -	This work
w/o	PH4	-	0.58±0.01 -	This work
w/o	w/o	-	0.47±0.03 -	This work

Table S5 Pairwise interaction of MBW components in Maize (*Z.mays*).

BD or ProtA fusion	AD or Luciferase fusion	Yeast two hybrid	LUMIER	References
PAC1	PAC1	-	0.67±0.00 -	This work
PAC1	MP1	-	0.65±0.02 -	This work
PAC1	R(Lc)	+	10.97±1.33 +	This work
PAC1	R(S)	+	10.34±0.71 +	This work
PAC1	B	+	10.84±0.49 +	This work
PAC1	C1	-	0.61±0.07 -	This work
PAC1	PL	-	0.52±0.05 -	This work
PAC1	P1	+	0.51±0.04 -	This work
PAC1	w/o	-	0.49±0.07 -	This work
MP1	PAC1	-	0.62±0.08 -	This work
MP1	MP1	-	0.65±0.02 -	This work
MP1	R(Lc)	-	0.70±0.12 -	This work
MP1	R(S)	-	0.63±0.03 -	This work
MP1	B	-	0.64±0.09 -	This work
MP1	C1	-	0.66±0.07 -	This work
MP1	PL	-	0.56±0.15 -	This work
MP1	P1	-	0.51±0.08 -	This work
MP1	w/o	-	0.47±0.05 -	This work
R(Lc)	PAC1	A	18.38±0.75 +	This work
R(Lc)	MP1	A	0.67±0.04 -	This work
R(Lc)	R(Lc)	A	9.63±0.84 +	This work
R(Lc)	R(S)	A	9.36±1.09 +	This work
R(Lc)	B	A	2.22±0.19 w	This work
R(Lc)	C1	A	48.68±2.07 +	This work
R(Lc)	PL	A	59.56±3.95 +	This work
R(Lc)	P1	A	0.52±0.09 -	This work
R(Lc)	w/o	A	0.49±0.06 -	This work
R(S)	PAC1	A	19.86±1.81 +	This work
R(S)	MP1	A	0.64±0.07 -	This work
R(S)	R(Lc)	A	8.44±0.84 +	This work

Table S5 Cont.

BD or ProtA fusion	AD or Luciferase fusion	Yeast two hybrid	LUMIER		References
R(S)	R(S)	A	10.29±1.40	+	[33, 145]
R(S)	B	A	2.16±0.15	w	This work
R(S)	C1	A	56.41±8.36	+	[43, 89, 145]
R(S)	PL	A	39.57±4.51	+	[43, 89]
R(S)	P1	A	0.53±0.10	-	[43, 89]
R(S)	w/o	A	0.50±0.05	-	This work
B	PAC1	+	12.51±1.20	+	This work
B	MP1	-	0.63±0.12	-	This work
B	R(Lc)	w	3.56±0.06	+	This work
B	R(S)	w	3.39±0.06	+	This work
B	B	-	3.90±0.09	+	This work
B	C1	-	0.66±0.16	-	[39, 43] conflict
B	PL	-	0.58±0.14	-	[39] conflict
B	P1	-	0.49±0.06	-	This work
B	w/o	-	0.51±0.05	-	This work
C1	PAC1	-	0.61±0.05	-	This work
C1	MP1	-	0.63±0.02	-	This work
C1	R(Lc)	+	35.56±3.66	+	This work
C1	R(S)	+	44.54±5.60	+	[43, 89, 145]
C1	B	w	1.73±0.19	-	[39, 43] conflict
C1	C1	+	0.52±0.16	-	This work
C1	PL	+	0.52±0.14	-	This work
C1	P1	-	0.53±0.06	-	This work
C1	w/o	-	0.53±0.01	-	This work
PL	PAC1	A	0.65±0.02	-	This work
PL	MP1	A	0.60±0.05	-	This work
PL	R(Lc)	A	47.19±3.91	+	This work
PL	R(S)	A	46.37±4.45	+	[43, 89, 145]
PL	B	A	0.63±0.18	-	[39, 43] conflict
PL	C1	A	0.57±0.14	-	This work

Table S5 Cont.

BD or ProtA fusion	AD or Luciferase fusion	Yeast two hybrid	LUMIER	References
PL	PL	A	0.53±0.10 -	This work
PL	P1	A	0.53±0.12 -	This work
PL	w/o	A	0.52±0.05 -	This work
P1	PAC1	-	0.63±0.05 -	This work
P1	MP1	-	0.57±0.09 -	This work
P1	R(Lc)	-	0.59±0.11 -	This work
P1	R(S)	+	0.65±0.09 -	[43, 89]
P1	B	-	0.63±0.08 -	This work
P1	C1	-	0.66±0.16 -	This work
P1	PL	-	0.55±0.12 -	This work
P1	P1	-	0.49±0.06 -	This work
P1	w/o	-	0.50±0.05 -	This work
w/o	PAC1	-	0.61±0.09 -	This work
w/o	MP1	-	0.56±0.05 -	This work
w/o	R(Lc)	-	0.62±0.10 -	This work
w/o	R(S)	-	0.60±0.08 -	This work
w/o	B	-	0.62±0.02 -	This work
w/o	C1	-	0.65±0.08 -	This work
w/o	PL	-	0.55±0.06 -	This work
w/o	P1	-	0.53±0.04 -	This work
w/o	w/o	-	0.51±0.02 -	This work

Table S6 Interaction between WD40 homologs and bHLHs/R2R3MYBs in Arabidopsis (*A. thaliana*).

ProtA fusion	Luciferase fusion	Luciferase activity: pulldown/input ratio (%)	References
AaTTG1	AtGL3	36.35±2.64 +	This work
GhTTG1	AtGL3	27.38±2.23 +	This work
GhTTG2	AtGL3	0.57±0.16 -	This work
GhTTG3	AtGL3	2.44±0.34 w	This work
GhTTG4	AtGL3	0.74±0.03 -	This work
AN11	AtGL3	17.18±1.64 +	This work
PAC1	AtGL3	26.44±8.70 +	This work
MP1	AtGL3	0.77±0.00 -	This work
w/o	AtGL3	0.58±0.06 -	This work
AaTTG1	AtEGL3	20.86±9.54 +	This work
GhTTG1	AtEGL3	25.92±1.71 +	This work
GhTTG2	AtEGL3	0.58±0.14 -	This work
GhTTG3	AtEGL3	6.16±4.64 +	This work
GhTTG4	AtEGL3	0.54±0.14 -	This work
AN11	AtEGL3	23.90±2.75 +	This work
PAC1	AtEGL3	28.14±3.96 +	This work
MP1	AtEGL3	0.50±0.09 -	This work
w/o	AtEGL3	0.55±0.07 -	This work
AaTTG1	AtTT8	23.15±3.19 +	This work
GhTTG1	AtTT8	17.83±4.90 +	This work
GhTTG2	AtTT8	0.59±0.07 -	This work
GhTTG3	AtTT8	1.21±0.15 -	This work
GhTTG4	AtTT8	0.60±0.10 -	This work
AN11	AtTT8	20.55±4.53 +	This work
PAC1	AtTT8	11.51±1.23 +	This work
MP1	AtTT8	1.05±0.17 -	This work
w/o	AtTT8	0.59±0.06 -	This work
AaTTG1	AtMYC1	41.01±0.08 +	This work
GhTTG1	AtMYC1	33.26±0.09 +	This work

Table S6 Cont.

ProtA fusion	Luciferase fusion	Luciferase activity: pulldown/input ratio (%)	References
GhTTG2	AtMYC1	0.69±0.12 -	This work
GhTTG3	AtMYC1	20.83±0.11 +	This work
GhTTG4	AtMYC1	0.71±0.07 -	This work
AN11	AtMYC1	13.79±2.04 +	This work
PAC1	AtMYC1	45.63±3.67 +	This work
MP1	AtMYC1	1.69±0.21 w	This work
w/o	AtMYC1	0.56±0.06 -	This work
AaTTG1	AtGL1	0.63±0.056 -	This work
GhTTG1	AtGL1	0.66±0.03 -	This work
GhTTG2	AtGL1	0.67±0.01 -	This work
GhTTG3	AtGL1	0.65±0.01 -	This work
GhTTG4	AtGL1	0.60±0.09 -	This work
AN11	AtGL1	0.61±0.01 -	This work
PAC1	AtGL1	0.65±0.10 -	This work
MP1	AtGL1	0.60±0.05 -	This work
w/o	AtGL1	0.57±0.07 -	This work
AaTTG1	AtWER	0.59±0.06 -	This work
GhTTG1	AtWER	0.63±0.07 -	This work
GhTTG2	AtWER	0.60±0.06 -	This work
GhTTG3	AtWER	0.61±0.04 -	This work
GhTTG4	AtWER	0.67±0.06 -	This work
AN11	AtWER	0.59±0.08 -	This work
PAC1	AtWER	0.69±0.09 -	This work
MP1	AtWER	0.64±0.01 -	This work
w/o	AtWER	0.58±0.06 -	This work
AaTTG1	AtMYB61	0.62±0.02 -	This work
GhTTG1	AtMYB61	0.60±0.01 -	This work
GhTTG2	AtMYB61	0.62±0.01 -	This work
GhTTG3	AtMYB61	0.68±0.10 -	This work
GhTTG4	AtMYB61	0.65±0.07 -	This work

Table S6 Cont.

ProtA fusion	Luciferase fusion	Luciferase activity: pulldown/input ratio (%)	References
AN11	AtMYB61	0.60±0.03 -	This work
PAC1	AtMYB61	0.63±0.01 -	This work
MP1	AtMYB61	0.62±0.02 -	This work
w/o	AtMYB61	0.57±0.01 -	This work
AaTTG1	AtTT2	0.71±0.07 -	This work
GhTTG1	AtTT2	1.13±0.11 -	This work
GhTTG2	AtTT2	0.68±0.15 -	This work
GhTTG3	AtTT2	2.02±0.21 w	This work
GhTTG4	AtTT2	0.69±0.05 -	This work
AN11	AtTT2	0.88±0.17 -	This work
PAC1	AtTT2	0.93±0.20 -	This work
MP1	AtTT2	0.69±0.02 -	This work
w/o	AtTT2	0.60±0.07 -	This work
AaTTG1	AtPAP1	0.71±0.07 -	This work
GhTTG1	AtPAP1	1.13±0.11 -	This work
GhTTG2	AtPAP1	0.68±0.15 -	This work
GhTTG3	AtPAP1	1.02±0.21 -	This work
GhTTG4	AtPAP1	0.69±0.05 -	This work
AN11	AtPAP1	0.88±0.17 -	This work
PAC1	AtPAP1	0.93±0.20 -	This work
MP1	AtPAP1	0.69±0.02 -	This work
w/o	AtPAP1	0.60±0.07 -	This work
AaTTG1	AtPAP2	0.66±0.04 -	This work
GhTTG1	AtPAP2	0.80±0.08 -	This work
GhTTG2	AtPAP2	0.69±0.05 -	This work
GhTTG3	AtPAP2	0.72±0.11 -	This work
GhTTG4	AtPAP2	0.62±0.07 -	This work
AN11	AtPAP2	0.88±0.17 -	This work
PAC1	AtPAP2	0.93±0.20 -	This work
MP1	AtPAP2	0.69±0.02 -	This work

Table S6 Cont.

ProtA fusion	Luciferase fusion	Luciferase activity: pulldown/input ratio (%)	References
w/o	AtPAP2	0.60±0.07 -	This work
AaTTG1	w/o	0.56±0.08 -	This work
GhTTG1	w/o	0.64±0.09 -	This work
GhTTG2	w/o	0.66±0.03 -	This work
GhTTG3	w/o	0.59±0.02 -	This work
GhTTG4	w/o	0.69±0.10 -	This work
AN11	w/o	0.67±0.05 -	This work
PAC1	w/o	0.69±0.06 -	This work
MP1	w/o	0.55±0.11 -	This work
w/o	w/o	0.54±0.01 -	This work
AtGL3	AaTTG1	23.29±8.03 +	This work
AtGL3	GhTTG1	20.11±7.74 +	This work
AtGL3	GhTTG2	0.64±0.05 -	This work
AtGL3	GhTTG3	26.89±6.41 +	This work
AtGL3	GhTTG4	0.72±0.13 -	This work
AtGL3	AN11	15.71±6.73 +	This work
AtGL3	PAC1	26.61±4.19 +	This work
AtGL3	MP1	0.70±0.03 -	This work
AtGL3	w/o	0.59±0.04 -	This work
AtEGL3	AaTTG1	27.06±3.13 +	This work
AtEGL3	GhTTG1	26.52±9.50 +	This work
AtEGL3	GhTTG2	0.71±0.06 -	This work
AtEGL3	GhTTG3	11.38±2.80 +	This work
AtEGL3	GhTTG4	0.66±0.13 -	This work
AtEGL3	AN11	18.03±9.12 +	This work
AtEGL3	PAC1	12.55±7.87 +	This work
AtEGL3	MP1	0.66±0.05 -	This work
AtEGL3	w/o	0.59±0.03 -	This work
AtTT8	AaTTG1	23.34±4.25 +	This work
AtTT8	GhTTG1	26.57±6.30 +	This work

Table S6 Cont.

ProtA fusion	Luciferase fusion	Luciferase activity: pulldown/input ratio (%)	References
AtTT8	GhTTG2	0.81±0.13 -	This work
AtTT8	GhTTG3	0.92±0.23 -	This work
AtTT8	GhTTG4	0.67±0.11 -	This work
AtTT8	AN11	8.31±1.41 +	This work
AtTT8	PAC1	20.50±4.54 +	This work
AtTT8	MP1	0.70±0.11 -	This work
AtTT8	w/o	0.59±0.08 -	This work
AtMYC1	AaTTG1	17.22±8.33 +	This work
AtMYC1	GhTTG1	26.87±7.34 -	This work
AtMYC1	GhTTG2	0.69±0.02 +	This work
AtMYC1	GhTTG3	23.63±5.74 -	This work
AtMYC1	GhTTG4	0.67±0.21 +	This work
AtMYC1	AN11	30.54±0.38 +	This work
AtMYC1	PAC1	9.17±1.17 +	This work
AtMYC1	MP1	0.70±0.40 -	This work
AtMYC1	w/o	0.55±0.01 +	This work
AtGL1	AaTTG1	0.67±0.08 -	This work
AtGL1	GhTTG1	0.66±0.02 -	This work
AtGL1	GhTTG2	0.69±0.06 -	This work
AtGL1	GhTTG3	0.68±0.14 -	This work
AtGL1	GhTTG4	0.71±0.09 -	This work
AtGL1	AN11	0.65±0.06 -	This work
AtGL1	PAC1	0.68±0.10 -	This work
AtGL1	MP1	0.68±0.08 -	This work
AtGL1	w/o	0.59±0.03 -	This work
AtWER	AaTTG1	0.67±0.08 -	This work
AtWER	GhTTG1	0.66±0.02 -	This work
AtWER	GhTTG2	0.69±0.06 -	This work
AtWER	GhTTG3	0.68±0.14 -	This work
AtWER	GhTTG4	0.71±0.09 -	This work
AtWER	AN11	0.65±0.06 -	This work

Table S6 Cont.

ProtA fusion	Luciferase fusion	Luciferase activity: pulldown/input ratio (%)	References
AtWER	PAC1	0.68±0.10 -	This work
AtWER	MP1	0.68±0.08 -	This work
AtWER	w/o	0.59±0.03 -	This work
AtMYB61	AaTTG1	0.67±0.08 -	This work
AtMYB61	GhTTG1	0.66±0.02 -	This work
AtMYB61	GhTTG2	0.69±0.06 -	This work
AtMYB61	GhTTG3	0.68±0.14 -	This work
AtMYB61	GhTTG4	0.71±0.09 -	This work
AtMYB61	AN11	0.65±0.06 -	This work
AtMYB61	PAC1	0.68±0.10 -	This work
AtMYB61	MP1	0.68±0.08 -	This work
AtMYB61	w/o	0.59±0.03 -	This work
AtTT2	AaTTG1	0.82±0.10 -	This work
AtTT2	GhTTG1	0.86±0.07 -	This work
AtTT2	GhTTG2	0.79±0.06 -	This work
AtTT2	GhTTG3	1.88±0.19 w	This work
AtTT2	GhTTG4	0.66±0.09 -	This work
AtTT2	AN11	0.62±0.03 -	This work
AtTT2	PAC1	0.64±0.05 -	This work
AtTT3	MP1	0.69±0.02 -	This work
AtTT4	w/o	0.58±0.00 -	This work
AtPAP1	AaTTG1	0.70±0.05 -	This work
AtPAP1	GhTTG1	0.68±0.01 -	This work
AtPAP1	GhTTG2	0.66±0.02 -	This work
AtPAP1	GhTTG3	0.66±0.04 -	This work
AtPAP1	GhTTG4	0.69±0.03 -	This work
AtPAP1	AN11	0.63±0.09 -	This work
AtPAP1	PAC1	0.68±0.02 -	This work
AtPAP1	MP1	0.64±0.03 -	This work
AtPAP1	w/o	0.59±0.01 -	This work

Table S6 Cont.

ProtA fusion	Luciferase fusion	Luciferase activity: pulldown/input ratio (%)	References
AtPAP2	AaTTG1	0.63±0.03 -	This work
AtPAP2	GhTTG1	0.65±0.04 -	This work
AtPAP2	GhTTG2	0.61±0.01 -	This work
AtPAP2	GhTTG3	0.60±0.06 -	This work
AtPAP2	GhTTG4	0.62±0.03 -	This work
AtPAP2	AN11	0.63±0.00 -	This work
AtPAP2	PAC1	0.67±0.08 -	This work
AtPAP2	MP1	0.63±0.06 -	This work
AtPAP2	w/o	0.58±0.07 -	This work
w/o	AaTTG1	0.67±0.06 -	This work
w/o	GhTTG1	0.63±0.00 -	This work
w/o	GhTTG2	0.68±0.08 -	This work
w/o	GhTTG3	0.63±0.01 -	This work
w/o	GhTTG4	0.62±0.00 -	This work
w/o	AN11	0.69±0.11 -	This work
w/o	PAC1	0.70±0.08 -	This work
w/o	MP1	0.62±0.00 -	This work
w/o	w/o	0.53±0.02 -	This work

Table S7 Interaction between bHLH homologs and AtTTG1/R2R3MYBs in Arabidopsis (*A. thaliana*).

ProtA fusion	Luciferase fusion	Luciferase activity: pulldown/input ratio (%)	References
AtTTG1	AaGL3	27.06±2.07 +	This work
AtTTG1	AaEGL3	14.60±1.96 +	This work
AtTTG1	AaMYC1	18.25±1.45 +	This work
AtTTG1	AaTT8	17.93±1.43 +	This work
AtTTG1	GhDEL61	8.84±1.78 +	This work
AtTTG1	GhDEL65	18.86±2.26 +	This work
AtTTG1	JAF13	29.06±4.13 +	This work
AtTTG1	AN1	19.27±1.78 +	This work
AtTTG1	R(Lc)	32.02±3.92 +	This work
AtTTG1	R(S)	28.75±3.24 +	This work
AtTTG1	B	26.26±3.56 +	This work
AtTTG1	w/o	0.60±0.01 -	This work
AtGL1	AaGL3	14.17±2.36 +	This work
AtGL1	AaEGL3	6.63±1.02 +	This work
AtGL1	AaMYC1	4.25±0.03 +	This work
AtGL1	AaTT8	7.85±0.41 +	This work
AtGL1	GhDEL61	12.75±0.79 +	This work
AtGL1	GhDEL65	8.66±0.10 +	This work
AtGL1	JAF13	12.76±2.61 +	This work
AtGL1	AN1	6.55±0.66 +	This work
AtGL1	R(Lc)	32.06±3.16 +	This work
AtGL1	R(S)	31.36±2.35 +	This work
AtGL1	B	0.95±0.01 -	This work
AtGL1	w/o	0.59±0.00 -	This work
AtWER	AaGL3	37.17±2.56 +	This work
AtWER	AaEGL3	16.09±1.58 +	This work
AtWER	AaMYC1	8.84±0.79 +	This work
AtWER	AaTT8	7.67±0.87 +	This work
AtWER	GhDEL61	20.60±0.21 +	This work
AtWER	GhDEL65	8.61±0.24 +	This work

Table S7 Cont.

ProtA fusion	Luciferase fusion	Luciferase activity: pull-down/input ratio (%)	References
AtWER	JAF13	30.55±2.63 +	This work
AtWER	AN1	22.92±3.75 +	This work
AtWER	R(Lc)	32.48±5.25 +	This work
AtWER	R(S)	38.22±3.55 +	This work
AtWER	B	0.90±0.02 -	This work
AtWER	w/o	0.60±0.00 -	This work
AtMYB61	AaGL3	0.98±0.02 -	This work
AtMYB61	AaEGL3	0.89±0.01 -	This work
AtMYB61	AaMYC1	0.86±0.00 -	This work
AtMYB61	AaTT8	1.22±0.03 -	This work
AtMYB61	GhDEL61	1.17±0.03 -	This work
AtMYB61	GhDEL65	1.11±0.02 -	This work
AtMYB61	JAF13	0.96±0.02 -	This work
AtMYB61	AN1	1.36±0.03 -	This work
AtMYB61	R(Lc)	1.08±0.04 -	This work
AtMYB61	R(S)	0.93±0.02 -	This work
AtMYB61	B	0.76±0.04 -	This work
AtMYB61	w/o	0.60±0.03 -	This work
AtTT2	AaGL3	16.19±2.87 +	This work
AtTT2	AaEGL3	8.58±0.41 +	This work
AtTT2	AaMYC1	9.18±1.37 +	This work
AtTT2	AaTT8	41.91±3.91 +	This work
AtTT2	GhDEL61	15.37±2.25 +	This work
AtTT2	GhDEL65	7.96±0.03 +	This work
AtTT2	JAF13	24.48±1.17 +	This work
AtTT2	AN1	40.54±7.54 +	This work
AtTT2	R(Lc)	22.88±2.56 +	This work
AtTT2	R(S)	25.48±3.02 +	This work
AtTT2	B	0.88±0.04 -	This work
AtTT2	w/o	0.60±0.01 -	This work

Table S7 Cont.

ProtA fusion	Luciferase fusion	Luciferase activity: pull-down/input ratio (%)	References
AtPAP1	AaGL3	5.63±0.52 +	This work
AtPAP1	AaEGL3	2.18±0.41 w	This work
AtPAP1	AaMYC1	5.90±0.62 +	This work
AtPAP1	AaTT8	6.91±1.10 +	This work
AtPAP1	GhDEL61	6.71±0.26 +	This work
AtPAP1	GhDEL65	5.96±1.10 +	This work
AtPAP1	JAF13	8.45±1.12 +	This work
AtPAP1	AN1	6.27±0.78 +	This work
AtPAP1	R(Lc)	8.21±0.67 +	This work
AtPAP1	R(S)	6.88±0.13 +	This work
AtPAP1	B	0.89±0.01 -	This work
AtPAP1	w/o	0.60±0.00 -	This work
AtPAP2	AaGL3	2.28±0.12 w	This work
AtPAP2	AaEGL3	1.09±0.14 -	This work
AtPAP2	AaMYC1	1.99±0.10 w	This work
AtPAP2	AaTT8	3.11±0.16 +	This work
AtPAP2	GhDEL61	8.01±0.09 +	This work
AtPAP2	GhDEL65	5.59±0.17 +	This work
AtPAP2	JAF13	2.15±0.46 w	This work
AtPAP2	AN1	4.12±0.23 +	This work
AtPAP2	R(Lc)	14.42±0.77 +	This work
AtPAP2	R(S)	16.68±2.11 +	This work
AtPAP2	B	0.86±0.02 -	This work
AtPAP2	w/o	0.60±0.03 -	This work
w/o	AaGL3	0.72±0.01 -	This work
w/o	AaEGL3	0.73±0.01 -	This work
w/o	AaMYC1	0.77±0.00 -	This work
w/o	AaTT8	0.72±0.01 -	This work
w/o	GhDEL61	0.70±0.00 -	This work
w/o	GhDEL65	0.73±0.02 -	This work
w/o	JAF13	0.73±0.01 -	This work

Table S7 Cont.

ProtA fusion	Luciferase fusion	Luciferase activity: pull-down/input ratio (%)	References
w/o	AN1	0.71±0.00 -	This work
w/o	R(Lc)	0.72±0.01 -	This work
w/o	R(S)	0.69±0.00 -	This work
w/o	B	0.69±0.02 -	This work
w/o	w/o	0.60±0.01 -	This work
AaGL3	AtTTG1	30.58±6.14 +	This work
AaEGL3	AtTTG1	27.55±3.65 +	This work
AaMYC1	AtTTG1	14.13±1.22 +	This work
AaTT8	AtTTG1	16.11±1.36 +	This work
GhDEL61	AtTTG1	5.86±0.84 +	This work
GhDEL65	AtTTG1	21.17±3.16 +	This work
JAF13	AtTTG1	10.44±2.16 +	This work
AN1	AtTTG1	16.28±2.14 +	This work
R(Lc)	AtTTG1	16.01±3.91 +	This work
R(S)	AtTTG1	7.87±2.15 +	This work
B	AtTTG1	18.31±3.10 +	This work
w/o	AtTTG1	0.57±0.03 -	This work
AaGL3	AtGL1	21.46±4.37 +	This work
AaEGL3	AtGL1	21.65±3.14 +	This work
AaMYC1	AtGL1	23.28±2.35 +	This work
AaTT8	AtGL1	6.16±0.39 +	This work
GhDEL61	AtGL1	10.85±1.84 +	This work
GhDEL65	AtGL1	10.79±2.09 +	This work
JAF13	AtGL1	10.25±1.07 +	This work
AN1	AtGL1	10.74±2.19 +	This work
R(Lc)	AtGL1	23.35±3.09 +	This work
R(S)	AtGL1	16.70±1.70 +	This work
B	AtGL1	0.77±0.04 -	This work
w/o	AtGL1	0.62±0.02 -	This work
AaGL3	AtWER	23.62±3.88 +	This work

Table S7 Cont.

ProtA fusion	Luciferase fusion	Luciferase activity: pull-down/input ratio (%)	References
AaEGL3	AtWER	20.87±1.27 +	This work
AaMYC1	AtWER	15.28±1.82 +	This work
AaTT8	AtWER	6.78±0.45 +	This work
GhDEL61	AtWER	11.82±1.51 +	This work
GhDEL65	AtWER	11.62±0.85 +	This work
JAF13	AtWER	6.96±0.73 +	This work
AN1	AtWER	14.55±2.19 +	This work
R(Lc)	AtWER	20.82±2.88 +	This work
R(S)	AtWER	20.08±1.08 +	This work
B	AtWER	0.86±0.05 -	This work
w/o	AtWER	0.61±0.00 -	This work
AaGL3	AtMYB61	0.91±0.11 -	This work
AaEGL3	AtMYB61	0.89±0.00 -	This work
AaMYC1	AtMYB61	0.87±0.03 -	This work
AaTT8	AtMYB61	1.74±0.21 w	This work
GhDEL61	AtMYB61	0.90±0.01 -	This work
GhDEL65	AtMYB61	0.93±0.03 -	This work
JAF13	AtMYB61	0.94±0.01 -	This work
AN1	AtMYB61	0.86±0.02 -	This work
R(Lc)	AtMYB61	0.93±0.03 -	This work
R(S)	AtMYB61	0.91±0.01 -	This work
B	AtMYB61	0.78±0.04 -	This work
w/o	AtMYB61	0.67±0.03 -	This work
AaGL3	AtTT2	5.72±0.28 +	This work
AaEGL3	AtTT2	6.60±0.89 +	This work
AaMYC1	AtTT2	9.46±0.50 +	This work
AaTT8	AtTT2	12.54±1.21 +	This work
GhDEL61	AtTT2	13.56±1.89 +	This work
GhDEL65	AtTT2	13.99±0.50 +	This work
JAF13	AtTT2	8.68±0.97 +	This work
AN1	AtTT2	14.25±0.94 +	This work

Table S7 Cont.

ProtA fusion	Luciferase fusion	Luciferase activity: pull-down/input ratio (%)	References
R(Lc)	AtTT2	17.23±1.06 +	This work
R(S)	AtTT2	16.74±1.73 +	This work
B	AtTT2	0.83±0.02 -	This work
w/o	AtTT2	0.55±0.01 -	This work
AaGL3	AtPAP1	5.32±0.90 +	This work
AaEGL3	AtPAP1	1.95±0.28 w	This work
AaMYC1	AtPAP1	3.24±0.48 +	This work
AaTT8	AtPAP1	8.13±0.85 +	This work
GhDEL61	AtPAP1	4.16±0.12 +	This work
GhDEL65	AtPAP1	4.02±0.26 +	This work
JAF13	AtPAP1	3.82±0.21 +	This work
AN1	AtPAP1	2.96±0.14 +	This work
R(Lc)	AtPAP1	8.50±0.69 +	This work
R(S)	AtPAP1	9.38±0.93 +	This work
B	AtPAP1	0.72±0.06 -	This work
w/o	AtPAP1	0.56±0.01 -	This work
AaGL3	AtPAP2	3.68±0.18 +	This work
AaEGL3	AtPAP2	1.09±0.21 -	This work
AaMYC1	AtPAP2	5.41±0.17 +	This work
AaTT8	AtPAP2	13.90±0.49 +	This work
GhDEL61	AtPAP2	2.12±0.50 w	This work
GhDEL65	AtPAP2	5.67±1.36 +	This work
JAF13	AtPAP2	2.10±0.32 w	This work
AN1	AtPAP2	6.45±0.35 +	This work
R(Lc)	AtPAP2	10.31±2.02 +	This work
R(S)	AtPAP2	15.15±1.15 +	This work
B	AtPAP2	1.06±0.30 -	This work
w/o	AtPAP2	0.55±0.00 -	This work
AaGL3	w/o	0.60±0.03 -	This work
AaEGL3	w/o	0.58±0.00 -	This work

Table S7 Cont.

ProtA fusion	Luciferase fusion	Luciferase activity: pull-down/input ratio (%)	References
AaMYC1	w/o	0.64±0.01 -	This work
AaTT8	w/o	0.60±0.03 -	This work
GhDEL61	w/o	0.60±0.04 -	This work
GhDEL65	w/o	0.58±0.03 -	This work
JAF13	w/o	0.61±0.03 -	This work
AN1	w/o	0.58±0.01 -	This work
R(Lc)	w/o	0.62±0.01 -	This work
R(S)	w/o	0.64±0.02 -	This work
B	w/o	0.65±0.03 -	This work
w/o	w/o	0.55±0.01 -	This work

Table S8 Interaction between R2R3MYB homologs and AtTTG1/bHLHs in Arabidopsis (*A. thaliana*).

ProtA fusion	Luciferase fusion	Luciferase activity: pulldown/input ratio (%)	References
AaGL1	AtGL3	17.75±0.60 +	This work
AaWER	AtGL3	31.37±2.86 +	This work
AaMYB23	AtGL3	35.42±2.57 +	This work
AaPAPL	AtGL3	7.53±0.62 +	This work
GhMYB2	AtGL3	19.01±1.83 +	This work
GhMYB3	AtGL3	18.16±1.47 +	This work
GhMYB25	AtGL3	0.48±0.02 -	This work
GhRLC1	AtGL3	7.56±1.57 +	This work
PhAN2	AtGL3	16.79±0.68 +	This work
PhAN4	AtGL3	9.41±0.12 +	This work
PhPH4	AtGL3	13.09±0.79 +	This work
ZmC1	AtGL3	21.36±0.56 +	This work
ZmPL	AtGL3	16.79±1.29 +	This work
ZmP1	AtGL3	0.43±0.01 -	This work
w/o	AtGL3	0.39±0.00 -	This work
AaGL1	AtEGL3	9.96±0.38 +	This work
AaWER	AtEGL3	19.69±1.72 +	This work
AaMYB23	AtEGL3	17.99±2.71 +	This work
AaPAPL	AtEGL3	5.52±0.36 +	This work
GhMYB2	AtEGL3	7.32±0.89 +	This work
GhMYB3	AtEGL3	10.86±1.11 +	This work
GhMYB25	AtEGL3	0.68±0.08 -	This work
GhRLC1	AtEGL3	5.56±1.42 +	This work
PhAN2	AtEGL3	10.12±1.28 +	This work
PhAN4	AtEGL3	4.15±0.05 +	This work
PhPH4	AtEGL3	4.53±0.32 +	This work
ZmC1	AtEGL3	5.90±0.05 +	This work
ZmPL	AtEGL3	9.13±0.72 +	This work
ZmP1	AtEGL3	0.44±0.02 -	This work
w/o	AtEGL3	0.50±0.01 -	This work

Table S8 Cont.

ProtA fusion	Luciferase fusion	Luciferase activity: pull-down/input ratio (%)		References
AaGL1	AtTT8	4.62±0.89	+	This work
AaWER	AtTT8	4.87±0.71	+	This work
AaMYB23	AtTT8	5.68±0.19	+	This work
AaPAPL	AtTT8	22.39±2.12	+	This work
GhMYB2	AtTT8	20.10±3.07	+	This work
GhMYB3	AtTT8	27.34±1.69	+	This work
GhMYB25	AtTT8	0.74±0.09	-	This work
GhRLC1	AtTT8	22.67±1.22	+	This work
PhAN2	AtTT8	41.41±4.82	+	This work
PhAN4	AtTT8	20.78±3.33	+	This work
PhPH4	AtTT8	30.98±0.49	+	This work
ZmC1	AtTT8	48.16±4.96	+	This work
ZmPL	AtTT8	46.53±3.54	+	This work
ZmP1	AtTT8	0.59±0.02	-	This work
w/o	AtTT8	0.61±0.04	-	This work
AaGL1	AtMYC1	12.28±0.80	+	This work
AaWER	AtMYC1	19.29±1.07	+	This work
AaMYB23	AtMYC1	17.42±0.82	+	This work
AaPAPL	AtMYC1	3.98±0.48	+	This work
GhMYB2	AtMYC1	11.94±1.42	+	This work
GhMYB3	AtMYC1	12.65±1.66	+	This work
GhMYB25	AtMYC1	0.59±0.00	-	This work
GhRLC1	AtMYC1	4.67±0.53	+	This work
PhAN2	AtMYC1	12.97±2.55	+	This work
PhAN4	AtMYC1	5.69±0.50	+	This work
PhPH4	AtMYC1	9.11±0.11	+	This work
ZmC1	AtMYC1	8.60±0.55	+	This work
ZmPL	AtMYC1	13.96±1.59	+	This work
ZmP1	AtMYC1	0.47±0.01	-	This work
w/o	AtMYC1	0.48±0.01	-	This work
AaGL1	AtTTG1	0.35±0.01	-	This work

Table S8 Cont.

ProtA fusion	Luciferase fusion	Luciferase activity: pull-down/input ratio (%)	References
AaWER	AtTTG1	0.36±0.00 -	This work
AaMYB23	AtTTG1	0.37±0.01 -	This work
AaPAPL	AtTTG1	0.35±0.00 -	This work
GhMYB2	AtTTG1	0.39±0.01 -	This work
GhMYB3	AtTTG1	0.36±0.02 -	This work
GhMYB25	AtTTG1	0.36±0.02 -	This work
GhRLC1	AtTTG1	0.39±0.02 -	This work
PhAN2	AtTTG1	0.38±0.02 -	This work
PhAN4	AtTTG1	0.35±0.01 -	This work
PhPH4	AtTTG1	0.34±0.01 -	This work
ZmC1	AtTTG1	0.39±0.01 -	This work
ZmPL	AtTTG1	1.63±0.06 w	This work
ZmP1	AtTTG1	0.37±0.00 -	This work
w/o	AtTTG1	0.35±0.00 -	This work
AtGL3	AaGL1	28.14±1.63 +	This work
AtGL3	AaWER	22.23±1.43 +	This work
AtGL3	AaMYB23	20.27±2.15 +	This work
AtGL3	AaPAPL	23.16±1.95 +	This work
AtGL3	GhMYB2	11.36±1.00 +	This work
AtGL3	GhMYB3	13.05±2.14 +	This work
AtGL3	GhMYB25	0.57±0.02 -	This work
AtGL3	GhRLC1	17.12±2.16 +	This work
AtGL3	PhAN2	13.38±2.66 +	This work
AtGL3	PhAN4	16.01±1.38 +	This work
AtGL3	PhPH4	17.52±2.70 +	This work
AtGL3	ZmC1	20.16±1.60 +	This work
AtGL3	ZmPL	25.80±3.49 +	This work
AtGL3	ZmP1	0.54±0.01 -	This work
AtGL3	w/o	0.45±0.00 -	This work
AtEGL3	AaGL1	24.85±2.63 +	This work
AtEGL3	AaWER	18.20±1.42 +	This work

Table S8 Cont.

ProtA fusion	Luciferase fusion	Luciferase activity: pull-down/input ratio (%)	References
AtEGL3	AaMYB23	19.64±1.87 +	This work
AtEGL3	AaPAPL	19.33±1.19 +	This work
AtEGL3	GhMYB2	14.26±1.34 +	This work
AtEGL3	GhMYB3	18.59±2.72 +	This work
AtEGL3	GhMYB25	0.59±0.02 -	This work
AtEGL3	GhRLC1	24.58±2.76 +	This work
AtEGL3	PhAN2	19.71±2.35 +	This work
AtEGL3	PhAN4	26.80±1.53 +	This work
AtEGL3	PhPH4	23.99±2.07 +	This work
AtEGL3	ZmC1	32.45±1.73 +	This work
AtEGL3	ZmPL	17.32±2.47 +	This work
AtEGL3	ZmP1	0.55±0.01 -	This work
AtEGL3	w/o	0.44±0.00 -	This work
AtTT8	AaGL1	11.41±1.58 +	This work
AtTT8	AaWER	11.19±3.43 +	This work
AtTT8	AaMYB23	14.45±1.79 +	This work
AtTT8	AaPAPL	24.25±3.34 +	This work
AtTT8	GhMYB2	10.69±1.11 +	This work
AtTT8	GhMYB3	9.64±1.64 +	This work
AtTT8	GhMYB25	0.60±0.01 -	This work
AtTT8	GhRLC1	25.59±2.67 +	This work
AtTT8	PhAN2	25.43±1.79 +	This work
AtTT8	PhAN4	23.29±3.84 +	This work
AtTT8	PhPH4	31.82±5.89 +	This work
AtTT8	ZmC1	30.53±3.81 +	This work
AtTT8	ZmPL	22.32±1.47 +	This work
AtTT8	ZmP1	0.58±0.03 -	This work
AtTT8	w/o	0.46±0.01 -	This work
AtMYC1	AaGL1	20.15±2.48 +	This work
AtMYC1	AaWER	16.77±0.59 +	This work
AtMYC1	AaMYB23	15.89±1.25 +	This work

Table S8 Cont.

ProtA fusion	Luciferase fusion	Luciferase activity: pull-down/input ratio (%)	References
AtMYC1	AaPAPL	16.86±1.24 +	This work
AtMYC1	GhMYB2	16.07±1.40 +	This work
AtMYC1	GhMYB3	15.49±2.16 +	This work
AtMYC1	GhMYB25	0.60±0.01 -	This work
AtMYC1	GhRLC1	21.56±2.68 +	This work
AtMYC1	PhAN2	20.65±2.27 +	This work
AtMYC1	PhAN4	22.90±1.23 +	This work
AtMYC1	PhPH4	20.19±1.48 +	This work
AtMYC1	ZmC1	30.00±1.44 +	This work
AtMYC1	ZmPL	21.69±3.95 +	This work
AtMYC1	ZmP1	0.57±0.00 -	This work
AtMYC1	w/o	0.48±0.02 -	This work
AtTTG1	AaGL1	0.75±0.05 -	This work
AtTTG1	AaWER	0.71±0.02 -	This work
AtTTG1	AaMYB23	0.64±0.05 -	This work
AtTTG1	AaPAPL	0.70±0.01 -	This work
AtTTG1	GhMYB2	0.71±0.02 -	This work
AtTTG1	GhMYB3	0.63±0.01 -	This work
AtTTG1	GhMYB25	0.54±0.01 -	This work
AtTTG1	GhRLC1	0.56±0.02 -	This work
AtTTG1	PhAN2	0.60±0.01 -	This work
AtTTG1	PhAN4	0.55±0.01 -	This work
AtTTG1	PhPH4	0.62±0.00 -	This work
AtTTG1	ZmC1	0.54±0.01 -	This work
AtTTG1	ZmPL	1.91±0.02 w	This work
AtTTG1	ZmP1	0.55±0.01 -	This work
AtTTG1	w/o	0.49±0.01 -	This work
w/o	AaGL1	0.70±0.02 -	This work
w/o	AaWER	0.66±0.03 -	This work
w/o	AaMYB23	0.61±0.01 -	This work
w/o	AaPAPL	0.62±0.01 -	This work

Table S8 Cont.

ProtA fusion	Luciferase fusion	Luciferase activity: pull-down/input ratio (%)	References
w/o	GhMYB2	0.65±0.02 -	This work
w/o	GhMYB3	0.57±0.03 -	This work
w/o	GhMYB25	0.48±0.01 -	This work
w/o	GhRLC1	0.50±0.01 -	This work
w/o	PhAN2	0.51±0.01 -	This work
w/o	PhAN4	0.54±0.02 -	This work
w/o	PhPH4	0.61±0.02 -	This work
w/o	ZmC1	0.55±0.02 -	This work
w/o	ZmPL	0.72±0.01 -	This work
w/o	ZmP1	0.56±0.02 -	This work
w/o	w/o	0.43±0.02 -	This work

APPENDIX B Protein motif analysis

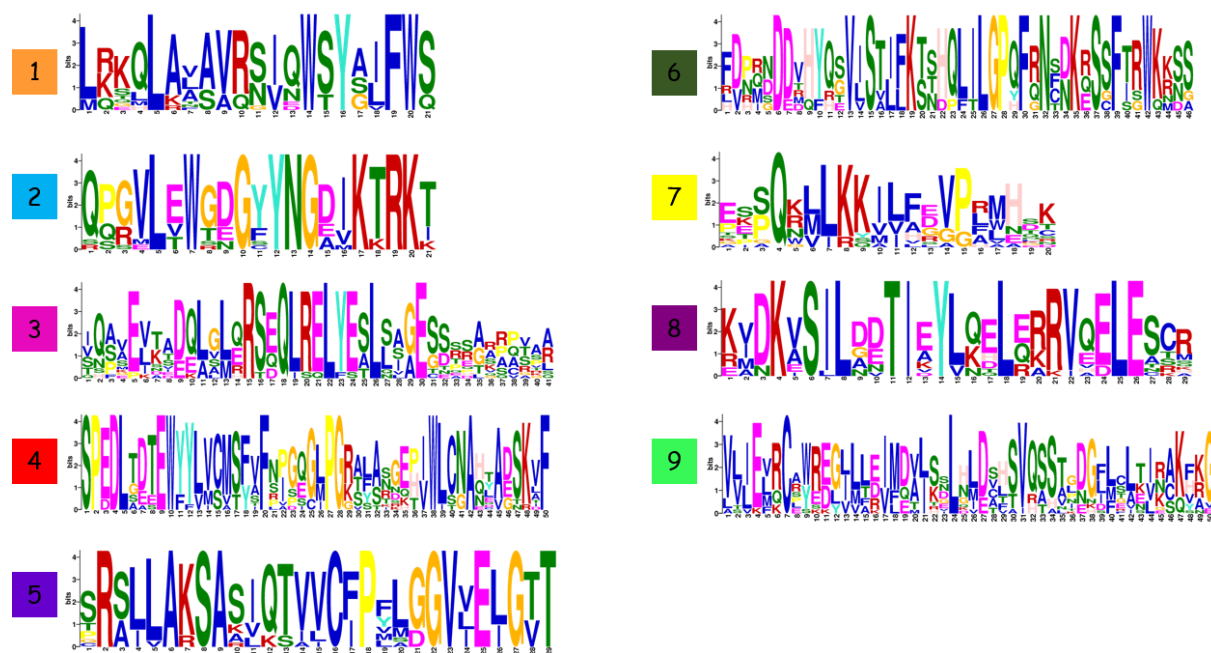
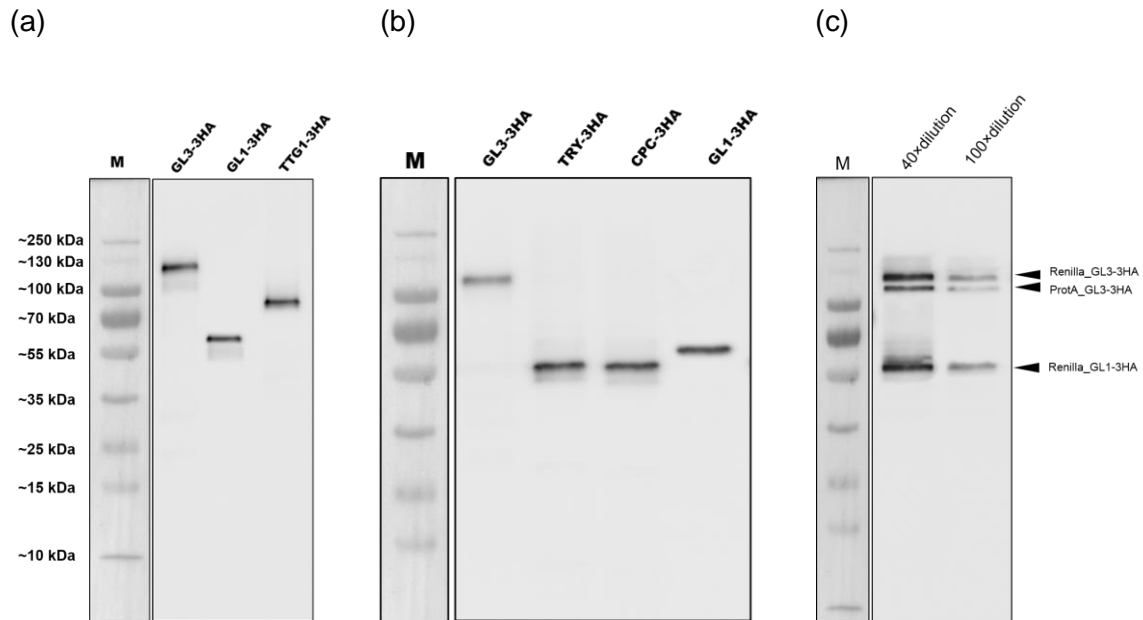


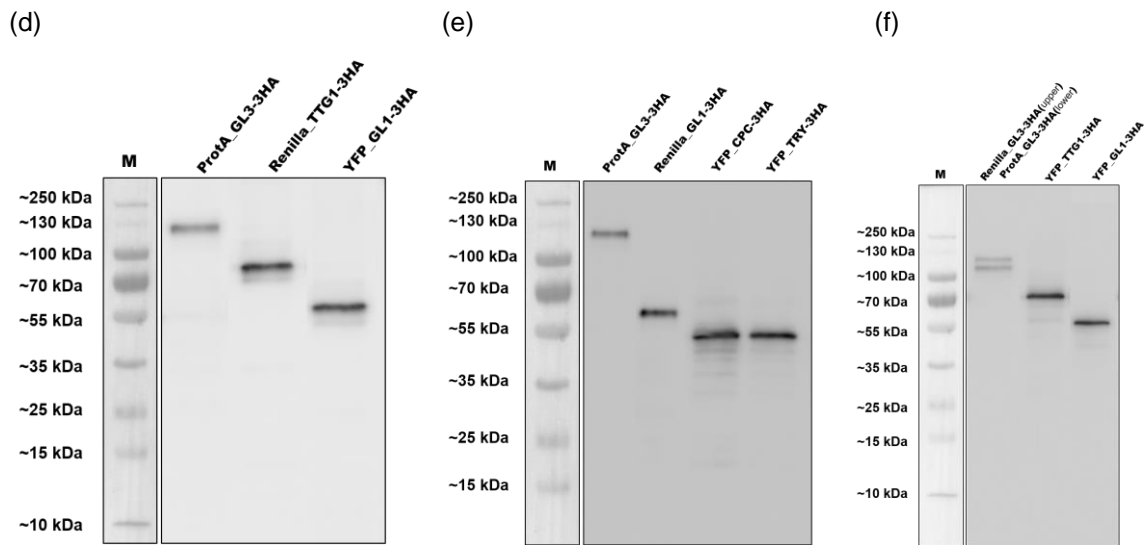
Figure S2 Sequence information of each motif in bHLH proteins.

APPENDIX C Western blot analysis of protein expressed in HEK cell



(a)Sample	%Peak	Relative density
ProtA_GL3-3HA	18,612	1
Renilla_GL1-3HA	15,394	0,827100795
Renilla_TTG1-3HA	15,541	0,834998925
(b)Sample	%Peak	Relative density
ProtA_GL3-3HA	10,752	1
Renilla_TRY-3HA	16,342	1,519903274
Renilla_CPC-3HA	16,456	1,530505952
Renilla_GL1-3HA	17,003	1,581380208
(c)Sample	%Peak	Relative density
ProtA_GL3-3HA	7,121	1
Renilla_GL3-3HA	8,462	1,188316248
Renilla_GL1-3HA	8,771	1,23170903

Figure S3 Western blot analysis of proteins fused with 3HA.



(d) Sample	%Peak	Relative density
ProtA_GL3-3HA	10,106	1
Renilla_TTG1-3HA	18,132	1,794181674
Renilla_GL1-3HA	13,993	1,384622996
(e) Sample	%Peak	Relative density
ProtA_GL3-3HA	8,996	1
Renilla_GL1-3HA	13,167	1,463650511
YFP_CPC-3HA	14,722	1,636505113
YFP_TRY-3HA	14,672	1,630947088
(f) Sample	%Peak	Relative density
ProtA_GL3-3HA	4,111	1
Renilla_GL3-3HA	4,098	0,996837752
Renilla_TTG1-3HA	14,593	3,549744588
Renilla_GL1-3HA	14,281	3,473850645

Figure S3 Cont. Western blot analysis of proteins fused with 3HA

Protein lysate was extracted from HEK cell and detected with Anti-HA-Peroxidase (5 mU/ml 1:2500 roth). Each Lane is 40x dilution of original lysate by lysis buffer. Relative density of each band is analysed in tables below by ImageJ (1.48v, National Institutes of Health, USA)

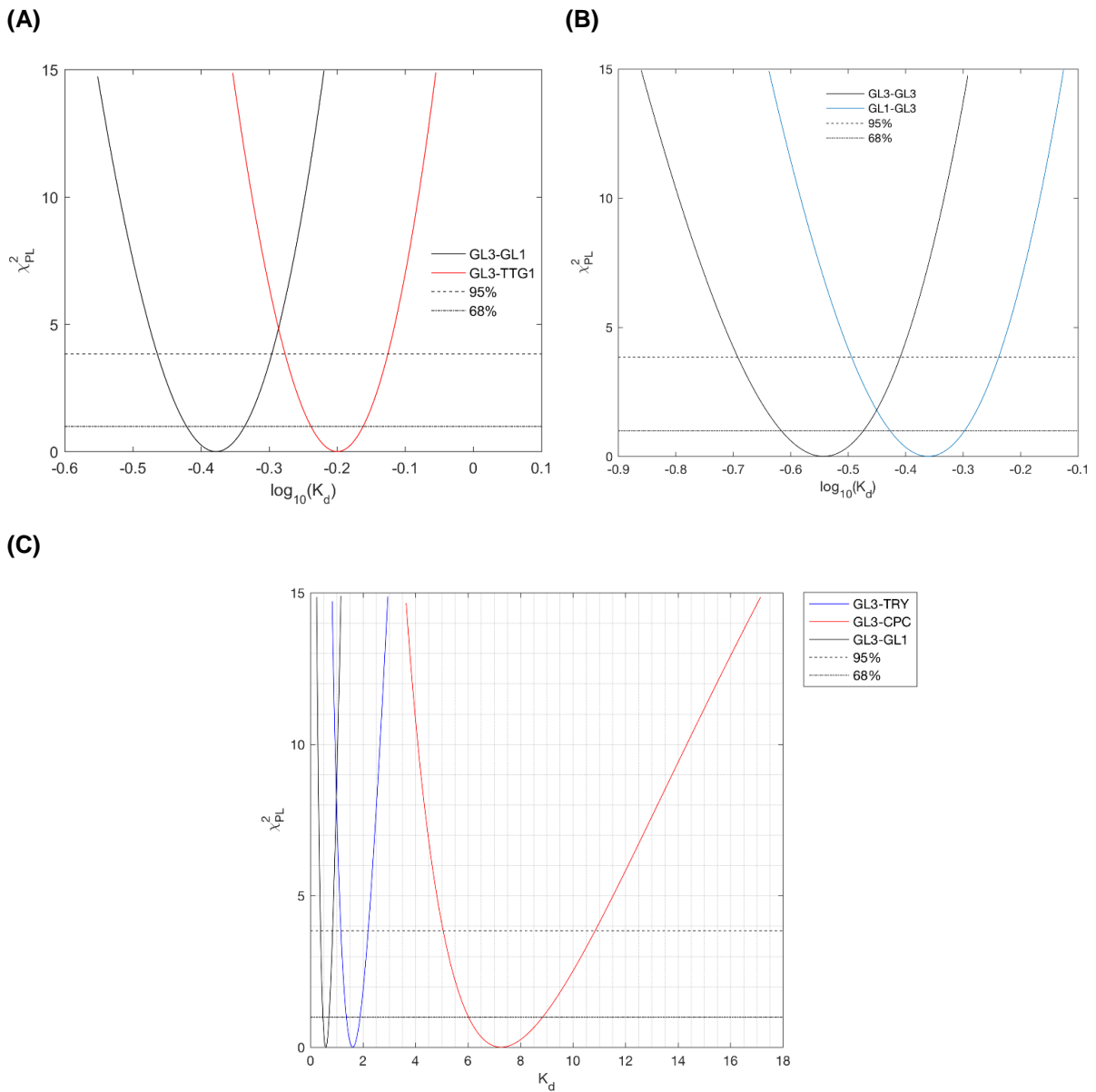


Figure S4 Likelihood profile ([195]).

(A) χ^2_{PL} for the estimates of the K_d for GL1 (black) and TTG1 (red).

(B) χ^2_{PL} for the estimates of the K_d for GL3 (black) and GL1 (blue).

(C) χ^2_{PL} for the estimates of the K_d for GL1 (black) and TRY (blue) and CPC (red).

Thresholds for confidence intervals are given by the dashed (95%) and dash-dotted lines (68%).

APPENDIX D Quantitative analyses of TTG1, GL3 and GL1 Protein Complex Formation

Table S 9-1 Binding affinity analysis of TTG1 (or GL1) and GL3 by titration (1st Biological replicate).

ProtA	Renilla	R1	R2	R3	Mean	Relative
20 µl AtGL3	-	213	224	223	220	-
20 µl AtGL3	5 µl AtTTG1	3385	3155	3108	3216	17,47%
20 µl AtGL3	10 µl AtTTG1	4698	4652	4711	4687	25,46%
20 µl AtGL3	15 µl AtTTG1	5521	5652	5600	5591	30,38%
20 µl AtGL3	20 µl AtTTG1	7490	7652	7691	7611	41,35%
20 µl AtGL3	25 µl AtTTG1	8813	9285	9123	9073,667	49,30%
20 µl AtGL3	30 µl AtTTG1	9971	9886	10034	9963,667	54,13%
20 µl AtGL3	35 µl AtTTG1	11815	12032	11882	11909,67	64,70%
20 µl AtGL3	40 µl AtTTG1	12477	12298	12465	12413,33	67,44%
20 µl AtGL3	50 µl AtTTG1	13064	12798	12976	12946	70,33%
20 µl AtGL3	60 µl AtTTG1	15167	15342	15198	15235,67	82,77%
20 µl AtGL3	70 µl AtTTG1	16298	16361	16233	16297,33	88,54%
20 µl AtGL3	80 µl AtTTG1	17639	17213	17367	17406,33	94,57%
20 µl AtGL3	90 µl AtTTG1	18397	18277	18545	18406,33	100,00%
20 µl AtGL3	100 µl AtTTG1	17842	18118	18397	18119	98,44%
20 µl AtGL3	150 µl AtTTG1	18385	18966	19038	18796,33	102,12%
20 µl AtGL3	w/o	215	222	217	218	-
20 µl AtGL3	5 µl AtGL1	6115	6032	5887	6011,333	26,62%
20 µl AtGL3	10 µl AtGL1	7369	7590	7330	7429,667	32,90%
20 µl AtGL3	15 µl AtGL1	9017	9326	9118	9153,667	40,54%
20 µl AtGL3	20 µl AtGL1	12777	12675	12338	12596,67	55,79%
20 µl AtGL3	25 µl AtGL1	13556	13378	13638	13524	59,89%

Table S9-1 Cont.

ProtA	Renilla	R1	R2	R3	Mean	Relative
20 µl AtGL3	30 µl AtGL1	13827	14009	14122	13986	61,94%
20 µl AtGL3	35 µl AtGL1	14735	14797	14890	14807,33	65,58%
20 µl AtGL3	40 µl AtGL1	15405	15218	15222	15281,67	67,68%
20 µl AtGL3	50 µl AtGL1	16939	17213	17098	17083,33	75,66%
20 µl AtGL3	60 µl AtGL1	18832	19027	18978	18945,67	83,91%
20 µl AtGL3	70 µl AtGL1	19966	20167	20259	20130,67	89,15%
20 µl AtGL3	80 µl AtGL1	21073	20897	21008	20992,67	92,97%
20 µl AtGL3	90 µl AtGL1	21771	22037	21853	21887	96,93%
20 µl AtGL3	100 µl AtGL1	22492	22545	22702	22579,67	100,00%
20 µl AtGL3	150 µl AtGL1	22498	22084	22632	22404,67	99,22%

Table S9-2 Binding affinity analysis of TTG1 (or GL1) and GL3 by titration LUMIER (2st Biological replicate).

ProtA	Renilla	R1	R2	R3	Mean	Relative
15 µl AtGL3	-	213	214	214	213,6667	-
15 µl AtGL3	5 µl AtTTG1	2785	2520	2578	2627,667	15,25%
15 µl AtGL3	15 µl AtTTG1	4398	4433	4365	4398,667	25,53%
15 µl AtGL3	30 µl AtTTG1	7599	7665	7773	7679	44,57%
15 µl AtGL3	45 µl AtTTG1	10413	10686	10226	10441,67	60,61%
15 µl AtGL3	60 µl AtTTG1	12094	11823	11906	11941	69,31%
15 µl AtGL3	75 µl AtTTG1	13470	13379	13400	13416,33	77,88%
15 µl AtGL3	90 µl AtTTG1	15094	14823	14906	14941	86,73%
15 µl AtGL3	120 µl AtTTG1	17279	17291	17112	17227,33	100,00%
15 µl AtGL3	150 µl AtTTG1	17015	17110	17187	17104	99,28%
15 µl AtGL3	180 µl AtTTG1	17544	18149	18101	17931,33	104,09%
15 µl AtGL3	240 µl AtTTG1	18447	17772	17447	17888,67	103,84%
15 µl AtGL3	w/o	215	222	224	220,3333	-
15 µl AtGL3	5 µl AtGL1	4105	4532	4387	4341,333	19,62%
15 µl AtGL3	15 µl AtGL1	7663	7698	7221	7527,333	34,03%
15 µl AtGL3	30 µl AtGL1	11915	12167	11832	11971,33	54,11%
15 µl AtGL3	45 µl AtGL1	14342	14177	14118	14212,33	64,24%
15 µl AtGL3	60 µl AtGL1	16933	16797	17019	16916,33	76,47%
15 µl AtGL3	75 µl AtGL1	18308	18002	18239	18183	82,19%
15 µl AtGL3	90 µl AtGL1	19833	20066	19666	19855	89,75%
15 µl AtGL3	120 µl AtGL1	21544	21476	21576	21532	97,33%
15 µl AtGL3	150 µl AtGL1	22045	22336	21986	22122,33	100,00%
15 µl AtGL3	180 µl AtGL1	22397	21966	22045	22136	100,06%
15 µl AtGL3	240 µl AtGL1	22157	22035	22233	22141,67	100,09%

Table S10 Binding affinity analysis of TRY (or CPC) and GL3 by titration LUMIER.

ProtA	Renilla	R1	R2	R3	Mean	Relative
10 µl AtGL3	-	224	226	224	224,6667	-
10 µl AtGL3	10 µl AtTRY	2177	2022	2167	2122	45,34%
10 µl AtGL3	20 µl AtTRY	3437	3330	3408	3391,667	72,47%
10 µl AtGL3	30 µl AtTRY	3654	3773	3610	3679	78,61%
10 µl AtGL3	40 µl AtTRY	3641	3801	3376	3606	77,05%
10 µl AtGL3	50 µl AtTRY	3950	4391	4226	4189	89,50%
10 µl AtGL3	80 µl AtTRY	4169	4232	4030	4143,667	88,53%
10 µl AtGL3	120 µl AtTRY	4590	4420	5028	4679,333	99,98%
10 µl AtGL3	160 µl AtTRY	5355	5302	4924	5193,667	110,97%
10 µl AtGL3	200 µl AtTRY	4600	4347	5094	4680,333	100,00%
10 µl AtGL3	w/o					-
10 µl AtGL3	10 µl AtCPC	2559	2418	2282	2419,667	43,86%
10 µl AtGL3	20 µl AtCPC	3200	3543	2632	3125	56,64%
10 µl AtGL3	30 µl AtCPC	2723	3072	3092	2962,333	53,69%
10 µl AtGL3	40 µl AtCPC	3103	3398	3525	3342	60,58%
10 µl AtGL3	50 µl AtCPC	3062	3095	2958	3038,333	55,07%
10 µl AtGL3	80 µl AtCPC	3472	3521	3755	3582,667	64,94%
10 µl AtGL3	120 µl AtCPC	5607	5148	5718	5491	99,53%
10 µl AtGL3	160 µl AtCPC	5324	5343	5494	5387	97,64%
10 µl AtGL3	200 µl AtCPC	5507	5597	5447	5517	100,00%
10 µl AtGL3	10 µl AtGL1	3681	3248	3612	3513,667	50,07%
10 µl AtGL3	20 µl AtGL1	4381	4327	4450	4386	62,50%
10 µl AtGL3	30 µl AtGL1	5002	5147	5289	5146	73,33%
10 µl AtGL3	40 µl AtGL1	6229	5996	5950	6058,333	86,33%

Table S10 Cont.

ProtA	Renilla	R1	R2	R3	Mean	Relative
10 µl AtGL3	50 µl AtGL1	6427	6678	6611	6572	93,65%
10 µl AtGL3	60 µl AtGL1	7058	6911	6757	6908,667	98,45%
10 µl AtGL3	70 µl AtGL1	6965	6847	6870	6894	98,24%
10 µl AtGL3	80 µl AtGL1	7248	6987	7266	7167	102,13%
10 µl AtGL3	120 µl AtTRY	7131	6918	7004	7017,667	100,00%
10 µl AtGL3	160 µl AtTRY	6427	6678	6611	6572	93,65%
10 µl AtGL3	200 µl AtTRY	7058	6911	6757	6908,667	98,45%

Table S11 Binding affinity analysis of TRY (or CPC) and GL3 by titration LUMIER.

ProtA	Renilla	R1	R2	R3	Mean	Relative
30 µl AtGL3	-	220	223	233	225,33	-
30 µl AtGL3	10 µl AtGL3	1003	929	1011	981,00	33,61%
30 µl AtGL3	20 µl AtGL3	1437	1522	1505	1488,00	50,98%
30 µl AtGL3	30 µl AtGL3	1751	2001	1800	1850,67	63,40%
30 µl AtGL3	40 µl AtGL3	2012	2188	2100	2100,00	71,94%
30 µl AtGL3	50 µl AtGL3	2340	2465	2488	2431,00	83,28%
30 µl AtGL3	60 µl AtGL3	2709	2691	2611	2670,33	91,48%
30 µl AtGL3	70 µl AtGL3	2986	2871	2900	2919,00	100,00%
30 µl AtGL3	80 µl AtGL3	2951	2790	2777	2839,33	97,27%
30 µl AtGL3	120 µl AtGL3	2890	3029	2928	2949,00	101,03%
30 µl AtGL3	160 µl AtGL3	3067	2988	2775	2943,33	100,83%
30 µl AtGL3	200 µl AtGL3	2807	2912	2994	2904,33	99,50%
30 µl AtGL3	w/o	234	222	230	228,67	-
30 µl AtGL3	10 µl AtGL1	3400	3112	3581	3364,33	38,95%
30 µl AtGL3	20 µl AtGL1	4612	4432	4450	4498,00	52,07%
30 µl AtGL3	30 µl AtGL1	5216	5248	5098	5187,33	60,05%
30 µl AtGL3	40 µl AtGL1	6009	5712	5657	5792,67	67,06%
30 µl AtGL3	50 µl AtGL1	6627	6278	6551	6485,33	75,08%
31 µl AtGL3	60 µl AtGL1	6910	7080	7110	7033,33	81,43%
32 µl AtGL3	70 µl AtGL1	7500	7521	7518	7513,00	86,98%
30 µl AtGL3	80 µl AtGL1	7958	7911	7757	7875,33	91,17%
30 µl AtGL3	120 µl AtGL1	8696	8747	8470	8637,67	100,00%
30 µl AtGL3	160 µl AtGL1	8724	8687	8500	8637,00	99,99%
30 µl AtGL3	200 µl AtGL1	8831	8503	8540	8624,67	99,85%

Table S12-1 Quantitative analysis of GL1 or TTG1 effect on GL3-GL3 dimerization by dosage-dependent LUMIER (1st Biological replicate).

ProtA	Renilla	YFP	R1	R2	R3	Mean	Relative	GL3_ProtA: GL3_Renilla: YFP_GL1
50 µl AtGL3	50 µl AtGL3	-	1900	2020	1927	1949,00	100,00%	-
50 µl AtGL3	50 µl AtGL3	w/o	1883	1985	1948	1938,67	99,47%	-
50 µl AtGL3	50 µl AtGL3	10 µl GL1	2188	2157	1923	2089,33	107,20%	1.2: 1: 1
50 µl AtGL3	50 µl AtGL3	20 µl GL1	2094	2078	2150	2107,33	108,12%	1.2: 1: 2
50 µl AtGL3	50 µl AtGL3	30 µl GL1	2136	2124	2003	2087,67	107,11%	1.2: 1: 3
50 µl AtGL3	50 µl AtGL3	40 µl GL1	2059	1903	2093	2018,33	103,56%	1.2: 1: 4
50 µl AtGL3	50 µl AtGL3	50 µl GL1	2054	2200	2204	2152,67	110,45%	1.2: 1: 5
50 µl AtGL3	50 µl AtGL3	60 µl GL1	2158	2171	2244	2191,00	112,42%	1.2: 1: 6
50 µl AtGL3	50 µl AtGL3	70 µl GL1	1936	2257	2179	2124,00	108,98%	1.2: 1: 7
50 µl AtGL3	50 µl AtGL3	80 µl GL1	2044	2053	1931	2009,33	103,10%	1.2: 1: 8
50 µl AtGL3	50 µl AtGL3	90 µl GL1	2098	1935	2005	2012,67	103,27%	1.2: 1: 9
50 µl AtGL3	50 µl AtGL3	100 µl GL1	2151	2036	1935	2040,67	104,70%	1.2: 1: 10
								GL3_ProtA: GL3_Renilla: YFP_TTG1
50 µl AtGL3	50 µl AtGL3	10 µl TTG1	1933	1916	1935	1928,00	98,92%	1.2: 1: 1
50 µl AtGL3	50 µl AtGL3	20 µl TTG1	1974	1947	2058	1993,00	102,26%	1.2: 1: 2
50 µl AtGL3	50 µl AtGL3	30 µl TTG1	1936	1915	1989	1946,67	99,88%	1.2: 1: 3
50 µl AtGL3	50 µl AtGL3	40 µl TTG1	2133	1910	2107	2050,00	105,18%	1.2: 1: 4
50 µl AtGL3	50 µl AtGL3	50 µl TTG1	1900	2073	1993	1988,67	102,04%	1.2: 1: 5
50 µl AtGL3	50 µl AtGL3	60 µl TTG1	2025	1948	1960	1977,67	101,47%	1.2: 1: 6
50 µl AtGL3	50 µl AtGL3	70 µl TTG1	2093	1919	1988	2000,00	102,62%	1.2: 1: 7
50 µl AtGL3	50 µl AtGL3	80 µl TTG1	1957	1990	2093	2013,33	103,30%	1.2: 1: 8
50 µl AtGL3	50 µl AtGL3	90 µl TTG1	1944	2093	1845	1960,67	100,60%	1.2: 1: 9
50 µl AtGL3	50 µl AtGL3	100 µl TTG1	2077	2013	1980	2023,33	103,81%	1.2: 1: 10

Table S12-2 Quantitative analysis of GL1 or TTG1 effect on GL3-GL3 dimerization by dosage-dependent LUMIER (2st Biological replicate).

ProtA	Renilla	YFP	R1	R2	R3	Mean	Relative	GL3_ProtA: GL3_Renilla: YFP_GL1
50 µl AtGL3	50 µl AtGL3	-	5433	5018	5648	5366,33	100,00%	-
50 µl AtGL3	50 µl AtGL3	w/o	5150	5342	5371	5287,67	98,53%	-
50 µl AtGL3	50 µl AtGL3	10 µl GL1	5905	5201	5584	5563,33	103,67%	1: 1: 0.7
50 µl AtGL3	50 µl AtGL3	20 µl GL1	5960	5714	5629	5767,67	107,48%	1: 1: 1.4
50 µl AtGL3	50 µl AtGL3	30 µl GL1	5762	5516	5664	5647,33	105,24%	1: 1: 2.1
50 µl AtGL3	50 µl AtGL3	40 µl GL1	5758	5723	5894	5791,67	107,93%	1: 1: 2.8
50 µl AtGL3	50 µl AtGL3	50 µl GL1	5404	5514	5892	5603,33	104,42%	1: 1: 3.5
50 µl AtGL3	50 µl AtGL3	60 µl GL1	5634	5698	5288	5540,00	103,24%	1: 1: 4.2
50 µl AtGL3	50 µl AtGL3	70 µl GL1	5505	5359	5823	5562,33	103,65%	1: 1: 4.9
50 µl AtGL3	50 µl AtGL3	80 µl GL1	6003	5712	5645	5786,67	107,83%	1: 1: 5.6
50 µl AtGL3	50 µl AtGL3	90 µl GL1	5622	5620	5669	5637,00	105,04%	1: 1: 6.3
50 µl AtGL3	50 µl AtGL3	100 µl GL1	5932	5790	5881	5867,67	109,34%	1: 1: 7.0
								GL3_ProtA: GL3_Renilla: YFP_TTG1
50 µl AtGL3	50 µl AtGL3	10 µl TTG1	5589	5334	5322	5415,00	100,91%	1: 1: 0.7
50 µl AtGL3	50 µl AtGL3	20 µl TTG1	5449	5720	5871	5680,00	105,85%	1: 1: 1.4
50 µl AtGL3	50 µl AtGL3	30 µl TTG1	5550	5883	5600	5677,67	105,80%	1: 1: 2.1
50 µl AtGL3	50 µl AtGL3	40 µl TTG1	5712	5354	5449	5505,00	102,58%	1: 1: 2.8
50 µl AtGL3	50 µl AtGL3	50 µl TTG1	5432	5489	5485	5468,67	101,91%	1: 1: 3.5
50 µl AtGL3	50 µl AtGL3	60 µl TTG1	5775	5606	5687	5689,33	106,02%	1: 1: 4.2
50 µl AtGL3	50 µl AtGL3	70 µl TTG1	5471	5480	5509	5486,67	102,24%	1: 1: 4.9
50 µl AtGL3	50 µl AtGL3	80 µl TTG1	5557	5690	5593	5613,33	104,60%	1: 1: 5.6
50 µl AtGL3	50 µl AtGL3	90 µl TTG1	5344	5700	5521	5521,67	102,89%	1: 1: 6.3
50 µl AtGL3	50 µl AtGL3	100 µl TTG1	5771	5588	5880	5746,33	107,08%	1: 1: 7.0

Table S13-1 Quantitative analysis of GL1 effect on TTG1-GL3 interaction by dosage-dependent LUMIER (1st Biological replicate).

ProtA	Renilla	YFP*	R1	R2	R3	Mean	Relative	GL3: TTG1: GL1
30 µl AtGL3	30 µl AtTTG1	-	7636	7255	7300	7397,00	100,00%	-
30 µl AtGL3	30 µl AtTTG1	10 µl AtGL1	6858	7024	7071	6984,33	94,42%	1: 1.7: 0.47
30 µl AtGL3	30 µl AtTTG1	20 µl AtGL1	6112	6006	6179	6099,00	82,45%	1: 1.7: 0.93
30 µl AtGL3	30 µl AtTTG1	30 µl AtGL1	5184	5385	5434	5334,33	72,11%	1: 1.7: 1.4
30 µl AtGL3	30 µl AtTTG1	40 µl AtGL1	4501	4570	4405	4492,00	60,73%	1: 1.7: 1.87
30 µl AtGL3	30 µl AtTTG1	50 µl AtGL1	4852	5001	4632	4828,33	65,27%	1: 1.7: 2.33
30 µl AtGL3	30 µl AtTTG1	60 µl AtGL1	5465	5716	5588	5589,67	75,57%	1: 1.7: 2.8
30 µl AtGL3	30 µl AtTTG1	70 µl AtGL1	5806	5901	5810	5839,00	78,94%	1: 1.7: 3.27
30 µl AtGL3	30 µl AtTTG1	80 µl AtGL1	5887	6133	6010	6010,00	81,25%	1: 1.7: 3.73
30 µl AtGL3	30 µl AtTTG1	90 µl AtGL1	5951	6122	6150	6074,33	82,12%	1: 1.7: 4.2
30 µl AtGL3	30 µl AtTTG1	100 µl AtGL1	6180	5952	6061	6064,33	81,98%	1: 1.7: 4.67
GL3: TTG1: TTG1-YFP								
30 µl AtGL3	30 µl AtTTG1	100 µl w/o	7230	7865	7370	7488,33	101,23%	-
30 µl AtGL3	30 µl AtTTG1	10 µl AtTTG1	4630	4552	4856	4679,33	63,26%	1: 1.7: 0.47
30 µl AtGL3	30 µl AtTTG1	20 µl AtTTG1	3509	3711	3876	3698,67	50,00%	1: 1.7: 0.93
30 µl AtGL3	30 µl AtTTG1	30 µl AtTTG1	3252	3151	3580	3327,67	44,99%	1: 1.7: 1.4
30 µl AtGL3	30 µl AtTTG1	40 µl AtTTG1	2420	2673	2241	2444,67	33,05%	1: 1.7: 1.87
30 µl AtGL3	30 µl AtTTG1	50 µl AtTTG1	2064	2169	1976	2069,67	27,98%	1: 1.7: 2.33
30 µl AtGL3	30 µl AtTTG1	60 µl AtTTG1	1703	1754	1715	1724,00	23,31%	1: 1.7: 2.8
30 µl AtGL3	30 µl AtTTG1	70 µl AtTTG1	1770	1720	1711	1733,67	23,44%	1: 1.7: 3.27
30 µl AtGL3	30 µl AtTTG1	80 µl AtTTG1	1861	1886	1899	1882,00	25,44%	1: 1.7: 3.73
30 µl AtGL3	30 µl AtTTG1	90 µl AtTTG1	1800	1721	1733	1751,33	23,68%	1: 1.7: 4.2
30 µl AtGL3	30 µl AtTTG1	100 µl AtTTG1	1727	1710	1681	1706,00	23,06%	1: 1.7: 4.67

* YFP_GL1, YFP_w/o and YFP_TTG1 are normalized by YFP fluorescence intensity

Table S13-2 Quantitative analysis of GL1 effect on TTG1-GL3 interaction by dosage-dependent LUMIER (2st Biological replicate).

ProtA	Renilla	YFP*	R1	R2	R3	Mean	Relative	GL3: TTG1: GL1
30 µl AtGL3	30 µl AtTTG1	-	8879	9005	8721	8868,33	100,00%	-
30 µl AtGL3	30 µl AtTTG1	10 µl AtGL1	8406	8501	8389	8432,00	95,08%	1: 2.0: 0.5
30 µl AtGL3	30 µl AtTTG1	20 µl AtGL1	7537	7620	7310	7489,00	84,45%	1: 2.0: 1.0
30 µl AtGL3	30 µl AtTTG1	30 µl AtGL1	6792	6518	6895	6735,00	75,94%	1: 2.0: 1.5
30 µl AtGL3	30 µl AtTTG1	40 µl AtGL1	5812	5931	6003	5915,33	66,70%	1: 2.0: 2.0
30 µl AtGL3	30 µl AtTTG1	50 µl AtGL1	6112	6018	5905	6011,67	67,79%	1: 2.0: 2.5
30 µl AtGL3	30 µl AtTTG1	60 µl AtGL1	6612	6731	6903	6748,67	76,10%	1: 2.0: 3.0
30 µl AtGL3	30 µl AtTTG1	70 µl AtGL1	7182	7119	7036	7112,33	80,20%	1: 2.0: 3.5
30 µl AtGL3	30 µl AtTTG1	80 µl AtGL1	7410	7221	7302	7311,00	82,44%	1: 2.0: 4.0
30 µl AtGL3	30 µl AtTTG1	90 µl AtGL1	7286	7250	7111	7215,67	81,36%	1: 2.0: 4.5
30 µl AtGL3	30 µl AtTTG1	100 µl AtGL1	7305	7222	7304	7277,00	82,06%	1: 2.0: 5.0
GL3: TTG1: TTG1_YFP								
30 µl AtGL3	30 µl AtTTG1	100 µl w/o	9010	8812	8858	8893,33	100,28%	-
30 µl AtGL3	30 µl AtTTG1	10 µl AtTTG1	5834	5807	6012	5884,33	66,35%	1: 2.0: 0.5
30 µl AtGL3	30 µl AtTTG1	20 µl AtTTG1	5100	5002	5120	5074,00	57,21%	1: 2.0: 1.0
30 µl AtGL3	30 µl AtTTG1	30 µl AtTTG1	4101	4200	4069	4123,33	46,50%	1: 2.0: 1.5
30 µl AtGL3	30 µl AtTTG1	40 µl AtTTG1	3215	3101	3134	3150,00	35,52%	1: 2.0: 2.0
30 µl AtGL3	30 µl AtTTG1	50 µl AtTTG1	2811	2529	2388	2576,00	29,05%	1: 2.0: 2.5
30 µl AtGL3	30 µl AtTTG1	60 µl AtTTG1	2302	2251	2212	2255,00	25,43%	1: 2.0: 3.0
30 µl AtGL3	30 µl AtTTG1	70 µl AtTTG1	2007	2155	2173	2111,67	23,81%	1: 2.0: 3.5
30 µl AtGL3	30 µl AtTTG1	80 µl AtTTG1	2195	1988	2024	2069,00	23,33%	1: 2.0: 4.0
30 µl AtGL3	30 µl AtTTG1	90 µl AtTTG1	1940	2055	2155	2050,00	23,12%	1: 2.0: 4.5
30 µl AtGL3	30 µl AtTTG1	100 µl AtTTG1	1912	2172	2091	2058,33	23,21%	1: 2.0: 5.0

* YFP_GL1, YFP_w/o and YFP_TTG1 are normalized by YFP fluorescence intensity

Table S 14-1 Quantitative analysis of TRY or CPC effect on GL3-GL1 interaction by dosage-dependent LUMIER (1st Biological replicate).

ProtA	Renilla	YFP	R1	R2	R3	Mean	Relative	GL3_ProtA: GL1_Renilla: YFP_TRY
30 µl AtGL3	30 µl AtGL1	-	7831	7762	7738	7777,00	100,00%	-
30 µl AtGL3	30 µl AtGL1	w/o	8018	7820	7918	7918,67	101,82%	-
30 µl AtGL3	30 µl AtGL1	10 µl TRY	2042	1900	1986	1976,00	25,41%	1: 1.5: 0.53
30 µl AtGL3	30 µl AtGL1	20 µl TRY	1989	1758	1679	1808,67	23,26%	1: 1.5: 1.07
30 µl AtGL3	30 µl AtGL1	30 µl TRY	1334	1398	1354	1362,00	17,51%	1: 1.5: 1.6
30 µl AtGL3	30 µl AtGL1	40 µl TRY	1205	1502	1337	1348,00	17,33%	1: 1.5: 2.13
30 µl AtGL3	30 µl AtGL1	50 µl TRY	1425	1313	1105	1281,00	16,47%	1: 1.5: 2.67
30 µl AtGL3	30 µl AtGL1	60 µl TRY	1164	1459	1380	1334,33	17,16%	1: 1.5: 3.2
30 µl AtGL3	30 µl AtGL1	70 µl TRY	1371	1171	1484	1342,00	17,26%	1: 1.5: 3.73
30 µl AtGL3	30 µl AtGL1	80 µl TRY	1275	1393	1325	1331,00	17,11%	1: 1.5: 4.28
30 µl AtGL3	30 µl AtGL1	90 µl TRY	1287	1226	1393	1302,00	16,74%	1: 1.5: 4.8
30 µl AtGL3	30 µl AtGL1	100 µl TRY	1300	1365	1290	1318,33	16,95%	1: 1.5: 5.33
								GL3_ProtA: GL3_Renilla: YFP_CPC
30 µl AtGL3	30 µl AtGL1	10 µl CPC	3069	2950	2906	2975,00	38,25%	1: 1.5: 0.27
30 µl AtGL3	30 µl AtGL1	20 µl CPC	2575	2456	2656	2562,33	32,95%	1: 1.5: 0.53
30 µl AtGL3	30 µl AtGL1	30 µl CPC	2043	2098	2181	2107,33	27,10%	1: 1.5: 0.8
30 µl AtGL3	30 µl AtGL1	40 µl CPC	1931	1987	1927	1948,33	25,05%	1: 1.5: 1.07
30 µl AtGL3	30 µl AtGL1	50 µl CPC	1735	1883	1758	1792,00	23,04%	1: 1.5: 1.33
30 µl AtGL3	30 µl AtGL1	60 µl CPC	1629	1554	1634	1605,67	20,65%	1: 1.5: 1.6
30 µl AtGL3	30 µl AtGL1	70 µl CPC	1404	1338	1302	1348,00	17,33%	1: 1.5: 1.87
30 µl AtGL3	30 µl AtGL1	80 µl CPC	1561	1323	1450	1444,67	18,58%	1: 1.5: 2.13
30 µl AtGL3	30 µl AtGL1	90 µl CPC	1441	1381	1303	1375,00	17,68%	1: 1.5: 2.4
30 µl AtGL3	30 µl AtGL1	100 µl CPC	1339	1400	1422	1387,00	17,83%	1: 1.5: 2.67

Table S14-2 Quantitative analysis of TRY or CPC effect on GL3-GL1 interaction by dosage-dependent LUMIER (2st Biological replicate).

ProtA	Renilla	YFP	R1	R2	R3	Mean	Relative	GL3_ProtA: GL1_Renilla: YFP_TRY
30 µl AtGL3	30 µl AtGL1	-	9019	9159	9562	9246,67	100,00%	
30 µl AtGL3	30 µl AtGL1	w/o	9322	9331	9277	9310,00	100,68%	
30 µl AtGL3	30 µl AtGL1	10 µl TRY	4023	4112	4029	4054,67	43,85%	1: 1.8: 0.33
30 µl AtGL3	30 µl AtGL1	20 µl TRY	3629	3518	3504	3550,33	38,40%	1: 1.8: 0.67
30 µl AtGL3	30 µl AtGL1	30 µl TRY	2901	3125	3054	3026,67	32,73%	1: 1.8: 1
30 µl AtGL3	30 µl AtGL1	40 µl TRY	2456	2350	2414	2406,67	26,03%	1: 1.8: 1.33
30 µl AtGL3	30 µl AtGL1	50 µl TRY	1910	2076	2038	2008,00	21,72%	1: 1.8: 1.67
30 µl AtGL3	30 µl AtGL1	60 µl TRY	1711	1604	1717	1677,33	18,14%	1: 1.8: 2
30 µl AtGL3	30 µl AtGL1	70 µl TRY	1689	1604	1744	1679,00	18,16%	1: 1.8: 2.33
30 µl AtGL3	30 µl AtGL1	80 µl TRY	1514	1604	1659	1592,33	17,22%	1: 1.8: 2.67
30 µl AtGL3	30 µl AtGL1	90 µl TRY	1709	1632	1637	1659,33	17,95%	1: 1.8: 3
30 µl AtGL3	30 µl AtGL1	100 µl TRY	1559	1662	1608	1609,67	17,41%	1: 1.8: 3.33
								GL3_ProtA: GL3_Renilla: YFP_CPC
30 µl AtGL3	30 µl AtGL1	10 µl CPC	4110	4218	4109	4145,67	44,83%	1: 1.8: 0.33
30 µl AtGL3	30 µl AtGL1	20 µl CPC	3809	3723	3702	3744,67	40,50%	1: 1.8: 0.67
30 µl AtGL3	30 µl AtGL1	30 µl CPC	3129	3275	3201	3201,67	34,63%	1: 1.8: 1
30 µl AtGL3	30 µl AtGL1	40 µl CPC	2702	2630	2615	2649,00	28,65%	1: 1.8: 1.33
30 µl AtGL3	30 µl AtGL1	50 µl CPC	2111	2002	2129	2080,67	22,50%	1: 1.8: 1.67
30 µl AtGL3	30 µl AtGL1	60 µl CPC	1623	1575	1630	1609,33	17,40%	1: 1.8: 2
30 µl AtGL3	30 µl AtGL1	70 µl CPC	1605	1627	1723	1651,67	17,86%	1: 1.8: 2.33
30 µl AtGL3	30 µl AtGL1	80 µl CPC	1660	1729	1652	1680,33	18,17%	1: 1.8: 2.67
30 µl AtGL3	30 µl AtGL1	90 µl CPC	1700	1621	1605	1642,00	17,76%	1: 1.8: 3
30 µl AtGL3	30 µl AtGL1	100 µl CPC	1656	1607	1700	1654,33	17,89%	1: 1.8: 3.33

Table S15 ANOVA test of effect of GL1 on the TTG1 binding to GL3.

		ProtA	Renilla	YFP*	Anova group
		30 µl AtGL3	30 µl AtTTG1	-	1
		30 µl AtGL3	30 µl AtTTG1	10 µl AtGL1	2
		30 µl AtGL3	30 µl AtTTG1	20 µl AtGL1	3
		30 µl AtGL3	30 µl AtTTG1	30 µl AtGL1	4
		30 µl AtGL3	30 µl AtTTG1	40 µl AtGL1	5
		30 µl AtGL3	30 µl AtTTG1	50 µl AtGL1	6
		30 µl AtGL3	30 µl AtTTG1	60 µl AtGL1	7
		30 µl AtGL3	30 µl AtTTG1	70 µl AtGL1	8
		30 µl AtGL3	30 µl AtTTG1	80 µl AtGL1	9
		30 µl AtGL3	30 µl AtTTG1	90 µl AtGL1	10
		30 µl AtGL3	30 µl AtTTG1	100 µl AtGL1	11
Group1	Group2	lower CI	mean diff	upper CI	P-value
1	2	65,912	436,333	806,755	9,47E-03
1	3	1008,912	1379,333	1749,755	7,37E-11
1	4	1762,912	2133,333	2503,755	9,30E-15
1	5	2582,578	2953,000	3323,422	9,07E-18
1	6	2486,245	2856,667	3227,088	1,85E-17
1	7	1749,245	2119,667	2490,088	1,07E-14
1	8	1385,578	1756,000	2126,422	5,43E-13
1	9	1186,912	1557,333	1927,755	6,39E-12
1	10	1282,245	1652,667	2023,088	1,90E-12
1	11	1220,912	1591,333	1961,755	4,11E-12
2	3	572,578	943,000	1313,422	1,04E-07
2	4	1326,578	1697,000	2067,422	1,10E-12
2	5	2146,245	2516,667	2887,088	2,79E-16
2	6	2049,912	2420,333	2790,755	6,41E-16
2	7	1312,912	1683,333	2053,755	1,30E-12
2	8	949,245	1319,667	1690,088	1,77E-10
2	9	750,578	1121,000	1491,422	4,22E-09
2	10	845,912	1216,333	1586,755	8,77E-10
2	11	784,578	1155,000	1525,422	2,38E-09
3	4	383,578	754,000	1124,422	4,94E-06
3	5	1203,245	1573,667	1944,088	5,16E-12
3	6	1106,912	1477,333	1847,755	1,86E-11
3	7	369,912	740,333	1110,755	6,66E-06
3	8	6,245	376,667	747,088	4,27E-02
3	9	-192,422	178,000	548,422	1,00E+00
3	10	-97,088	273,333	643,755	5,40E-01
3	11	-158,422	212,000	582,422	1,00E+00
4	5	449,245	819,667	1190,088	1,22E-06
4	6	352,912	723,333	1093,755	9,69E-06
4	7	-384,088	-13,667	356,755	1,00E+00
4	8	-747,755	-377,333	-6,912	4,20E-02
4	9	-946,422	-576,000	-205,578	2,96E-04
4	10	-851,088	-480,667	-110,245	3,10E-03
4	11	-912,422	-542,000	-171,578	6,77E-04
5	6	-466,755	-96,333	274,088	1,00E+00
5	7	-1203,755	-833,333	-462,912	9,21E-07
5	8	-1567,422	-1197,000	-826,578	1,20E-09
5	9	-1766,088	-1395,667	-1025,245	5,83E-11
5	10	-1670,755	-1300,333	-929,912	2,37E-10
5	11	-1732,088	-1361,667	-991,245	9,53E-11

Table S15 Cont.

Group1	Group2	lower CI	mean diff	upper CI	P-value
6	7	-1107,422	-737,000	-366,578	7,17E-06
6	8	-1471,088	-1100,667	-730,245	5,97E-09
6	9	-1669,755	-1299,333	-928,912	2,41E-10
6	10	-1574,422	-1204,000	-833,578	1,07E-09
6	11	-1635,755	-1265,333	-894,912	4,06E-10
7	8	-734,088	-363,667	6,755	5,92E-02
7	9	-932,755	-562,333	-191,912	4,12E-04
7	10	-837,422	-467,000	-96,578	4,37E-03
7	11	-898,755	-528,333	-157,912	9,48E-04
8	9	-569,088	-198,667	171,755	1,00E+00
8	10	-473,755	-103,333	267,088	1,00E+00
8	11	-535,088	-164,667	205,755	1,00E+00
9	10	-275,088	95,333	465,755	1,00E+00
9	11	-336,422	34,000	404,422	1,00E+00
10	11	-431,755	-61,333	309,088	1,00E+00

ANOVA results

Source	SS	df	MS	F	Prob>F
Columns	2,37E+07	10	2,37E+06	168,8782	2,07E-18
Error	3,08E+05	22	1,40E+04		
Total	2,40E+07	32			

REFERENCES

1. Kranz, H., K. Scholz, and B. Weisshaar, *c-MYB oncogene-like genes encoding three MYB repeats occur in all major plant lineages*. Plant J, 2000. **21**(2): p. 231-5.
2. Lipsick, J.S., *The C-MYB story--is it definitive?* Proc Natl Acad Sci U S A, 2010. **107**(40): p. 17067-8.
3. Ogata, K., et al., *Solution structure of a specific DNA complex of the Myb DNA-binding domain with cooperative recognition helices*. Cell, 1994. **79**(4): p. 639-48.
4. Sakura, H., et al., *Delineation of three functional domains of the transcriptional activator encoded by the c-myb protooncogene*. Proc Natl Acad Sci U S A, 1989. **86**(15): p. 5758-62.
5. Klempnauer, K.H. and A.E. Sippel, *The highly conserved amino-terminal region of the protein encoded by the v-myb oncogene functions as a DNA-binding domain*. EMBO J, 1987. **6**(9): p. 2719-25.
6. Klempnauer, K.H., T.J. Gonda, and J.M. Bishop, *Nucleotide sequence of the retroviral leukemia gene v-myb and its cellular progenitor c-myb: the architecture of a transduced oncogene*. Cell, 1982. **31**(2 Pt 1): p. 453-63.
7. Du, H., et al., *Genome-wide analysis of the MYB transcription factor superfamily in soybean*. BMC Plant Biol, 2012. **12**: p. 106.
8. Liu, J., A. Osbourn, and P. Ma, *MYB Transcription Factors as Regulators of Phenylpropanoid Metabolism in Plants*. Mol Plant, 2015. **8**(5): p. 689-708.
9. Braun, E.L. and E. Grotewold, *Newly discovered plant c-myb-like genes rewrite the evolution of the plant myb gene family*. Plant Physiol, 1999. **121**(1): p. 21-4.
10. Stracke, R., et al., *Differential regulation of closely related R2R3-MYB transcription factors controls flavonol accumulation in different parts of the Arabidopsis thaliana seedling*. The Plant Journal, 2007. **50**(4): p. 660-677.
11. Dubos, C., et al., *MYB transcription factors in Arabidopsis*. Trends in Plant Science, 2010. **15**(10): p. 573-581.
12. Paz-Ares, J., et al., *The regulatory c1 locus of Zea mays encodes a protein with homology to myb proto-oncogene products and with structural similarities to transcriptional activators*. EMBO J, 1987. **6**(12): p. 3553-8.
13. McClintock, B., *The origin and behavior of mutable loci in maize*. Proc Natl Acad Sci U S A, 1950. **36**(6): p. 344-55.
14. Zimmermann, I.M., et al., *Comprehensive identification of Arabidopsis thaliana MYB transcription factors interacting with R/B-like BHLH proteins*. Plant J, 2004. **40**(1): p. 22-34.
15. Pires, N. and L. Dolan, *Origin and diversification of basic-helix-loop-helix proteins in plants*. Mol Biol Evol, 2010. **27**(4): p. 862-74.
16. Grotewold, E., et al., *Identification of the residues in the Myb domain of maize C1 that specify the interaction with the bHLH cofactor R*. Proc Natl Acad Sci U S A, 2000. **97**(25): p. 13579-84.
17. Ludwig, S.R., et al., *Lc, a member of the maize R gene family responsible for tissue-specific anthocyanin production, encodes a protein similar to transcriptional activators and contains the myc-homology region*. Proc Natl Acad Sci U S A, 1989. **86**(18): p. 7092-6.
18. Murre, C., P.S. McCaw, and D. Baltimore, *A new DNA binding and dimerization motif in immunoglobulin enhancer binding, daughterless, MyoD, and myc proteins*. Cell, 1989. **56**(5): p. 777-83.
19. Massari, M.E. and C. Murre, *Helix-loop-helix proteins: regulators of transcription in eucaryotic organisms*. Mol Cell Biol, 2000. **20**(2): p. 429-40.
20. Toledo-Ortiz, G., E. Huq, and P.H. Quail, *The Arabidopsis Basic/Helix-Loop-Helix Transcription Factor Family*. The Plant Cell, 2003. **15**(8): p. 1749-1770.
21. van Nocker, S. and P. Ludwig, *The WD-repeat protein superfamily in Arabidopsis: conservation and divergence in structure and function*. BMC Genomics, 2003. **4**(1): p. 50.
22. Neer, E.J., et al., *The ancient regulatory-protein family of WD-repeat proteins*. Nature, 1994. **371**(6495): p. 297-300.
23. Smith, T.F., et al., *The WD repeat: a common architecture for diverse functions*. Trends Biochem Sci, 1999. **24**(5): p. 181-5.

24. Deng, X.W., et al., *COP1, an Arabidopsis regulatory gene, encodes a protein with both a zinc-binding motif and a G beta homologous domain*. Cell, 1992. **71**(5): p. 791-801.
25. Hoecker, U., J.M. Tepperman, and P.H. Quail, *SPA1, a WD-repeat protein specific to phytochrome A signal transduction*. Science, 1999. **284**(5413): p. 496-9.
26. Laubinger, S. and U. Hoecker, *The SPA1-like proteins SPA3 and SPA4 repress photomorphogenesis in the light*. Plant J, 2003. **35**(3): p. 373-85.
27. Walker, A.R., et al., *The TRANSPARENT TESTA GLABRA1 locus, which regulates trichome differentiation and anthocyanin biosynthesis in Arabidopsis, encodes a WD40 repeat protein*. Plant Cell, 1999. **11**(7): p. 1337-50.
28. Walker, A.R., et al., *The TRANSPARENT TESTA GLABRA1 locus, which regulates trichome differentiation and anthocyanin biosynthesis in Arabidopsis, encodes a WD40 repeat protein*. The Plant Cell, 1999. **11**(7): p. 1337-1350.
29. Payne, C.T., F. Zhang, and A.M. Lloyd, *GL3 encodes a bHLH protein that regulates trichome development in arabidopsis through interaction with GL1 and TTG1*. Genetics, 2000. **156**(3): p. 1349-1362.
30. Heim, M.A., et al., *The Basic Helix–Loop–Helix Transcription Factor Family in Plants: A Genome-Wide Study of Protein Structure and Functional Diversity*. Molecular Biology and Evolution, 2003. **20**(5): p. 735-747.
31. Baudry, A., et al., *TT2, TT8, and TTG1 synergistically specify the expression of BANYULS and proanthocyanidin biosynthesis in Arabidopsis thaliana*. The Plant Journal, 2004. **39**(3): p. 366-380.
32. Zimmermann, I.M., et al., *Comprehensive identification of Arabidopsis thaliana MYB transcription factors interacting with R/B-like BHLH proteins*. The Plant Journal, 2004. **40**(1): p. 22-34.
33. Feller, A., J.M. Hernandez, and E. Grotewold, *An ACT-like Domain Participates in the Dimerization of Several Plant Basic-helix-loop-helix Transcription Factors*. Journal of Biological Chemistry, 2006. **281**(39): p. 28964-28974.
34. Feller, A., et al., *Evolutionary and comparative analysis of MYB and bHLH plant transcription factors*. The Plant Journal, 2011. **66**(1): p. 94-116.
35. Zhao, H., et al., *A Single Amino Acid Substitution in IIIf Subfamily of Basic Helix-Loop-Helix Transcription Factor AtMYC1 Leads to Trichome and Root Hair Patterning Defects by Abolishing Its Interaction with Partner Proteins in Arabidopsis*. Journal of Biological Chemistry, 2012. **287**(17): p. 14109-14121.
36. Wang, Y., et al., *A Method for WD40 Repeat Detection and Secondary Structure Prediction*. PLOS ONE, 2013. **8**(6): p. e65705.
37. Winkel-Shirley, B., *Flavonoid Biosynthesis. A Colorful Model for Genetics, Biochemistry, Cell Biology, and Biotechnology*. Plant Physiology, 2001. **126**(2): p. 485-493.
38. Stafford, H.A., *Flavonoid Evolution: An Enzymic Approach*. Plant Physiology, 1991. **96**(3): p. 680-685.
39. Goff, S.A., K.C. Cone, and V.L. Chandler, *Functional analysis of the transcriptional activator encoded by the maize B gene: evidence for a direct functional interaction between two classes of regulatory proteins*. Genes & Development, 1992. **6**(5): p. 864-875.
40. Lloyd, A., V. Walbot, and R. Davis, *Arabidopsis and Nicotiana anthocyanin production activated by maize regulators R and C1*. Science, 1992. **258**(5089): p. 1773-1775.
41. Cone, K.C., et al., *Maize anthocyanin regulatory gene pl is a duplicate of c1 that functions in the plant*. The Plant Cell, 1993. **5**(12): p. 1795-805.
42. Carey, C.C., et al., *Mutations in the pale aleurone color1 Regulatory Gene of the Zea mays Anthocyanin Pathway Have Distinct Phenotypes Relative to the Functionally Similar TRANSPARENT TESTA GLABRA1 Gene in Arabidopsis thaliana*. The Plant Cell, 2004. **16**(2): p. 450-464.
43. Hernandez, J.M., et al., *Different Mechanisms Participate in the R-dependent Activity of the R2R3 MYB Transcription Factor C1*. Journal of Biological Chemistry, 2004. **279**(46): p. 48205-48213.
44. Quattrocchio, F., et al., *Regulatory Genes Controlling Anthocyanin Pigmentation Are Functionally Conserved among Plant Species and Have Distinct Sets of Target Genes*. The Plant Cell, 1993. **5**(11): p. 1497-1512.

45. Quattrocchio, F., et al., *Analysis of bHLH and MYB domain proteins: species-specific regulatory differences are caused by divergent evolution of target anthocyanin genes*. The Plant Journal, 1998. **13**(4): p. 475-488.
46. Spelt, C., et al., *anthocyanin1 of Petunia Encodes a Basic Helix-Loop-Helix Protein That Directly Activates Transcription of Structural Anthocyanin Genes*. The Plant Cell, 2000. **12**(9): p. 1619-1631.
47. Spelt, C., et al., *ANTHOCYANIN1 of Petunia Controls Pigment Synthesis, Vacuolar pH, and Seed Coat Development by Genetically Distinct Mechanisms*. The Plant Cell, 2002. **14**(9): p. 2121-2135.
48. Quattrocchio, F., et al., *PH4 of Petunia Is an R2R3 MYB Protein That Activates Vacuolar Acidification through Interactions with Basic-Helix-Loop-Helix Transcription Factors of the Anthocyanin Pathway*. The Plant Cell, 2006. **18**(5): p. 1274-1291.
49. Albert, N.W., et al., *Members of an R2R3-MYB transcription factor family in Petunia are developmentally and environmentally regulated to control complex floral and vegetative pigmentation patterning*. The Plant Journal, 2011. **65**(5): p. 771-784.
50. Schwinn, K., et al., *A Small Family of MYB-Regulatory Genes Controls Floral Pigmentation Intensity and Patterning in the Genus Antirrhinum*. The Plant Cell, 2006. **18**(4): p. 831-851.
51. de Vetten, N., et al., *The an11 locus controlling flower pigmentation in petunia encodes a novel WD-repeat protein conserved in yeast, plants, and animals*. Genes & Development, 1997. **11**(11): p. 1422-1434.
52. Selinger, D.A. and V.L. Chandler, *A Mutation in the pale aleurone color1 Gene Identifies a Novel Regulator of the Maize Anthocyanin Pathway*. The Plant Cell, 1999. **11**(1): p. 5-14.
53. Sompornpailin, K., et al., *A WD-repeat-containing putative regulatory protein in anthocyanin biosynthesis in Perilla frutescens*. Plant Molecular Biology, 2002. **50**(3): p. 485-495.
54. Morita, Y., et al., *Isolation of cDNAs for R2R3-MYB, bHLH and WDR Transcriptional Regulators and Identification of c and ca Mutations Conferring White Flowers in the Japanese Morning Glory*. Plant and Cell Physiology, 2006. **47**(4): p. 457-470.
55. Brueggemann, J., B. Weisshaar, and M. Sagasser, *A WD40-repeat gene from Malus x domestica is a functional homologue of Arabidopsis thaliana TRANSPARENT TESTA GLABRA1*. Plant Cell Reports, 2010. **29**(3): p. 285-294.
56. Pang, Y., et al., *A WD40 Repeat Protein from Medicago truncatula Is Necessary for Tissue-Specific Anthocyanin and Proanthocyanidin Biosynthesis But Not for Trichome Development*. Plant Physiology, 2009. **151**(3): p. 1114-1129.
57. Chopra, D., et al., *Analysis of TTG1 function in Arabis alpina*. BMC Plant Biology, 2014. **14**: p. 16-16.
58. Liu, K., et al., *TRANSPARENT TESTA GLABRA 1 ubiquitously regulates plant growth and development from Arabidopsis to foxtail millet (Setaria italica)*. Plant Science, 2017. **254**(Supplement C): p. 60-69.
59. Zhang, J., et al., *Map-based cloning and characterization of a gene controlling hairiness and seed coat color traits in Brassica rapa*. Plant Molecular Biology, 2009. **69**(5): p. 553-563.
60. Nemesio-Gorrioz, M., et al., *Identification of Norway Spruce MYB-bHLH-WDR Transcription Factor Complex Members Linked to Regulation of the Flavonoid Pathway*. Frontiers in Plant Science, 2017. **8**(305).
61. Miller, J.C., W.R. Chezem, and N.K. Clay, *Ternary WD40 Repeat-Containing Protein Complexes: Evolution, Composition and Roles in Plant Immunity*. Front Plant Sci, 2015. **6**: p. 1108.
62. Hedges, S.B., J. Dudley, and S. Kumar, *TimeTree: a public knowledge-base of divergence times among organisms*. Bioinformatics, 2006. **22**(23): p. 2971-2.
63. Lee, M.M. and J. Schiefelbein, *WEREWOLF, a MYB-Related Protein in Arabidopsis, Is a Position-Dependent Regulator of Epidermal Cell Patterning*. Cell, 1999. **99**(5): p. 473-483.
64. Penfield, S., et al., *MYB61 Is Required for Mucilage Deposition and Extrusion in the Arabidopsis Seed Coat*. The Plant Cell, 2001. **13**(12): p. 2777-2791.

65. Bernhardt, C., et al., *The bHLH genes GLABRA3 (GL3) and ENHANCER OF GLABRA3 (EGL3) specify epidermal cell fate in the Arabidopsis root*. *Development*, 2003. **130**(26): p. 6431-6439.
66. Zhang, F., et al., *A network of redundant bHLH proteins functions in all TTG1-dependent pathways of Arabidopsis*. *Development*, 2003.
67. Kirik, V., et al., *Functional diversification of MYB23 and GL1 genes in trichome morphogenesis and initiation*. *Development*, 2005. **132**(7): p. 1477-1485.
68. Bouyer, D., et al., *Two-Dimensional Patterning by a Trapping/Depletion Mechanism: The Role of TTG1 and GL3 in Arabidopsis Trichome Formation*. *PLoS Biology*, 2008. **6**(6): p. e141.
69. Morohashi, K. and E. Grotewold, *A Systems Approach Reveals Regulatory Circuitry for Arabidopsis Trichome Initiation by the GL3 and GL1 Selectors*. *PLOS Genetics*, 2009. **5**(2): p. e1000396.
70. Symonds, V.V., G. Hatlestad, and A.M. Lloyd, *Natural Allelic Variation Defines a Role for ATMYC1: Trichome Cell Fate Determination*. *PLOS Genetics*, 2011. **7**(6): p. e1002069.
71. Bruex, A., et al., *A Gene Regulatory Network for Root Epidermis Cell Differentiation in Arabidopsis*. *PLOS Genetics*, 2012. **8**(1): p. e1002446.
72. Romano, J.M., et al., *AtMYB61, an R2R3-MYB transcription factor, functions as a pleiotropic regulator via a small gene network*. *New Phytologist*, 2012. **195**(4): p. 774-786.
73. Liu, B., Y. Zhu, and T. Zhang, *The R3-MYB Gene GhCPC Negatively Regulates Cotton Fiber Elongation*. *PLOS ONE*, 2015. **10**(2): p. e0116272.
74. Humphries, J.A., et al., *Two WD-repeat genes from cotton are functional homologues of the Arabidopsis thaliana TRANSPARENT TESTA GLABRA1 (TTG1) gene*. *Plant Molecular Biology*, 2005. **57**(1): p. 67-81.
75. Gao, Z., et al., *The Promoter Structure Differentiation of a MYB Transcription Factor RLC1 Causes Red Leaf Coloration in Empire Red Leaf Cotton under Light*. *PLOS ONE*, 2013. **8**(10): p. e77891.
76. Shangguan, X.-X., et al., *Functional characterization of a basic helix-loop-helix (bHLH) transcription factor GhDEL65 from cotton (Gossypium hirsutum)*. *Physiologia Plantarum*, 2016. **158**(2): p. 200-212.
77. Martin, C. and B.J. Glover, *Functional aspects of cell patterning in aerial epidermis*. *Current Opinion in Plant Biology*, 2007. **10**(1): p. 70-82.
78. Brockington, S.F., et al., *Evolutionary Analysis of the MIXTA Gene Family Highlights Potential Targets for the Study of Cellular Differentiation*. *Molecular Biology and Evolution*, 2013. **30**(3): p. 526-540.
79. Glover, B.J., M. Perez-Rodriguez, and C. Martin, *Development of several epidermal cell types can be specified by the same MYB-related plant transcription factor*. *Development*, 1998. **125**(17): p. 3497-3508.
80. Payne, T., et al., *Heterologous myb genes distinct from GL1 enhance trichome production when overexpressed in Nicotiana tabacum*. *Development*, 1999. **126**(4): p. 671-682.
81. Serna, L. and C. Martin, *Trichomes: different regulatory networks lead to convergent structures*. *Trends in Plant Science*, 2006. **11**(6): p. 274-280.
82. Stracke, R., M. Werber, and B. Weisshaar, *The R2R3-MYB gene family in Arabidopsis thaliana*. *Current Opinion in Plant Biology*, 2001. **4**(5): p. 447-456.
83. Albert, N.W., et al., *A Conserved Network of Transcriptional Activators and Repressors Regulates Anthocyanin Pigmentation in Eudicots*. *The Plant Cell*, 2014. **26**(3): p. 962-980.
84. Lang, D., et al., *Genome-wide phylogenetic comparative analysis of plant transcriptional regulation: a timeline of loss, gain, expansion, and correlation with complexity*. *Genome Biol Evol*, 2010. **2**: p. 488-503.
85. Serna, L. and C. Martin, *Trichomes: different regulatory networks lead to convergent structures*. *Trends Plant Sci*, 2006. **11**(6): p. 274-80.
86. XU, W., *Deciphering the regulatory network controlling flavonoid biosynthesis by MYB-bHLH-WDR complexes in Arabidopsis seed* THÈSE DE DOCTORAT, 2014.
87. Zhang, B. and A. Schrader, *TRANSPARENT TESTA GLABRA 1-Dependent Regulation of Flavonoid Biosynthesis*. *Plants*, 2017. **6**(4): p. 65.
88. Sainz, M.B., E. Grotewold, and V.L. Chandler, *Evidence for direct activation of an anthocyanin promoter by the maize C1 protein and comparison of DNA binding by related Myb domain proteins*. *The Plant Cell*, 1997. **9**(4): p. 611-25.

89. Grotewold, E., et al., *Identification of the residues in the Myb domain of maize C1 that specify the interaction with the bHLH cofactor R*. Proceedings of the National Academy of Sciences, 2000. **97**(25): p. 13579-13584.
90. Burr, F.A., et al., *The maize repressor-like gene intensifier1 shares homology with the r1/b1 multigene family of transcription factors and exhibits missplicing*. The Plant Cell, 1996. **8**(8): p. 1249-1259.
91. Ludwig, S.R., et al., *Lc, a member of the maize R gene family responsible for tissue-specific anthocyanin production, encodes a protein similar to transcriptional activators and contains the myc-homology region*. Proceedings of the National Academy of Sciences, 1989. **86**(18): p. 7092-7096.
92. Chandler, V.L., et al., *Two regulatory genes of the maize anthocyanin pathway are homologous: isolation of B utilizing R genomic sequences*. The Plant Cell, 1989. **1**(12): p. 1175-83.
93. Pires, N. and L. Dolan, *Origin and Diversification of Basic-Helix-Loop-Helix Proteins in Plants*. Molecular Biology and Evolution, 2010. **27**(4): p. 862-874.
94. Sakamoto, W., et al., *The Purple leaf (Pl) Locus of Rice: the Plw Allele has a Complex Organization and Includes Two Genes Encoding Basic Helix-Loop-Helix Proteins Involved in Anthocyanin Biosynthesis*. Plant and Cell Physiology, 2001. **42**(9): p. 982-991.
95. Hu, J., V.S. Reddy, and S.R. Wessler, *The rice R gene family: two distinct subfamilies containing several miniature inverted-repeat transposable elements*. Plant Molecular Biology, 2000. **42**(5): p. 667-678.
96. Furukawa, T., et al., *The Rc and Rd genes are involved in proanthocyanidin synthesis in rice pericarp*. The Plant Journal, 2007. **49**(1): p. 91-102.
97. Li, Y., et al., *Two Illf Clade-bHLHs from Freesia hybrida Play Divergent Roles in Flavonoid Biosynthesis and Trichome Formation when Ectopically Expressed in Arabidopsis*. Scientific Reports, 2016. **6**: p. 30514.
98. Martin, C., et al., *Control of anthocyanin biosynthesis in flowers of Antirrhinum majus*. The Plant Journal, 1991. **1**(1): p. 37-49.
99. Tamagnone, L., et al., *The AmMYB308 and AmMYB330 transcription factors from antirrhinum regulate phenylpropanoid and lignin biosynthesis in transgenic tobacco*. The Plant Cell, 1998. **10**(2): p. 135-154.
100. Shang, Y., et al., *The molecular basis for venation patterning of pigmentation and its effect on pollinator attraction in flowers of Antirrhinum*. New Phytologist, 2011. **189**(2): p. 602-615.
101. Bai, Y., et al., *Flavonoid-related basic helix-loop-helix regulators, NtAn1a and NtAn1b, of tobacco have originated from two ancestors and are functionally active*. Planta, 2011. **234**(2): p. 363.
102. Nesi, N., et al., *The TT8 Gene Encodes a Basic Helix-Loop-Helix Domain Protein Required for Expression of DFR and BAN Genes in Arabidopsis Siliques*. The Plant Cell, 2000. **12**(10): p. 1863-1878.
103. Baudry, A., M. Caboche, and L. Lepiniec, *TT8 controls its own expression in a feedback regulation involving TTG1 and homologous MYB and bHLH factors, allowing a strong and cell-specific accumulation of flavonoids in Arabidopsis thaliana*. The Plant Journal, 2006. **46**(5): p. 768-779.
104. Gonzalez, A., et al., *TTG1 complex MYBs, MYB5 and TT2, control outer seed coat differentiation*. Developmental Biology, 2009. **325**(2): p. 412-421.
105. Koornneef, M., *The complex syndrome of ttg mutants*. Arabid. Inf. Serv., 1981. **18**: p. 45-51.
106. Teng, S., et al., *Sucrose-Specific Induction of Anthocyanin Biosynthesis in Arabidopsis Requires the MYB75/PAP1 Gene*. Plant Physiology, 2005. **139**(4): p. 1840-1852.
107. Cominelli, E., et al., *Expression analysis of anthocyanin regulatory genes in response to different light qualities in Arabidopsis thaliana*. Journal of Plant Physiology, 2008. **165**(8): p. 886-894.
108. Gonzalez, A., et al., *Regulation of the anthocyanin biosynthetic pathway by the TTG1/bHLH/Myb transcriptional complex in Arabidopsis seedlings*. The Plant Journal, 2008. **53**(5): p. 814-827.
109. Feyissa, D.N., et al., *The endogenous GL3, but not EGL3, gene is necessary for anthocyanin accumulation as induced by nitrogen depletion in Arabidopsis rosette stage leaves*. Planta, 2009. **230**(4): p. 747.

110. Qiu, J., et al., *Arabidopsis AtPAP1 transcription factor induces anthocyanin production in transgenic Taraxacum brevicorniculatum*. Plant Cell Reports, 2014. **33**(4): p. 669-680.
111. Jin, H., et al., *Transcriptional repression by AtMYB4 controls production of UV-protecting sunscreens in Arabidopsis*. The EMBO Journal, 2000. **19**(22): p. 6150-6161.
112. Yuan, Y., L.-W. Chiu, and L. Li, *Transcriptional regulation of anthocyanin biosynthesis in red cabbage*. Planta, 2009. **230**(6): p. 1141.
113. Ren, Y., et al., *Characteristics of Color Development in Seeds of Brown- and Yellow-Seeded Heading Chinese Cabbage and Molecular Analysis of Brsc, the Candidate Gene Controlling Seed Coat Color*. Frontiers in Plant Science, 2017. **8**: p. 1410.
114. Li, X., et al., *A Large Insertion in bHLH Transcription Factor BrTT8 Resulting in Yellow Seed Coat in Brassica rapa*. PLOS ONE, 2012. **7**(9): p. e44145.
115. Rahim, M.A., N. Busatto, and L. Trainotti, *Regulation of anthocyanin biosynthesis in peach fruits*. Planta, 2014. **240**(5): p. 913-929.
116. Ravaglia, D., et al., *Transcriptional regulation of flavonoid biosynthesis in nectarine (Prunus persica) by a set of R2R3 MYB transcription factors*. BMC Plant Biology, 2013. **13**(1): p. 68.
117. Taheri, A., et al., *A WD-repeat gene from peach (Prunus persica L.) is a functional ortholog of Arabidopsis thaliana TRANSPARENT TESTA GLABRA1*. In Vitro Cellular & Developmental Biology - Plant, 2012. **48**(1): p. 23-29.
118. Lin-Wang, K., et al., *An R2R3 MYB transcription factor associated with regulation of the anthocyanin biosynthetic pathway in Rosaceae*. BMC Plant Biology, 2010. **10**: p. 50-50.
119. Espley, R.V., et al., *Red colouration in apple fruit is due to the activity of the MYB transcription factor, MdMYB10*. The Plant Journal, 2007. **49**(3): p. 414-427.
120. Matoušek, J., et al., *Combinatorial analysis of lupulin gland transcription factors from R2R3Myb, bHLH and WDR families indicates a complex regulation of chs_H1 genes essential for prenylflavonoid biosynthesis in hop (Humulus Lupulus L.)*. BMC Plant Biology, 2012. **12**: p. 27-27.
121. Yoshida, K., et al., *Comparative Analysis of the Triplicate Proanthocyanidin Regulators in Lotus japonicus*. Plant and Cell Physiology, 2010. **51**(6): p. 912-922.
122. Li, P., et al., *Regulation of anthocyanin and proanthocyanidin biosynthesis by Medicago truncatula bHLH transcription factor MtTT8*. New Phytologist, 2016. **210**(3): p. 905-921.
123. Peel, G.J., et al., *The LAP1 MYB transcription factor orchestrates anthocyanidin biosynthesis and glycosylation in Medicago*. The Plant Journal, 2009. **59**(1): p. 136-149.
124. Hancock, K.R., et al., *Expression of the R2R3-MYB Transcription Factor TaMYB14 from Trifolium arvense Activates Proanthocyanidin Biosynthesis in the Legumes Trifolium repens and Medicago sativa*. Plant Physiology, 2012. **159**(3): p. 1204-1220.
125. Verdier, J., et al., *MtPAR MYB transcription factor acts as an on switch for proanthocyanidin biosynthesis in Medicago truncatula*. Proceedings of the National Academy of Sciences of the United States of America, 2012. **109**(5): p. 1766-1771.
126. Jun, J.H., et al., *The Transcriptional Repressor MYB2 Regulates Both Spatial and Temporal Patterns of Proanthocyanidin and Anthocyanin Pigmentation in Medicago truncatula*. The Plant Cell, 2015. **27**(10): p. 2860-2879.
127. Mellway, R.D., et al., *The Wound-, Pathogen-, and Ultraviolet B-Responsive MYB134 Gene Encodes an R2R3 MYB Transcription Factor That Regulates Proanthocyanidin Synthesis in Poplar*. Plant Physiology, 2009. **150**(2): p. 924-941.
128. Wang, L., et al., *The transcription factor MYB115 contributes to the regulation of proanthocyanidin biosynthesis and enhances fungal resistance in poplar*. New Phytologist, 2017. **215**(1): p. 351-367.
129. Yoshida, K., D. Ma, and C.P. Constabel, *The MYB182 Protein Down-Regulates Proanthocyanidin and Anthocyanin Biosynthesis in Poplar by Repressing Both Structural and Regulatory Flavonoid Genes*. Plant Physiology, 2015. **167**(3): p. 693-710.
130. Bogs, J., et al., *The Grapevine Transcription Factor VvMYBPA1 Regulates Proanthocyanidin Synthesis during Fruit Development*. Plant Physiology, 2007. **143**(3): p. 1347-1361.
131. Matus, J.T., et al., *Isolation of WDR and bHLH genes related to flavonoid synthesis in grapevine (Vitis vinifera L.)*. Plant Molecular Biology, 2010. **72**(6): p. 607-620.
132. Kobayashi, S., N. Goto-Yamamoto, and H. Hirochika, *Retrotransposon-Induced Mutations in Grape Skin Color*. Science, 2004. **304**(5673): p. 982-982.

133. Czemmel, S., et al., *The Grapevine R2R3-MYB Transcription Factor VvMYBF1 Regulates Flavonol Synthesis in Developing Grape Berries*. *Plant Physiology*, 2009. **151**(3): p. 1513-1530.
134. Hichri, I., et al., *The Basic Helix-Loop-Helix Transcription Factor MYC1 Is Involved in the Regulation of the Flavonoid Biosynthesis Pathway in Grapevine*. *Molecular Plant*, 2010. **3**(3): p. 509-523.
135. Xue, B., et al., *Characterization of a MYBR2R3 gene from black spruce (Picea mariana) that shares functional conservation with maize C1*. *Molecular Genetics and Genomics*, 2003. **270**(1): p. 78-86.
136. Bedon, F., et al., *Subgroup 4 R2R3-MYBs in conifer trees: gene family expansion and contribution to the isoprenoid- and flavonoid-oriented responses*. *Journal of Experimental Botany*, 2010. **61**(14): p. 3847-3864.
137. Bomal, C., et al., *Involvement of Pinus taeda MYB1 and MYB8 in phenylpropanoid metabolism and secondary cell wall biogenesis: a comparative in planta analysis*. *Journal of Experimental Botany*, 2008. **59**(14): p. 3925-3939.
138. Menand, B., et al., *An Ancient Mechanism Controls the Development of Cells with a Rooting Function in Land Plants*. *Science*, 2007. **316**(5830): p. 1477-1480.
139. Quattrocchio, F., et al., *The Regulation of Flavonoid Biosynthesis*, in *The Science of Flavonoids*, E. Grotenwold, Editor. 2006, Springer New York: New York, NY. p. 97-122.
140. Hernandez, J.M., et al., *The basic helix-loop-helix domain of maize R links transcriptional regulation and histone modifications by recruitment of an EMSY-related factor*. *Proceedings of the National Academy of Sciences*, 2007. **104**(43): p. 17222-17227.
141. Pattanaik, S., C.H. Xie, and L. Yuan, *The interaction domains of the plant Myc-like bHLH transcription factors can regulate the transactivation strength*. *Planta*, 2008. **227**(3): p. 707-715.
142. Thévenin, J., et al., *A new system for fast and quantitative analysis of heterologous gene expression in plants*. *New Phytologist*, 2012. **193**(2): p. 504-512.
143. Broun, P., *Transcriptional control of flavonoid biosynthesis: a complex network of conserved regulators involved in multiple aspects of differentiation in Arabidopsis*. *Current Opinion in Plant Biology*, 2005. **8**(3): p. 272-279.
144. Caro, E., M.M. Castellano, and C. Gutierrez, *GEM, a Novel Factor in the Coordination of Cell Division to Cell Fate Decisions in the Arabidopsis Epidermis*. *Plant Signaling & Behavior*, 2007. **2**(6): p. 494-495.
145. Kong, Q., et al., *Regulatory switch enforced by basic helix-loop-helix and ACT-domain mediated dimerizations of the maize transcription factor R*. *Proceedings of the National Academy of Sciences of the United States of America*, 2012. **109**(30): p. E2091-E2097.
146. Albert, N.W., et al., *A Conserved Network of Transcriptional Activators and Repressors Regulates Anthocyanin Pigmentation in Eudicots*. *The Plant Cell Online*, 2014.
147. Koes, R., W. Verweij, and F. Quattrocchio, *Flavonoids: a colorful model for the regulation and evolution of biochemical pathways*. *Trends in Plant Science*, 2005. **10**(5): p. 236-242.
148. Ramsay, N.A. and B.J. Glover, *MYB-bHLH-WD40 protein complex and the evolution of cellular diversity*. *Trends in Plant Science*, 2005. **10**(2): p. 63-70.
149. Pesch, M., et al., *TRANSPARENT TESTA GLABRA1 and GLABRA1 Compete for Binding to GLABRA3 in Arabidopsis*. *Plant Physiology*, 2015. **168**(2): p. 584-597.
150. Chopra, D., *Genetic analysis of trichome and root hair development in Arabis alpina*. PhD Dissertation, 2015.
151. Wang, G., et al., *Identification and Characterization of Cotton Genes Involved in Fuzz-Fiber Development*. *Journal of Integrative Plant Biology*, 2013. **55**(7): p. 619-630.
152. Lepiniec, L., et al., *GENETICS AND BIOCHEMISTRY OF SEED FLAVONOIDS*. *Annual Review of Plant Biology*, 2006. **57**(1): p. 405-430.
153. Zhao, M., et al., *The TTG1-bHLH-MYB complex controls trichome cell fate and patterning through direct targeting of regulatory loci*. *Development*, 2008. **135**(11): p. 1991-1999.
154. Barrios-Rodiles, M., et al., *High-Throughput Mapping of a Dynamic Signaling Network in Mammalian Cells*. *Science*, 2005. **307**(5715): p. 1621-1625.
155. Herman, P.L. and M.D. Marks, *Trichome Development in Arabidopsis thaliana. II. Isolation and Complementation of the GLABROUS1 Gene*. *The Plant Cell*, 1989. **1**(11): p. 1051-1055.

156. Marks, M.D. and K.A. Feldmann, *Trichome Development in Arabidopsis thaliana. I. T-DNA Tagging of the GLABROUS1 Gene*. The Plant Cell, 1989. **1**(11): p. 1043-1050.
157. Oppenheimer, D.G., et al., *A myb gene required for leaf trichome differentiation in Arabidopsis is expressed in stipules*. Cell, 1991. **67**(3): p. 483-493.
158. Borevitz, J.O., et al., *Activation Tagging Identifies a Conserved MYB Regulator of Phenylpropanoid Biosynthesis*. The Plant Cell, 2000. **12**(12): p. 2383-2393.
159. Hülskamp, M., S. Miséra, and G. Jürgens, *Genetic dissection of trichome cell development in Arabidopsis*. Cell, 1994. **76**(3): p. 555-566.
160. Wang, S., et al., *Control of Plant Trichome Development by a Cotton Fiber MYB Gene*. The Plant Cell, 2004. **16**(9): p. 2323-2334.
161. Wan, Q., et al., *Genome-Wide Transcriptome Profiling Revealed Cotton Fuzz Fiber Development Having a Similar Molecular Model as Arabidopsis Trichome*. PLOS ONE, 2014. **9**(5): p. e97313.
162. Guan, X., et al., *miR828 and miR858 regulate homoeologous MYB2 gene functions in Arabidopsis trichome and cotton fibre development*. Nature Communications, 2014. **5**: p. 3050.
163. Cedroni, M.L., et al., *Evolution and expression of MYB genes in diploid and polyploid cotton*. Plant Molecular Biology, 2003. **51**(3): p. 313-325.
164. Machado, A., et al., *The MYB transcription factor GhMYB25 regulates early fibre and trichome development*. The Plant Journal, 2009. **59**(1): p. 52-62.
165. Lloyd, A., et al., *Epidermal cell fate determination in Arabidopsis: patterns defined by a steroid-inducible regulator*. Science, 1994. **266**(5184): p. 436-439.
166. Dooner, H.K., *IDENTIFICATION OF AN R-LOCUS REGION THAT CONTROLS THE TISSUE SPECIFICITY OF ANTHOCYANIN FORMATION IN MAIZE*. Genetics, 1979. **93**(3): p. 703-710.
167. Patterson, G.I., et al., *Genetic analysis of B-Peru, a regulatory gene in maize*. Genetics, 1991. **127**(1): p. 205-220.
168. Jones, D.T., W.R. Taylor, and J.M. Thornton, *The rapid generation of mutation data matrices from protein sequences*. Bioinformatics, 1992. **8**(3): p. 275-282.
169. Tamura, K., et al., *MEGA6: Molecular Evolutionary Genetics Analysis Version 6.0*. Molecular Biology and Evolution, 2013. **30**(12): p. 2725-2729.
170. Bailey, T.L. and M. Gribskov, *Combining evidence using p-values: application to sequence homology searches*. Bioinformatics, 1998. **14**(1): p. 48-54.
171. Lai, Y., H. Li, and M. Yamagishi, *A review of target gene specificity of flavonoid R2R3-MYB transcription factors and a discussion of factors contributing to the target gene selectivity*. Frontiers in Biology, 2013. **8**(6): p. 577-598.
172. Pireyre, M. and M. Burow, *Regulation of MYB and bHLH Transcription Factors: A Glance at the Protein Level*. Molecular Plant, 2015. **8**(3): p. 378-388.
173. Nesi, N., et al., *The Arabidopsis TT2 Gene Encodes an R2R3 MYB Domain Protein That Acts as a Key Determinant for Proanthocyanidin Accumulation in Developing Seed*. The Plant Cell, 2001. **13**(9): p. 2099-2114.
174. Koornneef, M., *Mutations affecting the testa colour in Arabidopsis*. Arabidopsis Information Service, 1990. **27**: p. 1-4.
175. Kubasek, W.L., et al., *Regulation of Flavonoid Biosynthetic Genes in Germinating Arabidopsis Seedlings*. The Plant Cell, 1992. **4**(10): p. 1229-1236.
176. Ioannidi, E., et al., *Trichome patterning control involves TTG1 interaction with SPL transcription factors*. Plant Molecular Biology, 2016. **92**(6): p. 675-687.
177. Li, S.F., et al., *The Arabidopsis MYB5 Transcription Factor Regulates Mucilage Synthesis, Seed Coat Development, and Trichome Morphogenesis*. The Plant Cell, 2009. **21**(1): p. 72-89.
178. Pesch, M., et al., *Mutual control of intracellular localisation of the patterning proteins AtMYC1, GL1 and TRY/CPC in Arabidopsis*. Development, 2013. **140**(16): p. 3456-3467.
179. Schellmann, S., et al., *TRIPTYCHON and CAPRICE mediate lateral inhibition during trichome and root hair patterning in Arabidopsis*. The EMBO Journal, 2002. **21**(19): p. 5036-5046.
180. Liang, G., et al., *MYB82 functions in regulation of trichome development in Arabidopsis*. Journal of Experimental Botany, 2014. **65**(12): p. 3215-3223.
181. Gietz, R.D., et al., *Studies on the transformation of intact yeast cells by the LiAc/SS-DNA/PEG procedure*. Yeast, 1995. **11**(4): p. 355-360.

182. Jakoby, M.J., et al., *Transcriptional Profiling of Mature Arabidopsis Trichomes Reveals That NOECK Encodes the MIXTA-Like Transcriptional Regulator MYB106*. Plant Physiology, 2008. **148**(3): p. 1583-1602.
183. Friede, A., et al., *The Second Intron Is Essential for the Transcriptional Control of the Arabidopsis thaliana GLABRA3 Gene in Leaves*. Frontiers in Plant Science, 2017. **8**(1382).
184. Kuromori, T., et al., *A collection of 11 800 single-copy Ds transposon insertion lines in Arabidopsis*. The Plant Journal, 2004. **37**(6): p. 897-905.
185. Zhang, X., et al., *Agrobacterium-mediated transformation of Arabidopsis thaliana using the floral dip method*. Nat. Protocols, 2006. **1**(2): p. 641-646.
186. Landy, A., *Dynamic, Structural, and Regulatory Aspects of lambda Site-Specific Recombination*. Annual Review of Biochemistry, 1989. **58**(1): p. 913-941.
187. Magnani, E., L. Bartling, and S. Hake, *From Gateway to MultiSite Gateway in one recombination event*. BMC Molecular Biology, 2006. **7**: p. 46-46.
188. Bernard, P. and M. Couturier, *Cell killing by the F plasmid CcdB protein involves poisoning of DNA-topoisomerase II complexes*. Journal of Molecular Biology, 1992. **226**(3): p. 735-745.
189. Miki, T., et al., *Control of segregation of chromosomal DNA by sex factor F in Escherichia coli*. Journal of Molecular Biology, 1992. **225**(1): p. 39-52.
190. Koncz, C. and J. Schell, *The promoter of TL-DNA gene 5 controls the tissue-specific expression of chimaeric genes carried by a novel type of Agrobacterium binary vector*. Molecular and General Genetics MGG, 1986. **204**(3): p. 383-396.
191. Sambrook, J., *Molecular cloning : a laboratory manual / Joseph Sambrook, David W. Russell*, ed. D.W. Russell and L. Cold Spring Harbor. 2001, Cold Spring Harbor, N.Y: Cold Spring Harbor Laboratory.
192. Schroeder, M., et al., *Use of enhancer trapping to identify pathogen-induced regulatory events spatially restricted to plant-microbe interaction sites*. Molecular Plant Pathology, 2016. **17**(3): p. 388-397.
193. Morohashi, K., et al., *Participation of the Arabidopsis bHLH Factor GL3 in Trichome Initiation Regulatory Events*. Plant Physiology, 2007. **145**(3): p. 736-746.
194. Tominaga, R., et al., *Functional Analysis of the Epidermal-Specific MYB Genes CAPRICE and WEREWOLF in Arabidopsis*. The Plant Cell, 2007. **19**(7): p. 2264-2277.
195. Kreutz, C., et al., *Profile likelihood in systems biology*. FEBS Journal, 2013. **280**(11): p. 2564-2571.

Erklärung

Ich versichere, dass ich die von mir vorgelegte Dissertation selbständig angefertigt, die benutzten Quellen und Hilfsmittel vollständig angegeben und die Stellen der Arbeit einschließlich Tabellen, Karten und Abbildungen, die anderen Werken im Wortlaut oder dem Sinn nach entnommen sind, in jedem Einzelfall als Entlehnung kenntlich gemacht habe; dass diese Dissertation noch keiner anderen Fakultät oder Universität zur Prüfung vorgelegen hat; dass sie abgesehen von unten angegebenen Teilpublikationen noch nicht veröffentlicht worden ist, sowie, dass ich eine solche Veröffentlichung vor Abschluss des Promotionsverfahrens nicht vornehmen werde. Die Bestimmungen der Promotionsordnung sind mir bekannt. Die von mir vorgelegte Dissertation ist von Prof. Dr. Martin Hülskamp betreut worden.

Köln, den 05 März, 2018

Lebenslauf

Persönliche Daten

Name: Bipei

Vorname: Zhang

Geburtsdatum: 12 März 1984

Geburtsort: Zhejiang

Staatsangehörigkeit: China

E-mail: bzhang1@smail.uni-koeln.de



Ausbildung

Studienverlauf

seit April 2014 Promotionstudium am Botanisches Institut III

Universität zu Köln

September 2007 - Juni 2010 Master of Science (Genetics)

SUN-Yat-sen University, China

September 2003 - Juni 2007 Bachelor of Science (Biological Technics)

with First Class Honors
GuangXi University, China

Schulbildung

September 1997 - Juni 2003 Sekundarstufe I und II

Zhoushan Middle School

September 1992 - Juni 1997 Grundschule

Changtu Central School

